



# Kent Academic Repository

Walsh, Yvonne (2017) *PHARMACOLOGICAL REGULATION OF TREK1, TREK2 AND TRESK TWO PORE DOMAIN POTASSIUM CHANNELS*. Doctor of Philosophy (PhD) thesis, University of Kent,.

## Downloaded from

<https://kar.kent.ac.uk/68081/> The University of Kent's Academic Repository KAR

## The version of record is available from

## This document version

Author's Accepted Manuscript

## DOI for this version

## Licence for this version

UNSPECIFIED

## Additional information

## Versions of research works

### Versions of Record

If this version is the version of record, it is the same as the published version available on the publisher's web site. Cite as the published version.

### Author Accepted Manuscripts

If this document is identified as the Author Accepted Manuscript it is the version after peer review but before type setting, copy editing or publisher branding. Cite as Surname, Initial. (Year) 'Title of article'. To be published in *Title of Journal*, Volume and issue numbers [peer-reviewed accepted version]. Available at: DOI or URL (Accessed: date).

## Enquiries

If you have questions about this document contact [ResearchSupport@kent.ac.uk](mailto:ResearchSupport@kent.ac.uk). Please include the URL of the record in KAR. If you believe that your, or a third party's rights have been compromised through this document please see our [Take Down policy](https://www.kent.ac.uk/guides/kar-the-kent-academic-repository#policies) (available from <https://www.kent.ac.uk/guides/kar-the-kent-academic-repository#policies>).

**PHARMACOLOGICAL  
REGULATION OF TREK1, TREK2  
AND TRESK TWO PORE DOMAIN  
POTASSIUM CHANNELS**

**YVONNE WALSH**

**A thesis submitted in partial fulfilment of the  
requirements of the University of Kent and the  
University of Greenwich for the Degree of  
Doctor of Philosophy**

**September 2017**

## ***DECLARATION***

I certify that this work has not been accepted in substance for any degree, and is not concurrently being submitted for any degree other than that of Doctor of Philosophy being studied at the Universities of Greenwich and Kent. I also declare that this work is the result of my own investigations except where otherwise identified by references and that I have not plagiarised the work of others.

Yvonne Walsh

Alistair Mathie

# ACKNOWLEDGEMENTS

*Firstly, I would like to express my sincere gratitude to Prof. Alistair Mathie for the continuous support, motivation and advice during my PhD study. His tremendous contribution of time and ideas have made my PhD experience a happy, productive and rewarding one. I would also like to thank Dr. Michael Leach for his guidance throughout.*

*Many thanks to Dr. Emma Veale for her support and endless advice in the lab during these years. I would also like to thank the lab group: Dr. Ehab Al-Moubarak, Dr. Mustafa Hassan, Lee Mun Ching, Kevin Cunningham and Robyn Holden for their constant support, humour and encouragement. Thanks to all my colleagues and friends in Medway School of Pharmacy for their positivity and support.*

*My greatest thank you goes to my family, particularly my late father Dave, who is a lasting source of inspiration. This thesis is dedicated to him. To my mother, Beatrice, and siblings, Jackie and Keith, for their love and sacrifice. I am so grateful to have you all supporting me along the way. I would also like to thank my grandparents, Rena and Matt, who have always been a pillar of strength throughout. Finally thank you to Cameron, for your belief, encouragement and faithful support.*

# ABSTRACT

**Introduction:** Two pore domain potassium ( $K_{2P}$ ) channels are responsible for background currents that regulate membrane potential and neuronal excitability. Compounds which alter the activity of these channels are predicted to have therapeutic potential in treating CNS disorders. Members of the TREK family of  $K_{2P}$  channels (TREK1 and TREK2) have been shown to play an active role in neuroprotection, depression and pain, whilst TRESK, with high expression in sensory neurons, has a role in nociception. Sipatrigine, a neuroprotective agent and a derivative of the anticonvulsant lamotrigine, is a known antagonist of TREK channels whilst lamotrigine is thought to primarily inhibit TRESK channels. A new compound, Cen-092-C, has also been developed which is structurally similar to lamotrigine. However, its effects on  $K_{2P}$  channels are unknown. To understand the mechanism of channel inhibition by drugs, the structure of TREK2 was solved and was co-crystallised with norfluoxetine. This showed that fenestration sites were important in channel and current inhibition. Furthermore, TRESK docking studies showed that F145 and F352 function in a similar way to TREK2 fenestration site, as the bulky phenylalanine faces into the pore, and are thought to be important for compound binding. The aim of this study is to clarify to differences in the inhibitory effect of these compounds on the selected  $K_{2P}$  channels and to investigate the mechanism by which these compounds inhibit the channels current.

**Methods:** Wild-type (WT) and mutated human  $K_{2P}$  channels were transiently expressed in tsA-201 cells. The currents were measured using whole-cell patch-clamp electrophysiology.

**Results:** Sipatrigine was shown to inhibit both TREK1 and TREK2 current. Lamotrigine was also found to inhibit TREK1 and to a lesser extent TREK2. Cen-092-C was found to be less effective on TREK1 and TRESK current compared to sipatrigine, but similar to lamotrigine results. The sipatrigine inhibitory effect, but not lamotrigine, was reduced by mutations on the M4 region at the fenestration site of TREK1 and TREK2 (L286 and L320). This sensitivity is selective at this site as other mutations in the central cavity showed no change in sipatrigine inhibition. Interestingly, the gain-of-function mutation (TREK1 E306A) on the C terminus showed a reduced sipatrigine inhibition. The effect of sipatrigine on TREK2 showed an over-recovery of current following wash-off of the compound. The wash-off current increase was not seen if the N-terminus length is forced into intermediate and short isoform. Sipatrigine inhibition was significantly decreased when the N-terminus was truncated. Sipatrigine has been shown to strongly inhibit TRESK. Lamotrigine was seen to inhibit TRESK current, however significantly less effective compared to sipatrigine. Furthermore, lamotrigine did show state dependent inhibition when TRESK is in the fixed activated state. Cen-092-C was also found to inhibit TRESK to a similar degree to lamotrigine, however there was no state dependent inhibition on TRESK current. The effects of these antagonists on TRESK has been shown to be abolished by mutations on two sites at the central cavity (F145 and F352).

**Conclusion:** Lamotrigine was found not to be TRESK selective, contrary to other studies. Sipatrigine and lamotrigine inhibition works through binding to the channel. The fenestration site in both TREK1 and TREK2 has been found to be an important binding site of sipatrigine, differing from lamotrigine. This suggests that the structurally similar compounds bind to different regions of the TREK channels. Furthermore, the over recovery of TREK2 current after sipatrigine wash off is believed to show the compound's biphasic effect, where the underlying enhancement of current is hidden by the action of inhibition. The N-terminus is therefore believed to be important in regulating sipatrigine action on TREK2.

It remains unclear whether the TRESK potential binding sites (F145 and F352) are important in compound binding as the inserted mutation is believed to shift the channel to constant active state. The newly developed compound Cen-092-C shows a significantly greater degree of inhibition of TRESK when compared to TREK1. Cen-092-C and lamotrigine inhibition of TRESK is not significantly different. Lamotrigine inhibition of TRESK current is state dependent whereas sipatrigine and Cen-092-C inhibition of TRESK current is shown as state independent. All of this together could lead to a better understanding of how neuroprotective agents effect TREK and TRESK channels and could contribute to the design of more efficient ligands.

## Table of Contents

|  |    |
|--|----|
| <b>ACKNOWLEDGEMENTS</b> .....  | ii |
| <b>TABLES</b> .....  | vi |
| <b>Figures</b> .....   | vi |
| <b>ABSTRACT</b> .....  | ix |
| <b>LIST OF ABBREVIATIONS</b> .....   | x  |
| <b>CHAPTER 1</b> .....   | 1  |
| <b>1 General Introduction</b> .....  | 2  |
| 1.1 The voltage-gated ion channel super-family.....                              | 3  |
| 1.2 Evolution of ion channels.....   | 4  |
| 1.3 Ion channel nomenclature.....  | 6  |
| 1.4 Membrane potentials.....   | 14 |
| 1.5 The resting membrane potential and the estimation of membrane potential..... | 15 |
| 1.6 The pore structure of Kcsa.....  | 18 |
| 1.7 The selectivity filter in potassium channels.....                            | 19 |
| 1.8 Two pore domain potassium channels (K <sub>2P</sub> ).....                   | 21 |
| 1.9 Gating K <sub>2P</sub> channel.....  | 22 |
| 1.10 TREK channels.....  | 28 |
| 1.11 TRESK channel.....  | 38 |
| 1.12 Sipatrigine and its derivative lamotrigine.....                             | 47 |
| 1.13 Cen-092-C.....  | 50 |
| 1.14 Aims and objectives of thesis.....  | 51 |
| <b>CHAPTER 2</b> .....   | 52 |
| <b>2 Methods</b> .....   | 53 |
| 2.1 Preparation of poly-D-lysine (PDL) plates.....                               | 53 |
| 2.2 Cell culture.....  | 53 |
| 2.3 Calcium phosphate transfection.....  | 54 |
| 2.4 Mutagenesis.....   | 55 |
| 2.5 Electrophysiology experiments.....   | 56 |
| 2.6 Structure visualization.....   | 65 |

|  |           |
|--|-----------|
| <b>CHAPTER 3.....</b>  | <b>68</b> |
| <b>3 Regulation of TREK1 channels by sipatrigine and lamotrigine.....</b>                                      | <b>68</b> |
| 3.1 Complex neurobiological systems mediate pain.....  | 68        |
| 3.2 Somatosensory neurons and nociceptors.....   | 68        |
| 3.3 TREK1 is a novel pain target.....  | 68        |
| 3.4 K <sub>2P</sub> lateral fenestrations.....   | 69        |
| 3.5 Fenestration gating.....   | 70        |
| 3.6 Aim of this chapter.....   | 70        |
| 3.7 Sipatrigine inhibits TREK1 channels.....   | 75        |
| 3.8 Lamotrigine inhibition of TREK1 .....  | 75        |
| 3.9 TREK1 mechanism of action.....   | 76        |
| <b>CHAPTER 4.....</b>  | <b>83</b> |
| <b>4 Regulation of TRESK channels by sipatrigine and lamotrigine.....</b>                                      | <b>84</b> |
| 4.1 Physiological role of TRESK and pain.....  | 84        |
| 4.2 Regulatory pathways involving phosphorylation.....   | 85        |
| 4.3 Central cavity is important for blocking binding.....  | 85        |
| 4.4 Aim of the chapter.....  | 86        |
| 4.5 Sipatrigine inhibition of TRESK.....   | 87        |
| 4.6 Lamotrigine inhibition of TRESK.....   | 89        |
| 4.7 TRESK mechanism of action.....   | 90        |
| 4.8 Potential activators of TRESK.....   | 93        |
| <b>CHAPTER 5.....</b>  | <b>96</b> |
| <b>5 Regulation of TREK2 channels by sipatrigine and lamotrigine.....</b>                                      | <b>97</b> |
| 5.1 TREK2 linked to pain.....  | 97        |
| 5.2 Variation of the channel structure.....  | 97        |
| 5.3 Aim of this chapter.....   | 99        |
| 5.4 Sipatrigine inhibits TREK2 channels.....   | 100       |
| 5.5 Lamotrigine inhibits TREK2 channels.....   | 101       |
| 5.6 TREK2 predicted norfluoxetine interaction site is also predicted<br>as a sipatrigine interaction site..... | 102       |
| 5.7 TREK2 over recovery of current.....  | 104       |

|  |            |
|--|------------|
| 5.8 TREK2 isoforms generated by ATI change sipatrigine effect.....                             | 105        |
| 5.9 25 mM K <sup>+</sup> solution effect on TREK2 with sipatrigine.....                        | 108        |
| <b>CHAPTER 6.....</b>  | <b>111</b> |
| <b>6 Antagonist compound Cen-092-C effect on K<sub>2P</sub> channels.....</b>                  | <b>112</b> |
| 6.1 Cen-092-C.....   | 112        |
| 6.2 Aim of the chapter.....  | 113        |
| 6.3 Cen-092-C inhibition of TRESK is affected by the central cavity.....                       | 114        |
| 6.4 Is Cen-092-C inhibition on TRESK state dependent?.....                                     | 116        |
| 6.5 Cen-092-C inhibition on TREK1.....   | 117        |
| <b>CHAPTER 7.....</b>  | <b>118</b> |
| <b>7 GENERAL DISCUSSION.....</b>   | <b>119</b> |
| 7.1 Lamotrigine modulates TREK1, TREK2 and TRESK.....  | 119        |
| 7.2 Sipatrigine is a potent inhibitor of TREK1, TREK2 and TRESK.....                           | 120        |
| 7.3 The binding sites in the central cavity.....   | 121        |
| 7.4 Dynamic structural changes involving fenestrations in K <sub>2P</sub> channels.....        | 123        |
| 7.5 Access to TREK through fenestrations.....  | 124        |
| 7.6 Sipatrigine has a biphasic effect on TREK2 current.....                                    | 125        |
| 7.7 N-terminus is important in over-recovery of TREK2 current<br>following sipatrigine.....    | 126        |
| 7.8 Influence of TRESK central cavity.....   | 128        |
| 7.9 TRESK phosphorylation state influences lamotrigine<br>but not sipatrigine sensitivity..... | 129        |
| 7.10 Cen-092-C inhibition on TREK and TRESK current.....                                       | 130        |
| 7.11 Therapeutic implications of regulating TREK and TRESK channels.....                       | 131        |
| 7.12 Future work.....  | 134        |
| 7.13 Conclusion.....   | 135        |
| <b>REFERENCES.....</b>   | <b>136</b> |
| <b>8 APPENDIX.....</b>   | <b>157</b> |

## Tables

|   |    |
|---|----|
| Table 1.1: The 2TM potassium ion channel subfamily.....   | 6  |
| Table 1.2: The 6TM potassium ion channel subfamily.....   | 7  |
| Table 1.3: The 4TM potassium ion channel subfamily.....   | 8  |
| Table 1.3.1: Natural and chemical effectors of $K_{2P}$ channels including salient features and interacting partners..... | 9  |
| Table 1.4: The voltage-gated sodium ion channel subfamily and function.....   | 11 |
| Table 1.5: The voltage-gated calcium ion channel subfamily and function.....  | 12 |
| Table 1.6: The TRP ion channel subfamily names and what they stand for.....   | 13 |
| Table 2.1: Number of cycles needed of each type of mutation.....  | 56 |

## Figures

|   |    |
|---|----|
| Figure 1.1: Representation of the 143 members in seven ion channel families.....                          | 5  |
| Figure 1.2: The unequal distribution of ions found at the resting membrane potential.....                 | 15 |
| Figure 1.3: Nernst equation.....  | 16 |
| Figure 1.4: Goldman-Hodgkin-Katz equation.....  | 16 |
| Figure 1.5: Ribbon representation of the Kcsa $K^+$ channel (1BL8).....                                   | 19 |
| Figure 1.6: The ion binding in sodium and potassium channels.....   | 21 |
| Figure 1.7: TREK1 and C-terminus gating.....  | 26 |
| Figure 1.8: Model of coupling gates.....  | 26 |
| Figure 1.9: Structure of $K_{2P}$ TWIK1 channel (3UKM) with an open inner gate.....                       | 28 |
| Figure 1.10: TREK inhibition activated by $G\alpha_q$ and mediated by PKC or a depletion of $PIP_2$ ..... | 32 |
| Figure 1.11: Regulation of TREK via the fluctuation of cAMP concentration.....                            | 33 |
| Figure 1.12: Representation of human TRESK activation.....  | 41 |
| Figure 1.13: Representation of human TRESK regulation.....  | 43 |
| Figure 1.14: Structure of sipatrigine and lamotrigine.....  | 48 |
| Figure 1.15: Chemical structure of sipatrigine, lamotrigine and Cen-092-C.....                            | 50 |
| Figure 2.1: Patch clamp differential amplifier.....   | 57 |
| Figure 2.2: Membrane capacitor.....   | 59 |
| Figure 2.3: Simplified Voltage clamp circuit.....   | 60 |
| Figure 2.4: Formation of whole cell patch clamp.....  | 63 |
| Figure 2.5: Voltage protocol used to study $K_{2P}$ channels.....   | 64 |

|   |     |
|---|-----|
| Figure 3.1: Sipatrigine (100 $\mu$ M) inhibition of WT TREK1 channels.....  | 71  |
| Figure 3.2: Concentration-response curve of sipatrigine inhibition of TREK1 current.....                                  | 72  |
| Figure 3.3: Current density (pA/pF) of TREK1 WT and TREK1 E306A.....  | 73  |
| Figure 3.4: Sipatrigine effects on TREK1 E306A.....   | 73  |
| Figure 3.5: TREK1 E306A trace and reversal potential.....   | 74  |
| Figure 3.6: Lamotrigine inhibition of TREK1 WT.....   | 75  |
| Figure 3.7: Model and sequence of TREK1 L289A.....  | 76  |
| Figure 3.8: Current density and compound inhibition of TREK1 L289.....  | 77  |
| Figure 3.9: TREK1 T142A, T251A structure and current density (pA/pF).....   | 78  |
| Figure 3.10: Effects of sipatrigine (100 $\mu$ M) on TREK1 T142A and TREK1 T251A.....                                     | 79  |
| Figure 3.11: Effects of sipatrigine (100 $\mu$ M) on TREK1 T142A, T251A.....  | 80  |
| Figure 3.12: Effects of sipatrigine (100 $\mu$ M) in 25 mM $K^+$ solution.....  | 82  |
| Figure 3.13: Current density (pA/pF) of TREK1 WT and TREK1 T142A, T251A in 25 mM $K^+$ .....                              | 82  |
| Figure 3.14: Difference in sipatrigine (100 $\mu$ M) inhibition in 2.5 mM external solution and 25 mM $K^+$ solution..... | 82  |
| Figure 4.1: Sipatrigine (100 $\mu$ M) inhibition of TRESK WT channels.....  | 87  |
| Figure 4.2: Concentration-response curve of sipatrigine inhibition of TRESK current.....                                  | 88  |
| Figure 4.3: Lamotrigine (100 $\mu$ M) inhibition of WT TRESK channels.....  | 89  |
| Figure 4.4: Sipatrigine (100 $\mu$ M) inhibition of TRESK FF channels.....  | 90  |
| Figure 4.5: Lamotrigine (100 $\mu$ M) inhibition of TRESK FF channels.....  | 91  |
| Figure 4.6: The effect that the double FF mutation has on the inhibitory action of sipatrigine and lamotrigine.....       | 92  |
| Figure 4.7: Current density of TRESK mutations.....   | 92  |
| Figure 4.8: Effects of sipatrigine (100 $\mu$ M) and lamotrigine (100 $\mu$ M) on TRESK mutations.....                    | 93  |
| Figure 4.9: Effects of potential activators on TRESK WT.....  | 94  |
| Figure 4.10: TRESK WT current in the presence of low EGTA and potential activators.....                                   | 95  |
| Figure 5.1: Kozak scanning model.....   | 98  |
| Figure 5.2: Sipatrigine (100 $\mu$ M) effects of WT TREK2 channels.....   | 100 |
| Figure 5.3: Lamotrigine (100 $\mu$ M) effects of WT TREK2 channels.....   | 101 |
| Figure 5.4: TREK2 structure highlighting mutated residue.....   | 102 |
| Figure 5.5: TREK2 L320A is the presence and absence of sipatrigine (100 $\mu$ M) .....                                    | 103 |

|  |     |
|--|-----|
| Figure 5.6: Recovery of current after sipatrigine inhibition.....  | 104 |
| Figure 5.7: TREK2 in the presence of sipatrigine (100 $\mu$ M) after a longer exposure time.....   | 104 |
| Figure 5.8: Forced long form TREK2 in the presence of sipatrigine (100 $\mu$ M)<br>and the over recovery in the wash off of sipatrigine..... | 105 |
| Figure 5.9: Forced intermediate TREK2 in the presence of sipatrigine (100 $\mu$ M) and the<br>recovery of current in the wash off.....       | 105 |
| Figure 5.10: Forced short form of TREK2 in the presence of sipatrigine (100 $\mu$ M) and the<br>recovery of current in the wash off.....     | 106 |
| Figure 5.11: Current density of TREK2 WT and the forced AT1 isoforms of TREK2 .....  | 106 |
| Figure 5.12: Current density of TREK2 WT and isoforms.....   | 107 |
| Figure 5.13: Sipatrigine inhibition of TREK2 isoforms.....   | 107 |
| Figure 5.14: Current density of TREK2 WT in 2.5 mM compared to 25 mM K <sup>+</sup> external<br>solution.....                                | 108 |
| Figure 5.15: Current inhibition of TREK2 WT and isoforms in 25 mM K <sup>+</sup> solution .....  | 109 |
| Figure 5.16: Over recovery of current seen in TREK2 WT and short isoform.....  | 110 |
| Figure 6.1: The inhibition of TRESK WT current in the presence and<br>absence of Cen-092-C.....  | 114 |
| Figure 6.2: Cen-092-C effect on TRESK WT.....  | 115 |
| Figure 6.3: Cen-092-C (100 $\mu$ M) inhibition of TRESK WT, TRESK AA and TRESK EE.....   | 116 |
| Figure 6.4: The inhibition of TREK1 current in the presence of Cen-092-C.....  | 117 |
| Figure 7.1: Lamotrigine inhibition of TREK1, TREK2 and TRESK current.....  | 119 |
| Figure 7.2: Sipatrigine inhibition of TREK1, TREK2 and TRESK current.....  | 120 |
| Figure 7.3: Highlighted sites L289, T142 and T251 on TREK1 (4TWK) .....  | 122 |
| Figure 7.4: TREK2 states which show fenestrations being formed.....  | 125 |

# LIST OF ABBREVIATIONS

|                       |  |
|-----------------------|--|
| <b>4AP</b>            | 4-Aminopyridine                              |
| <b>5-HT</b>           | 5-Hydroxytryptamine                          |
| <b>AA</b>             | Arachidonic acid                             |
| <b>ASIC</b>           | Acid-sensing ion channel                     |
| <b>ATI</b>            | Alternative translational initiation         |
| <b>CaCC</b>           | Calcium-activated chloride                   |
| <b>cAMP</b>           | Cyclic adenosine monophosphate               |
| <b>Ca<sub>v</sub></b> | Voltage-gated calcium                        |
| <b>CIPS</b>           | Calcineurin-inhibitor induced pain syndrome  |
| <b>C<sub>m</sub></b>  | Membrane capacitance                         |
| <b>CnA</b>            | Calmodulin-dependent phosphatase calcineurin |
| <b>CNS</b>            | Central nervous system                       |
| <b>CNG</b>            | Cyclic nucleotide-gated                      |
| <b>CsA</b>            | Cyclosporine A                               |
| <b>CSD</b>            | Cortical spreading depression                |
| <b>DAG</b>            | Diacylglycerol                               |
| <b>Dauda</b>          | 11-dansylaminoundecanoic acid                |
| <b>DRG</b>            | Dorsal root ganglion                         |
| <b>DRN</b>            | Dorsal raphe nucleus                         |
| <b>EAE</b>            | Experimental autoimmune encephalomyelitis    |
| <b>ENaC</b>           | Epithelial sodium channel                    |
| <b>E<sub>Cl</sub></b> | Chloride equilibrium                         |
| <b>E<sub>m</sub></b>  | Membrane potential                           |
| <b>E<sub>Na</sub></b> | Sodium equilibrium                           |
| <b>E<sub>K</sub></b>  | Potassium equilibrium                        |
| <b>FFA</b>            | Flufenamic acid                              |

|                        |  |
|------------------------|--|
| <b>GFP</b>             | Green fluorescent protein  |
| <b>GHK</b>             | Goldman-Hodgkin-Katz   |
| <b>GOF</b>             | Gain-of-function   |
| <b>HEK 293</b>         | Human embryonic kidney 293 cells   |
| <b>HCN</b>             | Hyperpolarization-activated cyclic nucleotide-modulated                      |
| <b>IC50</b>            | The half maximal inhibitory concentration                                    |
| <b>I<sub>f</sub></b>   | Feedback current   |
| <b>I<sub>p</sub></b>   | Pipette current  |
| <b>IP<sub>3</sub></b>  | Inositol trisphosphate   |
| <b>K<sub>2P</sub></b>  | Two pore domain potassium  |
| <b>K<sub>Ca</sub></b>  | Calcium-activated potassium  |
| <b>K<sub>ir</sub></b>  | Inwardly rectifying potassium  |
| <b>LPA</b>             | Lysophosphatidic acid  |
| <b>Maxi Cl</b>         | Maxi chloride  |
| <b>MS</b>              | Multiple sclerosis   |
| <b>mGluR</b>           | Metabotropic glutamate receptor  |
| <b>MlotiK</b>          | Cyclic nucleotide-regulated potassium channel from <i>Mesorhizobium loti</i> |
| <b>Na<sub>v</sub></b>  | Voltage-gated sodium   |
| <b>NavAB</b>           | Voltage-gated Na <sup>+</sup> channel from <i>Arcobacter</i>                 |
| <b>NavMs</b>           | Voltage-gated sodium from <i>Magnetococcus marinus</i>                       |
| <b>NFAT</b>            | Nuclear Factor of Activated T cells  |
| <b>NMDA</b>            | N-methyl-D-aspartate   |
| <b>PDB</b>             | Protein data bank  |
| <b>PIP<sub>2</sub></b> | Phosphatidylinositol 4,5-bisphosphate  |
| <b>PKC</b>             | Protein kinase C   |
| <b>PLC</b>             | Phospholipase C  |
| <b>PMA</b>             | Phorbol 12-myristate-13-acetate  |

|                      |  |
|----------------------|--|
| <b>PUFA</b>          | Polyunsaturated fatty acids                                      |
| <b>QA</b>            | Quaternary ammonium  |
| <b>Ra</b>            | Access resistance  |
| <b>Rf</b>            | Feedback resistor  |
| <b>Rinput</b>        | Input resistance   |
| <b>Rm</b>            | Membrane resistance  |
| <b>RMP</b>           | Resting membrane potential                                       |
| <b>Rp</b>            | Pipette resistance   |
| <b>Rs</b>            | Series resistance  |
| <b>Rt</b>            | Total resistance   |
| <b>RyR1</b>          | Ryanodine receptors 1  |
| <b>SERT</b>          | Serotonin transporter  |
| <b>TASK</b>          | TWIK-related acid-sensitive K <sup>+</sup> channel               |
| <b>TEA</b>           | Tetraethylammonium   |
| <b>TM</b>            | Transmembrane  |
| <b>TRAAK</b>         | TWIK-related arachidonic acid-stimulated K <sup>+</sup> channel  |
| <b>TREK</b>          | TWIK-related K <sup>+</sup> channel                              |
| <b>TRESK</b>         | TWIK-related spinal cord K <sup>+</sup> channel                  |
| <b>TRP</b>           | Transient receptor potential                                     |
| <b>TRPV1</b>         | Transient receptor potential cation channel subfamily V member 1 |
| <b>tsA 201 cells</b> | Temperature-sensitive A-gene 201 cells                           |
| <b>Vcomm</b>         | Command voltage  |
| <b>Vm</b>            | Membrane potential   |
| <b>Vp</b>            | Pipette voltage  |
| <b>Vo</b>            | Voltage output   |
| <b>VRC</b>           | Volume regulated chloride  |
| <b>WT</b>            | Wild-type  |

# **CHAPTER 1**

## **General Introduction**

# 1 General introduction

Ion channels are pore forming proteins found in the plasma membrane and forms a passageway which allows of the flow of ions across the membrane. The human genome contains over 200 genes which code the primary ( $\alpha$ ) subunit that form ion channel and the number for ion channel proteins may be even greater because of the formation of heteromeric channel subunit arrangements (Alexander, Mathie and Peters 2011). There are ion channels that are voltage gated, for example most Na, K, Ca and Cl channels. However, there are others that are insensitive to voltage and use secondary messengers and other intracellular and /or extracellular mediators to gate the channels. Along with this, neurotransmitter activated, ligand-gated ion channels are gated by the binding of neurotransmitter which triggers changes in conduction of ions across the plasma membrane (Overington, Al-Lazikani and Hopkins 2006)

Characterising ion channels can be greatly improved by understanding their structure, various gating processes and functional states. The mechanism by which ion channels interact and recognise modulators is essential in the understanding of how ion channels are regulated. Improving our knowledge of ion channel structure will also emphasise any differences between other ion channel sequences and overall structures. The potential importance of the specific structural differences could contribute to a better understanding of the function and sensitivity of the channel (Bagal et al 2013).

Ion channels are responsible for the flux of ions from one side of the membrane to the other which will generate the action potential. The availability of pharmacological tools to target ion channels is therefore important for potential therapeutic effects. New therapies for diseases could result from new drugs designed to target ion channels (Mathie 2010). There have also been recent advances in information about ion channel structure aiding research into ion channels function.

This introduction will focus on the evolution of ion channels and their common structural features such as pore structures with a particular focus on K channels. This then leads to comparing different ion channels and how structural information about the Kcsa channel led to a better understanding of the selectivity filter of  $K_{2P}$  channels. This is followed by a review of recent ideas of how  $K_{2P}$  channels gate, which is an important aspect for this thesis. The final section of the introduction will investigate how TREK1, TREK2 and TRESK are regulated and what therapeutic potential these channels hold.

## 1.1 The voltage-gated ion channel super-family

The voltage-gated ion channel protein superfamily is one of the largest families of signal transduction proteins and contains over 140 members. The basis of the ion channel families is centred on four variations surrounding the common pore-forming structure (Yu et al 2005).

Sodium channels were the first members of the superfamily to be identified as a protein and also the first amino acid sequence to be solved (Catterall 2000; Noda et al 1984). The voltage-gated sodium channel is a large, complex which consists of four domains (1TM-4TM) which forms the common structural motif for the family. Each of the domains contains six  $\alpha$ -helical transmembrane segments (S1-S6). There is an embedded membrane - reentrant loop between helices S5 - S6 which forms the narrow, ion-selective filter at the extracellular end of the pore. The intracellular end of the pore is formed by four S6 segments (Yu and Catterall 2003). The voltage-gated calcium ( $Ca_v$ ) channels are structurally similar to that for the  $Na_v$  channel. The  $\alpha$  subunit of  $Ca_v$  channel is similar to sodium channels as it is comprised in four homologous domains with six transmembrane segments. The S4 segment sense changes in the electric field and is important in channel gating. The transmembrane segments S5 and S6 contains a pore loop and determines ion conductance and selectivity (Hofmann et al 1994).

Voltage-gated potassium ( $K_v$ ) channels were first sequenced after analysis of the *Shaker* mutation in the fruit fly *Drosophila* (Papazian et al 1987).  $K_v$  channels are similar to the channels described above as the  $\alpha$  subunits is a tetramer which resembles domains found in sodium and calcium channels. There are several other families of ion channels which have the same structure including;

- Calcium-activated potassium ( $K_{Ca}$ )
- Cyclic nucleotide-gated (CNG)
- Hyperpolarization-activated cyclic nucleotide-modulated (HCN)
- Transient receptor potential (TRP)

Recent studies in structural modelling have found that ryanodine receptors 1 (RyR1) hold structure similarities to  $K_{Ca}$  channel. The region of similarity has been identified as important in gating the  $K_{Ca}$  channel and thus could also be important in gating RyR1. Therefore, the ryanodine receptor family could be added into to superfamily as there share structure features (Efremov et al 2015).

The inwardly rectifying potassium channel ( $K_{ir}$ ) is the simplest structure compared the channels above. The channel is formed from four subunits that consist of only two transmembrane segments (TM1 and TM2) which corresponds to the pore forming segments of  $Na_v$ ,  $Ca_v$ , and  $K_v$  channels (S5 and S6). Two pore potassium channel ( $K_{2P}$ ) are formed from two  $K_{ir}$  that are linked together (Yu et al 2005).

## 1.2 Evolution of ion channels

In  $K_v$  channels, the subunits are separate proteins and consists of 6TM and forms a tetramer of four protein subunits.  $K_v$  channels are thought to have evolved by the addition of the voltage-sensing region (S1 – S4) from a basic protein structure which consists of two transmembrane (2TM) segments that is connected by a pore forming loop (Jiang et al 2003). Ligand-gated channels such as calcium-activated potassium channels ( $K_{Ca}$ ), cyclic nucleotide-gated (CNG) channels and hyperpolarization-activated cyclic nucleotide-gated (HCN) channels are 6TM domain proteins that also assembles into a tetrameric structure and holds a pore-forming region which is made up of four highly similar domains (Mocydowski and Latorre 1983). There are also combinations of voltage-gating regions and pore forming modulates such as two 2TM pore modulates ( $K_{2P}$ ), which forms a dimer with two subunits (Lesage et al 1996a). However, it must be noted that in  $K_v$  channels each domain is a separate protein, whereas  $Na_v$  and  $Ca_v$  channels hold a pore-forming single protein which makes up the four domains. This evidence shows strongly that  $Na_v$  and  $Ca_v$  is evolved from  $K_v$  channels. It must also be noted that domains I and III in  $Na_v$  are more similar to one another compared to domains II and IV (Strong, Chandy and Gutman 1993). A further look at channel expression in lower eukaryotes show that most protozoans use  $Ca^{2+}$  as the inward charge carrier. Purely  $Na^+$  dependent action potentials are not found until early metazoans. Therefore, it is thought that  $Na_v$  channels evolved as a result of gene duplication of ancestral  $Ca_v$  channel, as the four domains of  $Na_v$  are more similar to the corresponding  $Ca_v$  domains than to each other. There is low similarity when compared to  $K_v$  channel (Hille 1984). This would suggest that the four-domain precursor protein leads to the formation of  $Na^+$  and  $Ca^{2+}$  channels and came about through two round gene duplication of the single-domain 6TM channel. The initially formation of these channels are believed to have started when a single domain of a two-domain protein results in the formation of the four-domain channel (Anderson and Greenberg 2001). The evidence would suggest that there is a common evolutionary pathway from a 2TM ancestor like the bacterial  $KcsA$  or  $K_{ir}$  channel despite the ion selectivity and gating differences. Many bacteria have 2TM potassium

channels similar to  $K_{ir}$ . Bacteria also express 6TM voltage-gated potassium channels (Booth, Edwards and Miller 2003).

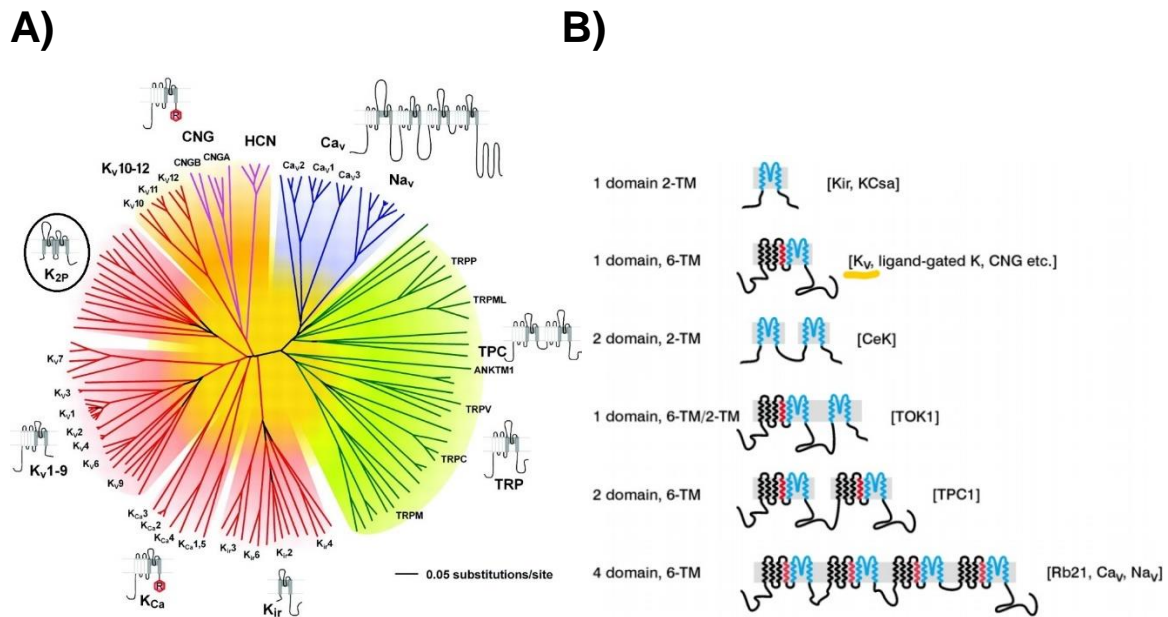


**Figure 1.1:** A) Representation of the 143 members in seven ion channel families (adapted from Yu et al 2005, Anderson) B) Evolution of the voltage gated ion channel superfamily (adapted from Greenberg 2001).

Evolution of ion channels have led to additional intracellular regulatory domains which are used in ligand binding and 4TM domain induced voltage-dependent gating. This allows for the ability to assemble information from different sources to control cell physiology and more complex processes such as learning, memory and muscle movements. This link to these important functions makes them targets for current therapy and could be used in the development of novel therapeutic agents (Yu et al 2005).

## 1.3 Ion channel nomenclature

Ion channel improved resolution of structures has been a great influence on understanding the structural basis of how an ion channel functions and it has been shown that many ion channels share a similar structure as they are thought to have evolved from a mutual ancestor. Cl channels, aquaporins and connexins on the other hand differ from this common structure and therefore evolved independently (Alexander, Mathie and Peters 2011).

### 1.3.1 Potassium channels

Potassium channels contribute to the frequency and the shape of the action potential and are central regulators of excitability. The different channels are grouped into families depending on their structure and function. The three main families grouping (2TM, 4TM and 6TM) is dependent on the transmembrane (TM) numbers (Alexander, Mathie and Peters 2011).

#### 1.3.1.1 The 2TM family

The 2TM family is characterised as the inward-rectifier K channel family. The family is grouped into seven subfamily;  $K_{IR1.x}$  –  $K_{IR7.x}$ . The  $\alpha$  subunit found at the pore can form tetramers and heteromeric channels within the subfamilies for example  $K_{IR3.2}$  can bind with  $K_{IR3.3}$ . These channels are strongly inward-rectifiers with  $K_{IR3.x}$  being a G protein-activated inward-rectifier and  $K_{IR6.x}$  is ATP-sensitive (Snyders 1999).

| Subfamily   | Channels                   |
|-------------|----------------------------|
| $K_{IR1.x}$ | $K_{IR1.1}$ (ROMK1)        |
| $K_{IR2.x}$ | $K_{IR2.1- 2.4}$ (IRK1-4)  |
| $K_{IR3.x}$ | $K_{IR3.1- 3.4}$ (GIRK1-4) |
| $K_{IR4.x}$ | $K_{IR4.1- 4.1}$           |
| $K_{IR5.x}$ | $K_{IR5.1}$                |
| $K_{IR6.x}$ | $K_{IR6.1- 6.2}$ (KATP)    |
| $K_{IR7.x}$ | $K_{IR7.1}$                |

**Table 1.1:** *The 2TM potassium ion channel subfamily*

### 1.3.1.2 The 6TM family

The 6TM family contains the voltage-gated K<sub>v</sub> subfamilies (K<sub>v</sub>1.x-K<sub>v</sub>12.x). The K<sub>v</sub> subfamily can then be divided again into subtypes based on what the channels are related to. Four sequence-related potassium channels genes – shaker, shaw, shab and shal- were first identified in *Drosophila*. The homologs genes have been found in humans. This gene encodes a member of the potassium channel- voltage-gated, shaker-related subfamily. The member this subfamily is made up of 6TM and shows delayed rectification. The members of this subfamily will allow for repolarisation of nerve cells following the action potential. The channels also play a role in T-cell proliferation and activation (Jiménez-Pérez et al 2016; Roberds and Tamkun 1991).

| Subfamily               | Type   |
|-------------------------|--|
| Kv1.1-Kv1.8:            | Shaker-related   |
| Kv2.1-2.2:              | Shab-related   |
| Kv3.1-3.4               | Shal-related   |
| Kv4.1-4.3:              | Shaw-related   |
| Kv7.x:                  | KCNQ   |
| Kv10.x, Kv11.x, Kv12.x: | EAG which include hERG channel   |
| KCa 2.x, KCa3.x:        | Ca <sup>2+</sup> activated SK subfamily                                      |
| KCa1.x, KCa4.x, KCa5.x: | Ca <sup>2+</sup> -activated Slo subfamily which is actually comprised of 7TM |

**Table 1.2:** *The 6TM potassium ion channel subfamily*

### 1.3.1.3 The 4TM family

The 4TM family is referred to as the two-pore domain ( $K_{2P}$ ) family as the pore-forming  $\alpha$  subunit contains two pore domains and is therefore thought to form dimers instead of tetramers which are more usually seen in potassium channels. This family is grouped into six subfamilies based on structure and functional properties (Ketchum et al 1995).

| Subfamily  | Channels        |                 |                 |
|--|-----------------|-----------------|-----------------|
| TWIK: Tandem of P-domains in a Weakly Inward rectifying K <sup>+</sup> channel | K2P1.1 (TWIK1)  | K2P6.1 (TWIK2)  | K2P7.1 (KNCK7)  |
| TREK: TWIK-related K <sup>+</sup> channel                                      | K2P2.1 (TREK1)  | K2P10.1 (TREK2) | K2P4.1 (TRAAK)  |
| TASK: TWIK-related acid sensitive K <sup>+</sup> channels                      | K2P3.1 (TASK1)  | K2P9.1 (TASK3)  | K2P15.1 (TASK5) |
| TALK: TWIK-related alkaline activated K <sup>+</sup> channel                   | K2P16.1 (TALK1) | K2P5.1 (TASK2)  | K2P17.1 (TASK4) |
| THIK: tandem pore domain halothane inhibited K <sup>+</sup> channel            | K2P13.1 (THIK1) | K2P12.1 (THIK2) |                 |
| TRESK: TWIK-related spinal cord K <sup>+</sup> channel                         | K2P18.1 (TRESK) |                 |                 |

**Table 1.3:** *The 4TM potassium ion channel subfamily*

### 1.3.1.3.1 Classification of K<sub>2P</sub> channels

Table 1.3.1 shows each individual K<sub>2P</sub> channel, including six subfamilies, and a summary of their key properties.

| Name                                 | Activators  |   |  | Inhibitors  |  | Remarkable features  | Interacting partners                 |
|--------------------------------------|---|---|--|---|--|--|--------------------------------------|
| <b>TWIK1</b><br>K <sub>2P</sub> 1.1  | Gi-coupled receptors-mediated trafficking to the cell membrane. |   |  | Acid pH <sub>i</sub><br>Protein kinase C                |  | Dynamic ion selectivity<br>Heterodimerization with K2P<br>Weak inward rectification  | EFA6/ ARF6 <sub>GDP</sub>            |
| <b>TWIK2</b><br>K <sub>2P</sub> 6.1  |   |   |  |   |  | Slow inactivation  |                                      |
| <b>KCNK7</b><br>K <sub>2P</sub> 7.1  |   |   |  |   |  | No current   |                                      |
| <b>TREK1</b><br>K <sub>2P</sub> 2.1  | Gβγ<br>NO<br>Copper<br>Substituted<br>caffeate<br>esters        | Acid pH <sub>i</sub><br>Volatile<br>anesthetics<br>ML67-33<br>Halothane | Stretch<br>PUFA<br>(Arachidonic<br>acid)<br>Lysophospholipid<br>Heat<br>Riluzole | Zinc<br>Acid pH <sub>o</sub><br>Fluoxetine<br>Spadin    | G <sub>s</sub> -coupled<br>protein<br>G <sub>q</sub> -coupled<br>protein | Multiple unitary conductances with<br>alternative transcription initiation<br>Heterodimerization within the TREK<br>family | AKAP150<br>Mtap2<br>Phospholipase D2 |
| <b>TREK2</b><br>K <sub>2P</sub> 10.1 | Acid pH <sub>o</sub><br>G <sub>i</sub>                          |   |  | Alkaline pH <sub>o</sub><br>Fluoxetine<br>Ruthenium Red |  |  |                                      |
| <b>TRAAK</b><br>K <sub>2P</sub> 4.1  | Alkaline pH <sub>i</sub>  |   |  | Acidic pH <sub>i</sub><br>Ruthenium Red                 |  |  |                                      |

|                                      |   |                                   |                                     |  |   |                                   |                                  |                 |
|--------------------------------------|---|-----------------------------------|-------------------------------------|--|---|-----------------------------------|----------------------------------|-----------------|
| <b>TASK1</b><br>K <sub>2p</sub> 3.1  | Alkaline pH <sub>o</sub>  | Volatile anesthetics<br>Halothane | Hypoxia                             | Acid pH <sub>o</sub><br>G <sub>q</sub> coupled protein<br>Sanshool | Heteromerization TASK1/TASK3<br>Dynamic ion selectivity<br>Slow time-dependent activation |                                   | P11<br>Syntaxin-8                | 14-3-3<br>Cop-1 |
| <b>TASK3</b><br>K <sub>2p</sub> 9.1  |   | Alkaline pH <sub>o</sub>          | Copper<br>Zinc<br>Ruthenium Red     |  |   |                                   |                                  |                 |
| <b>TASK5</b><br>K <sub>2p</sub> 15.1 |   |                                   |                                     |  | No measurable current   |                                   |                                  |                 |
| <b>TASK2</b><br>K <sub>2p</sub> 5.1  | Alkaline pH <sub>i</sub>  | Alkaline pH <sub>o</sub>          | Gβγ                                 |  | Slow time-dependent activation  |                                   |                                  |                 |
| <b>TALK1</b><br>K <sub>2p</sub> 16.1 | NO<br>Reactive oxygen species   |                                   |                                     |  |   |                                   |                                  |                 |
| <b>TALK2</b><br>K <sub>2p</sub> 17.1 |   |                                   |                                     |  |   |                                   |                                  |                 |
| <b>THIK1</b><br>K <sub>2p</sub> 13.1 | PUFA (arachidonic acid)   |                                   | Hypoxia                             | Halothane  | No change with pH   | Heterodimerisation<br>THIK1/THIK2 |                                  |                 |
| <b>THIK2</b><br>K <sub>2p</sub> 12.1 |   |                                   |                                     |  | ER retention  |                                   |                                  |                 |
| <b>TRESK</b><br>K <sub>2p</sub> 18.1 | Volatile anesthetics<br>Calcium<br>G <sub>q</sub><br>Protein kinase C |                                   | PUFA (arachidonic acid)<br>Sanshool |  | Asymmetrical gating<br>No change with pH  |                                   | 14-3-3<br>Calcineurin<br>Tubulin |                 |

**Table 1.3.1:** Natural and chemical effectors of K<sub>2P</sub> channels including salient features and interacting partners. PUFA, polyunsaturated fatty acid; LP, lysophospholipid; ER, endoplasmic reticulum; COP-I, coat protein 1; AKAP-150, A-kinase anchoring protein 150; Mtap2, microtubule-associated protein; NO, Nitric oxide (adapted from Feliciangeli et al 2011)

### 1.3.2 Sodium channels

Sodium channels are voltage gated and have one pore-forming  $\alpha$  subunit. Sodium channels contain four domains (I-IV) which has six transmembrane segments (S1-S6) and a pore forming loop. The S4 is positively charged and therefore acts as the voltage sensor for voltage gating. Voltage-gated sodium channels are important in the generation of the action potential as when the channels open, this will shift the membrane potential to a more positive value and will depolarise the cell. An important feature for these sodium channels is the carry out rapid voltage activation and inactivation of the channel. Inactivation of the channel involves closing the channel and preventing it from reopening until full recovery, which is important for the action potential (Armstrong 1973). The inactivation state has also been found to hold some clinically useful benefits as local anaesthetics and antiarrhythmic drugs will bind to the channel and stabilise the channel in the inactivated state. The subfamilies are characterised by their inactivation rate.

| Subfamily      | Function                                   |
|----------------|--|
| Nav1.1-Nav1.7  | Fast inactivation (between 0.5 ms – 1 ms). |
| Nav1.8-Nav1.9: | Slow inactivation (between 6 ms – 16 ms).  |

**Table 1.4:** *The voltage-gated sodium ion channel subfamily and function*

Fast inactivation works as a “ball-and-chain” mechanism where portion of the cytoplasmic region blocks the pore by binding to a docking region. During sustained membrane depolarization, the channel will further inactivate to a non-conducting state which is referred to as slow inactivation. Slow inactivation of the channel involves a conformational change in the structure of the sodium channel (Goldin 2003). A functional difference that is used to characterise the channels is its sensitivity to tetrodotoxin (TTX) as Nav1.5, and the slow inactivated Nav1.8 and Nav1.9 are less responsive to TTX compared to the other channels (Sangameswaran L et al 1996).

Another type of sodium channel is the sodium leak, non-selective channel which has a similar structure to the voltage-gated sodium channel family. However, it differs from the voltage gated sodium channels as Nav2.1 is unresponsive to voltage and is also insensitive to TTX (Ren 2011).

### 1.3.3 Calcium channels

Calcium ( $\text{Ca}^{2+}$ ) channels are voltage-gated ion channels that are located in the membrane of many excitable cells.  $\text{Ca}^{2+}$  channels form hetero-oligomeric complexes and contain pore-forming  $\alpha 1$  subunit which offers extracellular binding site(s). A  $\alpha 1$  subunit contains of four domains (I-IV) with each comprising of six transmembrane segments (S1-S6) and a pore-forming region between S5 and S6. The S4 segment is positivity charge and is therefore thought to be associated with gating. The 10  $\alpha 1$  subunits and characterised into three families (Simms and Zamponi 2014).

| Subfamily | Function  |
|-----------|---|
| Cav1.x    | L-type: High voltage activated dihydropyridine-sensitive family |
| Cav2.x    | High voltage activated dihydropyridine-insensitive family       |
| Cav3.x    | T-type: Low-voltage activated                                   |

**Table 1.5:** *The voltage-gated calcium ion channel subfamily and function*

### 1.3.4 Chloride channels

Chloride channels are anion selective channels which are involved in the regulation of excitability of neurons, skeletal, cardiac and smooth muscle cells. They are also involved in salt transport, inter- and extracellular acidification, cell cycle regulation and volume regulation. GABA<sub>A</sub> and glycine receptors are characterised as chloride channels but is gated by neurotransmitters. The voltage-sensitive ClC-1 and ClC-2 are found in the plasma membrane. ClC-Ka and ClC-Kb channels are also found in the plasma membrane and the other members of the ClC family are localised intracellular. Other chloride channels included the CFTR which are cAMP regulated found in the epithelial cell membrane and is involved in fluid transport. Chloride channels activated by intracellular calcium (CaCC) are expressed in excitable and non-excitable cells (Dutzler et al 2002).

### 1.3.5 Hyperpolarization – activated, cyclic nucleotide gated (HCN) channels

The hyperpolarisation-activated, cyclic nucleotide-gated (HCN) are cation channels which are both permeable to sodium and potassium. The HCN channel family are comprised of 4 members (HCN 1-4), which are expressed in the heart and the nervous system. These

channels are involved in setting the equilibrium potential of sodium, which shifts the resting potential of the whole cell more positive to that of the reversal potential of the potassium channel. These channels are activated by hyperpolarisation at -50mV and more negative voltages. To activate the channel, the cyclic nucleotides cAMP and cGMP act directly on the channel which causes the activation curve to shift to more positive voltages. The members are separated by their speed in activated (DiFrancesco 1993).

### 1.3.6 Transient receptor potential (TRP) cation channels

TRP contains six transmembrane domains which are used to form homo- or hetero-tetramers to form cation selective channels. TRP channels are widely distributed in different tissues and cell types. Activated TRP channels are involved in depolarisation of the cellular membrane. This will activate voltage-dependent ion channels, which will change the intracellular concentration of calcium. This is important for the function of intracellular organelles for example endosomes and lysosomes. The TRP superfamily is classified into six subfamilies (Nilius and Owsianik 2011).

| Subfamily | Acronym    |
|-----------|------------|
| TRPC      | Canonical  |
| TRPV      | Vanilloid  |
| TRPM      | Melastatin |
| TRPP      | Polycystin |
| TRPML     | Mucolipin  |
| TRPA      | Ankyrin    |
| TRPN      | NOMPC-like |

**Table 1.6:** *The TRP ion channel subfamily names and what they stand for.*

### 1.3.7 Other ion channels

There are many other ion channels for example; the epithelial sodium channels (ENaC) are responsible for sodium reabsorption in the distal part of the nephron and the collecting duct of the kidney. Cyclic nucleotide-gated (CNG) are responsible for signalling in the primary sensory cells of the vertebrate. Aquaporins and aquaglyceroporins are membrane channels which allow the permeation of water. Acid-sensing ion channels (ASICs) are members of the

sodium channel superfamily and form proton-gated, voltage-insensitive sodium permeable channels. CatSper channels are voltage-gated calcium permeant channels and there are four members of this family (CatSper 1-4) (Alexander, Mathie and Peters 2011).

## **1.4 Membrane potentials**

In cells, there is an electrical potential difference between the intracellular compartment and the surrounding external environment. Transported substances in cells will carry a net charge. The movement will be influenced by its concentration gradient and the membrane potential, the electric potential (voltage) across the membrane. These two forces combined is called the electrochemical gradient and will establish the energetically favourable direction of charged molecules across the membrane. The electric potential that is seen across most membrane is caused by a small imbalance in the concentration of positively and negatively charged ions on the two sides of the membranes. This separation of charge between the two locations is measured in units of volts. Neurons can conduct, transmit, and receive electric signals. This characteristic is a result of specific ion channels in the neuron plasma membrane. Therefore, ion channels are essential for normal functioning of neurons (Lodish et al 2000).

### **1.4.1 Neuronal Signalling**

The central nervous system (CNS) is composed of different cell types; including many different neurons, astrocytes, microglia and oligodendrocytes. Neurons are used to process information entering the CNS. Neurons have the ability to communicate information over great distances by propagating a transient electrical signal across their axonal membranes (Lodish et al 2000). This electrical signal (action potential) will reach the presynaptic membrane, connected to the dendrite, and will trigger the release of neurotransmitters across the chemical synapses. The action potential will drive the  $\text{Ca}^{2+}$  ions influx via voltage-gated calcium ion channels along the presynaptic membrane. Another mechanism of calcium concentration increase is through the release of  $\text{Ca}^{2+}$  from intracellular stores (Eilers, Plant and Konnerth 1996). The calcium will then bind to synaptotagmin which is found on the membrane of the synaptic vesicles. This newly formed protein will bind with SNAREs which will induce vesicle fusion with the presynaptic membrane. This will therefore trigger the neurotransmitter glutamate in synaptic vesicles to be released and diffuse across the synaptic cleft. Glutamate will bind to a specific transmembrane receptor called the N-methyl-D-aspartate (NMDA). Neurotransmitters can affect the postsynaptic cell by initiating an excitatory postsynaptic potential (EPSP) and therefore influencing the likelihood of the firing

of an action potential by depolarizing towards threshold. When the neurotransmitter binds to the postsynaptic receptor, this will induce EPSP activity (Purves et al 2001).

Signalling is necessary for neural function and is regulated by a flow of ions through ion channels. Binding of the neurotransmitter triggers changes in the ion permeability of the postsynaptic plasma membrane which changes the electric potential of the membrane (Lodish et al 2000).

## 1.5 The resting membrane potential and the estimation of membrane potential

The concentration of  $K^+$  ions is greater intracellularly than extracellularly, whereas it is the opposite for  $Na^+$  and  $Cl^-$  ions.

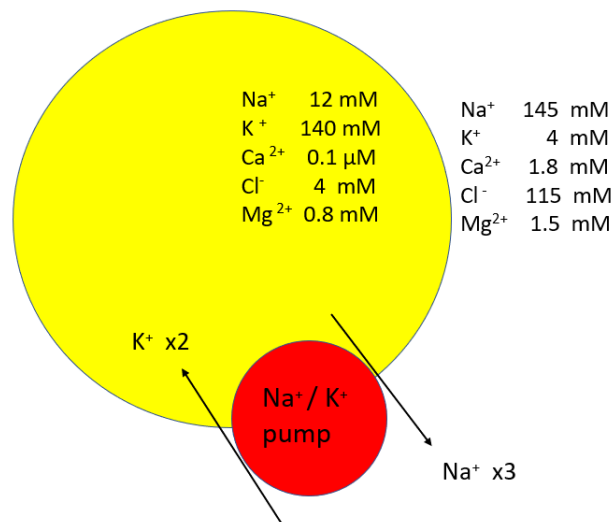


**Figure 1.2:** *The unequal distribution of ions found at the resting membrane potential*

The different ion concentration is sustained by ATP-dependent pumps, mostly notably the  $Na^+/K^+$  pump. The pump transports three  $Na^+$  ions out of the cell, and two  $K^+$  ions into the cell (Barnett and Larkman 2007).

The plasma membrane also contains open “resting” or “leaky”  $K_{2P}$  channels which are ion specific. The resting potential is therefore determined by the selective permeability of these  $K_{2P}$  channels and the movement of  $K^+$  ions. This movement of  $K^+$  across the membrane causes an excess of negative charge to be left behind. If  $K^+$  ions were the only movement of ions than the resting membrane potential would be the exact value of potassium equilibrium ( $E_k$ ) which is around -90mV. A key determinant of the membrane resting potential has been linked to  $K_{2P}$  channels. The increased potassium permeability imparted by leak  $K^+$  currents

through  $K_{2P}$  channel causes an increase  $K^+$  conductance and stabilizes cells at the hyperpolarised resting membrane potential (RMP) (MacKenzie, Franks and Brickley 2015).

The Nernst equation calculates the potential for a single permeable ion.

$$E_{ion} = \frac{RT}{zF} \ln \frac{\{ion\}_o}{\{ion\}_i}$$

**Figure 1.3:** Nernst equation.  $E_{ion}$ : equilibrium potential,  $R$ : universal gas constant,  $T$ : temperature (K),  $z$ : charge of the ion,  $F$ : Faraday constant,  $(ion)_o$ : the extracellular ion concentration,  $(ion)_i$ : the intracellular ion concentration (Copper 2012).

However, in reality, the resting membrane potential is less than  $E_K$  (between -50mV and -80mV) as  $Na^+$  ions contribute to the value. The main source for setting the resting membrane potential is  $K^+$  so the  $E_K$  is closer to the resting potential in comparison to  $E_{Na}$  (+65mV) (Purves, Augustine, Fitzpatrick, et al 2001).  $E_{Cl}$  has a similar potential to  $E_K$  however there are only a few  $Cl^-$  channels open and therefore could not contribute to the resting membrane potential in a significant way (Lodish et al 2000).

The Goldman-Hodgkin-Katz equation is used to estimate the membrane potential using the net flow of all the ions across the membrane. It is the same concept as the Nernst equation as it takes into account the charges of the ion. However, it also looks at the relative permeability of the membrane of each of the different ion channels (Copper 2012)

$$V_m = \frac{RT}{F} \ln \left( \frac{p_K [K^+]_o + p_{Na} [Na^+]_o + p_{Cl} [Cl^-]_i}{p_K [K^+]_i + p_{Na} [Na^+]_i + p_{Cl} [Cl^-]_o} \right)$$

**Figure 1.4:** Goldman-Hodgkin-Katz equation.  $V_m$ : membrane potential,  $R$ : gas constant,  $T$ : temperature (K),  $F$ : Faraday constant,  $(ion)_i$ : the intracellular ion concentration,  $(ion)_{out}$ : the extracellular ion concentration,  $P_{ion}$ : ion permeability (Copper 2012).

### 1.5.1 The action potential

The action potential begins with the opening of voltage-gated  $Na^+$  channels. This movement of high external  $Na^+$  ions diffuses down the concentration gradient into the neuron. The external  $Na^+$  ions will also diffuse down the electrochemical gradient as the  $Na^+$  ions are attracted to the negative internal charge of the neuron. The  $Na^+$  ions carry a net positive electrical charge and will allow the neuron the approach  $E_{Na}$  (the peak of action potential)

while leaving an excess of negative ions outside the membrane face. The movement is known as depolarization. If depolarization reaches threshold it will lead to an action potential. The shift of charge is represented as a spike on an action potential trace (Barnett and Larkman 2007).

As the membrane voltage increases, most gates in the voltage-sensitive  $\text{Na}^+$  channels will open. However, this increase will also close the channels inactivation gate at a slower rate. Therefore, when membrane voltage is raised suddenly, the  $\text{Na}^+$  channels open initially but due to the slower inactivation gate will close. This will lower the membranes permeability to  $\text{Na}^+$  which will drive the membrane voltage towards the negative voltage. The net movement of  $\text{Na}^+$  ions into the neuron will cease also because the concentration gradient is balanced by  $E_{\text{Na}}$  found inside the neuron.

The newly developed positive voltage of the neuron will cause voltage sensitive  $\text{K}^+$  channels to open. This efflux of  $\text{K}^+$  ions will drive the membrane voltage towards  $E_{\text{K}}$  as the membrane permeability changes between  $\text{Na}^+$  to  $\text{K}^+$  ions and repolarisation of the neuron will take place. The outward movement of  $\text{K}^+$  begins the progression toward resting membrane potential (Lodish, et al 2000).

The next stage is hyperpolarisation as the neurons slowly recover from the overshoot of the resting potential. The membrane becomes excessively negative and undershoots the resting potential (-70mV) (Barnett and Larkman 2007). The  $\text{K}^+$  channels remain open because of the influx of calcium during the action potential (Copper 2012). The  $\text{K}^+$  channels do not inactivate and thus the  $\text{K}^+$  ion movement is ceased by the closure of the activation gate. This closure of the gate however is slow and means the channel remains open for a longer phase and results in the described overshoot which generates this after-hyperpolarisation step (Barnett and Larkman 2007).

Each action potential is then followed by a refractory period which involves two stages; an absolute refractory period which cannot evoke an action potential and the relative refractory period which can induce an action potential but requires a very strong stimulus. The absolute refractory period is caused by the inactivation of the  $\text{Na}^+$  channels and the channel cannot be opened again (Copper 2012). When the  $\text{Na}^+$  channels reach back to its resting state and several voltage-gated  $\text{K}^+$  channels remain open, it makes it very difficult to stimulate a new action potential. This is known as relative refractory period. There are a number of class 1B antiarrhythmics for example lidocaine and phenytoin which are known to block sodium voltage-gated channels which may underly the therapeutic potential as it decreases

excitability of abnormally firing cells. In addition to this, these compounds will accelerate cellular repolarization by increasing potassium efflux and also decrease the duration of the action potential and the refractory period (Catterall 1987). Lidocaine is also a local anesthetic which is used in neuropathic pain conditions but also in acute and chronic pain (Golzarı et al 2014; Kosharskyy et al 2013). When all the voltage gated  $K^+$  channels are closed and the “leaky”  $K_{2P}$  channels are all open, the membrane potential begins to stabilize and return to the resting membrane potential, below the firing threshold. Therefore,  $K_{2P}$  channels are important in influencing the level of stimulation needed to initiate the action potential and regulates the shape, frequency, and magnitude of each spike (Plant 2012). Subsequent action potentials can now be fired. When an action potential is fired, its signal is carried along the axon until it reaches the axon terminal. This signal is continued to the next neuron via neurotransmission (Copper 2012).

## 1.6 The pore structure of Kcsa

The structure of Kcsa was the first structure that revealed the pore structure of a  $K^+$  channel. The three-dimensional structure of Kcsa showed a two trans-membrane (2TM) bacterial potassium channel. The channel shows a conical shape where four subunits surround the central ion pathway. The M1 and M2 segments are arranged around the pore. The pore is characterized by four short loops which contain the signature sequence of the  $K^+$  channel. The intracellular side of the channel is comprised of four inner helices that would pack against each other to form the helix bundle crossing. Thus, the Kcsa is thought to have been solved in the closed configuration (Doyle et al 1998). In the inwardly-rectifying potassium channel, which is analogous with Kcsa, the TM2 segment after each pore loop will make up the intracellular portion of the ion cavity pathway. These potassium channels are formed as tetramers with one pore loop in each subunit however  $K_{2P}$  channels consists of two pore loops in a single subunit. Therefore, four pore loops from two subunits comprises  $K_{2P}$  channels, which is how the name two-pore domain potassium channel was assigned. M1 and M3 are the outer helices of the P domain 1 and 2 and M2 and M4 are the inner helices of P domain 1 and 2 (Kollewe et al 2009). The pore structure of Kcsa is also shared with the cyclic nucleotide-regulated channel (MlotiK), voltage-gated  $Na^+$  channel from *Arcobacter butzleri* (NavAB), voltage gated sodium channel and the NaK.

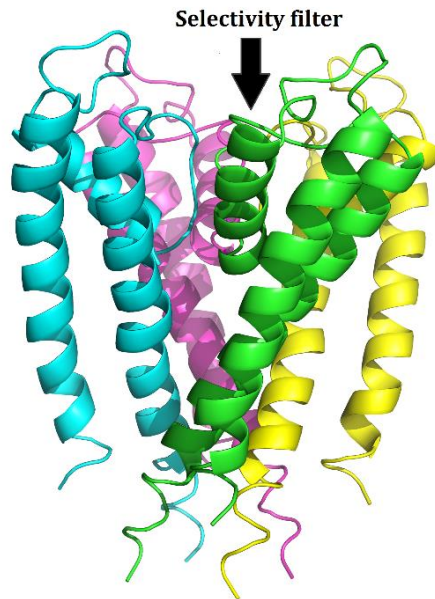


**Figure 1.5:** *Ribbon representation of the KcsA K<sup>+</sup> channel (1BL8) with four subunits coloured differently. The channel is oriented with the extracellular solution on top.*

## 1.7 The selectivity filter in potassium channels

Potassium channels are characterized by a common selectivity filter. The sequence of the K channel selectivity filter is a salient feature of K<sub>2P</sub> channel which indicates identical properties of the channels. The highly conserved K<sup>+</sup> channel signature sequence is XTTXGXG is important in the diffusion of potassium ions.

Potassium ions are hydrated in the central cavity and then dehydrated at the selectivity filter. The K<sup>+</sup> ions are then rehydrated in the extracellular entryway of the channel. The binding sites for ions inside the selectivity filter are comprised of eight oxygen atoms in the extracellular entry of KcsA K<sup>+</sup> channel. These sites, when not bond to potassium ion, are occupied by water molecules. In the K<sup>+</sup> selectivity filter, four binding sites of oxygen atoms are seen and therefore the sequence of binding goes between two configurations; where K<sup>+</sup> bind at position 1 and 3 (K<sup>+</sup>-water-K<sup>+</sup>-water) and position 2 and 4 (water-K<sup>+</sup>-water-K<sup>+</sup>).

There is also a concentration-dependent path where a third ion enters the selectivity filter and another ion exits from the other end. Conformational change in the channel is caused by different concentrations of ions. The main differences come down to changes in the shape of the selectivity filter with the remainder of the channel unchanged. In the low-potassium structure it is seen that G77 faces into the pore and could therefore block the pathway after the alpha carbon twists the residue. The twisting also gives the filter an hourglass shape. This low concentration of potassium ions causes the channel to become non-conducting as the selectivity filter is pinched shut. In high concentration of potassium ion, the channel is ion

conducting as the residue G77 is identified as providing two binding sites for two  $K^+$  ions. (Zhou and MacKinnon 2003). The channel is only conducting once the filter is straight, which is seen in high  $K^+$  structure. The high conductance of potassium ions and binding to the selectivity filter are examined by electrostatic repulsions between the ions. Two ions in the filter would stop the cavity from collapsing and would also repulse one of the ions out of the channel. This will cause tension in this two ion conformation and will lead to a decrease in affinity for  $K^+$  ions (MacKinnon 2004).

The ion-dependent conformation change is believed to switch in accordance to a timescale of gating (milliseconds) rather than ion conduction (nanoseconds). It should also be noted that the activation gate is important in identifying the ion concentration as the activation gate is found in between the selectivity filter and the cytoplasm. The position allows the activation gate to open the filter to sense the concentration of potassium ions (Zhou et al 2001).

### **1.7.1 Ion permeability of potassium and sodium channels**

In molecular dynamic simulations of the bacterial potassium channel (Kcsa), differences between the interactions of the selectivity filter and the ions potassium and sodium are shown. It was identified that  $K^+$  ions and water molecules bind within the filter and translocate between adjacent sites on a nanosecond timescale, while in contrast  $Na^+$  ions are bound in a more fixed matter to their sites within the filter. The ions also differ in how they like to bind in the channel.  $K^+$  ions are held within a cage of eight oxygen atoms contained in the filter while on the other hand,  $Na^+$  ions bind with the ring of four oxygen atoms (Shrivastava et al 2002). Regarding the sodium channel permeability, there are important conditions that improve  $Na^+$  channels selectivity of  $Na^+$  ions over  $K^+$  ions. The pore preferring  $Na^+$  ions provides three instead of four protein ligands to coordinate the ion. The hydration of  $Na^+$  ions is also less important and the  $Na^+$  ions favour the pore to be relatively rigid, constricted, and solvent exposed. It was also revealed that factors that favour  $Na^+$  ions over  $K^+$  ions in  $Na^+$  channels will cause  $K^+$  channels to prefer  $Na^+$  ions over  $K^+$  ions (Dudev and Lim 2010).

New crystal structure of the prokaryotic sodium channel from *Magnetococcus marinus* (NavMs) shows the pore only containing sodium ions. This structure was able to identify the binding sites of the three  $Na^+$  ions in the centre in the selectivity filter. The selectivity filter of sodium channels contains a highly conserved glutamate region which therefore allows hydrated sodium ions to pass through the pore, unlike  $K^+$  channels. Potassium ions are prevented from passing through the pore as the  $K^+$  ions would need to be desolvated to fit through the NavMs selectivity filter. The crystal structure also showed that NavM channel

has a much wider pore compared to K channels, which allows space for intervening water molecules (Naylor et al 2016).

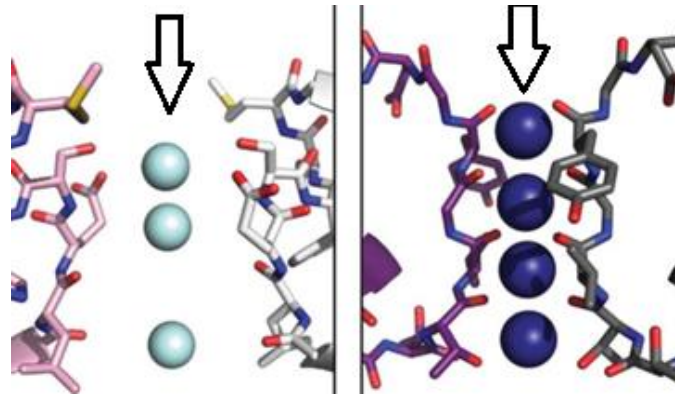


**Figure 1.6:** The ion binding in sodium and potassium channels. Left: sodium ions in the selectivity filter of the NavMs channels. Right: potassium ions in the selectivity filter of Kcsa channel (adapted from Naylor et al 2016).

All this evidence suggests that there are distinctions between sodium and potassium permeability in the respective ion channels. However, some ion channels have shown changes in ion channels selectivity. Evidence emerged that showed that the ion selectivity of TWIK1 changes to conduction of sodium at acidic pH and when the extracellular potassium is lowered (Chatelain et al 2012). Sodium ion selectivity in TREK1 will become TWIK1-like if a mutation is made at the selectivity filter (I267T) that is homogenous to TWIK1. However, BL-1249 will restore the K<sup>+</sup> ion permeability as it's believed to stabilize the selectivity filter (Decher et al 2017).

## 1.8 Two pore domain potassium channels (K<sub>2P</sub>)

### 1.8.1 Discovery of K<sub>2P</sub> channels

The first member of the K<sub>2P</sub> family to be discovered was TOK1 and was cloned from *Saccharomyces cerevisiae*. An important characteristic that was identified was that the channel contained two P domains or pore domain. The signature P domain (XXTTXGXG), as previously described, was used to identify in *S.Cerevisiae* genome and was subsequently translated to the amino acid sequence. The family was therefore predicted to have two pore like domains that consist of these eight residues. This was the first example of an outwardly rectifying potassium ion channel to be involved in the resting membrane potential (Ketchum et al 1995; Lesage et al 1996b). Subsequent studies showed however that K<sub>2P</sub> channels cloned from *Drosophila melanogaster* predicted a four transmembrane segment and was therefore referred to as TWIK- (Tandem of P domains in Weakly Inward Rectifying K<sup>+</sup>) related channels channel (Goldstein et al 1996, Lesage et al 1996a). The human genome contains at least 70 genes that code for potassium ion channels. The unique two pore/ four

transmembrane features have helped in identifying fifteen genes that encode the  $K_{2P}$  channels (Goldstein et al 2005).

## 1.9 Gating of $K_{2P}$ channels

### 1.9.1 C-type inactivation in $K_{2P}$ channels

Voltage-gated potassium (Kv) channels contain an outer pore gate that produces “C-type” inactivation. The conformation changes seen at the gating of  $K_{2P}$  channels shows a resemblance to the external pore C-type inactivation of Kv channels (Cohen, Ben-Abu and Zilberberg 2009). The evidence of this similarity is seen when comparing Kv channels and the two pore KCNKØ channels to their effects to zinc and tetraethylammonium (TEA).

In voltage gated *Shaker-delta*  $K^+$  channel, the C-type gate is controlled at position T449. A cysteine mutation at this location allows for inhibition by zinc and cadmium at a relatively small concentration compared to WT. The ions bind weakly when the channel is in an open state and slows the movement of the channel into the inactivation state. However, there is higher binding affinity when the channel starts in the inactivation state (T449C), which shows that there is a structural change in the external mouth of the pore during inactivation gating (Yellen et al 1994). Zinc is a potent inhibitor of KCNKØ channels and extracellular histidine 29 is required for zinc block. It would therefore appear that this interaction requires structural changes in the external mouth of the pore similar to that of the C-type inactivation gate (Zilberberg, Ilan and Goldstein 2001). Choi, Aldrich and Yellen (1991) showed that external tetraethylammonium (TEA) blocks the slow inactivation of the C-type gate in Kv channels. In relation to this, KCNKØ channels current is also blocked by TEA reducing the single channel conductance.

More similarities are seen as both  $K_{2P}$  channels and Kv channels show C-type inactivation gating in the presence of external permeant ions. In *Shaker-delta* potassium ion channel, a reversibly slowed closure of the inactivation gate was seen in high external potassium solution (López-Barneo et al 1993). This is a similar response to that of KCNKØ channels which showed that in high external potassium there is a high probability of an open state leading to an increase in current (Zilberberg, Ilan and Goldstein 2001).

As mentioned above, the importance of T449 in *Shaker* potassium channel has been connected to the C-type activation gate. The analogous site in  $K_{2P}$  channel is found in the first P loop T112. The mutation of this site (T112Y) allows for stability in the closed state of the channel and alters the C-type gate, as a faster inhibition speed from zinc is seen

(Zilberberg, Ilan and Goldstein 2001). In the attempt to discover more about the inactivation gate, the negatively charged glutamate 418 in *Shaker* channels was identified. This residue, found in most VGK and KCNK subunits, is believed to be involved in the interaction between the S4 movement and the pore in slow inactivation. To examine the role of E418, the *Shaker* channel was compared to the known structure KcsA. This structure suggested potential binding between G452 and V451 in S6 with E418 in S5. Therefore, cysteine mutations were carried out on these sites and E418C was seen to hold disulphide bonds to G452C and V451C. This indicated that the channel was stabilised in the inactivated state. These results suggested that E418 forms hydrogen bonds with the external end of S6 which holds the gate fixed in the open conformation. However, when these bonds are broken after rotations in the channel, it leads to closed inactivation state (Larsson and Elinder 2000). Zilberberg, Ilan and Goldstein (2001) carried out similar experiments on E28 and T115  $K_{2P}$  channels, which are analogous to the *Shaker* sites E418 and G452. Cysteine mutations showed that disulphide bonds could be formed and that these bonds could be broken in a similar fashion to that of the *Shaker* channel. All this evidence taken together confirms that there is indeed a functional upper gate found near the selective filter in  $K_{2P}$  channels and that the transition between open and closed is associated with conformational changes in the extracellular side of the pore (Cohen, Ben-Abu and Zilberberg 2009).

Kv channels have a well-defined method in controlling its opened and closed conformation involving both an upper inactivation gate and a lower activation gate. It was found that the state of the activation gate is connected to the state of the inactivation gate and vice versa. This cross-talk communication is negatively coupled as the opening of one causes the closure of the other. This negative cross-talk is believed to be involved in controlling the activity of the action potential (Panyi, and Deutsch 2006). With  $K_{2P}$  channels containing one similar gate, it was then thought that  $K_{2P}$  channel could have a similar lower gate.

## **1.9.2 Is there a functional activation gate in $K_{2P}$ channels?**

Voltage-gated potassium channels holds a well-defined activation gate. This gate is formed by a four-helix bundle which is located at the intracellular side of the pore on the sixth transmembrane segment (S6) (Tombola et al 2006). When investigating the role of this gate in  $K_{2P}$  channels it was important to note that voltage gating at this time was poorly understood in  $K_{2P}$  channels. A study with quaternary ammonium (QA) showed that there is no gating at the helix bundle crossing. QA has the ability to bind to TREK1 channel pore when it is positioned in its closed and open state. There is also a similar binding affinity in both states. Thus, the bundle is constantly open and is not directly involved in blocking the ion conductance (Piechotta et al 2011). It is also believed that  $K_{2P}$  channels are open over a

wide range of membrane voltage and therefore it was theorised that the mechanism is different to that of Kv channels (Renigunta et al 2015). However, a recent study has shown how  $K_{2P}$  channels operate as a voltage-dependent channel without a conventional voltage-sensor site.

It was found that excluding TWIK1,  $K_{2P}$  channels are dependent on the movement of ions in the channel and creating an electrochemical potential difference. Physiological activation by lipids, membrane stretch and intracellular acidification can switch from voltage dependence to leak mode. It is believed that voltage dependence is caused by three to four ions moving into the selectivity filter. When the channel is in the “ion depleted” state, the channel contains none or one ion in the selectivity filter at negative potentials. Upon depolarisation, there will be a flux of ions into the pore to fully occupy the selectivity filter and allow for the outward rectification of  $K^+$  ions (Schewe et al 2016).

It was originally hypothesised that the inner bundle crossing is important in activation of voltage gating in TASK3 channels (Ashmole et al 2009). The voltage gate activation is weak compared to the Schewe et al (2016) study. Mutating these channels at the pore lining in TM2 and TM4 however can enhance the activity of the voltage gate. The mutations did not affect extracellular acidification inhibition which is known to occur at the selectivity filter, thus suggesting two separate gates (Ashmole et al 2009; Niemeyer et al 2016). Further support was seen in Ben-Abu et al (2009) which showed that in *Shaker* Kv channels in the closed state are intrinsically more stable than the open state. Whereas  $K_{2P}$  channels have a higher open probability compared to the closed state. The difference in preferential states is believed to be directly caused by the activation gate site. In Kv channels the activation gate region is lined with hydrophobic residues termed the “hydrophobic seal” whereas the corresponding activation gate region found in  $K_{2P}$  channels consists of several glycine residues. Mutating these hydrophobic residues with glycine in Kv channels would stabilise the open state and mutating the glycine residues with hydrophobic residues in  $K_{2P}$  channels showed a non-conducting state (Ben-Abu et al 2009).

Ben-Abu et al (2009) also wanted to show the presence of the lower activation gate in  $K_{2P}$  channels and so developed a Kv- $K_{2P}$  chimera channel that contained the first pore domain of  $K_{2P}$  and the voltage sensor end of the Kv channel. This would demonstrate that  $K_{2P}$  channel could close in response to change in voltage by adding the functioning voltage sensor found in the Kv channel. This chimera channel showed its ability to close in a voltage-dependent manner in milliseconds, which is a characteristic of the lower activation gate movements. It must also be noted that the new tetrameric structure of the chimera could influence the

movement of TM2 that could not be seen in the native dimeric structure (Niemeyer et al 2016).

Further evidence seen in a molecular dynamic simulation study on TWIK1 crystal structure showed an interesting mechanism separate from the C-type gating. It was found that the pore lining below the selectivity filter is highly hydrophobic which creates a dewetting area. This region may form an energy barrier which blocks the ion passage with residues L146 and L261 forming the “hydrophobic cuff”. This therefore suggests a hydrophobic gating mechanism for regulating TWIK1 and account for the low functional activity (Aryal, Sansom and Tucker 2015).

### **1.9.3 Importance of C-terminus for gating**

The carboxyl terminal domain of TREK1 is essential for regulatory properties (Honoré 2007). However, mutations at the C-type gate causes a change in activation response linked to the C-terminal of TREK1. Mutagenesis scanning discovered the highly conserved W275S residue on the N-terminal portion of the M4 transmembrane segment of TREK1. This site is also close to the selective filter and the upper C-type gate. The mutation substantially blunted activity by regulatory modulators, such as temperature, which act on the C-terminus. These results therefore supported the idea that these sites close to the selectivity filter are used in regulation even if the action is on the C-terminus. This also shows that the mutation uncouples the sensors used by each stimulus from its gating mechanics. It was seen that the mutation abolished any inhibition of TREK1 through extracellular acidosis. An increase in extracellular potassium concentration would antagonise the inhibition of TREK1 current by external acidosis. However, the mutation TREK1 W275S showed a diminished response and was seen to have failed sensitivity to potassium concentration. Another mutation, F276L, discovered in this study did not show the change in response which shows that residue W275 is important in the gating mechanism. As can be seen there are modulators that act on the C-terminal but cause a reaction from the C-type gate. (Bagriantsev et al 2011). Therefore, how did the signals from the C-terminal effect the C-type gate and open the selective filter?

It was hypothesised that there was clear cross-talk between the lower gate and the upper gate found at the selectivity filter. An important site on TREK1 for this new gating mechanism was identified as G137. The mutation, G137I would halt any inhibition through acidosis and was seen to stabilise the C-type gate. Indeed, both W275S and G137I showed a reduced effect of membrane potential on the channel which may be linked to their close proximity to one another (Bagriantsev, Clark and Minor 2012).

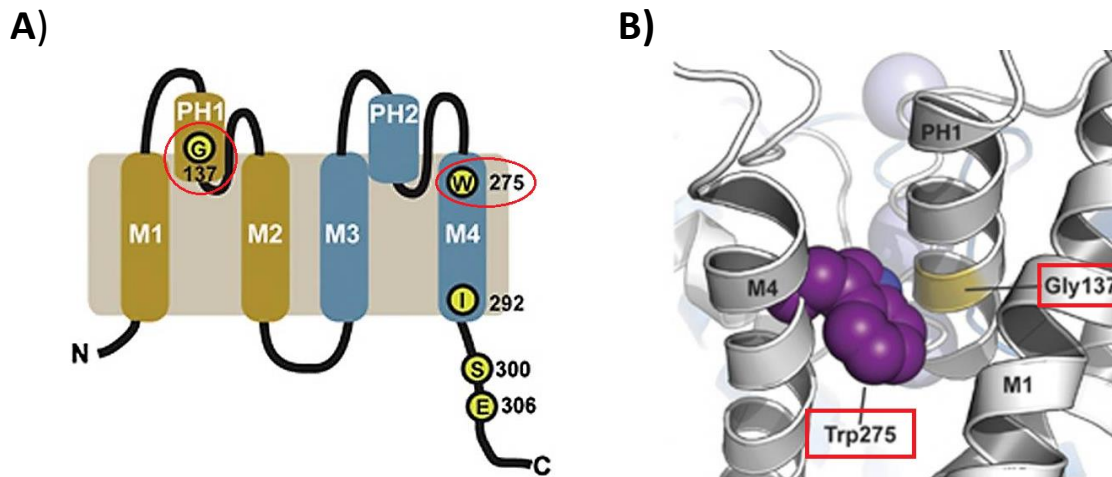


**Figure 1.7:** *TREK1 and C-terminus gating. A) shows important residue sites in relation to cross talk gating and C-terminus gating. B) TREK1 channel, based on TRAAK model, showing the location of W275 and G137 (adapted from Bagriantsev et al 2012).*

To further investigate cross-talk through M4 transduction, M4-Ct region was uncoupled from the intracellular domains which were achieved by mutating I262-G293-D294 to glycine or alanine. The mutation using glycine adds flexibility and alanine removes sidechain interactions. These mutations did in fact eliminate the C-terminus function and kept the channels extracellular acidosis sensitivity. More importantly, both mutations were insensitive to changes in membrane potential whereas the WT did alter. The lack of response is caused by uncoupling of the C tail from the bilayer and not from the C-type gate. Activation caused by increase in temperature is abolished by the triple mutations and therefore is also believed that this stimulus relies on the C terminus binding to the pore as the pore domain has temperature sensors. This shows that a signal moves from the C-terminal through the M4 segment to communicate to the extracellular C-type gate (Maingret et al 2000).

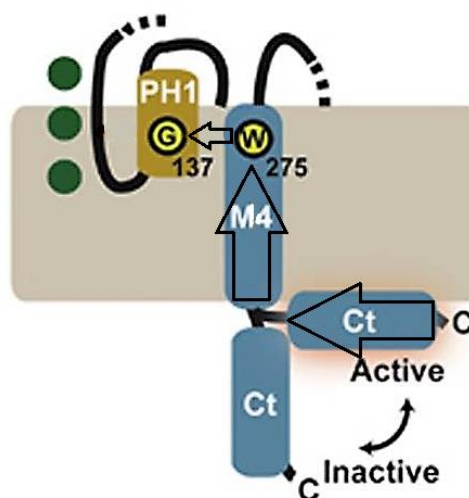


**Figure 1.8:** *Model of coupling gates: Shows the activation and inactive state based on the binding of C terminus and the membrane bilayer (adapted from Bagriantsev et al 2012).*

All this evidence together would strongly suggest that  $K_{2P}$  channels do not have a functional bundle crossing gate or functional activation gate, but that this lower gate is open and is insensitive to stimulation. It is in fact the upper C-type gate found near the selective filter that is the primary gate. This also correlates to the finding from Ben-Abu et al (2009), which reported movement made by the lower gate would affect the state of the C-type gate at the selectivity filter. More recently, evidence supporting a continually open activation gate was found as solved crystal structure of  $K_{2P}$  channels were developed.

### **1.9.4 $K_{2P}$ channel gating structure**

The first proposed gating system of  $K_{2P}$  channels has been extrapolated from crystallographic three-dimensional structures of two bacterial channels, KcsA (Doyle et al 1998) and MthK (Jiang et al 2002). In closed conformation, it is seen that the pore inner helices are straight and point outwards. This will allow a helix bundle to form at the intercellular region of the pore. In the opened conformation, the inner helices will bend at a 'glycine hinge', which causes the cytoplasmic region of the pore to open (Cohen, Ben-Abu and Zilberberg 2009).

However, after the crystal structure for TRAAK and TWIK1 were defined, considerable differences were observed (Brohawn 2015). One of the most interesting differences between the old prospective  $K_{2P}$  model and the new crystal structures of TRAAK and TWIK1 is that the inner helical gate is indeed constantly open. It is seen that when P1 domain of TRAAK is most constricted, it is similar to the most open conformation of MthK ( $\sim 12$  Å). The P1 domain is less open than when it is most restricted ( $\sim 10$  Å), however this is more expressive than the open conformation of Kv channels (Brohawn, Del Mármol and MacKinnon 2012). The TWIK1 cavity is also measured at similar values to that of open state channels ( $\sim 11$  Å) (Fig 1.9) (Miller and Long 2012). Another  $K_{2P}$  channel structure, TREK2 has also be visualised as a crystal structure with norfluoxetine. This channel also has a continually open cytoplasmic gate even in a closed state (Dong et al 2015).

All the structural information together supports the idea that  $K_{2P}$  does not gate at the lower structure and most therefore gate further up the channel.

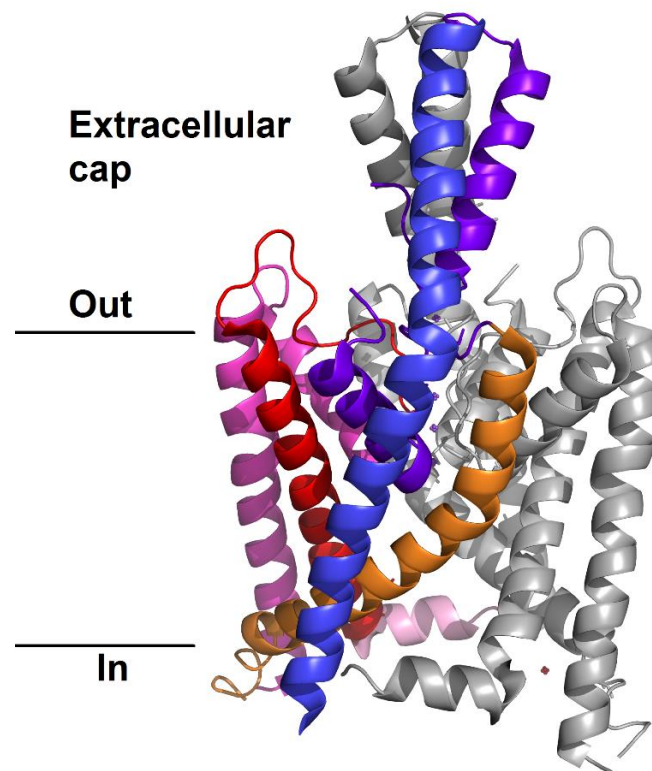


**Figure 1.9:** Structure of  $K_{2P}$  TWIK1 channel (3UKM) with an open inner gate. Subunit A is coloured and Subunit B is grey. TM1 is labelled in blue. TM2 is orange. TM3 is labelled pink and TM4 is labelled red. C helix coloured in light pink.

## 1.10 TREK channels

### 1.10.1 TREK tissue distribution and diversity

TREK1 is widely distributed in the CNS with expression at its highest in the striatal tissue, spinal cord and other areas in the brain for example cortex, hippocampus, hypothalamus, amygdala and the olfactory. To a lesser extent, it is also found in the GI tract (Medhurst et al 2001). TREK2 has similar distribution with less expression found in the brain; however, TREK2 was also seen in peripheral tissues like kidney and pancreas (Bang et al 2000; Medhurst et al 2001). TREK channels are known to form several different isoforms. TREK1 produces two isoforms and TREK2 form three isoforms through alternative translation initiation.  $K_{2P}$  channels are naturally widely expressed in areas which overlap each other channels so it has been widely thought that TREK channels form more heterodimer bonds than previously considered (Honoré 2008).

Heterodimerization is also an important part of channel diversity without increasing the number of genes. Combinations of different properties of the bound channels can change the channel's sensitivity to pharmacological agents. It was once believed that TWIK1, a non-functional channel, can become functional after achieving heterodimer binding with TREK1

(Mi Hwang et al 2014). However, after repeat experiments it was found that no interaction was found between the two channels. It was in fact established that all ATI isoforms of TREK1 and TREK2 can form a heterodimer bond with each other and with the TRAAK channel. TREK1 has a high binding affinity to itself and TREK2; however, it does not bind as efficiently to TRAAK. Heterodimerisation have seen changes in drug sensitivity for these channels. A TREK1 and TRAAK activator ML67, has seen intermediate degree of activation when interacting with the heterodimer TREK1/TRAAK. Changes in sensitivity was also seen in fluoxetine, which is a known TREK1 inhibitor and has no effect on TRAAK. The heterodimer TREK1/TRAAK has a lesser degree of fluoxetine inhibition when compared to TREK1 WT. Therefore, for compounds that are less specific, heterodimerisation has a moderate effect on their action however more targeted compounds could have an increase in their spectrum of effect with heterodimerisation (Levitz et al 2016).

## **1.10.2 Regulation of TREK channels**

### **1.10.2.1 Mechanical stimulation and polyunsaturated fatty acids activation**

TREK1 was the first identified  $K_{2P}$  channel to be regulated by mechanical stress. It was indicated that the shape of the membrane has a direct effect on channel functions. In an inside out patch clamp approach, negative pressure shows a significant effect on opening of TREK1 and TREK2 channels when compared to positive pressure. Therefore, specific changes in cell shape where convex curvature of the membrane allows for the opening of the channel (Patel et al 1998; Bang, Kim and Kim 2000). The mechano sensitivity of TREK1 was found in both cell attached and inside out recordings. TREK1 contains a charged region between D294 and E309 that, when truncated, showed a marked resistance to stretch. Therefore, the C-terminus in TREK1 is believed to be important in mechanoactivation (Patel et al 1998; Maingret et al 1999). The importance of the cytoskeletal network has also been investigated as methods which disrupts actin cytoskeleton (cytochalasin D for example) activates the channel which suggests the cytoskeleton acts as an inhibitory agent of mechanoactivation (Lauritzen et al 2005).

TREK channels are also reversibly opened by polyunsaturated fatty acids (PUFAs) for example arachidonic acid (AA). In fact, TRAAK (another  $K_{2P}$  channel) is an acronym for TWIK-related arachidonic acid-stimulated  $K^+$  channel. PUFAs part in activation is similar to that of stretch and mechanoactivation in TREK channels, as the C terminus has been shown to play a role (Patel et al 1998). Anionic amphipaths (negatively charged) can insert into the membrane leaflet and this creates a convex curved membrane. It is the opposite when

discussing cationic amphipaths (positively charged) where is membrane formed in a concave shape and caused the channel to close (Martinac, Adler and Kung 1990).

Stretch activation and mechanosensitivity is also believed to be affected by conformational changes of the channel and influence gating of the channel. Force which causes membrane tension will change the shape of TM4 and TM2-TM3 which creates a flatter membrane surface. An increase in stretch sensitivity can be seen in TREK1 I267T which suggests that the selectivity filter is important mechano activation. High tension at the membrane will cause the channel to open as the energy caused by the movement of the channel from closed to open will deform the lipid bilayer. In addition, PUFAs are believed to promote activation of TREK channels in the lipid bilayer even in low tension by lowering the lipid deformity barrier as PUFAs decrease the bilayer bending modulus. TREK1 I267T shows a significant decrease in AA sensitivity which suggests a link between stretch and lipid-activation (Decher et al. 2017).

### **1.10.2.2 Evidence of voltage dependency of TREK1**

$K_{2P}$  channels have traditionally been thought of as “leak” channels and therefore voltage independent. The channels exhibit an outwardly rectifying current which is was believed to be caused by the difference in concentration of  $K^+$  ions across the membrane which is predicted by the Goldman-Hodgkin-Katz (GHK) equation. This equation predicts that the flow of ions will increase across the membrane from the side with a higher concentration of  $K^+$  ions and that there is no voltage dependent gating (Goldstein et al 2001). This equation also assumes that permeating ions do not interact with each other however in the case of  $K_{2P}$  channels multiple ions are known to enter the pore simultaneously and their movement will affect each other. TREK1 displays a strong outward current in response to voltage steps instead of a linear current predicted by the GHK equation. This prominent outward rectifying current shows that the channel adheres to voltage-dependent activation gating (Schewe et al 2016). To discover where the voltage gating occurs on the channel, deletional and chimeric analysis on TREK1 where carried out and the C terminal domain thought to regulate the voltage- dependent gating. Phosphorylation by protein kinase A of S333 in the C terminal was proposed as the voltage regulation site. However, dephosphorylation mutation on this site (S333A) did not show any difference from TREK1 WT and is not thought to be involved in voltage gating (Maingret et al 2002).

A more recent study has shown that voltage-dependent gating site is located within the selectivity filter, similar to Kv channels. It found that the threonine within the  $K^+$  signature motif (TIGFG) is responsible to voltage-dependent gating. These threonine sites are highly

conserved in all  $K_{2P}$  channels and therefore is important in the voltage-dependent gating mechanism within the  $K_{2P}$  family. Mutations on TREK1 (T142C and T251C) exhibited a linear current-voltage relationship caused by a loss of  $K^+$  binding on the S1 and S4 in the channel pore. Therefore, ion binding is central to voltage gating. When the pore is ion-depleted (containing one and zero ions) the channel enters a conformation similar the C-type inactivation observed in Kcsa channels. Upon depolarization, three-four ions enter the filter via the electrochemical  $K^+$  gradient and enters an active, conductive state. TRAAK channels however still show limited voltage-independent activation as stimulation by AA converts the channel to the classical leak conformation at higher concentrations. Moreover, the voltage-gating mutated TRAAK (T212C) abolishes the activation by AA which shows the importance of the primary gate at the selective filter. Subsequently these channels have been proposed to be described as “ion-flux-gated” channels instead of “leak” (Schewe et al 2016).

### **1.10.2.3 Regulation by pH**

Internal acidification is known to cause a shift in atmospheric pressure which cause positive pressure onto the membrane and ultimately sensitizes that channel to stretch activation. E306 in TREK1 and E333 in TREK2 were identified as a proton sensor using alanine scanning mutagenesis. This site also falls into the charged cluster region which is critically for mechano-gating. Protonation of this site and removing the negative charge converts the channel from a mechano-gated channel to an open, leak channel. E306 in the presence of a low pH will reduce binding to the cytoskeleton and allows stretch activation to occur. It is also interesting to note that E306A locks the channel into the activated conformation and is a gain-of-function mutation (Honoré et al 2002).

TREK1 WT is strongly inhibited by high extracellular pH. TREK2 is also sensitive to extracellular pH however it differs from TREK1 as it is strongly activated by acidification. Alanine screening mutagenesis was carried out and resulted in finding that if TREK1 H126 and its counterpart TREK2 H151 is mutated, it causes to channel to lose its regulation. It was therefore concluded that these are proton sensors and that they play a key component in extracellular acidification control. These two histidines however act in opposite ways when comparing TREK1 and TREK2. TREK1 H126 is flanked by negatively charged residues and therefore protonated side chains will be attracted to the region. The bonds formed between the side chains and the histidine site will cause the selective filter to collapse. On the other hand, TREK2 H151 is partnered next to basic residues and therefore no attraction takes place when the protonation occurs. It is most likely to repulse side chains and therefore open the channel (Sandoz et al 2009).

The heterodimerisation of TREK1/TREK2 showed a unique change in pH sensitivity as extracellular acidification and alkalization resulted in activation of the channel. The pH sensors of the individual channels are still functional in the heterodimer however as mutation of one channel's pH sensors will lead to the other channel in the dimer to operate as if it was in a homodimer. Unlike TREK1 and TREK2, TRAAK is activated by internal alkalinisation. However, TREK1/TRAAK show a weak increase in activity when in the presence of an increased or decreased intracellular pH. This shows that separate pH regulators found in TREK1, TREK2 and TRAAK individually sense the intracellular pH and are active in heterodimers. These changes in pH from physiological values will increase hyperpolarising outward potassium current which could help prevent damaging hyperexcitation and lead to neuroprotection of neurons (Levitz et al. 2016).

### 1.10.2.4 Phospholipid regulation of TREK channels

The neurotransmitter glutamate activates group 1 metabotropic glutamate receptors (1 mGluRs). This activation will lead to depolarisation of the cell membrane and an increase in cell firing and neuronal excitability. Group 1 mGluRs are primarily coupled to G $\alpha_q$  protein (Czirjak and Enyedi 2002). Activation of G $\alpha_q$  stimulates the enzyme phospholipase C (PLC) which then leads to the hydrolysis of PIP<sub>2</sub> into the secondary messenger DAG and inositol trisphosphate (IP<sub>3</sub>). IP<sub>3</sub> will activate the release of calcium from intracellular stores and DAG stimulates the activation of protein kinase C. Neither IP<sub>3</sub> nor intracellular calcium has any effect on the conductance of the TREK channel. However, a depletion of PIP<sub>2</sub> will cause inhibition of TREK, as PIP<sub>2</sub> is thought to be used to maintain normal activity. PIP<sub>2</sub> regulates this pathway as it can lead to an increase in activity after cationic molecule inhibition (Chemin et al. 2003; Kang et al 2006). It has also been hypothesised that following PLC activation, direct inhibition of TREK occurs via diacylglycerol (DAG) independently of protein kinase C (PKC). However experimental studies showed that DAG produces minimal inhibition of current when directly applied (Lopes et al 2005).

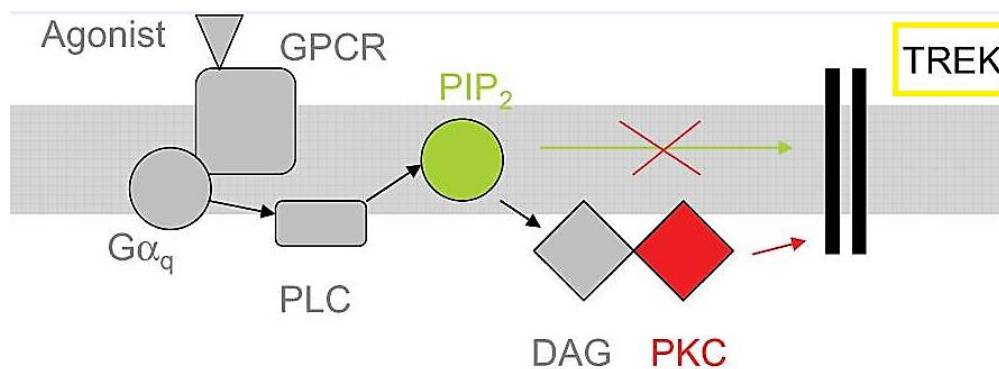


**Figure 1.10:** TREK inhibition activated by G $\alpha_q$  and mediated by PKC or a depletion of PIP<sub>2</sub> (adapted from Chemin et al 2003; Kang et al 2006; Mathie 2007).

Along with inhibition via G $\alpha_q$  activation, there is a second hypothesis that inhibition of TREK can be activated by G $\alpha_s$  protein. Activation of G $\alpha_s$  leads to an elevation of the concentration of cyclic adenosine monophosphate (cAMP). TREK channels are phosphorylated by cAMP which converts the channels behaviour from a leak conductance channel to a channel with a much lower open probability. This also lead to the hypothesis that if an increase in cAMP causes a decrease in TREK current, a decrease in cAMP caused by G $\alpha_i$  will lead to an increase TREK current (Patel et al 1998; Lesage et al 2000).

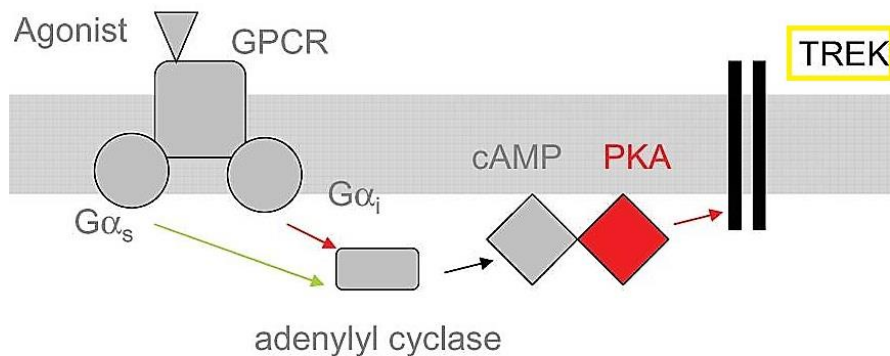


**Figure 1.11:** Regulation of TREK via the fluctuation of cAMP concentration (adapted from Mathie 2007; Murbartián et al 2005; Patel et al 1998).

There are two phosphorylation sites which have been identified for PKA- and PKC- mediated inhibition on TREK1 channel, S333 and S300. It was found that with alanine mutations, the channels inhibition would be abolished. Through these mutation studies it was also determined that phosphorylation of TREK1 at site S333 by PKA predisposes the channel for consequent phosphorylation by PKC at S300. Thus, there is a link between these serine sites on the C terminus for both the G $\alpha_q$  and G $\alpha_s$  inhibition cascade (Murbartián et al 2005).

### 1.10.2.5 Lysophospholipids

In contrast to phospholipids, extracellular lysophospholipids activate TREK. This stimulatory effect is dependent on the length of the carbonyl chain and the presence of a large polar head group. The conical shape of lysophospholipids is believed to cause the activity of the channel. Intracellular lysophospholipids on the other hand, are seen to inhibit TREK because of its concave shape (Patel, Lazdunski and Honoré 2001).

TREK1 is also strongly activated by lysophosphatidic acid (LPA). This activation is seen when applied to the intracellular side of the channel. LPA is thought to convert the voltage, pH, stretch sensitive K $^+$  channel to a leak conductance channel (Chemin et al 2005).

### **1.10.2.6 General anaesthesia**

Both TREK1 and TREK2 are opened by xenon, nitrous, chloroform, diethyl ether, halothane and isoflurane (Patel et al 1999; Gruss et al 2004). It is also seen that in TREK1 knockout mice, there is a decreased sensitivity in these types of anaesthesia. Anaesthesia, interestingly, has no effect on TRAAK. Deletion of the carboxyl terminus eliminates the activation of TREK current via anaesthesia's and therefore is a critical region of the channel (Patel et al 1999). Therefore, when extensive mutagenesis was studied this region was of particular interest. Mutations of TASK3 L241A and L242A saw a reduction in activation and was predicted to interrupt hydrophobic side chain interactions. However, it could not be ruled out that the mutation interfere with channel gating (Bertaccini et al 2014). Furthermore, an alanine mutation on the C terminus site E306A showed to almost abolish the effect of anaesthetics (xenon, nitrous oxide and cyclopropane) on TREK1 current again showing the importance of the C- terminus in anaesthetic sensitivity (Gruss et al 2004).

### **1.10.2.7 Thermosensitivity**

Thermal nociceptors are localised in the dorsal root ganglion which also expresses TREK channels. When these thermal nociceptors detect noxious heat, the neurons will begin to fire. TREK channels are activated gradually over a broad temperature spectrum. The rate of increase in activation is at its highest between 22 and 42°C (Maingret et al 2000). It was believed that the C-type gate was important in temperature sensing as mutation of G137I near the selectivity filter abolishes any response to heat. This function however is dependent on a C-terminal as mutations added between M4 and Ct will cause the channel to become insensitive to heat. The absence of this communication had a profound effect on heat sensitivity with no effect on the functional C-type gate. Indeed, the Ct domain is the structural element needed for heat sensing which then leads to the opening of the heat-insensitive C-type gate via an allosteric mechanism (Bagriantsev, Clark and Minor 2012).

## **1.10.3 TREK as potential target for treatments**

### **1.10.3.1 TREK links to pain**

Chronic pain is associated with the activity of nociceptive neurons that will transmit stimuli from the periphery to the central nervous system (CNS). This works as the signal, which is causing the pain, is sensed by ion channel and receptors found on nociceptor peripheral terminal. The signal is then transmitted to the CNS through dorsal root ganglion (DRG) neurons. The opening of K<sup>+</sup> channels will cause current hyperpolarization across the plasma

membrane as the efflux of potassium ions will limit neuronal excitability. Therefore, it is thought that TREK channels could be novel targets for treatment in pain (Tsantoulas and McMahon 2014).

TREK1 is highly expressed in small and medium DRG sensory neurons and are also co-localised with the transient receptor potential cation channel subfamily V member 1 (TRPV1) channels. These channels are capsaicin-activated nonselective ion channel which are known to recognise the sensation of pain (nociception) and noxious heat (>42 °C). The sensitivity of TRPV1 in response to these noxious stimuli is thus important for the latency and intensity of pain (Caterina et al 2000). When tissue damage occurs, inflammatory mediators for example prostaglandins and bradykinin are released. The inflammatory agents will activate the phospholipase C pathway leading to phosphorylation of TRPV1. Overall, the inflammatory mediators release will increase the sensitivity to hyperalgesia with non-painful stimuli (Katanosaka et al 2008). Mice lacking TRPV1 does not abolish pain sensitivity in general but lacks sensitivity to noxious temperatures (Caterina et al 2000). It is therefore proposed that TRPV1 antagonist is an analgesic agent. However, it is also known that the TRPV1 agonist capsaicin can also be used in pain relief. It was seen that application of a low-dose or single application at a high dose, shows relief from painful neuropathic conditions. The TRPV1 agonist is thought to desensitise the receptor and the neurons. Indeed, it is still argued that TRPV1 receptor agonist and antagonist may provide complementary treatments for analgesia (Derry et al 2009; Knotkova, Pappagallo and Szallasi 2008) TREK1 is known to be modulated by heat. TREK1 increase in activity contributes to the peripheral C-fibre heat nociception at the range of between noxious warmth and painful heat. TREK1 knockout results in hypersensitivity to heat at this range. The change in sensitivity to pain occurs in the noxious heat region between non-painful and painful stimulation. These results show that TREK1 channels are associated with the lower threshold of thermal pain and results in allodynia. Further mice experiments showed that TREK1<sup>-/-</sup> are more sensitive to mechanical stimuli and showed when in inflammation conditions (injection of intraplantar with carrageenan to produce inflammation) there was an increase in thermal and mechanical hyperalgesia (Alloui et al 2006). TREK2 channels are important to determine between moderate heat perceptions as TREK2<sup>-/-</sup> observe non-harmful heat, near 40°C, as aversive. This observation is seen in cold perception also between non-painful low temperatures and aversive cold (Pereira et al 2014). It was therefore suggested that TREK activators could have analgesic effect.

It is also believed that morphine has direct action on TREK1 channels. Morphine, acting on mu opioid receptors, enhances TREK1 current and has significantly less effect of an analgesic effect when depleted. The deletion of TREK1 channel however has no effect on

the three main side effects; constipation, respiratory depression and dependence. It is therefore concluded that the side effects and the analgesic effect do not involve the same mechanism and that activation of TREK1, downstream from mu opioid receptors, could be a possible target for pain relief (Devilliers et al 2013). However, activation of TREK1 channels for analgesia can also have adverse effects including depression (Heurteaux et al 2006).

### **1.10.3.2 TREK links to depression**

Depression is a mental disorder with symptoms that include depressed mood, worthlessness, and suicidal ideation. Serotonin (5-HT) is a neurotransmitter involved in the transmission of nerve impulses and has been linked to depression. The neurons of the dorsal raphe nuclei (DRN) are the principal source of 5-HT release in the brain (Ressler and Nemeroff 2000). 5-HT is transported into vesicles in the serotonergic neuron towards the presynaptic membrane into the synaptic cleft. Once here, 5-HT will diffuse across the synapse and bind to postsynaptic serotonin receptors transmitting the signal which will change the electrical state of the cell. However, the serotonin transporter (SERT) on the presynaptic neuron will recycle 5-HT at the synaptic cleft, thereby regulating the signal. Furthermore, presynaptic serotonin 1A (5-HT<sub>1A</sub>) is an autoreceptor and upon stimulation, the autoreceptor will inhibit the firing of 5-HT neuron. This will ultimately result in less serotonin levels (Newman-Tancredi 2011; Ressler and Nemeroff 2000) TREK channels have long been known to be a homolog of the *Aplysia* S-type channel. The *Aplysia* S-type channel is highly controlled by serotonin and this is the same as TREK1, therefore it is important to note its relationship to TREK1 and depression (Siegelbaum 1982). TREK1 is also highly expressed in regions of the brain that are important in cognitive attributes of depression (prefrontal cortex and the hippocampus) (Tally et al 2001). In TREK1<sup>-/-</sup> mice there is an increase in the activity of 5-HT transmission which is realized as increased firing of 5-HT neuron from DRN. In fact, the firing rate of 5-HT in TREK1<sup>-/-</sup> mice is two-fold larger than TREK1<sup>+/+</sup>. It could therefore be said that TREK<sup>-/-</sup> leads to a longer depolarisation rate and overall an increased firing rate in neurons. However, this antidepressant like property is not established in all K<sub>2P</sub> channels. TRAAK<sup>-/-</sup> showed no depression resistant phenotype. Thus, it is not as simple as a change in the efflux of potassium, but it is a specific characteristic to the TREK1 channel. This specific factor could be linked to TREK1 inhibition through G protein-coupled receptors which does not affect TRAAK. A G protein-coupled receptor that is important in depression is 5-HT<sub>1A</sub>. This receptor mediates inhibitory neurotransmission and are also a part of a serotonin negative feedback loop. The presynaptic 5-HT<sub>1A</sub> receptors are used as autoreceptors which triggers the serotonin feedback loop. This will lead to a reduction in neuronal activation and serotonin release leaving fewer serotonin molecules in

the synapse (Heurteaux et al 2006). 5-HT<sub>1A</sub> receptors are known to inhibit cAMP which is known to enhance TREK1 current causing hyperpolarisation of the neuron. This will cause an overall decrease in neuron firing rate and serotonin excretion. This shows that this abolishing TREK1 activity could be an important factor in disrupting the negative feedback loop which can alleviate depression (Gordon and Hen 2006).

It has been shown that TREK<sup>-/-</sup> mice show resistance to “depression-like” symptoms. In fact, the TREK<sup>-/-</sup> mice showed behaviour which was similar to that seen in TREK1<sup>+/+</sup> mice treated with the anti-depressant fluoxetine with no further effect on their behaviour. The resistance to ‘depression-like’ symptoms was tested using four distant models of antidepressant activity. The first was the Porsolt forced swim test (FST) which is based on the rodents’ immobility time when placed in an inescapable tank of water. The immobility time in the wildtype mice were found to be twice as long compared to the TREK1<sup>-/-</sup> mice (178 ± 2 s and 87 ± 8 s). The second test was the tail suspension test (TST) which again showed a shorter immobility time compared to the wildtype. In the conditioned suppression of motility test (CSMT) measures the conditioned suppression of motility when placed in an area which had previously set an electric shock through the foot. This showed a 44% reduction in conditioned suppression in TREK1<sup>-/-</sup> compared with the TREK1<sup>+/+</sup> mice. The fourth and final test is linked to chronic antidepressant use leading to stopping learned helplessness. It was found that the wild-type mice became helpless, as these mice showed increased escape latencies after exposure to shock compared to non-shocked control mice. TREK1<sup>-/-</sup> however showed significantly short escape latencies after training in the inescapable shock environment compared to the TREK1<sup>+/+</sup> mice. There was also no significant difference between shocked TREK1<sup>-/-</sup> and untrained control TREK1<sup>-/-</sup>. These results were interpreted as the TREK1<sup>-/-</sup> mice being less susceptible to induced ‘depression-like’ phenotype states (Heurteaux et al 2006).

### **1.10.3.3 TREK links to neuroprotection**

Astrocytes are specialized glial cells which are known to play a functional role in ischemic neuronal death. It has been demonstrated that also maintain ionic homeostasis involving glutamate uptake. It is also thought that K<sub>2P</sub> channels including TREK1 is involved in astrocytic passive conductance and contribute to the negative membrane potential (Chu et al 2010). The lipid and mechano-gated TREK1 channel is connected to conditions such as ischemia and epilepsy. TREK channels are known to be activated by PUFAs (poly unsaturated fatty acids) for example arachidonic acid and lysophospholipids (LPLs). These are both potent neuroprotective agents which protects against ischemia and seizures (Wu et al 2013). It has been seen in mice models that TREK1<sup>-/-</sup> display an increased sensitivity to both ischaemia and epilepsy when compared the WT mice. In TREK1 KO mice, there was a

lack of neuroprotection when PUFA was applied when compared to WT mice via seizure scores and mortality rate. TREK1 channels are therefore believed to protect neurons from ischemia induced excitotoxicity. However, it must be noted that TRAAK<sup>-/-</sup> mice showed no change in ischemia sensitivity showing that neuroprotection linked to TREK1 activity is a specific effect and is not due to any K<sup>+</sup> channel action (Heurteaux et al 2004). When ischemia occurs in the brain, arachidonic acid (AA) is released and the intracellular pH will become more acidic leading to neuronal swelling. The acidic intracellular pH will increase TREK current and lead to hyperpolarisation. This will subsequently reduce activation of presynaptic Ca<sup>2+</sup> channels and inhibit glutamate release at a presynaptic level and lower excitability of the neurons. At the postsynaptic level, hyperpolarisation will assist in Mg<sup>2+</sup> blocking NMDA (N-methyl-D-aspartate) glutamate receptors causing a shift towards more negative potentials. This will limit Ca<sup>2+</sup> release and therefore lower glutamate release and excitability of neurons (Franks and Honoré 2004). Therefore, a potential mechanism of neuroprotection is TREK1 activation. TREK1 is also found to be activated by volatile anaesthetics such as sevoflurane and that preconditioning cells with sevoflurane causes neuroprotection by increasing the expression of TREK1 channels. This preconditioning is believed to protect neurons from ischaemic injury. This may be caused by reduction in the inhibitory effect on the glutamate release which leads to a reduction in the excitatory neuron transmission leading to a possible mechanism of neuroprotection (Tong et al 2014). TREK2 channels have also been found to be up-regulated and that this activity will help maintain the membrane potential of astrocytes and will lower extracellular glutamate release during ischemia (Kucheryavykh et al 2009).

## **1.11 TRESK channel**

### **1.11.1 TRESK tissue distribution**

Human TRESK channel was identified in the human genome database and was originally only thought to be found in the spinal cord, hence the acronym TWIK-related spinal cord K<sup>+</sup> channel (TRESK) (Sano et al 2003). However further expression was detected primarily in the nervous system. Localisation of TRESK has been found using RT-PCR to determine the distribution of TRESK in mouse tissue where results showed expression in dorsal root ganglion (DRG) neurons (Kang and Kim 2006) the cerebrum, cerebellum, brainstem (Czirják, Tóth and Enyedi 2004) and in the sympathetic and parasympathetic ganglia (Cadaveira-Mosquera et al 2012). The channel was then subsequently found in human brain with a particularly high expression rate in the DRG and the trigeminal ganglion (Liu, C., et al. 2004). Through these experiments, they have also found expression of mouse TRESK in

non-nervous tissues such as testis (Czirják, Tóth and Enyedi 2004), spleen, thymus and heart (Kang and Kim 2006). The presence of TRESK was also identified using immunostaining which also identified a high expression rate in the dorsal root ganglion which is important to note as this region is thought to be involved in nociceptive trafficking and pain perception (Yoo et al 2009). It was thought by Kang, Mariash and Kim (2004) that a previously uncharacterised mouse ortholog of TRESK was discovered, an isoform called mTRESK-2. mTRESK-2 showed a 65% similarity with hTRESK. However further investigation identified the mouse genome and human database each only contains a single TRESK gene, which share a 92% similarity sequence identity. This indicates variable TRESK subunits between the two species (Keshavaprasad et al 2005).

## **1.11.2 Regulation of TRESK**

### **1.11.2.1 Calcium signalling regulation**

Gq-coupled receptor stimulation leads to an increase in TRESK activation. This increase is not a direct effect from the Gq-coupled receptor but is thought to be from an elevation of cytoplasmic calcium. It can be seen in experiments that after activation from calcium the TRESK channel remained in an activate state long after the calcium concentration had normalised. This would suggest that the calcium activation is in fact an indirect effect. This is confirmed in single-channel currents experiments, when calcium is applied to intracellular side and fails to effect TRESK current (Enyedi and Czirják 2014). The calcium ion does not bind to the channel protein, which can be seen in the classical  $Ca^{2+}$ -activated  $K^+$  channels. To look further into what is causing the activation, a specific inhibitor of the protein phosphatase calcineurin called cyclosporine A (CsA) was studied with an ionomycin induced enhancement of TRESK. It was seen that even in low concentrations of the compound, the enhancement was completely eliminated. This lead to the strong suggestion that calcineurin is involved in activation of TRESK channel. TRESK channel is the only  $K_{2P}$  channel that is regulated by calcineurin. The study went even further and applied another calcineurin inhibitor FK506. This again showed an abolished enhancement of current. A rigid active calcineurin (CnA 1-441) was developed and coexpressed with TRESK along with the regulatory B subunit of calcineurin. CnA 1-441 lacks any C-terminal and therefore lacks any inhibitory properties. It resulted in the triple expression causing higher basal currents than TRESK alone and calcium signal by ionomycin. This indicates that active calcineurin allows TRESK to enter its activated state, and cannot be further stimulated by calcium (Czirják, Tóth and Enyedi 2004).

### 1.11.2.2 Calcineurin binding partner

The enzyme/substrate relationship between TRESK and calcineurin has been identified; however there have been further binding partners and interactions which take place that are important in the activation of TRESK via calcineurin. Calcineurin has been seen to interact with TRESK via NFAT-like docking site (Czirják and Enyedi 2006). The non-catalytic surface of calcineurin is necessary for the binding of this enzyme to the Nuclear Factor of Activated T cells (NFAT) (Li et al 2007). The interaction was first identified in mouse TRESK with the amino acid sequence PQIVID, found in the N-terminal side of the intracellular loop. Mutations of the PQIVID motif (PQIVIA, PQIVAD and PQAVAD) were shown to decrease any calcium-dependent activation using a microinjection of the VIVIT peptide. This peptide is designed to eliminate the calcineurin-PQIVID site interaction which prevents any TRESK activation in the mouse model. The human ortholog sequence was identified as PQIIIS and acts identically to mouse TRESK in regard to calcium signalling (Czirják and Enyedi 2006).

A further interacting site for calcineurin-TRESK activation has been identified in the human TRESK loop close to the serine cluster called LQLP. It was revealed that combined inactivating mutation of PQIIIS and LQLP (PQAAAS and AQAP) abolished the calcium-dependent regulation of TRESK channel. The AQAP mutation on its own was also shown to slow down its sensitivity to high calcium, reducing the rate of activation. Binding experiments that replaced PQIIIS amino acid sequence with a high calcineurin binding affinity sequence PVIVIT, determined whether LQLP was an auxiliary binding site or a major determinant of the calcium sensitivity of TRESK regulation. The loss of function mutation (AQAP) was co-expressed with the gain of function motif PVIVIT. This resulted in the conclusion that the two sites are not functionally equal and that the gain-of-function action could not compensate for the loss of function brought about by the AQAP mutation. There is also suggestion that the binding of calcineurin to TRESK is observed in two consecutive steps as the binding of calcineurin to LQLP is calcium-dependent.

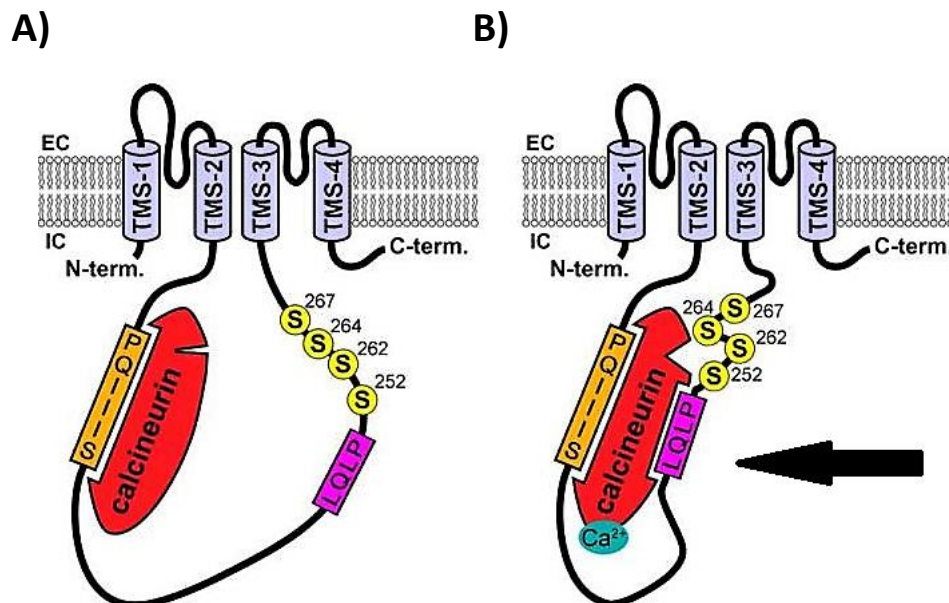


**Figure 1.12:** Representation of human TRESK activation. A) Calcineurin binds the PQQIS motif independently from cytoplasmic calcium. B) LQLP binds to calcineurin under calcium signalling and causes the serine residues to reside closer to calcineurin (adapted from Czirják and Enyedi 2014).

As seen in the diagram above calcineurin is attached to PQQIS at rest. As the cytoplasmic calcium level increase, calcineurin anchors to the LQLP motif and subsequently it is positioned near the regulatory serine cluster. It could be said that PQQIS is used for calcineurin availability and LQLP brings the adjacent serine residue into the proximity of the activated phosphatase calcineurin (Czirják and Enyedi 2014).

### 1.11.2.3 Regulation through 14-3-3 proteins

14-3-3 proteins are highly conserved regulatory proteins and has been implicated in a number of cellular processes. It has also been show to associate with many ion channels. In the  $K_{2P}$  family, it has been recognised that all isoforms of 14-3-3 protein interacts with the C-terminus of the TASK subfamily. This binding is central for membrane targeting of the channel (Rajan et al 2002).

The 14-3-3 protein binds to the RSNSCPE motif and was firstly identified in mouse TRESK and subsequently in the human TRESK in the intracellular loop region (Czirják, Vuity and Enyedi 2008). Protein kinase A enzyme is thought to be the auxiliary channel inhibitor as it phosphorylates the S252 which will lead to the recruitment of 14-3-3 protein (Czirják and Enyedi 2010). The phosphorylation of the S252 in this sequence is required for the interaction to occur (Enyedi, Braun, and Czirják 2012). Indeed, it has also been shown that 14-3-3 protein was responsible for halting the return to the currents previous resting state after calcineurin-mediated activation. It was originally believed that association of 14-3-3

protein to the newly phosphorylated S252 residue in TRESK would interfere with re-phosphorylation of the regulatory S264 residue and would hinder current recovery (Czirják, Vuity and Enyedi 2008). However new evidence shows a more complex mechanism, which involves different forms of inhibitory phosphorylation, connected to 14-3-3 protein.

#### **1.11.2.4 Inhibition pathway of TRESK**

There are two pathways that inhibit TRESK activation. The first involves phosphorylation of S252 by protein kinase A which then leads to the consequent union of the 14-3-3 protein to the serine residue. When the single site S252 was in a functional state (TRESK-S264E) it was observed that the basal activity was heightened in the absence of 14-3-3 protein. Therefore, it was concluded that the binding of 14-3-3 to S252 would enhance the inhibitory effect. The second pathway implicates the inhibition of TRESK by phosphorylation of the serine cluster. However surprisingly, this action is obstructed by 14-3-3 protein (Czirják and Enyedi 2010).

MARK, microtubule affinity-regulating kinase, is believed to have a regulatory effect on TRESK as it has been identified as a binding partner of the intracellular loop of TRESK. MARK1, MARK2 and MARK3 accelerate the return of the TRESK resting state following calcium-dependent activation. However, 14-3-3 protein inhibits the kinases phosphorylation of the serine cluster. MARK2 has previously demonstrated a negative response to 14-3-3 protein and was therefore identified as a potential new TRESK-inhibitory kinase. 14-3-3 protein plays a role in the involvement of MARK2 and the recovery of basal kinetics in TRESK. The quantity of 14-3-3 in the cytoplasm has been reported to affect the recovery of basal recovery. However, MARK kinases did increase activity in a reduced amount of 14-3-3 protein and overexpression of 14-3-3, but does not abolish the result of MARK on TRESK. It was also shown that even in the removal of 14-3-3 binding to MARK using a double mutation (S400A/T539A); it did not deter the action of MARK on TRESK. Therefore, it can be concluded that MARK is not completely influenced by 14-3-3 protein and is vital in TRESK regulation. The target for MARK2 was investigated and showed that even if S252 TRESK was mutated, the current would return to its resting state. This would indicate that the S252 site is not phosphorylated by MARK2 but targets the serine cluster (Braun et al 2011).

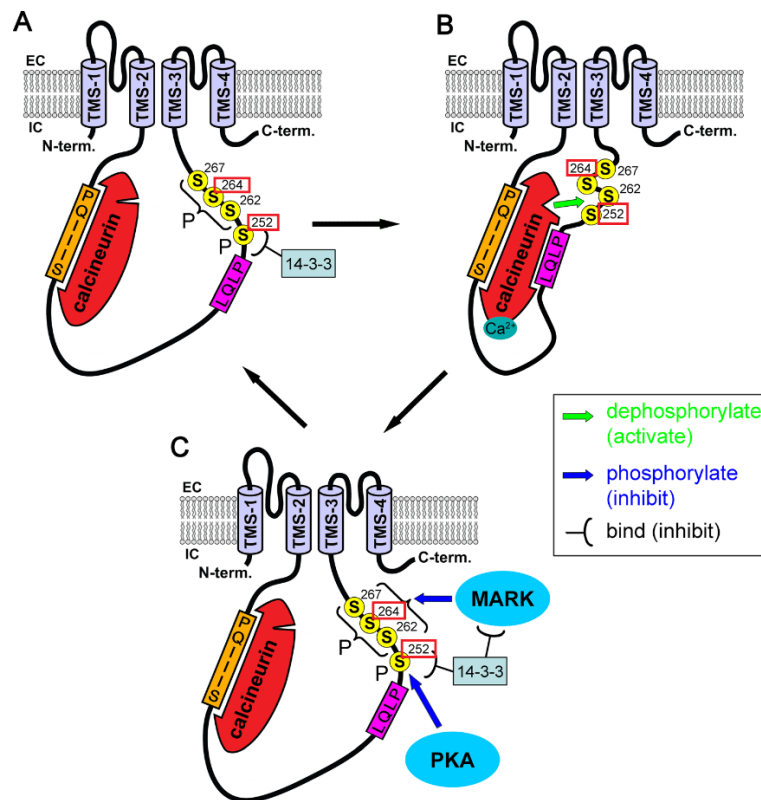


**Figure 1.13:** Representation of human TRESK regulation A) TRESK channel is constitutively phosphorylated under resting conditions. Phosphorylation occurs at S252 and leads to 14-3-3 protein binding to this serine site. This phosphorylation and protein binding leads to an inhibitory effect. B) Through calcium signalling, LQLP will bind to calcineurin and the calcineurin phosphatase will become activated and will lead to dephosphorylation. This also causes a detachment of 14-3-3 protein from the channel. C) The channel will then slowly phosphorylate and will return to its basal state. PKA and MARK kinases are involved in this process. The pathway is extended in the presence of 14-3-3 (adapted from Enyedi and Czirják 2014).

### 1.11.2.5 Activation by protein kinase C

Further activation pathways were investigated using mouse TRESK channel. It was found that the PKC activator phorbol 12-myristate-13-acetate (PMA) did not affect mouse TRESK and PKC did not influence the return to this original resting state after activation. However consequent human TRESK studies showed PMA contributed to activation of the channel. Mutations of potential PKC phosphorylation sites were identified (none of which are found in mouse sequence) but it did not affect the PMA-induced increase of current. This would suggest that the PKC activation is an indirect effect and is not mediated through direct binding to the human TRESK channel. However, the possibility of other PKC-phosphorylation sites cannot be ruled out (Rahm et al 2012).

### **1.11.2.6 TRESK pharmacological characteristics**

Like other  $K_{2P}$  channels, TRESK is inhibited by high concentration of extracellular  $Ba^{2+}$ , quinine and quinidine.  $Ba^{2+}$  is thought to bind to the channel at the plasma membrane as inhibition is seen at negative membrane potential. Quinine and quinidine accomplishes inhibition by blocking the channel. However, the channel also shows differential properties from that for the other  $K_{2P}$  channel as it is unaffected by classic  $K_{2P}$  blockers for example 4-aminopyridine, apamin, CsCl and ATP-sensitive  $K^+$  blockers tolazamide and glipizide (Enyedi and Czirják 2014).

Both mouse and human TRESK channels are also sensitive to several different anaesthetics. Isoflurane, halothane, sevoflurane and desflurane are all volatile anaesthetics that increase the TRESK current three-fold (Liu et al 2004). In vivo experiments show that TRESK knockout mice were less sensitive to isoflurane but show the sensitivity to desflurane, halothane and sevoflurane was unchanged (Chae et al 2010). This difference in sensitivity would suggest that TRESK is substituted by other anaesthetic-sensitive channels or TRESK is not the major target of the anaesthetic effect (Enyedi, Braun and Czirják. 2012). It was also found that the mortality rate increased in the KO mice compared to the WT (Chae et al 2010). This could suggest that TRESK is required for survival under these conditions; however, this process is not fully understood (Enyedi, Braun and Czirják 2012). There is a uniquely longer loop segment found in TRESK which differs from other members of the  $K_{2P}$  family. This loop connects the second and third transmembrane together. It is thought that it is this region that makes TRESK more sensitive to volatile anaesthetics than other  $K_{2P}$  channels, however more studies are needed in this region. Local anaesthetics are found to inhibit TRESK but at concentrations larger than those compared to the other  $K_{2P}$  channels. The target site for local anaesthetics is believed to be intracellularly or on the membrane. IV anaesthetics did not enhance TRESK channels at any significant level. Furthermore, the nonimmobilizer compound 1,2-dichlorohexafluorocyclobutane had no effect on TRESK (Liu et al 2004).

### **1.11.2.7 Difference between TRESK species**

There are certain characteristics of TRESK channels that exhibited species-specific variations. Human TRESK channels are found to be weakly sensitive or insensitive to extracellular pH whereas mouse TRESK is strongly regulated by extracellular pH. As the pH reaches pH 6, there is a drop in current. While an alkalisation of pH increases the current in mouse TRESK. The homologous histidine in mouse TRESK (His-132) is responsible for the proton sensor activity and is only conserved in mouse TRESK. This residue is found

directly downstream from the selectivity filter sequence (GYG). This site has also been seen to be significant for pH sensitivity in TASK-1 and TASK-3. It can be seen however that a mutation of the human TRESK analogue from a tyrosine to a histidine (Y121H) is sufficient for the channel to become pH dependent. A replacement of the mouse TRESK histidine to an asparagine will eliminate any pH sensitivity (H132N) (Dobler et al 2007).

Another species-specific variation for TRESK is zinc inhibition. Mouse TRESK is inhibited by zinc whereas human TRESK is resistant. The histidine residue mentioned for pH sensitivity has proved to be responsible for zinc binding (Czirják and Enyedi 2006).

### **1.11.3 TRESK involvement in pathological processes**

#### **1.11.3.1 Pain pathway**

As previously discussed, TRESK is highly expressed in DRG neurons. Following nerve injury, DRG is the source of increased nociceptive signals and because of the increase in neuronal excitability. It is also an important messenger to transport this pain signal from the periphery system to the central nervous system. Sensory neurons during hyperexcitability will prompt the enhancement of depolarisation and assists in reaching the action potential threshold. Hyperexcitability is also characterised by its decrease in nerve impulses and repetitive firing during extended depolarising stimuli.

Changes in the expression of ion channels have been seen to influence the action potential by increasing the amount of open TRESK channels and decreasing the action potential threshold. Chronic nerve damage and inflammation will down regulate the expression of TRESK and it is therefore believed to be linked with pain (Tulleuda et al 2011).

An important insight into the regulation and function of TRESK was discovered through the ENU-derived mouse knockout. It was seen that if a missense mutation was used, the channel will completely lose function. TRESK is believed to decrease membrane excitability, seeing as the loss-of-function TRESK mutation (G339R) increases DRG excitability (Dobler et al 2007). Down regulation of TRESK in neuropathic pain models also induces hyperexcitability and blocking or silencing the channel via pharmacological means results in the activation of sensory neurons and nociceptive fibres that begins the algescic effect (Tulleuda et al 2011). This affect can be seen in through calcineurin-inhibitor induced pain syndrome (CIPS). CIPS is described by severe pain after calcineurin inhibitor, has been known to affect patients after organ and stem-cell transplantations (Huang, Yu and Fan 2008).

In rats, it has been found that chronic nerve damage and inflammation will alter the expression level of TRESK mRNA. Over-expression of TRESK has been seen to inhibit the DRG-released capsaicin mediated substance P, which is used in the transmission of nociceptive impulses at the spinal cord level. TRESK over – expression also alleviates mechanical allodynia caused by nerve injury. The results therefore indicate that over-expression of TRESK and therefore an increase in channel activity diminishes the sensitivity of neurons to harmful stimuli (Guo and Cao 2014). Taking all these results together suggests that a TRESK-specific activator may display analgesic effects as ultimately this will lead to a significant decrease in the excitability of DRG neurons.

### **1.11.3.2 Migraine with aura**

Migraine is a highly prevalent condition and has been described as one of the top 20 causes of disabling chronic disorders among adults of all ages. The aura is associated with cortical spreading depression (CSD), which causes neuronal depolarisation that spreads to the cortical regions of the brain. Migraine is caused by hyperexcitation of neurons (Enyedi and Czirják 2014). This hyperexcitation activates CSD signals over the brain, which acts directly onto nerves in the trigeminal ganglion to release pro-inflammatory peptides (capsaicin mediated substance P for example) in the meninges. The meninges will start to inflame and promote the activation of trigeminal nerves and will lead to a painful throbbing headache (Lafrenière et al 2010). Under calcineurin inhibitor immunosuppressant treatment, patients began to develop headache symptoms. It was stated that 74 organ transplant patients received calcineurin inhibitors and that 38% of the patients developed migraines within three years of the organ transplantation. This showed indirect evidence that through the inactivation of calcineurin and therefore the inhibition of TRESK, lead to an increase in the frequency of migraine headaches (Ferrari et al 2005).

To delve deeper into the relationship between migraine and pain linked to TRESK, the KCNK18 gene was sequenced in a multigenerational family who suffered with migraines. It was discovered that a mutant KCNK18 gene was found in members of the family that were affected with typical migraine headaches. The mutant gene contains an F139WfaX24 frameshift mutation which causes a 2-bp deletion at position 414-415 at the C-terminal and truncation of the protein at position 162 in the second transmembrane segment. This mutation caused the channel to be non-functional and that the gene was inherited in a dominant fashion and causes a dominant-negative suppression of WT channel function (Lafrenière et al 2010). This F139WfaX24 mutation has also been found in a different, unrelated migraine sufferer which reinforces the conclusion that the dominant-negative mutation is directly linked with this type of rare migraine (Enyedi, Braun and Czirják 2012). In

additional screening for KCNK18 mutation discovered another missense variant C110R. C110R showed a loss-of-function similar to that of the TRESK framework mutation as it was able to reduce activity from co-expressed TRESK WT channels. However, the mutation was found to have no correlation with migraine sufferers and showed that a single non-functional mutation is not enough to develop migraine (Andres-Enguix et al 2012). This screening also showed an interesting site S231 in relation to migraine. The original study showed that TRESK S231P had no effect on TRESK activity. However, this site was identified in a female patient in Poland suffering with migraine with aura. Therefore, this site may contribute to migraine with typical aura (Domitrz et al 2015).

Millan-Guerrero et al (2008) discussed the role of TRESK coupling with the histamine H1 receptor as histamine activates TRESK channels. It has been suggested that TRESK is involved in “dampening” the activation of a cellular action involved in inflammation as histamine is known to be released in response to inflammation. The findings of this paper say that migraine symptoms decreased by ~50% when patients used subcutaneous histamine as a treatment for migraine.

Migraines are known to be linked to inflammation of the meninges and therefore the role of TRESK is deemed to be regulating the excitability of neurons during inflammation. It is therefore thought that the TRESK framework mutation causes an increase in excitability of trigeminal nociceptive pathway which ultimately allows for a higher predisposition to migraine headaches (Lafrenière and Rouleau 2011). It is not however believed that the dominant-negative mutation is directly responsible for the aura symptoms as the mutation does not induce CSD. The WT TRESK channel stabilises the normal neuronal activity by preventing the activation of neurons that trigger CSD. The dominant-negative mutation may delete this protective mechanism and cause the aura symptoms. These results would indicate that upregulating TRESK activity using a channel specific agonist could be a potential treatment for migraine sufferers (Enyedi, Braun and Czirják 2012).

## **1.12 Sipatrigine and its derivative lamotrigine**

Sipatrigine (BW 619C89) is a compound derived from the antiepileptic agent lamotrigine, which has a substituted pyrimidine into the structure. The change in chemical structure was developed to improve the neuroprotective effect seen with lamotrigine (Leach et al 1993). *In vivo* lamotrigine has been found to be a less potent neuroprotectant compared to sipatrigine, whilst lamotrigine is a better anticonvulsant (Hainsworth et al 2000).

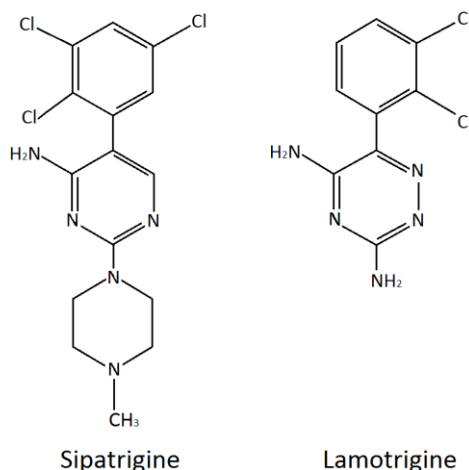


**Figure 1.14:** Structure of sipatrigine and lamotrigine

Both compounds were originally described as “glutamate release inhibitors”. *In vitro* experiments showed that sipatrigine inhibited glutamate release from brain slices which was found to be an animal model for neuroprotection and cerebral ischemia (Leach et al 1993). However, sipatrigine is not believed to have a direct effect on glutamate receptors as this compound has a weak affinity for excitatory amino acid binding sites. There was also no effect on glutamate release when measuring excitatory potentials in the presence of sipatrigine (100  $\mu$ M) in rat hippocampal brain slices. Lamotrigine was also identified to protect against ischaemic damage and this is completely independent of direct glutamate action (Garthwaite et al 1999).

### 1.12.1 Sipatrigine inhibition of ion channels

Sipatrigine has been shown to act in a reversible manner to inhibit voltage-gated  $\text{Na}^+$  current. The compound was shown to be a dose and voltage-dependent inhibitor of native  $\text{Na}^+$  and type 11A  $\text{Na}^+$  channels. The inhibitor is believed to work on these channels by stabilising the inactivated states of the channels. Therefore, this inhibition is believed to prevent membrane depolarization which is an effective strategy against neuroprotection (Garthwaite et al 1999). However, sipatrigine is not channel specific as it is equally effective as a calcium channel inhibitor. Sipatrigine was seen to inhibit human P and /N-type  $\text{Ca}^{2+}$  and was likely to provide cerebral protective effect.  $\text{Ca}^{2+}$  channels are important for release of glutamate from presynaptic terminals and inhibition could therefore decrease excitability of neurons (Garthwaite et al 1999; McNaughton et al 1997). Furthermore, low-voltage-activated T-type  $\text{Ca}^{2+}$  channels mediated by channels with  $\alpha_{11}$  subunits have also been found to be inhibited by sipatrigine. In fact, sipatrigine was more effective on T-type  $\text{Ca}^{2+}$  than type- 11

Na<sup>+</sup> channels or N-type Ca<sup>2+</sup> channels. Therefore T-type Ca<sup>2+</sup> channels are believed to contribute to the neuroprotective and anticonvulsant effect (McNaughton et al 2000).

The action of sipatrigine on Ca<sup>2+</sup> and Na<sup>+</sup> channels do show several shared features, as inhibition of both channels are reversible and enhanced antagonism of the channels is seen when the membrane is depolarized. It can therefore be suggested that sipatrigine binds more strongly when the channels are in the inactivated state. Furthermore, inhibition of voltage-gated K<sup>+</sup> by sipatrigine in hippocampal neurons have been observed. The inhibition of outward K<sup>+</sup> currents in the presence of 10 μM sipatrigine was ~ 30% at a holding potential of -90 or -60 mV. Sipatrigine did however show a greater affinity to inactivated Na<sup>+</sup> whilst inhibition of inactivated K<sup>+</sup> current was voltage-independent. This would indicate a selectivity to Na<sup>+</sup> channels over K<sup>+</sup> at less negative potentials (Xie and Garthwaite 1996; (McNaughton et al 1997).

### **1.12.1.1 Sipatrigine effect of K<sub>2P</sub> channels**

The action of sipatrigine is believed to have a broader effect on K<sub>2P</sub> channels compared to lamotrigine. TASK1 current showed to be inhibited by sipatrigine (10 μM) by ~ 37%. A member of the TREK family, TRAAK, produced sipatrigine inhibition of ~ 45% at a concentration of 10 μM. Sipatrigine was characterised as an effective inhibitor of TREK1 channels with a 75% decrease in current using 10μM of sipatrigine (Meadows et al 2001). TREK1 inhibition by sipatrigine has been associated with an antidepressant effect as its believed to be disrupting the serotonin feedback (Tsai 2008). Sipatrigine inhibition of K<sub>2P</sub> channels is thought to be involved in neuroprotection as chronic depolarisation block of glutamate release. It was also noted that the inhibition of TREK1 by sipatrigine and the subsequent wash off saw an over recovery of current not seen in the related TRAAK (Meadows et al 2001). Up until this work, no experiments have been carried out on TRESK. Little is known of how the different channels are regulated by sipatrigine and lamotrigine and insight into this could lead to new information about the structure and gating of the channels.

### **1.12.2 Lamotrigine inhibition of ion channels**

Lamotrigine has similar pharmacology to sipatrigine; however, it is deemed less potent in comparison (Hainsworth et al 2000). The ability of lamotrigine to modulate neuronal activity has made it useful in treating epilepsy and bipolar disorder. Lamotrigine is known to inhibit presynaptic voltage Na<sup>+</sup> channels which blocks glutamate release and decrease neuron excitation. However, the affinity of sipatrigine to inactivated Na<sup>+</sup> is four times higher than lamotrigine. This leads to lamotrigine being less effective in neuroprotection compared to

sipatrigine (Xie and Garthwaite 1996). Regarding  $\text{Ca}^{2+}$  channels, lamotrigine is known to inhibit both N- and P-type  $\text{Ca}^{2+}$  channels which would play a role in decreasing the  $\text{Ca}^{2+}$  dependent excitability of neurons. The difference however between lamotrigine and sipatrigine is that lamotrigine has no effect on T-type  $\text{Ca}^{2+}$  currents (Hainsworth et al 2000).

### 1.12.2.1 Effect of lamotrigine on $\text{K}_{2\text{P}}$ channels

The actions of lamotrigine have been characterised with TRESK channel and was shown as a potent inhibitor. It was found that for mouse TRESK, lamotrigine ( $30 \mu\text{M}$ ) inhibited the current by  $\sim 50\%$  followed by recovery of current with wash-out in an inside-out patch configuration. Therefore, it is believed that the inhibition is both a direct action on the channel and also involves intracellular mechanism (Kang et al 2008). These experiments also established that lamotrigine had little to no effect on all members of the TREK family (Kang et al 2008; Meadows et al 2001). This believed selectivity of lamotrigine on TRESK has been used in studies to show inhibition in cultured TG neurons. It was therefore concluded that lamotrigine primarily acts on TRESK channel (Liu et al 2013).

## 1.13 Cen-092-C

Cen-092-C, a newly developed compound, antagonises  $\text{Na}^+$  channels with an  $\text{IC}_{50}$  of  $29.5 \mu\text{M}$  in rat model (unpublished data, Leach). Cen-092-C is derived from lamotrigine and has a similar structure to sipatrigine. The difference between Cen-092-C and lamotrigine is the replacement of fluorine to chloride in different position.

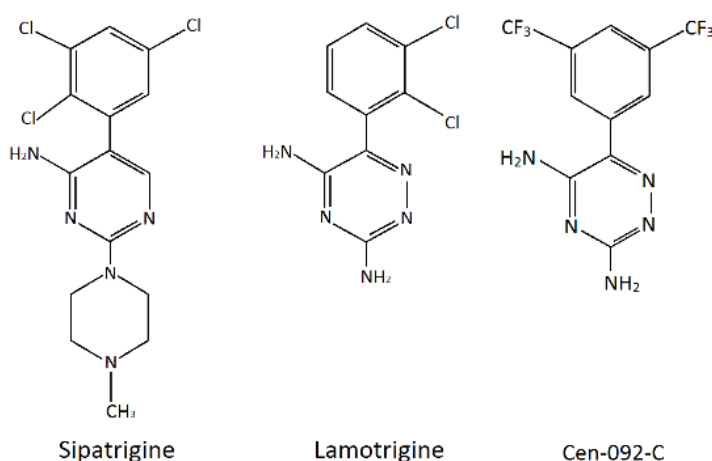


**Figure 1.15:** Chemical structure of sipatrigine, lamotrigine and Cen-092-C

Cen-092-C was used in a multiple sclerosis study in an EAE (experimental autoimmune encephalomyelitis) model and showed to nullify any clinical EAE symptoms when compared to untreated models (unpublished data, Leach). As this is a new compound, its testing has

been limited and has not been used on  $K_{2P}$  channels. Therefore, because of its close relation to lamotrigine, it would be interesting to find if the same degree of inhibition occurs on each  $K_{2P}$  channel.

## **1.14 Aims and objectives of thesis**

The aim of this research is to investigate the effect and mechanism of action of sipatrigine and lamotrigine on TREK1 (chapter 3), TRESK (chapter 4) and TREK2 (chapter 5).

Furthermore, the effect of the related compound Cen-092-C was also investigated on TREK1 and TRESK (chapter 6). This was all carried out using site directed point mutations and whole cell patch clamp electrophysiology.

Chapter 3 involves clarifying the effect of sipatrigine and lamotrigine on TREK1. A potential binding site of the compound at the fenestration site (L286) was examined. Furthermore, important binding sites for activators at the central cavity was also investigated. The effect of sipatrigine on the gain-of-function mutated TREK1 was also investigated to further examine the importance of the fenestration sites in sipatrigine binding.

In chapter 4, TRESK current inhibition by sipatrigine and lamotrigine were identified and the identified potential binding sites in the central cavity (F145 and F352) were mutated to investigate if these sites were important in compound binding. State dependent inhibition of TRESK was also studied in all selected compounds to further investigate how these inhibitory compounds act on the channels. TRESK activation has been linked to analgesia, therefore novel agonists of TRESK were also tested.

Chapter 5 investigates the degree of lamotrigine and sipatrigine inhibition on TREK2. Similar to chapter 3, the fenestration site was investigated for sipatrigine binding. Moreover, TREK2 isoforms were created through alternative translation initiation to further investigate sipatrigine effects on TREK2 current.

Chapter 6 investigates the novel compound Cen-092-C effect on TREK1 and TRESK channels. Cen-092-C binding on TRESK was investigated by mutation at potential binding target found at the central cavity sites (F145 and F352). Furthermore, the effect the compounds has when the channel is in different phosphorylation state was also examined, to further investigate to full action of this novel compound. This chapter's aim is to explore any antagonist effect on current using electrophysiology.

# **CHAPTER 2**

## **Methods**

## 2 Methods

### 2.1 Preparation of poly-D-lysine (PDL) plates

For electrophysiology experiments, Nunclon 4-well dishes (ThermoFisher Scientific) were prepared in advance. The cover slips (13mm circular, VWR) were first washed in a petri dish of distilled water to remove any glass debris. The cover slips were then removed individually using forceps and allowed to dry. The cover slips were then added to a petri dish of ethanol. When completely dried, the coverslips were transferred into four well plates. In a microbiological safety cabinet, 300  $\mu$ l of PDL (0.1mg/ml) was dropped onto each cover slip to ensure good cell adhesion. The plates were allowed to dry for 20-30 minutes. Any leftover PDL was removed with a pasteur pastette and allowed to dry completely. The plates were then transferred to a UV hood for sterilisation for 1-2 hours. The plates were stored at -20°C

### 2.2 Cell culture

The tsA 201, modified human embryonic kidney (HEK) cell line was chosen to transfection and electrophysiology because of its quick, manageable reproduction and maintenance, high efficiency of transfection when expressing protein of interest, and the small cell size suitable for voltage-clamp experiments.

This cell line was cultured in media containing Dulbecco's modified Eagle's medium (88%), with Earl Salts, heat-inactivated foetal bovine serum (10%), NEAA (1%), 2 mM L-Glutamine, and penicillin-streptomycin (1%). The cells were kept in two different sized flasks, 75cm<sup>2</sup> and 25cm<sup>2</sup>. These cultured flasks were incubated at 37°C tissue culture incubator with 5% CO<sub>2</sub> and 95% air. Cells were sub-cultured every 2-3 days if using 25cm<sup>2</sup> flask and every 4-5 days if using 75cm<sup>2</sup> flask. Cells should be 70-80% confluent at this stage. The cells were detached using Trypsin-EDTA (0.25%). When the cells are adhered to the smaller 25cm<sup>2</sup>, 1.5ml of Trypsin-EDTA is used. The larger flasks (75cm<sup>2</sup>) use 3ml of Trypsin-EDTA cell dissociation solution. The flasks were agitated gently and the left in the incubator for 3-5 minutes. The cells were removed from incubator and placed back in the fume hood. The cells were agitated again to ensure the cells have been dispersed from the bottom of the flask. Added 5ml of fresh media to the flask and pipetted up and down to ensure no clumping of cells and to remove any further cells from the bottom of the flask. Transferred 5ml of stock solution to a 15ml falcon tube. The falcon tube was placed into a centrifuge and spun at room temperature at 800rpm for 3 minutes. The supernatant was then poured out and the

cells were then re-suspended in 5ml fresh media and diluted for passage into a new flask. For cell passage, 20ml of fresh media is added to 75cm<sup>2</sup> flask and then 0.5ml of stock cell solution. If cell passage uses 25cm<sup>2</sup> flask, 5ml fresh media was added and then 0.5ml of stock cell solution. For electrophysiology experiments, 8.5ml of fresh solution was added to a falcon tube, followed by 0.5ml cell stock solution. Transfer 0.5ml of resuspended cells into each well of the plate. Cells prefer to grow between two surfaces, which can cause you to get a lot of cells growing on the bottom of the coverslip, rather than the top. Leave in incubator and allow cells to grow over night.

## 2.3 Calcium phosphate transfection

Calcium phosphate transfection is a popular method for introducing foreign DNA plasmid into cells. tsA 201 cells can be transiently transfected using the calcium-phosphate method. The HEPES-buffered saline solution containing negatively charged phosphate ions will combine with the positively charged calcium chloride solution containing the DNA. This combination will form a fine precipitate and will bind to the DNA on its surface. The suspension of the precipitate is then added to the cells to be transfected. The DNA-calcium phosphate precipitate is then internalised by the cells through endocytosis. Transfection begins 24 hours after the cells were plated. The tsA 201 cells are transfected with a plasmid encoding the cDNA of WT or mutated K<sub>2P</sub> channel and cDNA of green fluorescent protein (GFP). GFP is used as a reporter of expression and is exhibited in the cytosol of the cells that has been transfected. GFP will then emit a bright green fluorescence under UV light at a wavelength of 395 nm, which can be seen under the fluorescent microscope (Nikon Eclipse TS100). It is then easy to know which cells have been successfully transfected.

Two solutions are needed for this method of transfection. Tube A consists of 0.5 µg of the channel of interest, 0.5 µM GFP, 22.5 µl CaCl<sub>2</sub> and deionised water to reach the total volume of 100 µl. Tube B consists of 100 µl phosphate-free Buffer (HEPES) and 1.8 µl phosphate buffer. Tube B is then added to Tube A dropwise and left for 5-20 minutes to form a CaPO<sub>4</sub>/DNA precipitate. The newly formed precipitate is mixed gently and 50 µl is pipetted into each of the 4- well plate. The cells are then washed 4-8 hours later twice with 1 ml PBS and then 50 µl of media is added to each well plate. The plate is then left in an incubator for 12 hrs for electrophysiology experiments.

## 2.4 Mutagenesis

Point mutations were introduced by site-directed mutagenesis into  $K_{2P}$  channel clones using the Quikchange II site-directed mutagenesis kit (Agilent). The mutagenic oligonucleotide primers are all designed individually for the desired mutation. When creating the mutagenic primers there are parameters that need to be met. The mutagenic primers must contain the desired mutation site and anneal must match the opposite strand of the plasmid. The primers should be between 25-45 bases in length with the mutation site sitting in the middle of the primer with ~ 10-15 bases on either side of the desired mutation site. Anything over that length could lead to the formation of a secondary structure. The primer should also contain 40%-60% glycine and cysteine (GC) content and end on either a C or G base. The two newly synthesised complementary oligonucleotides containing the desired mutation is now ready to be prepared for thermal cycling reaction.

To prepare the LB agar plates, add 35g pre-mixed LB agar powder to 1L ddH<sub>2</sub>O and mix. Autoclave the liquid and when this is completed, remove from autoclave and allow to cool. Add 500  $\mu$ l of 50mg/ml antibiotic ampicillin into 1L of LB agar. Next pour the liquid into a polystyrene petri dish (100mm x 15 mm) on a sterile bench and near a Bunsen burner for sterilisation. Cover with lid and allow the solution to solidify and cool which takes around 30-60 minutes. Label plates with antibiotic and date and allow sit in plastic bags with an absorbent material at 4°C to reduce condensation.

To prepare synthesis of the mutant strand it is important that all solutions are kept on ice and are as cold as possible at all times. To prepare a control reaction, add 5  $\mu$ l of 10x reaction buffer, 2  $\mu$ l of control plasmid and 1.25  $\mu$ l of each control primer into a PCR tube. Next, add 1  $\mu$ l of dNTP mix and 39.5  $\mu$ l of double-distilled water (ddH<sub>2</sub>O). Finally add 1  $\mu$ l of *PfuTurbo* DNA polymerase. To prepare the sample reaction in a PCR tube, add 5  $\mu$ l of 10x reaction buffer, 1  $\mu$ l of the sample dsDNA template. Following this add 1.25  $\mu$ l of each oligonucleotide primers, 1  $\mu$ l of dnTP mix, 3  $\mu$ l of QuikSolution reagent to improve linear amplification. The solution final volume should be reach 50  $\mu$ l by adding ddH<sub>2</sub>O. Then add the final solution of 1  $\mu$ l of *PfuTurbo* DNA polymerase.

The number of cycles and temperature settings depends on what type of mutation is needed, which is described in Table 2.1.

| Type of mutation desired                    | Number of cycles |
|---|------------------|
| Point mutations                             | 12               |
| Single amino acid changes                   | 16               |
| Multiple amino acid deletions or insertions | 18               |

**Table 2.1:** *Number of cycles needed of each type of mutation*

Following temperature cycling, the reaction should be placed in ice for 2 minutes so that the reaction reaches a temperature of  $\leq 37^{\circ}\text{C}$ .

Add the restriction enzyme, *Dpn I* to the reaction tube. When the enzyme is added, gently mix the solution through pipetting up and down. Spin the solution down and incubate at room temperature for an hour.

The next stage is transformation of XL1-Blue cells. The cells are gently thawed out on ice. For each reaction, aliquot 40  $\mu\text{l}$  of the supercompetent cells into a pre-chilled 14ml BD Falcon polypropylene round-bottom tube. Transfer 3  $\mu\text{l}$  of *Dpn I*-treated DNA from each reaction to separate aliquots of the supercompetent cells. Swirl the transformation reactions to gently mix the solutions and incubate the reactions on for 30 minutes. The transformation reactions should then be heat pulsed for 45 seconds at  $42^{\circ}\text{C}$  and then placed on ice for 2 minutes. Add 350  $\mu\text{l}$  of preheated NZY<sup>+</sup> broth and incubate the transformation reaction at  $37^{\circ}\text{C}$  for an hour with shaking at 225-250 rpm. Plate 5  $\mu\text{l}$  of transformation solution onto a LB-ampicillin agar plate and spread. The plate can then be incubated at  $37^{\circ}\text{C}$  for >16 hours. This process was carried out by Emma Veale.

## 2.5 Electrophysiology experiments

### 2.5.1 Voltage clamp technique

The road to modern day voltage patch clamping started with Cole (1949) and, Hodgkin and Huxley (1952) and their experiments using giant squid axon in their study of ionic conductance. Hodgkin and Huxley used a two-electrode voltage clamp where the membrane voltage was controlled via a feedback amplifier and the current was measured to analyse ion channel activities. However, the disadvantage of this technique is that it could only be used

on larger cells (>20µm) and could not be used in tissue cells (Sontheimer and Ransom 2002).

Neher and Sakmann (1976) went on to develop the patch clamp method further by using a relatively large-tip pipette which did not penetrate the cell but formed a seal. This seal was stronger than the membrane, thus pulling the pipette away from the cell would cause the membrane to rupture around the patch but keep the seal intact. This introduced single channel recordings from the membrane patch to come into contact with defined media (Hamill et al 1981).

The voltage clamp method is useful in two different ways. Firstly, it separates the membrane ionic current from the capacitive current. Secondly, the membrane voltage is controlled. Therefore, the currents being recorded are measured under uniform conditions and experience the same voltage (Halliwell et al 1994).

Patch clamping is a form of voltage clamp, as it uses a feedback amplifier to set the membrane potential ( $V_m$ ) of the cell to the command voltage ( $V_{comm}$ ). The clamping amplifier passes current to control  $V_m$ .  $V_m$  is measured by the voltage follower. The feedback amplifier is a differential amplifier that compares the difference between the two voltage inputs,  $V_m$  and  $V_{comm}$  and makes it equal to the output ( $V_o$ ).

$$V_o = V_{comm} - V_m$$

The amplifier contains a feedback resistor ( $R_f$ ), with a known value, which allows the flow of a feedback current ( $I_f$ ) to make the  $V_m$  equal to  $V_{comm}$ .

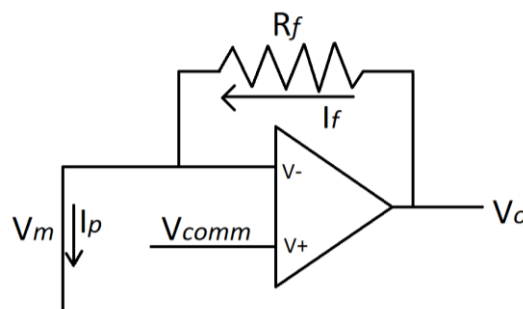


**Figure 2.1:** The patch clamp differential amplifier works to ensure the pipette voltage equals the command voltage

The feedback resistance is located between the output and the negative input. This is important as Ohm's law states that a current will flow through this resistance proportional to

the voltage difference between the two ends of the resistance, thus the current flow is a result of the difference between the  $V_o$  and  $V_m$ . The causes  $V_m$  to always be at  $V_{comm}$ .

This will allow for the calculation of the ionic current, which is equal to the amount of current which passed through the pipette to sustain  $V_m = V_{comm}$ . As stated previously, the  $R_f$  will cause  $V_m$  to equal  $V_{comm}$

$$\mathbf{I_p = (V_{comm} - V_o) / R_{feedback}}$$

Now that we have the  $V_{comm}$  and  $R_f$ , we can now conclude the  $I_p$ , pipette current, by measuring  $V_o$ . Therefore, the feedback amplifier function as a current ( $I_p$ )-to-voltage ( $V_o$ ) converter. It is assumed in these equations that  $V_m$  is equal to  $V_p$ , pipette voltage (Halliwell et al 1994).

$$\mathbf{V_o = - I_p R_f + V_{comm}}$$

## 2.5.2 Electrical Properties of the Cell Membrane

The phospholipid barrier acts as a barrier to ions and, in contrast, the intra and extracellular media act as effective conductors of ions due to its dilute saline solutions. Therefore, the membrane has a conductor-insulator-conductor sequence which makes an excellent capacitor. However, the insulation is not perfect as the membrane contains numerous ion channels which will lead to some leaks.

The membrane potential ( $E_m$ ) is the potential difference between the inside and the outside of the cell. This movement of ions across the membrane is expressed in current. There are two factors that determine the size of the flow of ions: driving force and membrane resistance. The driving force is defined as the difference between the equilibrium potential and the membrane potential. The greater the distance between the two potentials; the higher the net flow of a particular ion. Thus, current is proportional to driving force (volts). The current is also limited by resistance of the membrane. Current is inversely proportional to resistance.

Input resistance ( $R_{input}$ ) will determine the change in membrane voltage ( $\Delta V$ ) in response to current ( $I$ ).  $R_{input}$  depends on the size of the cell, the membrane resistance and the density of opened channels.

$$\Delta V = I R_{input}$$

As stated before a membrane is a capacitor. A capacitor has the ability to store electrical charge. The membrane exerts an electromagnetic field on both sides on the bilayer. This will allow charged particles to gather at the membrane. The amount of charge stored at the membrane can be calculated.

$$Q = E_m C$$

**Figure 2.2:**  $Q$  is the charge stored,  $E_m$  is the potential difference and  $C$  is the membrane capacitance (in farad).

This equation shows that the capacitance is the measure of the membranes ability to store charge at any potential. This capacitance needs to be charged to alter the voltage and this current pass is not instantaneous and therefore imparts a delay. Membrane capacitance is also linked to physical dimensions of the membrane, as the bigger the membrane the larger accumulation of charge. The membrane thickness is uniform however the capacitance is proportional to the circumference of the cell membrane.

For that reason, the capacitance is a good estimation of the membrane surface area (Molleman 2003). The membrane time constant also determines the rate of change in membrane potential. The time constant is proportional to the input resistance and the capacitances

$$\tau = RC$$

The greater the time constant, the more time is needed for the membrane to reach the step voltage.

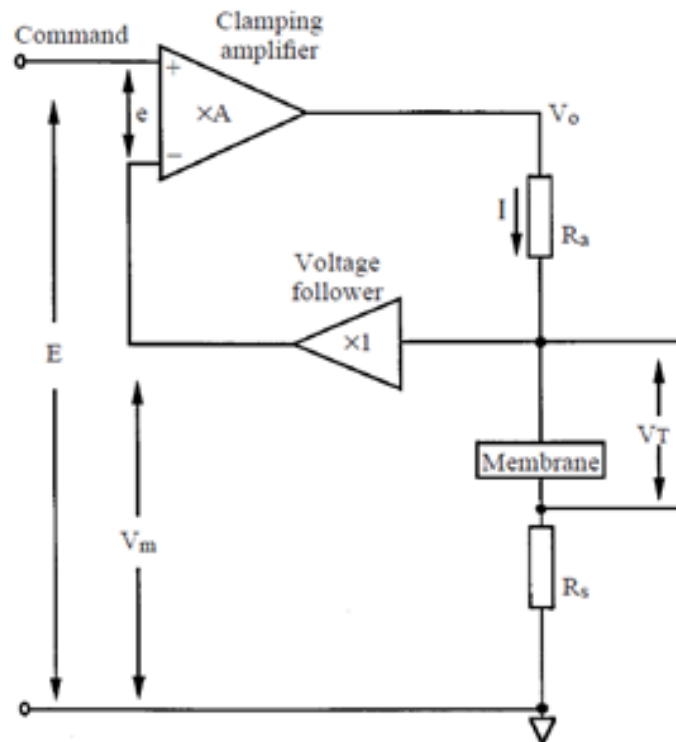


**Figure 2.3:** Simplified Voltage clamp circuit.  $E = V_{command}$ ,  $V_T$ : True membrane potential,  $R_s$ : serial resistant,  $R_a$ : access resistant,  $V_o$ : amplifier output (Halliwell et al 1994).

### 2.5.3 Series resistance and capacitance compensation

During whole cell patch clamping, there are resistance in series with the membrane and the electrode. The series resistance ( $R_s$ ) is the sum of the pipette (electrode) resistance ( $R_p$ ) and access resistance ( $R_a$ ) which is located between the end of the electrode and the interior of the cell. There are problems that can result from the  $R_s$ . The first is that the membrane potential measured and controlled at  $V_p$  and the voltage at the membrane may be different due to current flowing across the  $R_s$ . This will lead to a voltage drop. The second problem caused by  $R_s$  is its interaction with the membrane capacitance. The resistance and the capacitance are linearly proportional to the time constant ( $RC$ ). A rapid step change in the  $V_{comm}$  will change the  $V_m$ . However, there will be a delay by a few millisecond by  $R_s$  caused by a strong low-pass filtering effect which will increase the time constant. Therefore, the voltage step will not be immediately changed at the membrane (Sontheimer and Ransom 2002). The size of the series resistance error is  $I \times R_s$ , this can be significant in large current measurements. If it is significant,  $R_s$  compensation can be actualised through adding voltage signal depending on the membrane current and to the  $V_{comm}$  (Halliwell et al 1994).

Capacitance compensation can be important as rapid voltage changes are used to record the behaviour of the ion channels. As the membrane potential is changing, a transient capacitance current is produced. This transient current needs to be suppressed as the current will become too large to pass through the resistor. The system would become saturated and the step voltage change would be prolonged. In most voltage clamp experiments, the voltage change is in the form of a square step. This voltage step will cause a rapid spike of capacity current before the rate of voltage change ( $dV/dt$ ) is zero at which the voltage step is at a steady state and the current can be recorded. It must also be noted that the electrode wall acts as an insulator between two conductors (the bath solution and the electrode solution). To compensate this saturation, the approximate current is passed through the amplifier input (Yamane 2007).

## 2.5.4 Pipettes and internal solution

Patch clamping technique uses two electrodes: the pipette electrode and the bath electrode. Both are made from silver chloride. Silver chloride electrode is a silver wire or pellet which has been immersed in bleach of 10-15 minutes which results in chloriding of the silver wire. This will allow the wire to become a reversible electrode. To establish the membrane potential, a redox reaction takes place between the metals and the salt solutions. In experimental situations, if the metal-liquid junction potentials are not equal, it will cause offset current which could be incorrectly cancelled out. It is therefore important to use identical material with similar surface area so that you will get matching but opposite solid-liquid potentials on both sides and it can cancel each other out. Other problem can occur is electrode polarisation. This can occur when ions accumulate near electrodes that have direct current (DC) potential difference. Cations move to the negative electrode and anions move towards the positive electrode. This will lead to delays in potential changes and increases resistance. Electrode polarisation is subject to material, and silver chloride is the weakest polarisation material (Molleman 2003).

Patch pipettes (or electrodes) are made from thick-walled glass capillaries which are heated until molten and stretched into shape. This is a two-stage process carried out by a vertical puller (Narishige). The first stage is the heated coil is set at 76 degrees. The glass capillaries are thinned in the middle at this heat. The second stage consists of the glass capillaries being re-centred to the thinnest point and in respect to the heated coil. The coil is set at 60 degrees. This results in the capillaries breaking at the thinnest part, which will fashion two pipettes. The pipette tip should be 1-2  $\mu\text{m}$  wide with a resistance measuring between 3 -6  $\text{M}\Omega$  for whole-cell patch clamping. The second stage temperature can be adjusted if the resistance is not in this range (Halliwell et al 1994). This is seen as relatively blunt tip in

comparison to other patch clamp techniques however the blunt tip is needed to achieve and sustain a stable electrode-membrane seal (Sontheimer and Ransom 2002). Patch pipette were filled with standard (high EGTA) internal solution. Internal solution contains 150mM KCl, 3mM MgCl<sub>2</sub>, 5mM EGTA and 10mM HEPES and was then adjusted to pH7.4 using KOH. This internal solution contains electrolytes and other concentration solutions that are similar to the cytoplasm.

## **2.5.5 The whole cell configuration and current recording**

The whole cell patch clamp technique is used to study the properties of a small patch of the membrane. Current was recorded from cells clearly expressing WT or mutant K<sub>2P</sub> channels. Patch pipette were filled with internal solution and mounted to the pipette holder. The pipette holder is controlled by its manipulator which allows to experimenter to move the pipette in 3D movements. The pipette is lowered into the bath solution. A square pulse is used to measure the resistance of the pipette. If the resistance is between the parameters, the pipette can be lower towards the target cell. To start the formation for a high resistance seal (Giga-ohm) by first applying light contact on a tiny area, or patch, of cell membrane. A small amount of negative pressure is applied using a 5ml syringe connected to the pipette holder. The length of time taken to form this seal varies however it should take around 30 seconds. When the giga-ohm seal forms, the displayed resistance of the electrode seen as the square current will disappear. It is an all-or nothing process. The giga-ohm seal should remain intact after the pressure is released. A tight seal is important as it prevents the leakage of current and diffusion of small molecules. At this stage in experiment has entered the cell-attached configuration.

After this, higher but shorter negative pressure then follows to break the patch of the cell membrane giving a 'whole cell'. The pressure must break the patch between the pipette tip and the cytoplasm without disrupting the seal at the pipette edge and the membrane. Now at the whole cell configuration, the interior of the pipette and the cytoplasm are in contact and this allows for the recording of the exchange of ions and drug molecules. The Membrane Test in Clampfitx 10.2 produces a definable voltage pulse which can then be used to read a range of measurements. This included: Membrane capacitance (C<sub>m</sub>), Access resistance (R<sub>a</sub>), Membrane resistance (R<sub>m</sub>) and Total resistance (R<sub>t</sub>). The current is filtered by a low pass filter at 2kHz and then sampled 5kHz.

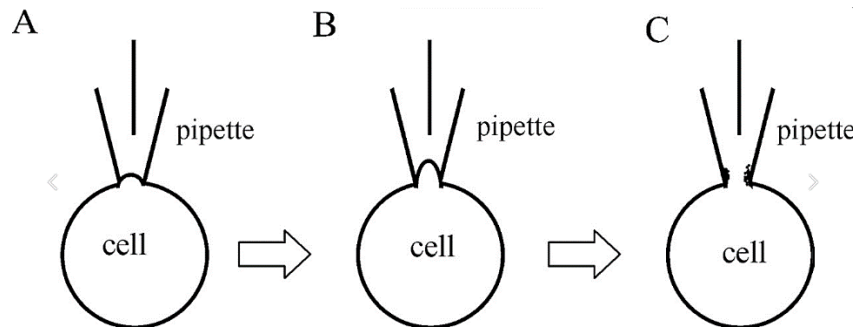


**Figure 2.4:** Formation of whole cell patch clamp. A) the patch pipette is placed on the transfected cell which is indicated by a small increase in the pipette resistance. B) cell-attached was achieved using negative pressure to form a giga-ohm seal. C) quick application of negative pressure would break the membrane patch and form the whole cell mode (Li 2008).

## 2.5.6 Electric circuit

The pipette holder (Warner Instruments) is attached to the amplifier stage head. The pipette holder contains a AgCl wire which is connected to the stage head. This allows for an internal solution filled pipette to become in contact with the wire and therefore the rest of the circuit. A ground pipette, also AgCl, is placed in the bath to close the circuit.

The circuit is connected to a digitiser interface (Digidata 1440A) which is used to visualise the cellular electrical signals onto the computer. A specific stimulation was entered on the computer and converted into an electrical current by the interface to be sent to the pipette inside the electrode. This electrical signal was then converted into a digital signal for the computer. The circuit is also connected to the amplifier (Axopatch 200B) which filters and converts the current the voltage coming from the electrode in the external bath by a low pass filter set at 2kHz.

Other important features to the rig set-up are the microscope with the epi-fluorescence attachment (Nikon Eclipse TS100) which are used to identify transfected cells under UV light at a wavelength of 395 nm. A vibration isolation table (TMC, Micro-g lab table) is used to keep a minimal mechanical interference. A faraday cage (Scientifica) was used to eliminate any electrical noise or hum from the environment. A piezo-electric manipulator (Scientifica) was used to maneuver the pipette and patch the cell. The computer software (Clampx 10.2) was used to set up the protocol of the electric circuit.

## 2.5.7 Protocol

Voltage-clamp recordings were made using the whole cell recording techniques. A step-ramp protocol was used in the recording. The cells were held at a holding potential of -60 millivolt (mV). The cells were then hyperpolarised from -60mV to -80mV for 100ms and then held at -40mV for 500ms. This concludes the step part of the protocol. The cells are then held at -120mV for 100ms before beginning the ramp to +20mV which lasts for 500ms. After the ramp, the cells are held at -80mV for 100ms before resuming to -60mV holding potential. The protocol lasts for 1.5 seconds, including sampling at the holding potential. The protocol was repeated every 5 seconds (sweep) with constant superfusion of external bath solution. As the voltage changes the current is measured and plotted. Currents were low pass filtered at 2kHz and digitized at 5kHz using a Digidata 1440A.

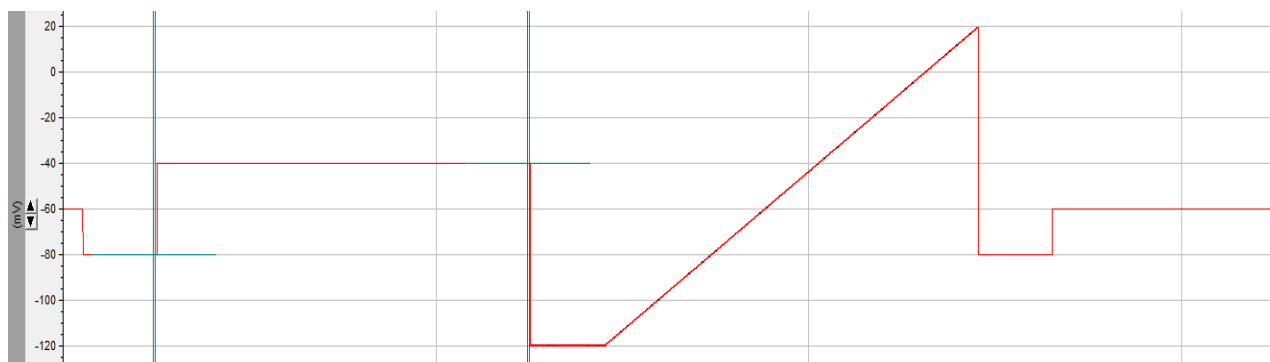


**Figure 2.5:** Voltage protocol used to study  $K_{2P}$  channels. The cursors show where the currents were measured from (-80mV and -40mV).

$K_{2P}$  channels are activated at wide ranges of voltages. This allows us to measure at -80 mV, close to  $K^+$  equilibrium ( $\sim -90$  mV), and at -40 mV. This step produces a driving force for current to flow through the conductive channel. The -40mV step is designed to ensure that there is no contamination from endogenous Kv channels found in tsA 201 cells. The current amplitude is measured by subtracting the current at -80 mV from the current at -40 mV. If the current at the holding potential is below 0 pA, it is seen as a leaky current. Also, if the current at -80 mV is below -200pA is it deemed a leak current. These recordings are then excluded. The protocol ramp also allows assessment of the quality of the recording. If the ramp is seen as linear during a change in current it could suggest a leak current.

## 2.5.8 Data Analysis

Current obtained was analysed using pClamp 10.2 software (Molecular Devices). Any further analysis and statistical tests were performed using Excel (Microsoft) and GraphPad Prism (GraphPad Software). Data are expressed as mean  $\pm$  standard error of the mean. Unpaired Welch's t-tests were used as to assume unequal variances and when there were unequal

sample sizes. It must be noted however that testing for variance can lead to Type 1 error and has therefore been advised to use the unequal variance without preliminary tests (Ruxton, G. D. 2006). The two-tailed Welch's t-test was used to test both directions of the relationship. The one-tailed Welch's t-test was used if the question is the difference is significantly greater or less, it cannot test for both. One-way ANOVA tests were used when more than two data sets were analysed. The Dunnett's method was used in ANOVA where every mean is compared to the control mean. The Tukey test is a post-hoc ANOVA test which shows the overall significance of the whole data set (Rowe 2016).

## **2.5.9 Drug application**

Extracellular solution (1litre) was made up of 145mM NaCl, 2.5mM KCl, 3mM MgCl<sub>2</sub>, 1mM CaCl<sub>2</sub> and 10mM HEPES and was then titrated to pH 7.4 with NaOH. Stock solutions of compounds were made using DMSO or ethanol and stored in the required environment. Drug solutions were made fresh every day performing electrophysiology. Drug solutions were made at the intended concentration for the electrophysiology experiments via dilutions from a stock solution into the extracellular solution. Recordings were carried out with the cells superfused with the drug free extracellular solution, and then drug solution accordingly. The drug solution was then washed off by control to evaluate the reversibility of its effect. All compounds were applied from the extracellular side of the membrane by bath perfusion. Complete exchange of bath solution occurred within 100-120s. All data were collected at room temperature (19-22°C).

## **2.6 Limitations**

The compound stock solutions were made up in 100% DMSO or ethanol to a final concentration of 10 mM. The stock solutions were then diluted down in external solution to the respective concentrations described. However, control DMSO and ethanol were not used, and this may be a limitation in the experiments.

## **2.7 Structure visualisation**

### **2.7.1 Channel mutation creation**

All channels need a PDB (Protein Data Bank) file to carry out mutations. These PDB files can be opened using PyMol software. PyMol creates a three-dimensional model structure of the ion channel. Modeller 9.12 software was used in mutating PDB channel files as needed. Python 2.3 (software language) was installed and Modeller was installed under the Python

directory. The mutate model script was created by the laboratory of Andrej Sali ([www.salilab.org](http://www.salilab.org)). This script is activated through Modeller to be used to mutate the selected channel. The script takes the selected PDB file and mutates a single residue of the channel. The new mutated ion channel is saved as a PDB file and can therefore be opened in PyMol. If multiple residues need to be mutated, the script is run multiple times and this creates multiple PDB files each time. It must be noted however that the script only works on one subunit at a time so for  $K_{2P}$  channels, the script must be run on both subunits.

# **CHAPTER THREE**

## **Regulation of TREK1 channels by sipatrigine and lamotrigine**

# Introduction

## 3.1 Complex neurobiological systems mediate pain

Pain is a system caused by diseases of the brain, spinal cord and nerves in the nervous system. Pain has proved to be a complex challenge which has been approached by various medicines. The most common drugs used to manage pain are opioid and non-opioid analgesics. Unfortunately, a wide range of medicines for pain are inadequate or can cause adverse drug reactions (ADRs) and addiction (National Research Council (US) Committee 2009).

## 3.2 Somatosensory neurons and nociceptors

The somatosensory systems process information of several somatic sensations for example temperature and touch. The somata of the sensory neurons are found in the dorsal root ganglia (DRG). The DRG is located between the dorsal root and the spinal nerve. It is understood that after injury, these neurons will increase nociceptive signalling through the generation of neuronal excitability. DRG neurons diverge from the axon into the peripheral and central afferent fibers. Nociceptors are neurons containing peripheral fibers that are stimulated by noxious sensory inputs. The largest group of nociceptors which diffuses pain are unmyelinated C-fibers. These C-fibers conduct slowly and respond to noxious stimuli and carry electrical impulses along the peripheral axon of the nociceptor into the CNS. There are also ion channels called transient receptor potential vanilloid (TRPV1) on nociceptor terminals that act as molecular transducers to depolarize these neurons. TRPV1 are known targets for inflammatory pain relief by antagonists and agonists (National Research Council (US) Committee 2009).

## 3.3 TREK1 is a novel pain target

Neuropathic pain is caused by a dysfunction of DRG and it is a difficult type of pain to treat. It is known that after injury to afferent neurons, ion channels will produce a greater generator potential which leads to an increased probability of action potential. Injury also leads to a decrease in threshold of sodium channels to initiate the spike in the action potential. All this together develops into DRG hyperexcitation. The symptoms of neuropathic pain include hypersensitivity to mechanical and thermal stimuli which is then addressed by nociceptors in the somatosensory system (Campbell and Meyer 2006). TREK channels are present on sensory neurons including DRG neurons and are co-localised with TRPV1. However, there is little information about the expression and role of TREK1 and TREK2 in neuropathic pain.

Using markers for the highly expressed IB4 and TREK channels it was found that there was coexpression in the DRG in neuropathic pain mouse model. When investigating expression of TREK1 it was identified that the channel was up-regulated and activated in the neuropathic pain mouse model. It is thought that this over expression is linked to TRPV1 activity and its contribution to neuropathic pain management. Therefore, it suggests that TREK1 downregulation could play an important role in neuropathic pain management (Han et al 2016). Intuitively one would predict that activators of  $K_{2P}$  channels would be useful in pain as they will dampen excitability of DRG neurons by hyperpolarising the membrane. However, there is an argument that  $K_{2P}$  channel blockers are also effective because depolarisation will inactivate voltage-gated Na channels and block AP firing (see discussion and, for example, Meadow et al 2001, Mathie 2010).

### **3.4 $K_{2P}$ lateral fenestrations**

Fenestrations were first characterised in voltage-gated sodium channels. It was seen that lipids could enter the four lateral openings and would occlude the cavity and block ion conductance (Payandeh et al 2011). The revelation of  $K_{2P}$  structures through a series of crystallisation and electrophysiology studies have provided a good insight into the gating function of the channels. So far  $K_{2P}$  channels which have been crystallised have been shown to hold lateral openings at the M2 helix and the M4 helix. These so-called openings or “fenestrations” allow a connection between the transmembrane pore and the membrane lipid bilayer (Brohawn, Campbell and MacKinnon 2013). In TWIK1 channels it was found that acyl chain lipids from the bilayer leaflet were able to enter the upper fenestration however it was not long enough to enter the pore. It is therefore not believed to block the inner pore. It is a similar situation with the lower fenestration as again lipid tails are found at the entrance but they are not long enough to block the pore cavity (Aryal et al 2015). TRAAK channels differ from TWIK1 as it was revealed that acyl chain lipids may protrude into the cavity. (Brohawn, Campbell, and MacKinnon 2014). Moreover, TREK2 co-crystallised channel with norfluooxetine identified the same intramembrane-side fenestrations below the selectivity filter. It is unclear whether TREK channels also allow acyl chain lipid into the cavity. If alkyl chains do enter the pore through the lateral fenestrations, it might impact the conductance and pharmacological properties of these  $K_{2P}$  channels (Dong et al 2015).

## 3.5 Fenestration gating

The lateral fenestrations seen in  $K_{2P}$  channels are a result of conformational changes at the M2 and M4 helices alongside bending of the highly conserved glycine hinges. Therefore, it is believed that  $K_{2P}$  channels enter into two different conformations.

The “up state” shows an upward movement which results in kinking of the M4 helix at the glycine hinge. This upward movement also bends the glycine hinges at M2. This movement opens the cavity and closes the fenestrations. This allows for full occupation of ions into the selectivity filter. And it therefore believed to be conductive.

The “down state” holds the M4 down wards and pushed the glycine hinges towards the cytoplasm. This movement creates the fenestration between the M4 and M2. Thus, the cavity is in contact with the lipid membrane. This results in no ions observed in the pore cavity and the channel is therefore non-conductive (Brohawn et al 2015; Dong et al 2015)

TREK1 and TREK2 has already been discussed as containing the structurally important fenestrations seen in both TWIK1 and TRAAK. TREK2 co-crystallised with norfluoxetine shows the “down state” and “up state” which represents the non-conductive and conductive states, respectively. The fenestrations are only present in the down state as the openings are blocked in the up state by the new positioning of the F316 and L320 residues. It is also important to note that the co-crystallised structure of TREK2 with the state-dependent drug norfluoxetine is in the down configuration. The binding is believed to be dependent on site L320 as mutation of this site reduces the inhibition which can only occur if the fenestrations are present (Dong et al 2015).

## 3.6 Aim of this chapter

The aim of this chapter is to clarify the difference between lamotrigine and sipatrigine and its inhibition of TREK1. To investigate the mechanism of how the channel is regulated, whole-cell patch clamp electrophysiology and site directed mutagenesis will be carried out by TREK1.

# Results

## 3.7 Sipatrigine inhibits TREK1 channels

Currents through wild-type (WT) human TREK channels transiently expressed in tsA-201 cells were measured using whole-cell patch-clamp electrophysiology. The currents were measured in the presence and absence of sipatrigine (100  $\mu$ M) which significantly reduced the TREK1 current ( $87 \pm 2\%$ , mean  $\pm$  S.E.M.,  $n = 19$ ). Current inhibition was reversed by  $70 \pm 11\%$  ( $n = 17$ ) when washing the cells with a drug free external solution. The following shows a representation of general TREK1 WT currents (see Fig 3.1).

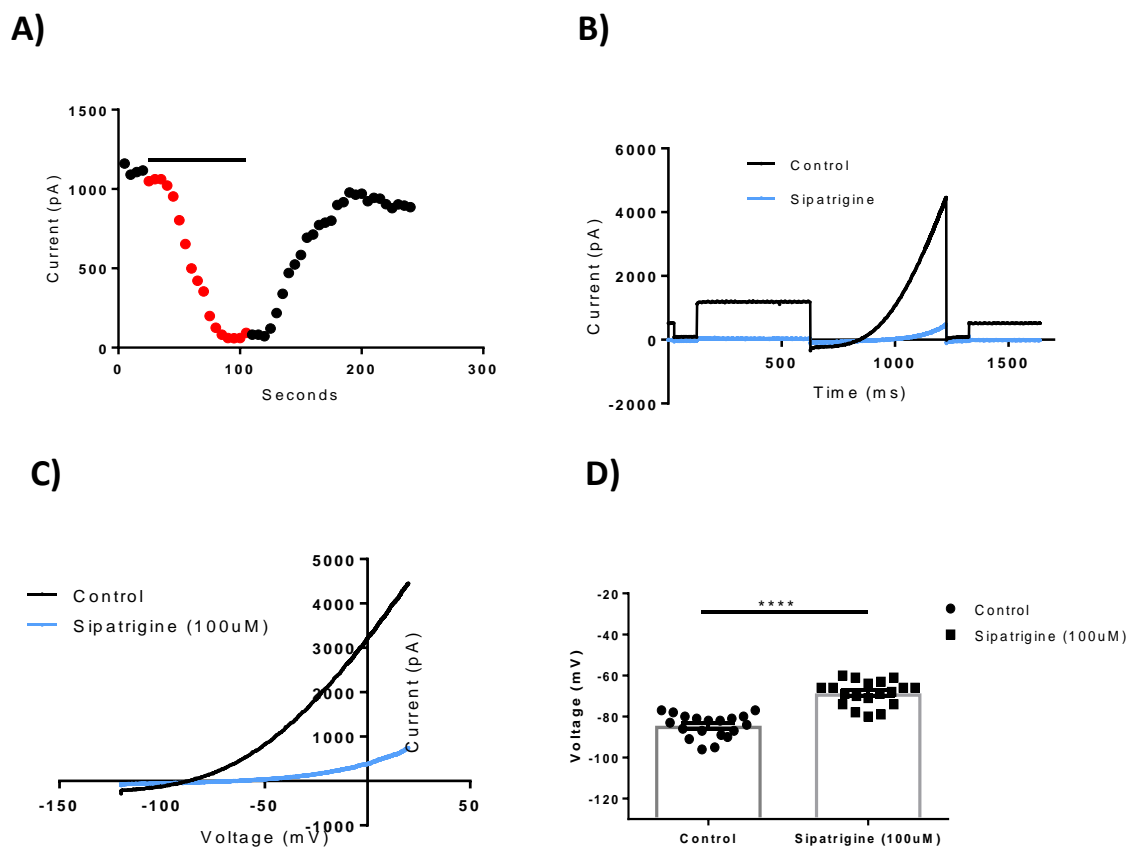


**Figure 3.1:** Sipatrigine (100  $\mu$ M) inhibition of WT TREK1 channels. (A) Time-course plot of sipatrigine effect on TREK1. Points show current in the presence and absence of sipatrigine. (B) Trace of current at different voltages controlled by the protocol. Each trace is an average of five consecutive traces in the presence and absence of sipatrigine. (C) Current-voltage relationship of TREK1 obtained from the ramp voltage changes in the presence and absence of sipatrigine. (D) Average reversal potential of TREK1 current, in control and in the presence of sipatrigine ( $n = 19$ ). Paired Student *t*-tests was used.

The reversal potential of TREK1 current was measured to investigate the effect of sipatrigine on TREK1 ion selectivity. The TREK1 reversal potential changed to  $-69 \pm 1$  mV when sipatrigine was in the presence of the channel, compared to  $-85 \pm 1$  mV before the drug was applied ( $n = 19$ ) (see Fig 3.1 C-D).

### 3.7.1 TREK1 inhibition by sipatrigine is concentration dependent

Experiments were carried out to investigate how different sipatrigine concentrations may affect TREK1 channels. Sipatrigine was applied to TREK1 channels at concentrations of 30  $\mu\text{M}$ , 10  $\mu\text{M}$ , 3  $\mu\text{M}$  and also at 100  $\mu\text{M}$  which has already been discussed. Sipatrigine (30  $\mu\text{M}$ ) concentration inhibited current by  $56 \pm 5\%$  ( $n = 13$ ), while the 10  $\mu\text{M}$  concentration of sipatrigine produced  $40 \pm 5\%$  ( $n = 10$ ). The lowest concentration (3  $\mu\text{M}$ ) inhibited the channel by only  $27 \pm 4\%$  ( $n = 8$ ). The fitted curve showed that sipatrigine inhibited TREK1 channels with an  $\text{IC}_{50} = 15.94 \mu\text{M}$ . 95% Confidence intervals (12.49 – 20.34  $\mu\text{M}$ ). The Hill slope was 0.82 with the 95% Confidence interval between 0.6 – 1 (see Fig 3.2). However, as can be seen the dose response curve does not measure 100% inhibition and more concentrations could be used to measure this (see Fig 3.2).

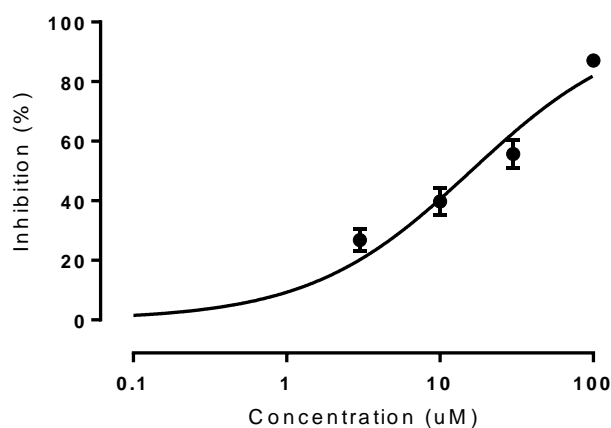


**Figure 3.2:** Dose- response curve for sipatrigine inhibition of TREK1 current

### 3.7.2 Sipatrigine inhibition of E306A TREK1 channels

The residue E306 is located between the TM4 and the intracellular C terminus which is a key location for gating regulation. It was found that mutation of this site to an alanine will mimic the effects of protonation and will lock the channel into a permanently open state (Honoré et al 2002). The mutated site E306A showed a significant increase in resting current density ( $137 \pm 26$  pA/pF,  $n = 9$ ) compared to TREK1 WT ( $87 \pm 7$  pA/pF,  $n = 25$ ), shown in Fig 3.3.

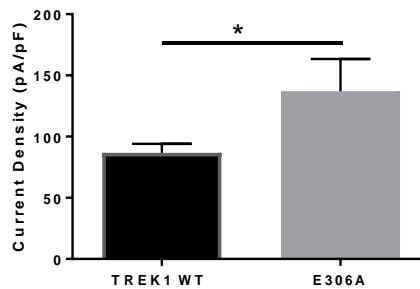
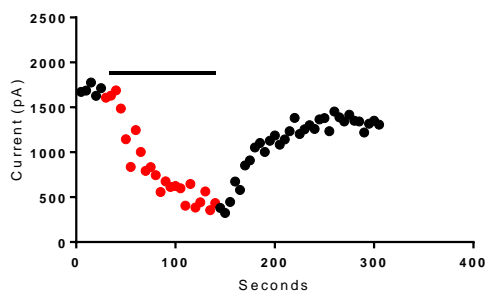


**Figure 3.3:** Current density (pA/pF) of TREK1 WT ( $n = 25$ ) compared to the gain-of-function mutated TREK1 E306A ( $n = 9$ ). Unpaired one-tailed Welch's *t*-tests was used.

It was also found that sipatrigine ( $100\mu\text{M}$ ) did produce an inhibitory effect of  $64 \pm 4\%$ ,  $n = 7$  on TREK1 E306A current. This is significantly less than TREK1 WT inhibition ( $87 \pm 1\%$ ,  $n = 19$ ).

**A)**



**B)**

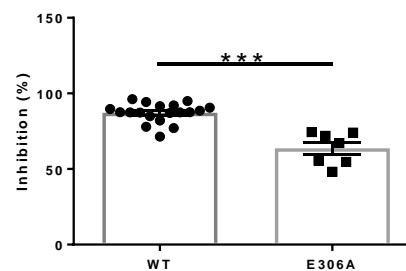
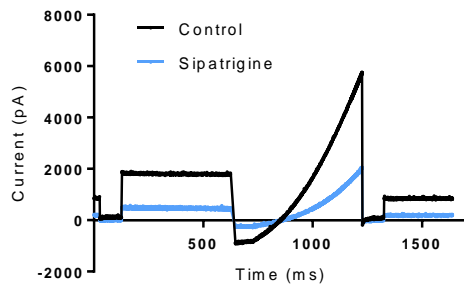


**Figure 3.4:** Sipatrigine ( $100\mu\text{M}$ ) has a significantly effect on TREK1 E306A. A) Time-course of sipatrigine ( $100\mu\text{M}$ ) effect of TREK1 E306A in the presence and absence of sipatrigine. B) Inhibition of WT ( $n = 19$ ) and mutated TREK1 E306A ( $n = 7$ ) with sipatrigine ( $100\mu\text{M}$ ). Unpaired two-tailed Welch's *t*-test was used.

The reversal potential of TREK1 E306A current was investigated and was shown that no significant change was seen in the presence of sipatrigine.

**A)**



**B)**

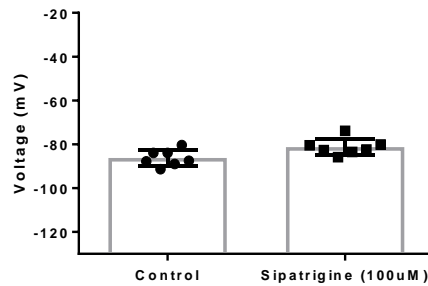


**Figure 3.5:** A) Trace of current at different voltages controlled by the protocol. Each trace is an average of five consecutive traces in the presence and absence of lamotrigine. B) Average reversal potential of TREK1 E306A current, in control and in the presence of sipatrigine ( $n = 7$ ). Paired Student *t*-tests was used.

The results here show that sipatrigine has a decreased degree of inhibition for the channel with the gain of function mutation E306A. This would suggest that sipatrigine inhibition may favour the closed state but can still function in the more open state.

### 3.8 Lamotrigine inhibition of TREK1

TREK1 (WT) channels were transiently transfected in tsA-201 cells and currents were again measured using whole-cell patch-clamp electrophysiology. All currents were measured in the presence and absence of lamotrigine (100  $\mu$ M) showed current inhibition of  $30 \pm 6\%$  ( $n = 6$ ). The following shows a representation of general TREK1 WT currents (see Fig 3.5).

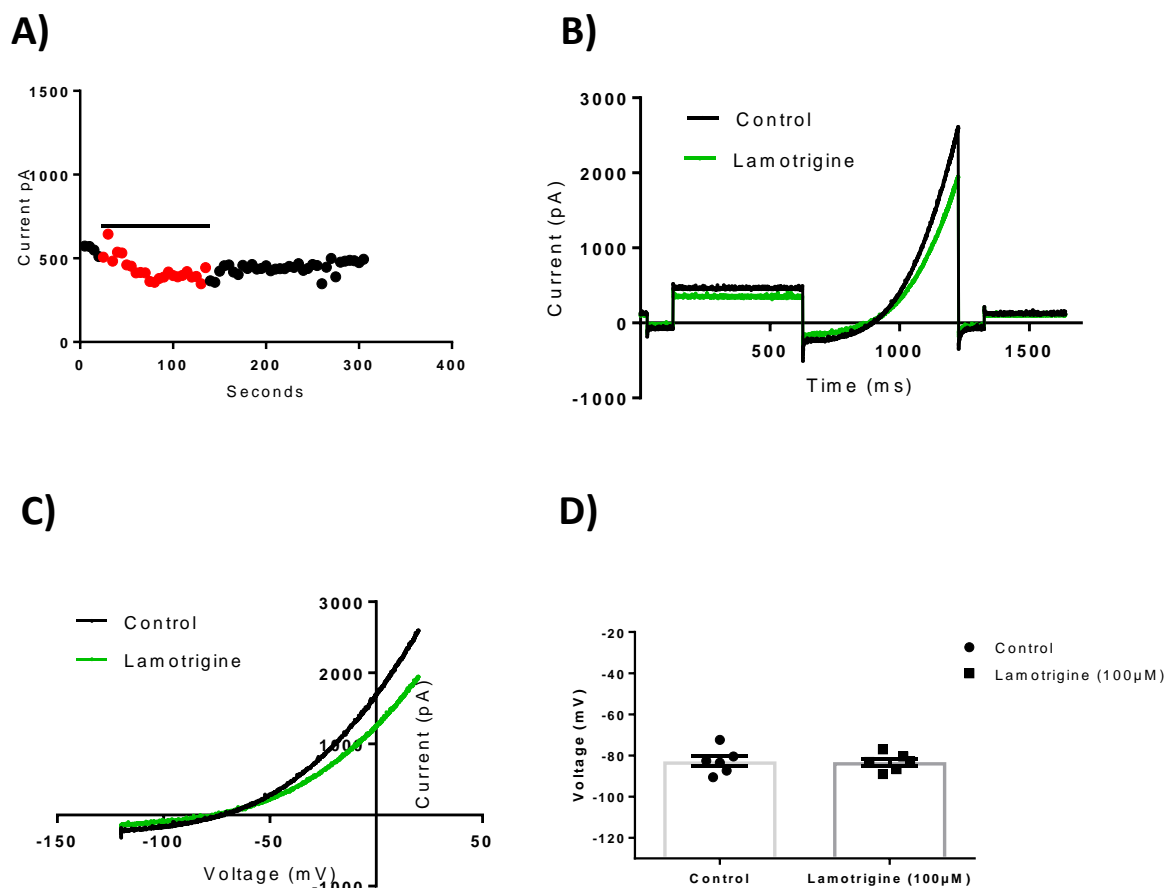


**Figure 3.6:** Lamotrigine (100  $\mu$ M) inhibition of WT TREK1 channels. (A) Time-course plot of lamotrigine effect on TREK1. Points show current in the presence and absence of lamotrigine. (B) Trace of current at different voltages controlled by the protocol. Each trace is an average of five consecutive traces in the presence and absence of lamotrigine. (C) Current-voltage relationship of TREK1 obtained from the ramp voltage changes in the presence and absence of lamotrigine. (D) Average reversal potential of TREK1 current, in control and in the presence of lamotrigine ( $n = 6$ ). Paired Student *t*-test was used.

The results show that lamotrigine does indeed inhibit TREK1 channels, in contrast to results obtained for the same WT channel which were expressed in HEK293 at a concentration of 10  $\mu$ M (Meadows et al 2001). The reversal potential showed little to no change shifting to  $-83 \pm 2$  mV from its original potential of  $-83 \pm 3$  mV.

## 3.9 Sipatrigine mechanism of action on TREK1 current

### 3.9.1 TREK2 docking to predict binding site(s)

The co-crystallised structure of TREK2 with norfluoxetine showed important binding sites. This study showed that the residue leucine at position 320 holds importance in the binding and inhibition of norfluoxetine. This residue is located in the fenestration site when the channel is in the up state. Norfluoxetine is known to only bind when TREK2 is in the closed conformation and therefore when the channel is in the down state. The fenestration site L320 is used as a binding site for norfluoxetine as the channel shifts to expose the residue. Therefore, I investigated if the same site is important in sipatrigine inhibition.

### 3.9.2 TREK1 mutation at predicted sipatrigine binding site

To investigate the effect of sipatrigine on TREK1, the TREK2 L320 homologues site was identified on TREK1. The homologues site was TREK1 L289 (see Figure 3.5).

A)

```
TREK2 K P L V W F W I L V G L A Y F A A V L S M I 320
TREK1 K P V V W F W I L V G L A Y F A A V L S M I 289
```

B)

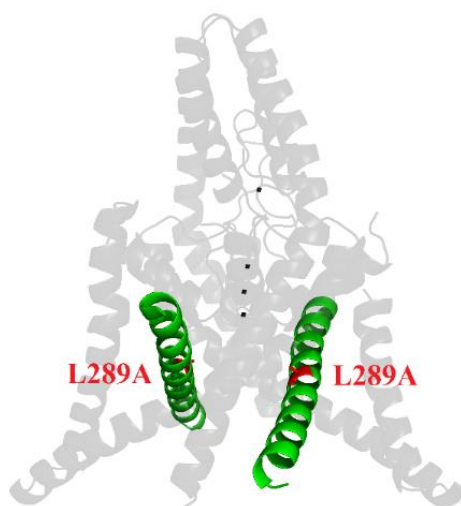


**Figure 3.7:** A) sequence highlighting TREK2 and TREK1 residue important of inhibition (yellow). B) TREK1 structure highlighting mutated residue (red)

After identifying the homogenous site, a mutated TREK1 was produced and electrophysiology could be carried out.

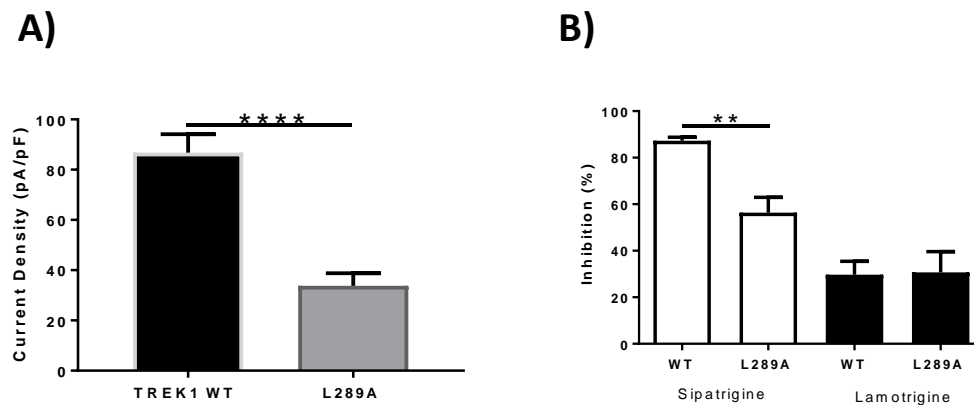


**Figure 3.8:** A) Current density (pA/pF) of TREK1 WT ( $n = 25$ ) compared to the mutated TREK1 L289A ( $n = 9$ ). B) TREK1 WT ( $n = 19$ ) inhibition compared to TREK1 L289A ( $n = 9$ ) with sipatrigine and lamotrigine at a concentration of 100  $\mu$ M. Unpaired two-tailed Welch's  $t$ -test was used.

The current density (pA/pF) of TREK1 WT ( $87 \pm 7$  pA/pF,  $n = 25$ ) was significantly greater compared to the mutated TREK1 L289A ( $34 \pm 5$  pA/pF,  $n = 9$ ). The results show that sipatrigine inhibition was decreased when the channel was mutated. The mutated channel showed an inhibition of  $56 \pm 7\%$  ( $n=9$ ), compared to the WT at  $87 \pm 2\%$  ( $n=19$ ). However, lamotrigine sensitivity did not change when the channel was mutated ( $31 \pm 9\%$ ,  $n=6$ ) compared to the WT ( $30 \pm 6\%$ ,  $n=6$ ).

### 3.9.3 Sipatrigine interaction with double mutations in the central cavity of TREK1

There have been two positions on the  $K_{2P}$  pore which have been identified as important in the activation of these channels. It was found that mutation of one of these sites on TRAAK results in the abolished activation by arachidonic acid (AA) and phosphoinositides ( $PIP_2$ ). It was also seen that a single mutation would shift the  $K_{2P}$  channel from a voltage gated channel to a linear leak channel. The equivalent amino acids in TREK1 were identified (T142 and T251) as the important residue for AA and  $PIP_2$  activation (Schewe et al 2016).

Furthermore, these sites showed to be important in  $Ba^{2+}$  inhibition as mutations reduced the blockade of TREK1 current (Ma et al 2011). These residues were mutated from a threonine to an alanine (see Fig 3.7 A-B). These mutated TREK1 channels were used with sipatrigine (100  $\mu$ M) to see if there was a reduced inhibition.

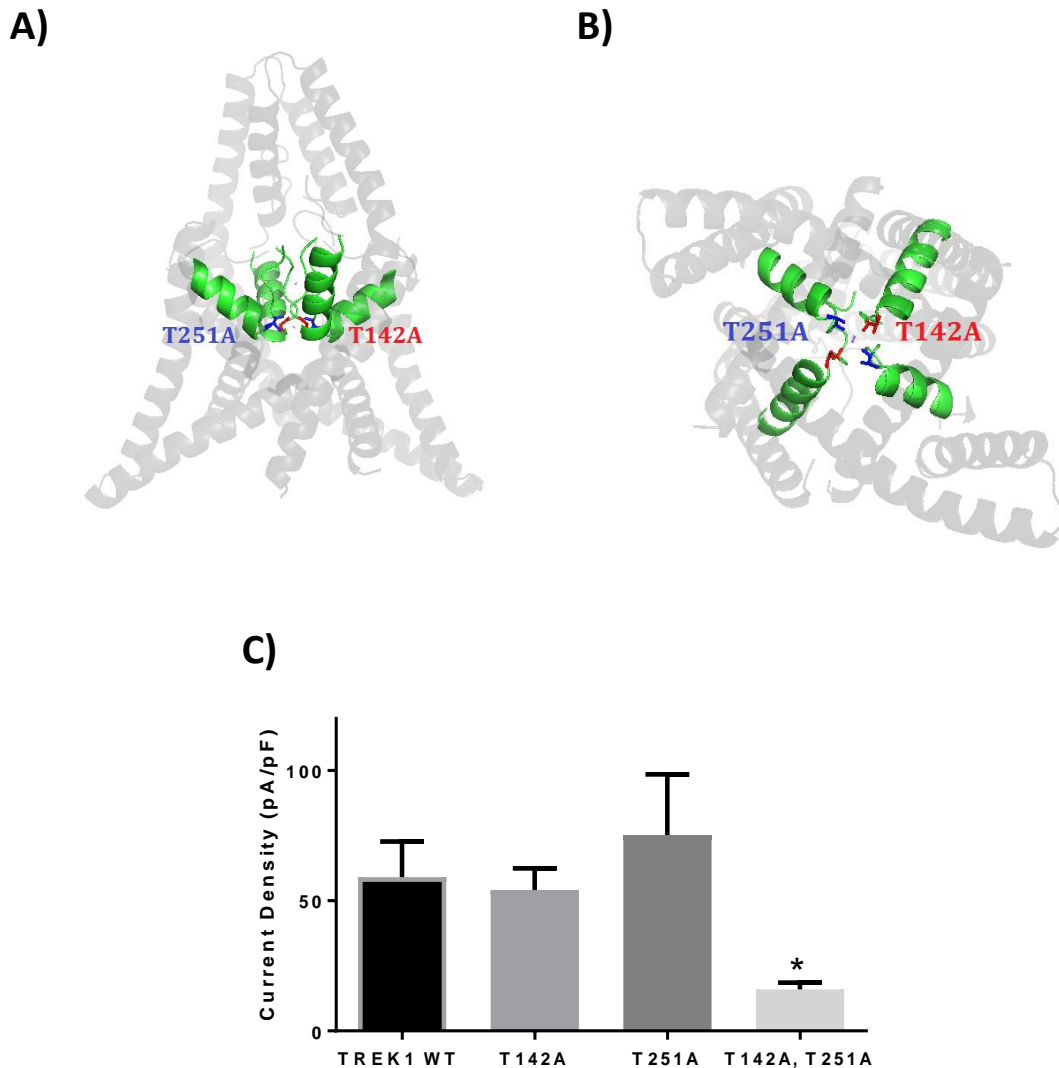


**Figure 3.9:** A) *TREK1* structure highlighting mutated residues T142A (red) and T251A (blue). B) View of *TREK1* structure highlighting the mutated residues at the pore. C) Current density of *TREK1* WT ( $n = 8$ ) and the mutations T142A ( $n = 10$ ), T251A ( $n = 7$ ) and double mutation ( $n = 7$ ). One-way ANOVA applying post hoc Dunnett's test was used.

It was also made clear that the current density of the double mutation was significantly smaller ( $16 \pm 3$  pA/pF,  $n = 7$ ) compared to *TREK1* WT ( $60 \pm 14$  pA/pF,  $n = 8$ ). The current density of the single mutation T142A was  $54 \pm 8$  pA/pF ( $n = 10$ ) and T251A was  $75 \pm 23$  pA/pF ( $n = 7$ ). The single mutations were not significantly different to *TREK1* WT. The following shows a representation of general *TREK1* T142A and *TREK1* T251A currents (see Fig 3.9).

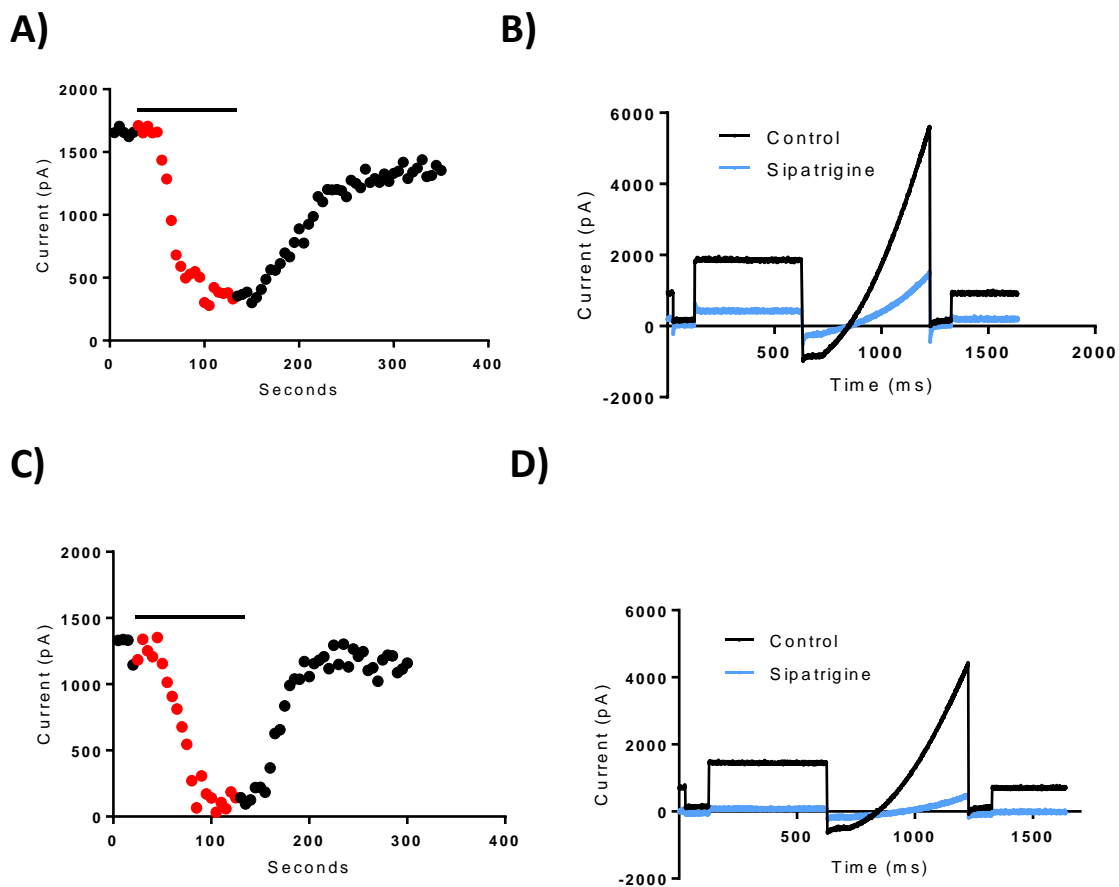


**Figure 3.10:** A) TREK1 T142A in the presence and absence of sipatrigine (100 $\mu$ M). B) Trace of TREK1 T142A current at different voltages controlled by the protocol. Each trace is an average of five consecutive traces in the presence and absence of sipatrigine. C) TREK1 T251A in the presence and absence of sipatrigine (100 $\mu$ M). D) Trace of TREK1 T251A current at different voltages controlled by the protocol. Each trace is an average of five consecutive traces in the presence and absence of sipatrigine.

TREK1 WT current inhibition by sipatrigine was  $80 \pm 5\%$  ( $n = 11$ ), which is similar to TREK1 T142A ( $67 \pm 5\%$ ,  $n = 8$ ) and TREK1 T251A ( $81 \pm 4\%$ ,  $n = 8$ ) (see Fig 3.10). The only significant difference was seen between TREK1 WT and the double mutated channel TREK1 T142A, T251A ( $45 \pm 6\%$ ,  $n = 6$ ). However, as the current is significantly lower compared to the WT and single mutations, it does become more difficult to measure the degree of inhibition. It can therefore be questioned if the measurement is accurate.

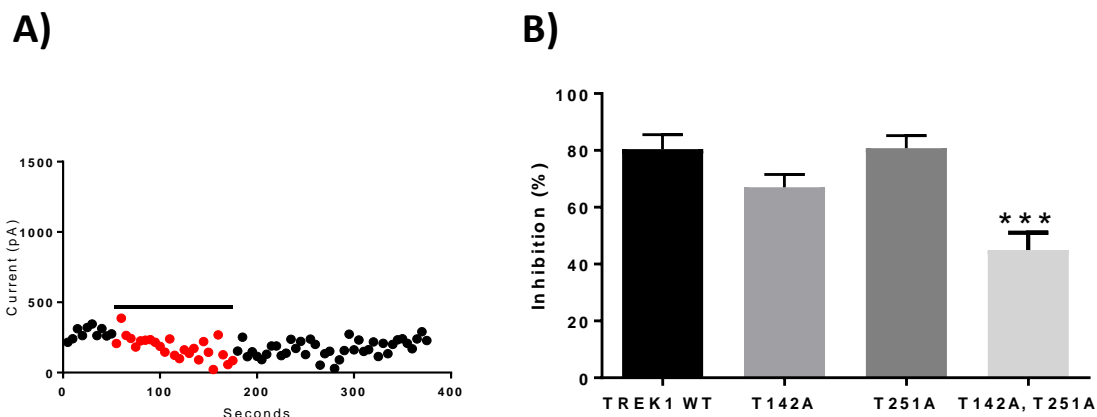
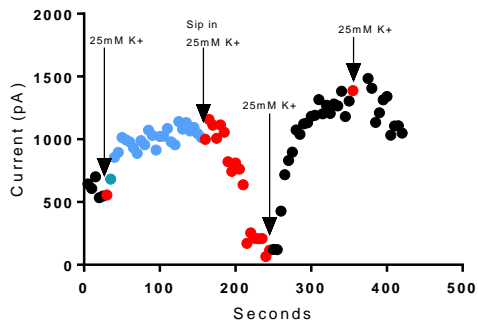


**Figure 3.11:** A) *TREK1 T142A, T251A* in the presence and absence of sipatrigine (100 $\mu$ M). B) *TREK1 WT* ( $n = 11$ ) sipatrigine inhibition is similar to *TREK1 T142A* ( $n = 8$ ) and *TREK1 T251A* ( $n = 8$ ). Significant difference was seen between *TREK1 WT* and *TREK1 T142A, T251A* ( $n = 6$ ). One-way ANOVA applying post hoc Dunnett's test was used.

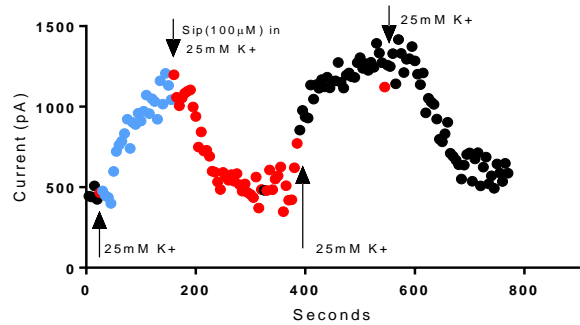
### 3.9.4 25 mM K<sup>+</sup> solution effect on TREK1 with sipatrigine

The low basal current of the double *TREK1* mutation (*T142A, T251A*) made measuring the degree of inhibition by sipatrigine difficult. Therefore, an increased KCL external solution from 2.5 mM K<sup>+</sup> to 25 mM K<sup>+</sup> was used. This increase in extracellular potassium concentration will cause the potassium gradient to decrease across the membrane. This shifts the reversal membrane potential for potassium to more positive voltages (around -40mV, see Fig 3.10). To investigate the resting basal current and sipatrigine inhibition, a different external potassium concentration was used. The current was measured in 2.5 mM K<sup>+</sup> solution and then at 25 mM K<sup>+</sup> solution. Sipatrigine (100  $\mu$ M) was made in 25mM K<sup>+</sup> solution. The effect and sipatrigine was then washed off using 25 mM K<sup>+</sup> solution and then the normal 2.5 mM K<sup>+</sup> was then added. The following shows a representation of general *TREK1 T142A, T251A* currents (see Fig 3.11).

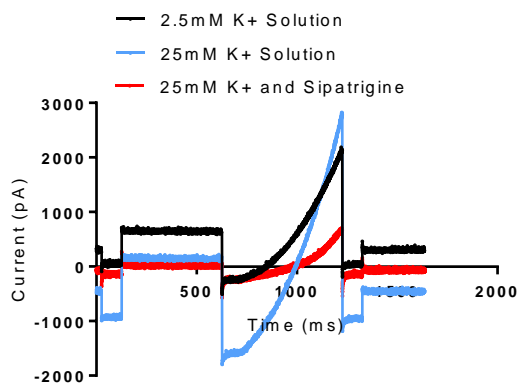
A)



B)



C)



D)

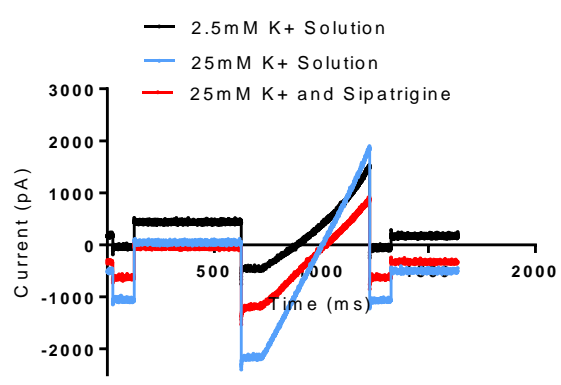


**Figure 3.12:** A) *TREK1* WT current increase is due to the change in external potassium concentration and current inhibition was caused by sipatrigine(Sip) ( $100 \mu\text{M}$ ). B) *TREK1* T145A, T251A current increase is due to the change in external potassium concentration and current inhibition was caused by sipatrigine (Sip) ( $100 \mu\text{M}$ ). C) *TREK1* WT reversal potential shifts to the more positive  $-40 \text{ mV}$ . *TREK1* WT current was decreased in  $25 \text{ mM K}^+$  and sipatrigine. D) *TREK1* T142A, T251A reversal potential shifts to the more positive  $-40 \text{ mV}$ . *TREK1* T142A, T251A current was slightly decreased in  $25 \text{ mM K}^+$  and sipatrigine, compared to *TREK1* WT.

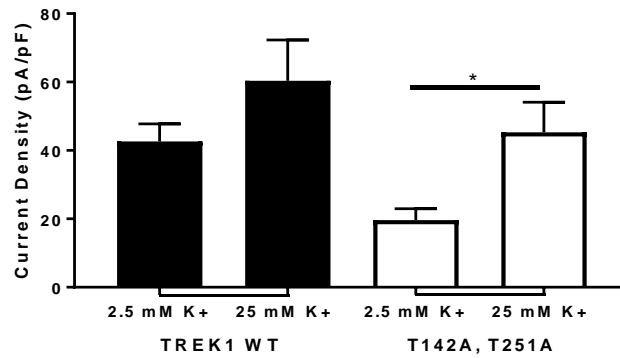


**Figure 3.13:** Current density (pA/pF) of TREK1 WT ( $n = 6$ ) in 2.5mM K<sup>+</sup> solution compared to the same cell in 25mM K<sup>+</sup> solution. Current density (pA/pF) of TREK1 T142A, T251A ( $n = 6$ ) in 2.5mM K<sup>+</sup> solution compared to the same cell in 25mM K<sup>+</sup> solution. Paired Student t-test was used.

TREK1 WT and mutated channels were characterised and it was found that there was an increase in current. However it was found not to be significantly different between TREK1 WT in 2.5 mM K<sup>+</sup> external solution (43 ± 5 pA/pF,  $n = 6$ ) and 25 mM K<sup>+</sup> solution (60 ± 12 pA/pF,  $n = 6$ ). There was significant difference between the TREK1 T142A, T251A in 2.5 mM K<sup>+</sup> solution (20 ± 3 pA/pF,  $n = 6$ ) and 25 mM K<sup>+</sup> solution (45 ± 9 pA/pF,  $n = 6$ ).

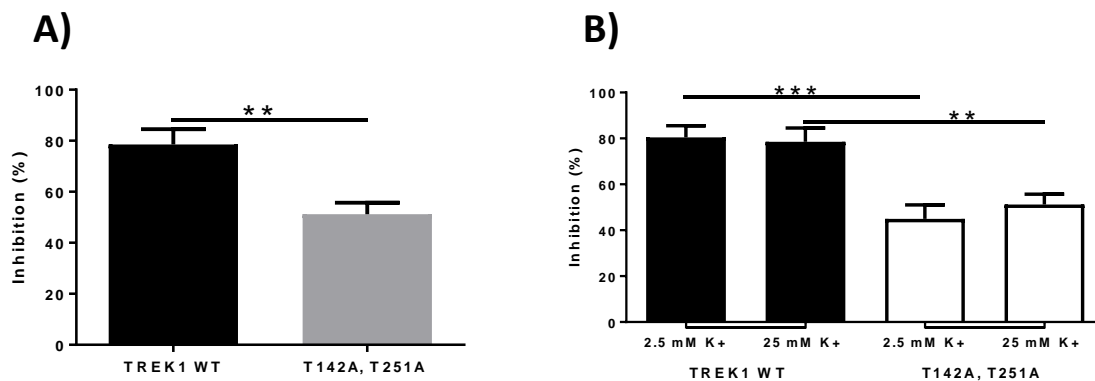


**Figure 3.14:** A) The inhibitory effect of sipatrigine (100  $\mu$ M) in 25 mM K<sup>+</sup> external solution on TREK1 WT ( $n = 6$ ) compared to TREK1 T142A, T251A ( $n = 6$ ). B) Inhibition of TREK1 WT ( $n = 11$ ) current and TREK1 T142A, T251A ( $n = 6$ ) in sipatrigine (100  $\mu$ M) in 2.5 mM K<sup>+</sup> external solution versus 25 mM K<sup>+</sup> external solution. Unpaired two-tailed Welch's t-test was used for 2.5 mM K<sup>+</sup> solution. Unpaired one-tailed Welch's t-test was used for 25 mM K<sup>+</sup> solution.

Sipatrigine in 25 mM K<sup>+</sup> solution produced inhibition of TREK1 current (79 ± 6%,  $n = 6$ ). The double mutated TREK1 T142A, T251A current showed a significantly reduced degree of inhibition of sipatrigine (100  $\mu$ M) in 25 mM K<sup>+</sup> solution compared to the WT (51 ± 5%,  $n = 6$ ), see Fig 3.11 A. The increase in the resting current also showed to have no change in the degree of sipatrigine inhibition when compared to the normal 2.5 mM extracellular solution (Fig 3.11 B). This shows that the degree of inhibition seen in 2.5 mM external and sipatrigine is accurate.

# **CHAPTER FOUR**

## **Regulation of TRESK channels by sipatrigine and lamotrigine**

# Introduction

## 4.1 Physiological role of TRESK and pain

The DRG are very important in transmitting nociception as it relays the pain signal to the nervous central system. DRG contains the cell bodies of primary afferent neurons which is used for transmitting sensory information from the periphery to the central nervous system. It has been proven that hyperexcitability and increased discharge of DRG signals plays a role in pain models. As TRESK channels are known to be expressed on the DRG neurons and modulate the resting background current, the channel could be involved in the discussed electrical conduction in neuropathic pain (Tulleuda et al 2011).

In chronic pain, the condition is regulated by altering the nociceptive function. Stimulation from inflammatory mediators released in tissue produced by injury act on GPCRs. GPCR, expressed on DRG, activate intracellular signalling systems such as  $G\alpha_q$  which evokes the release of cytoplasmic calcium stores. This elevation of intracellular calcium promotes the release of neurotransmitters at the presynaptic terminal and thereby activating calcineurin, which is known to increase TRESK activity (Ji and Woolf 2001). There is further evidence of this as lysophosphatidic acid (LPA), an inflammatory mediator, signalling influences neurological disorders such as neuropathic pain. It is known that during tissue damage, LPA is released from activated platelets or microglia. This release will alter the activity of ion channels and influence the excitability of neurons. In heterologous systems, LPA will strongly activate TRESK through  $G\alpha_q$ -coupled receptors. This activation of TRESK is believed to down regulate depolarisation of DRG neurons and thereby attenuates nociception. This is contrary to LPA action on TREK1, as it has an inhibitory effect which evokes excitation for nociceptors (Kollert et al 2015).

The natural analgesic hydroxy- $\alpha$ -sanshool (sanshool) is known to excite a subset of capsaicin-sensitive sensory neurons and inhibites TRESK channels. Sanshool is responsible for the tingling or numbing sensations associated with Szechuan peppers (Bautista et al 2008). Another compound Aristolochic acid (AristA) also occurs naturally and has been used in traditional medicine to relieve pain. This compound is unique however as it selectively inhibits TRESK while activating TREK1 and TREK2 (Veale and Mathie 2016). It remains unclear how the inhibition of TRESK current results in the analgesic effect seen by these compounds. One thought is that the tingling and numbing effect by the natural compounds will desensitise the excited neurons which results in pain relief, similar to that seen with the nociceptive agent capsaicin. It is also important to consider what we know about TRESK and

the pain linked the migraine. As previously discussed, the mutated gene which encodes for TRESK leads to a non-functional TRESK indicating that enhancement of TRESK current is important in treating migraines (Lafrenière et al 2010). Taking all this information together could be useful in understanding the exact role of TRESK and its therapeutic potential to target pain.

## **4.2 Regulatory pathways involving phosphorylation**

Calcium-dependent activation of TRESK targets calcineurin and the docking motif PQIIS. The serine residues (S252 and S264) have been identified as important sites for phosphorylation/dephosphorylation dependent regulation. Serine 264 is found in the intracellular loop and is the target for MARK kinases phosphorylation. Serine 252 is also found in the intracellular loop and is phosphorylated by PKA. Substitution of these residues to alanine changes the channel to the dephosphorylated state, as the serine residues now cannot be phosphorylated. This shift is seen with high basal current and a reduced response to the calcium signal which suggest the channels are in this active configuration. Mutating the same serine residue to a negative charged glutamic acid is also thought to mimic permanent phosphorylated state which shows to have a low basal current and also reduced response to calcium. (Czirják and Enyedi 2010).

## **4.3 Central cavity is important for blocker binding**

Two key mouse TRESK residues, F156 and F364, were found to be involved in binding blockers of K<sup>+</sup> channels, such as propafenone and lidocaine, and resulting in current inhibition. This evidence is based on homology modelling and molecular docking simulations. These phenylalanine residues are conserved in human TRESK channels as F145 and F352. Both residues face into the central cavity and form a narrow pore for ion conduction. It is therefore likely that these residues interact with TRESK blockers. It is believed that inhibitors of TRESK form  $\pi$ - $\pi$  stacking interactions with the phenylalanine residues. It was demonstrated in the mouse model of TRESK that the aromatic rings of the blockers will form  $\pi$ - $\pi$  interactions at the two phenylalanine sites (Kim et al 2013). Alanine mutations on both sites would diminish inhibition of TRESK blockers quinine, propafenone, and lidocaine. Therefore, the two phenylalanine residues have been proposed as important in forming the narrow gate region and for binding for these inhibitors (Bruneret al 2014). Therefore, I used the same mutations to see if the same residues are involved in another compound's inhibition.

## **4.4 Aim of the chapter**

I investigated the effect of sipatrigine and lamotrigine on TRESK. This study will aim to understand the mechanism by which the drugs act on the channel using direct mutagenesis and electrophysiology recording. Additionally, I aim to investigate the action of novel activators on TRESK through the same means as previously described.

# Results

## 4.5 Sipatrigine inhibition of TRESK

TRESK (WT) channels were transiently expressed in tsA-201 cells and currents were measured using whole-cell patch-clamp electrophysiology. The current was measured in the presence of sipatrigine (100  $\mu$ M) and it was found to significantly reduce TRESK current ( $73 \pm 3\%$ ,  $n = 17$ ). Current inhibition was recovered by  $51 \pm 6\%$  ( $n = 13$ ) after wash-off with a drug free external solution. The reversal potential of TRESK current in external solution was  $-75 \pm 2$  mV ( $n = 16$ ), however there is a shift to a more positive  $-64 \pm 3$  mV ( $n = 16$ ) in sipatrigine (100  $\mu$ M). The following shows a representation of general TRESK currents (see Fig 4.1).

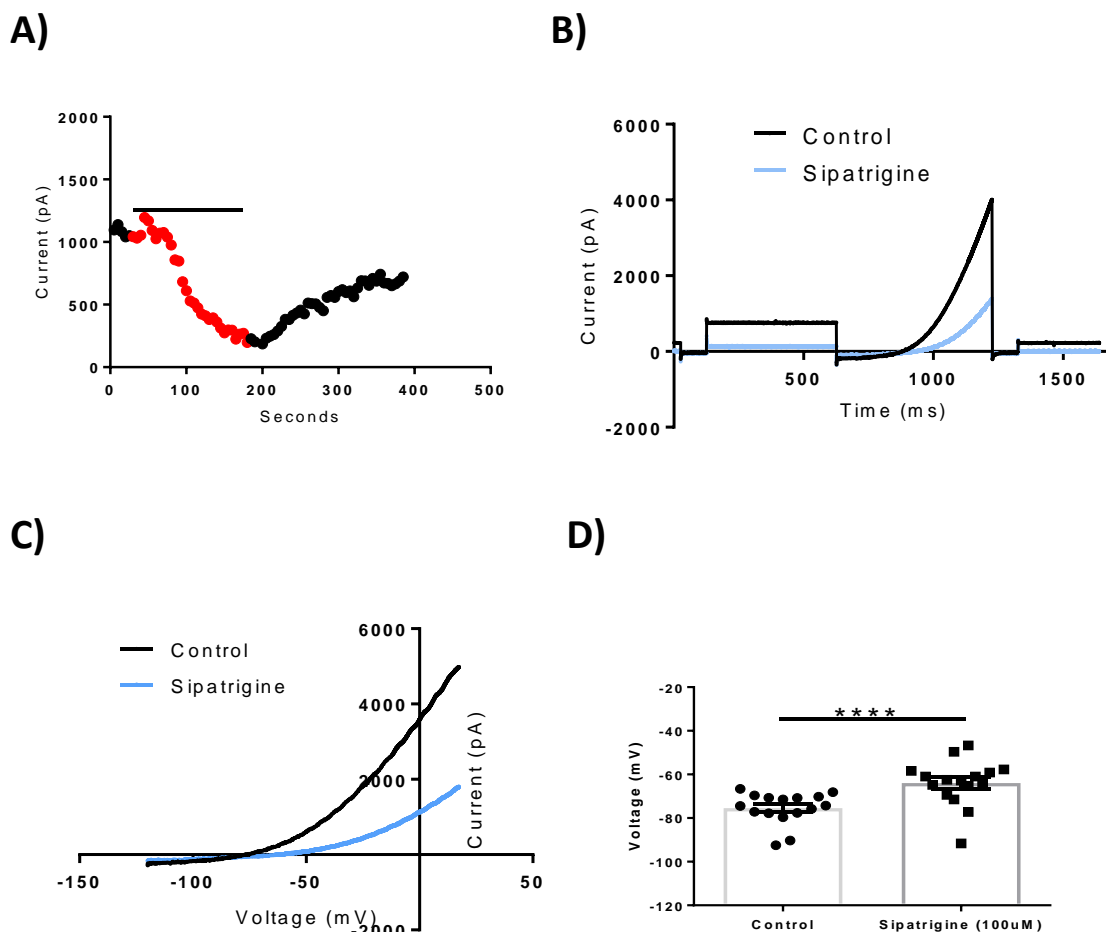


**Figure 4.1:** Sipatrigine (100  $\mu$ M) inhibition of TRESK WT channels. (A) The effect on TRESK current in the presence and absence of sipatrigine. (B) Trace of current at different voltages controlled by the protocol. Each trace is an average of five consecutive traces in the presence and absence of sipatrigine. (C) Current-voltage relationship of TRESK obtained from the ramp voltage changes in the presence and absence of sipatrigine. (D) Average reversal potential of TRESK current ( $n = 16$ ). Paired Student t-test was used.

### 4.5.1 TRESK inhibition by sipatrigine is concentration dependent

Sipatrigine was applied to TRESK channels at concentrations of 3  $\mu\text{M}$ , 10  $\mu\text{M}$ , 30  $\mu\text{M}$  and 100  $\mu\text{M}$ , which has already been discussed. Sipatrigine (30  $\mu\text{M}$ ) concentration inhibited the channel by  $46 \pm 3\%$  ( $n = 19$ ), while the 10  $\mu\text{M}$  concentration of sipatrigine produced  $24 \pm 4\%$  ( $n=11$ ). Sipatrigine (3  $\mu\text{M}$ ) concentration only inhibited TRESK channels by  $11 \pm 3\%$  ( $n = 8$ ). TRESK inhibition by sipatrigine showed that sipatrigine an  $\text{IC}_{50} = 36.57 \mu\text{M}$ . The 95% Confidence intervals was between (30.68 – 43.61  $\mu\text{M}$ ). The Hill slope was 0.91 with the 95% Confidence interval between 0.7 – 1 (see Fig 4.2). It must be noted however that this dose response curve does not measure 100% inhibition and that more concentrations could be used to measure this.

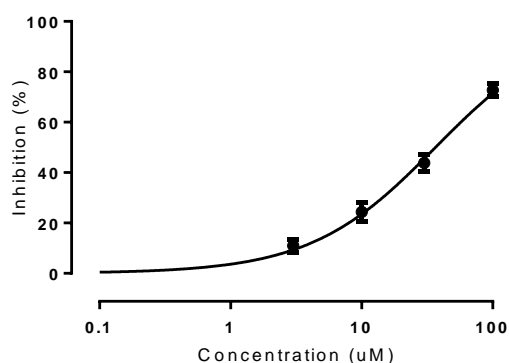
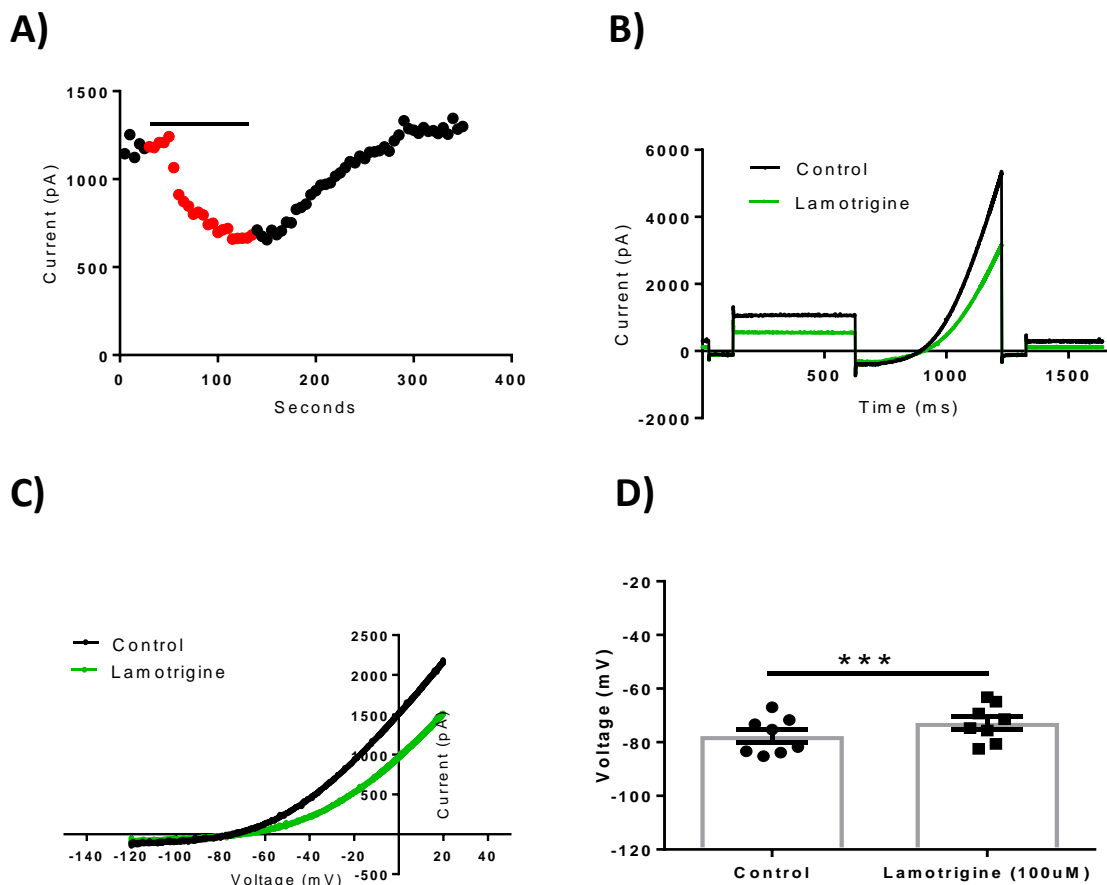


Figure 4.2: Dose - response curve of sipatrigine inhibition of TRESK current

## 4.6 Lamotrigine inhibition of TRESK

TRESK (WT) channels were transiently transfected in tsA-201 cells and currents were again measured using whole-cell patch-clamp electrophysiology. TRESK current was measured in the presence of lamotrigine (100  $\mu$ M) showed current inhibition of  $35 \pm 4\%$ ,  $n = 8$ . The reversal potential of TRESK current in external solution was  $-78 \pm 2$  mV ( $n = 8$ ), however there is a shift to a more positive  $-73 \pm 2$  mV ( $n = 8$ ) in sipatrigine (100  $\mu$ M). The following shows a representation of general TRESK currents (see Fig 4.3).



**Figure 4.3:** Lamotrigine (100  $\mu$ M) inhibition of WT TRESK channels. (A) Effect of lamotrigine on TRESK. Time-course plot show current in the presence and absence of lamotrigine. (B) TRESK current at different voltages controlled by the protocol. Each trace is an average of five consecutive traces in the presence and absence of lamotrigine. (C) Current-voltage relationship of TRESK obtained from the ramp voltage changes in the presence and absence of lamotrigine. (D) The reversal potential of current in the presence of lamotrigine on TRESK WT ( $n = 8$ ). Paired Student *t*-test was used.

## 4.7 Sipatrigine and lamotrigine mechanism of action on TRESK current

### 4.7.1 F156A/ F364A mutation reduces pharmacological inhibition on TRESK

Sipatrigine (100  $\mu\text{M}$ ) was applied on TRESK F145A/F352A to investigate its effect on the TRESK mutant. Sipatrigine (100  $\mu\text{M}$ ) was found to have little or no effect on TRESK F145A/F352A ( $10 \pm 2$ ,  $n = 9$ ). The results show a significant difference in sipatrigine (100  $\mu\text{M}$ ) inhibition between the WT TRESK and the FF mutated TRESK which suggests that this location is important in sipatrigine inhibitory effect. The following shows a representation of general TRESK F156A/ F364A currents (see Fig 4.4).

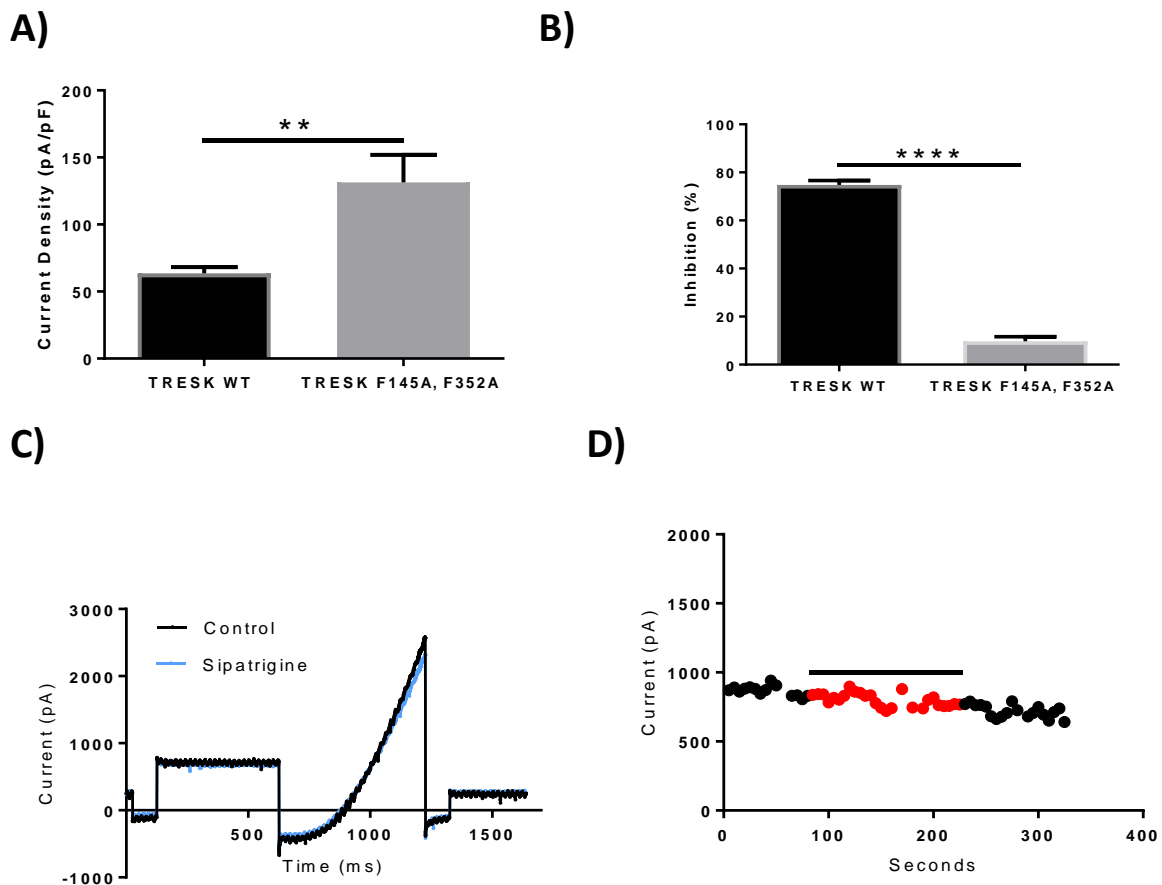


**Figure 4.4:** Sipatrigine (100  $\mu\text{M}$ ) inhibition of TRESK FF channels. (A) Current density (pA/pF) of TRESK WT ( $n = 28$ ) versus TRESK double mutation ( $n = 10$ ). (B) Comparison between TRESK WT ( $n = 17$ ), and TRESK FF ( $n = 9$ ) current inhibition in the presence of sipatrigine (100  $\mu\text{M}$ ). (C) TRESK current at different voltages controlled by the protocol. Each trace is an average of five consecutive traces in the presence and absence of sipatrigine. (D) The effect on TRESK in the presence and absence of sipatrigine. Unpaired two-tailed Welch's *t*-test was used.

Lamotrigine (100  $\mu\text{M}$ ) was applied on TRESK F145A/F352A ( $5 \pm 2\%$ ,  $n = 11$ ) which saw little or no effect compared to TRESK ( $35 \pm 4\%$ ,  $n = 8$ ). The results show a significant difference in lamotrigine (100  $\mu\text{M}$ ) between the WT TRESK and the FF mutated TRESK which again shows that these residues are important for blockers.

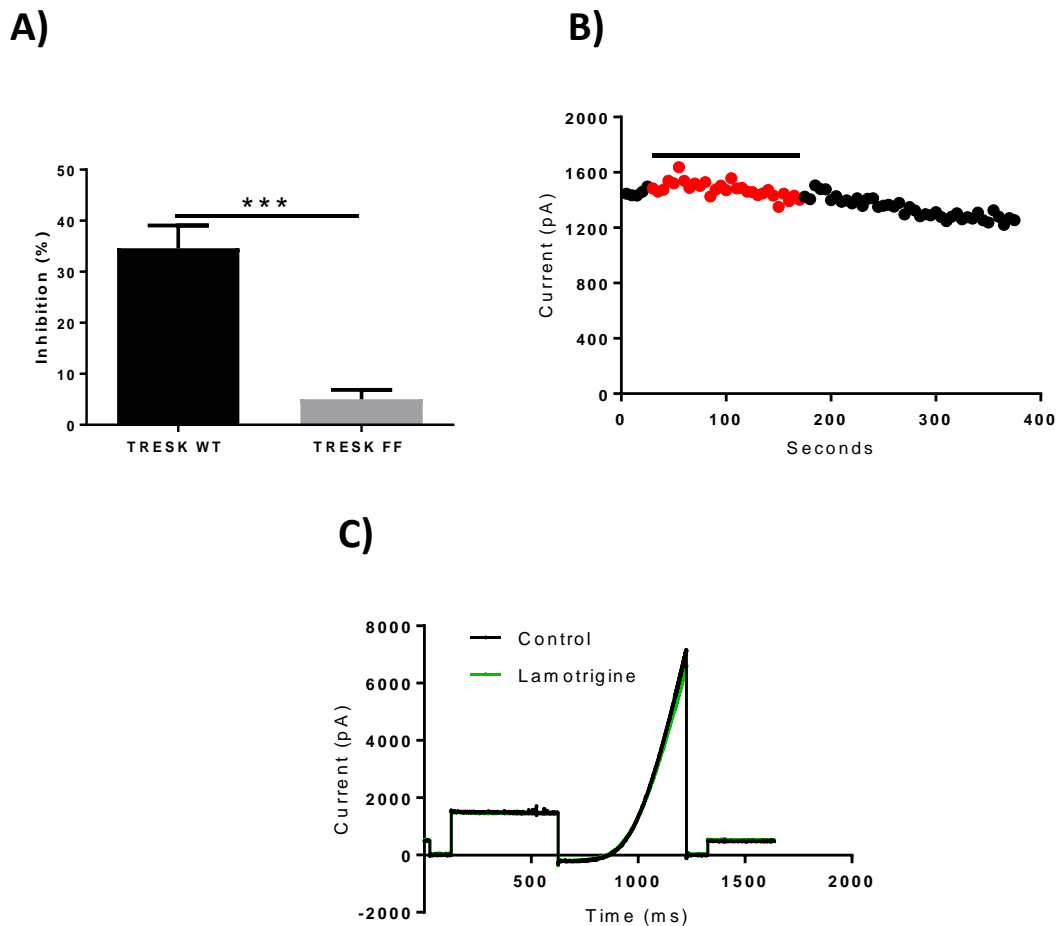


**Figure 4.5:** Lamotrigine (100  $\mu\text{M}$ ) inhibition of TRESK FF channels. (A) Comparison between TRESK WT ( $n = 8$ ) and TRESK FF ( $n = 11$ ) current inhibition in the presence of lamotrigine (100  $\mu\text{M}$ ). Unpaired two-tailed Welch's  $t$ -test was used. (B) The effect on TRESK FF in the presence and absence of lamotrigine (100  $\mu\text{M}$ ). (C) TRESK current at different voltages controlled by the protocol. Each trace is an average of five consecutive traces in the presence and absence of lamotrigine.

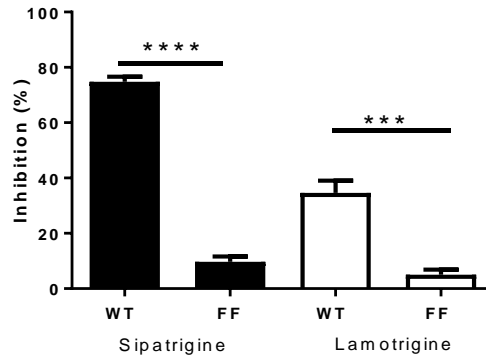


**Figure 4.6:** The effect that the double FF mutation has on the inhibitory action of sipatrigine and lamotrigine. The inhibitory effect of sipatrigine on TRESK WT ( $n = 16$ ) versus TRESK F145A, F352A ( $n = 9$ ). The inhibitory effect of lamotrigine on TRESK WT ( $n = 8$ ) versus TRESK F145A, F352A ( $n = 11$ ). Unpaired two-tailed Welch's *t*-test was used.

#### 4.7.2 Is TRESK inhibition state dependent?

It come as no surprise that the S252A, S264A mutated channel had a significantly larger current density ( $95 \pm 9$  pA/pF,  $n = 14$ ) than the WT ( $64 \pm 5$  pA/pF,  $n = 28$ ) as that mutation mimics the forced open dephosphorylated state. The phosphorylated S252E, S264E ( $80 \pm 12$  pA/pF,  $n = 15$ ) had a similar current density to WT. Mutation of the bulky residues (F142 and F352) in the M2 and M4 inner pore regions of the channel showed a significantly greater current density compared to WT ( $134 \pm 17$  pA/pF,  $n = 13$ ).

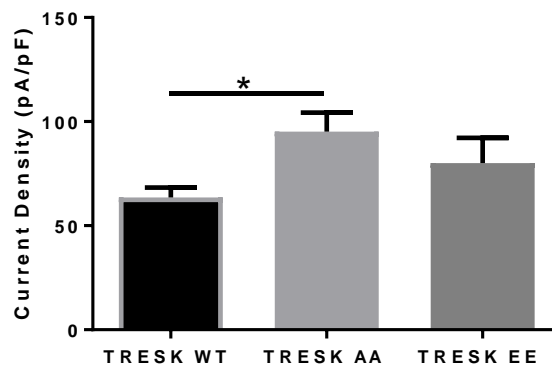


**Figure 4.7:** Current density (pA/pF) of TRESK WT ( $n = 28$ ) compared to dephosphorylated ( $n = 14$ ) and phosphorylated state ( $n = 15$ ) of the channel. One-way ANOVA applying post hoc Dunnett's test was used.

To investigate whether the phosphorylation state of the TRESK channel affects the degree of inhibition of certain compounds, electrophysiology recording were used to measure inhibition.

The sipatrigine inhibition of TRESK WT current was  $75 \pm 2\%$  ( $n = 16$ ). The inhibition of the two forced states were similar to TRESK WT with the degree of inhibition of  $70 \pm 4\%$  ( $n = 6$ ) for the TRESK AA channel and  $79 \pm 2\%$  ( $n = 6$ ) for TRESK EE (see Fig 4.8-A).

Lamotrigine (100  $\mu$ M) showed a significant difference in inhibition between WT ( $35 \pm 4\%$ ,  $n = 8$ ) and TRESK AA ( $57 \pm 3\%$ ,  $n = 9$ ). There was no significant with TRESK EE inhibition ( $49 \pm 6\%$ ,  $n = 7$ ) and TRESK WT lamotrigine inhibition (see Fig 4.8-B).

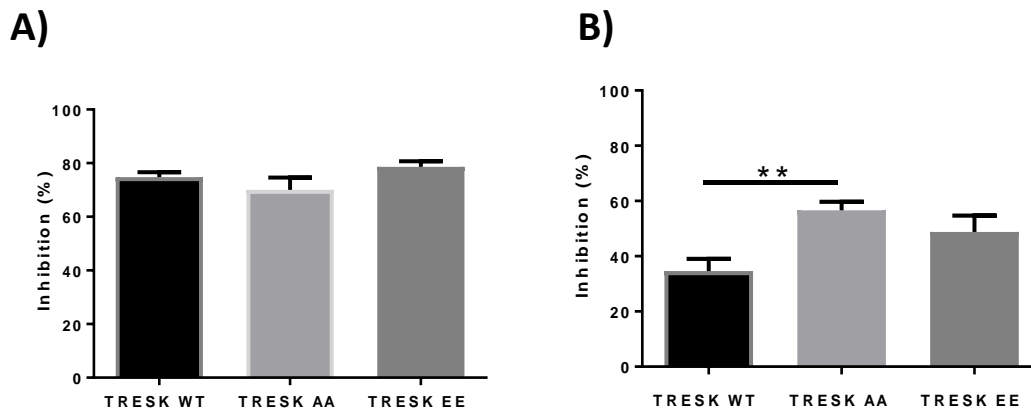


**Figure 4.8:** A) Sipatrigine (100  $\mu$ M) inhibition of TRESK WT ( $n = 16$ ), TRESK AA ( $n = 6$ ) and TRESK EE current ( $n = 6$ ). B) Lamotrigine (100  $\mu$ M) inhibition of TRESK WT ( $n = 8$ ), TRESK AA ( $n = 9$ ) and TRESK EE current ( $n = 7$ ). The inhibitory effect of lamotrigine on TRESK WT versus TRESK AA. One- way ANOVA applying post hoc Dunnett's test was used.

## 4.8 Potential activators of TRESK

Downregulation of TRESK is known to induce hyperexcitability that results in activation of sensory neurons and nociceptive fibres. This causes a pro-algesic effect. (Guo and Cao 2014). Migraine is also caused by hyperexcitation of neurons. Therefore, a TRESK-specific activator may display analgesic effects and could be a potential treatment for migraine patients as ultimately this will lead to a significant decrease in the excitability of DRG neurons (Enyedi, Braun, and Czirjak 2012). Two novel compounds (PD0307243 and PD0322388) were suggested to be activators of TRESK channels on the basis of data from high throughput screening carried out at Pfizer Neusentis. The effects of these two compounds were investigated using whole-cell patch-clamp electrophysiology.

### 4.8.1 PD0307243 and PD0322388 had no effect on TRESK current

PD0307243 (100  $\mu$ M) was applied to TRESK WT and TRESK F145A/F352A to investigate if it enhances the current of TRESK. PD0307243 was found to have little or no effect on TRESK WT ( $-2 \pm 4\%$ ,  $n = 8$ ) or TRESK F145A/F352A ( $-2 \pm 3\%$ ,  $n = 7$ ) (see Fig 4.9 A-B). PD0322388 (100  $\mu$ M) was also applied to TRESK WT and TRESK F145A/F352A to see if the compound has effect on current enhancement. Little enhancement of TRESK WT current was measured after the presence of PD0322388 ( $7 \pm 8\%$ ,  $n = 6$ ). TRESK F145A/F352A

showed little current activation also at  $4 \pm 2$  ( $n = 5$ ) (see Fig 4.9 C-D). The results show that the potential TRESK activator compounds has no direct action on TRESK channel. The following shows a representation of general TRESK currents (see Fig 4.9).

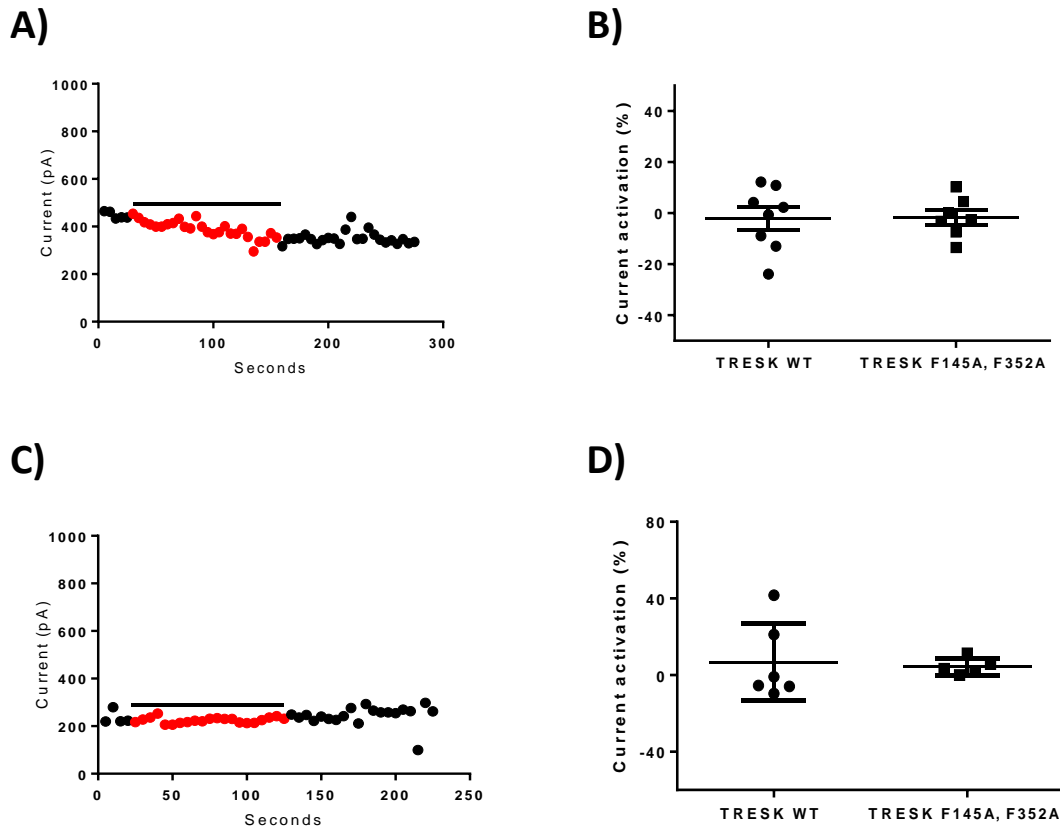


**Figure 4.9:** A) TRESK WT in the presence of the potential activator PD0307243. B) Comparison of PD0307243 enhanced current in TRESK WT ( $n = 8$ ) and TRESK FF mutation channel ( $n = 7$ ). C) TRESK WT in the presence of the other potential activator PD0322388. D) Comparison of PD0322388 enhanced current between TRESK WT ( $n = 6$ ) and TRESK FF mutation ( $n = 5$ ). Unpaired two-tailed Welch's *t*-test was used.

## 4.8.2 Potential TRESK current enhancers do not work via the calcineurin pathway

TRESK channels are known to be indirectly activated by calcium through the calcineurin/NFAT signalling pathway. Potential activators of TRESK could affect this pathway however the internal solution contains EGTA. EGTA is a chelating agent that buffers calcium. This is used in whole cell patch as rupture of the cell's membrane will release  $\text{Ca}^{2+}$  from intracellular store and damage the seal. To see if the potential activators of TRESK work indirectly, low EGTA internal solution (0.1 mM, compared to 5 mM) was used. This will allow calcineurin pathway upon cellular calcium uptake.

Electrophysiology recordings with electrode solution now containing low EGTA were carried out in the presence of PD0307243 and PD0322388, respectively. PD0307243 (100  $\mu\text{M}$ )

showed little activation ( $1 \pm 5\%$ ,  $n = 8$ ) and TRESK FF also showed no activation ( $-9 \pm 3$ ,  $n = 5$ ) (see Fig 4.10 A-B). PD0322388 showed similar results with TRESK WT showing  $-1 \pm 4\%$  ( $n = 7$ ) and TRESK FF mutation with  $3.1 \pm 5\%$  activation ( $n = 3$ ) (see Fig 4.10 C-D). The following shows a representation of general TRESK currents (see Fig 4.10).

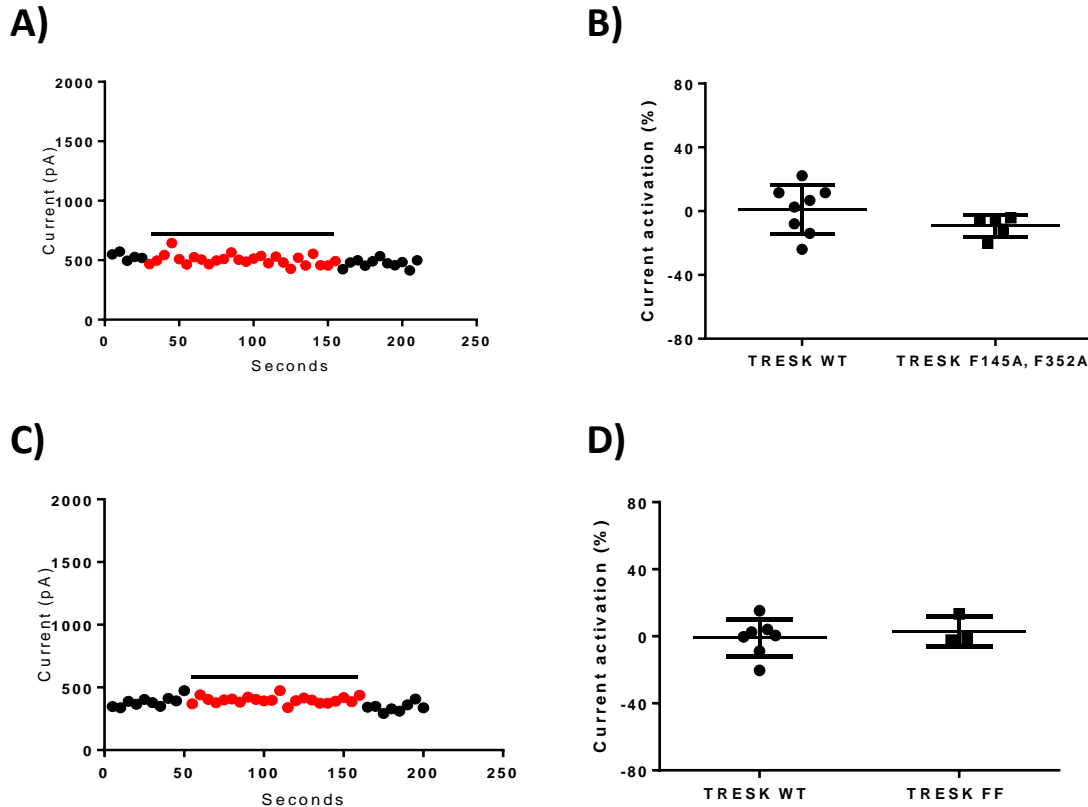


**Figure 4.10:** A) TRESK WT in the presence of low EGTA internal solution and potential activator PD0307243. B) Comparison between TRESK WT ( $n = 8$ ) and TRESK FF enhanced current ( $n = 5$ ) when in the presence of PD0307243 and in low EGTA internal solution. C) TRESK WT in the presence of low EGTA internal solution and the other potential activator PD0322388. D) Comparison between TRESK WT ( $n = 7$ ) and TRESK FF ( $n = 3$ ) enhanced current when in PD0322388 and in low EGTA internal solution. Unpaired two-tailed Welch's *t*-test was used.

# **CHAPTER FIVE**

## **Regulation of TREK2 channels by sipatrigine and lamotrigine**

# Introduction

## 5.1 TREK2 linked to pain

TREK2 is closely related to TREK1 with their sequence being 78% similar however the expression level of TREK2 in DRG neurons is low in comparison. The importance of TREK2 however has been identified in its contribution to the resting K<sup>+</sup> current. TREK2 is the most active conductive channel at 37°C in DRG neurons (69%), compared to TRESK (16%), TREK1 (12%) and TRAAK (3%) (Kang and Kim 2006). This high rate in current conductance could be important in spontaneous pain as TREK2 is selectively expressed in selectin B4 binding (IB4<sup>+</sup>) C-fiber nociceptors in small DRG neurons. In neuropathic pain models in rats, the spontaneous firing rate are connected to the membrane potential which is highly defined by TREK2. It was also seen that rats with a greater amount of spontaneous foot lifting measured a lower amount of TREK2 activity. This shows that TREK2 may limit spontaneous pain *in vivo* (Acosta et al 2014). It is therefore not surprising that the neuroprotective agent baicalein and wogonin active TREK2 current, which is thought to suppress neuronal excitability of DRG neurons (Kim et al 2010). It has been reported however that antidepressants with analgesic effects inhibit TREK2 channels including amitriptyline, citalopram, escitalopram, and fluoxetine. This study however could not determine the relationship between the analgesic inhibitions to pain. It was noted that activation of inhibitory interneurons caused by depolarization of the resting potential could lead to treatment to pain, however there are no accounts of TREK2 expression on inhibitory interneurons (Park et al 2016).

## 5.2 Variation of the channel structure

For manufacturing protein, the information in DNA is transferred to a messenger RNA (mRNA) by transcription. The DNA is used as a template for complementary base pairing and an enzyme called RNA polymerase transcribes primary transcript mRNA (pre-mRNA) molecule into the mature mRNA. The mature mRNA molecules must leave the nucleus and travel to the ribosomes. This resulting mRNA is a single-stranded gene, which will be translated into a protein molecule. The translation of mRNA begins when the small subunit of the ribosome and a transfer RNA (tRNA) molecule assemble on the mRNA transcript. Each tRNA contains a set of three nucleotides called an anticodon. The anticodon tRNA will bind to the specific AUG start codon of the mRNA transcript. The tRNA molecule also carries a methionine, the amino acid that the tRNA binds to. The ribosome will move along the mRNA

in the 5'-to-3' direction. Termination will occur when the stop codons are recognized by proteins (Flinta et al 1986).

When it comes to diversity of ion channels to alter channel function and neuronal excitability, alternative translation initiation (ATI) plays a key role. ATI has also been shown to further increase the molecular and functional complexity of K<sup>+</sup> channels. ATI is thought to occur on eukaryotic mRNA that contains a weak Kozak sequence which is skipped by the scanning ribosome and translation is initiated at a different start codon (Thomas et al 2008). The optimal sequence for translation transpires when the start codon is flanked by strong Kozak consensus sequence. The third nucleotide base (-3) before the start codon must be an alanine or guanine and the fourth nucleotide base (+4) after the start codon must be a guanine (Simkin et al 2008).

**-3      +4**  
**GCCATGG**      or      **ACCATGG**

**Figure 5.1:** Kozak scanning model for optimum translation where A is position one and ATG is the start codon (Simkin, Cavanaugh and Kim 2008).

The ATI produces an isoform of TREK1 where the first 56 amino acids, found at the N-terminal, are truncated because of the “leaky” scanning. This shorter isoform yields smaller currents when compared to the full-length gene and the shorter isoform loses its selective permeability to potassium as the reversal potential shows an increase in permeability to sodium. It has been noted that the shorter isoform is involved with depolarisation in rat hippocampal neurons (Thomas et al 2008).

There are three TREK2 isoforms that can form: The “full length” protein is established when the first start codon is translated. The first start codon is a weak Kozak sequence as it flanked only by adequate sequence for translation. The full-length protein is created by mutating the second (M60) and third (M72) initiation sites to an isoleucine. This will force the first start codon to be translated even though it is weak site. The second protein that can arise is “intermediate length” as the first start codon is skipped and translation begins at the second codon site. The second site for initiation has a strong consensus sequence and therefore is routinely translated from methionine. The channel was truncated (1-56Δ) and the third translation site is mutated (M72I). This will force translation is begin at M60. The third isoform is “short length” and is formed when both the first and second start codons are skipped. The third methionine is flanked by an “adequate” consensus sequence. This site is believed not to be a popular initiation site for translation due to the previous strong consensus sequence. The formation of the short ATI was created by truncation of the N-terminus (1-63Δ) which caused translation to begin at M72. The forced long form TREK2

isoform creates the small and large conductance channel while, the two shorter isoforms produces the large conductance channel only. TREK2 isoforms differs from the TREK1 isoform as the reversal potential of potassium is unchanged from the TREK2 wildtype (Simkin et al 2008).

These isoforms have shown to affect the drug sensitivity of ion channels. This has been shown in the case of both TREK1 and TREK2. It was seen that truncated isoforms of  $K_{2P}$  were 2.6 -5-fold less sensitive to the drug carvedilol. It was speculated that the change in sensitivity could have been exhibited because of the increase in sodium permeability of the channel. However, this increase in sodium conductance is only seen in TREK1 and not TREK2. It is therefore indicated that the N-terminal is critical region for regulation of the channel (Kisselbach et al 2014; Veale et al 2014).

### **5.3 Aim of this chapter**

The aim is to clarify the differences in the inhibition of TREK2 by lamotrigine and sipatrigine and to investigate the mechanism of TREK2 is regulated by these compounds. The mechanism of action of sipatrigine and lamotrigine on TREK2 will be investigated by site directed mutagenesis and whole cell patch clamp electrophysiology.

# Results

## 5.4 Sipatrigine inhibits TREK2 channels

TREK2 currents were measured in the absence of sipatrigine (100  $\mu$ M) and showed inhibition of  $85 \pm 3\%$  ( $n = 10$ ). The reversal potential showed TREK2 at  $-92 \pm 1$  mV at control and then a significant but minor shift to  $72 \pm 4$  mV in the presence of sipatrigine ( $n = 10$ ). The TREK2 WT current after sipatrigine wash off was significantly higher than the baseline current before the application of the drug. Sipatrigine at a concentration of 100  $\mu$ M showed a large over recovery of current after inhibition ( $201 \pm 28\%$ ,  $n = 7$ ), (see Fig 5.2). The following shows a representation of general TREK2 WT currents (see Fig 5.2).

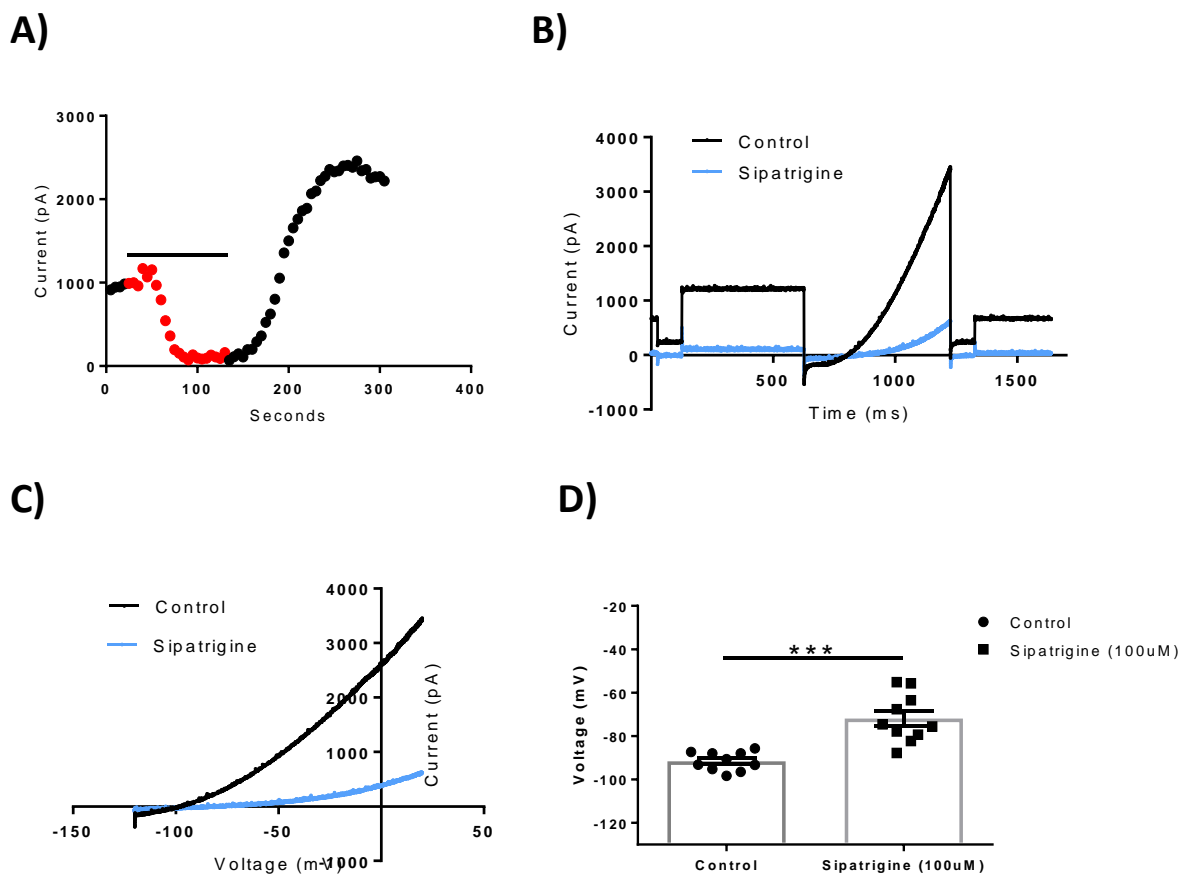


**Figure 5.2:** Sipatrigine (100  $\mu$ M) inhibition of WT TREK2 channels. (A) Time-course plot of sipatrigine effect on TREK2. Points show current in the presence and absence of sipatrigine. (B) Trace of current at different voltages controlled by the protocol. Each trace is an average of five consecutive traces in the presence and absence of sipatrigine. (C) Current-voltage relationship of TREK2 obtained from the ramp voltage changes in the presence and absence of sipatrigine. (D) Average reversal potential of TREK2 current ( $n = 10$ ). The reversal potential of current after the presence of sipatrigine. Paired Student *t*-test was used.

## 5.5 Lamotrigine inhibits TREK2 channels

TREK2 currents were measured in the absence of lamotrigine (100  $\mu\text{M}$ ) and showed inhibition of  $14 \pm 3\%$ ,  $n = 10$ . The reversal potential showed TREK2 at  $-87 \pm 2 \text{ mV}$  at control and then a negligible shift to  $-87 \pm 2 \text{ mV}$  in the presence of lamotrigine ( $n = 10$ ). The following shows a representation of general TREK2 WT currents (see Fig 5.2).

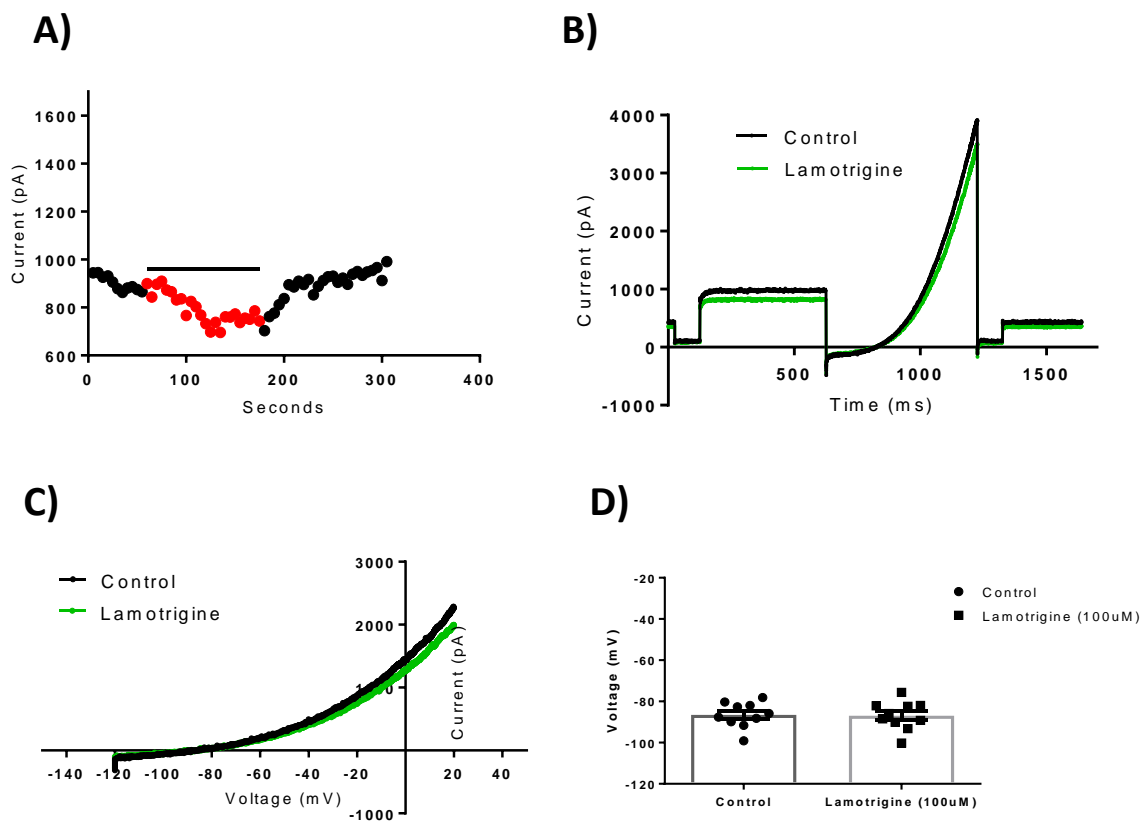


**Figure 5.3:** Lamotrigine (100  $\mu\text{M}$ ) inhibition of WT TREK2 channels. (A) Lamotrigine time course effect on TREK1. Points show current in the presence and absence of lamotrigine. (B) Trace of current at different voltages controlled by the protocol. Each trace is an average of five consecutive traces in the presence and absence of lamotrigine. (C) Current-voltage relationship of TRE2 using ramp voltage changes in the presence and absence of sipatrigine. (D) Average reversal potential of TREK2 current, in control and in lamotrigine ( $n = 10$ ). Paired Student  $t$ -test was used.

## 5.6 TREK2 predicted norfluoxetine interaction site is also predicted as a sipatrigine interaction site

It has been identified that norfluoxetine activity is reduced when TREK2 is mutated at site 320. This site is found at the fenestration and is believed to be an important residue for norfluoxetine interaction. To examine whether this site is involved in sipatrigine inhibition, the residue was mutated from a leucine to an alanine.

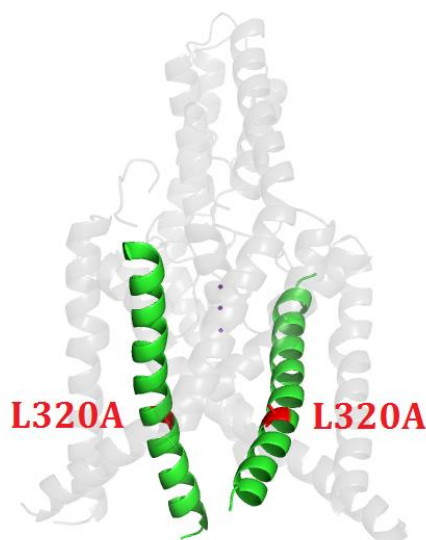


**Figure 5.4:** *TREK2* structure highlighting mutated residue (red)

The mutated TREK1 was produced and electrophysiology could therefore be carried out. TREK2 L320A showed inhibition at  $67 \pm 3\%$  ( $n=9$ ) in the presence of  $100\mu\text{M}$  sipatrigine. The recovery of current after inhibition was  $98 \pm 13\%$  ( $n=9$ ). The results show that sipatrigine inhibition was significantly decreased when the channel was mutated at the site compared to the WT at  $85 \pm 3\%$  ( $n = 10$ ) (see Fig 5.5 -C). It must also be noted that the TREK2 L320A has a similar degree of inhibition to that for the homologues site found on TREK1 L289A ( $56 \pm 7\%$ ,  $n=9$ ). The following shows a representation of general TREK2 L320A currents (see Fig 5.5).

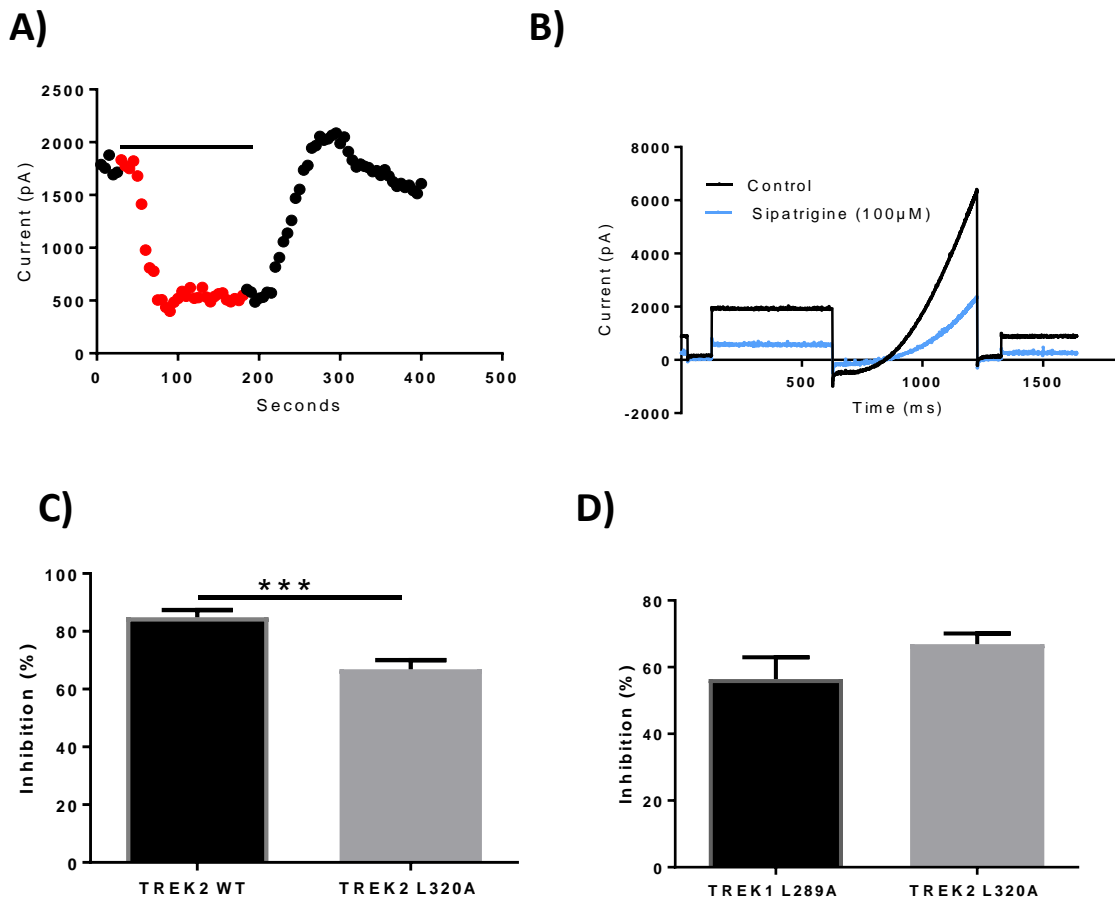


**Figure 5.5:** A) *TREK2* L320A is the presence and absence of sipatrigine (100 μM). B) *TREK2* L320A trace of current at different voltages controlled by the protocol. Each trace is an average of five consecutive traces in the presence and absence of sipatrigine. C) *TREK2* WT ( $n = 10$ ) sipatrigine inhibition (100 μM) compared to *TREK2* L320A ( $n = 9$ ). D) *TREK1* L289A ( $n = 9$ ) inhibition compared to the homogenous site on *TREK2* (L320A) ( $n = 9$ ) in the presence of sipatrigine (100 μM). Unpaired two-tailed Welch's *t*-test was used.

## 5.7 TREK2 over recovery of current

Sipatrigine was used at concentrations of 100  $\mu\text{M}$  and 30  $\mu\text{M}$  to study its effects on TREK2 WT current. TREK2 WT inhibition at 30  $\mu\text{M}$  was  $66 \pm 4\%$  ( $n = 11$ ) and inhibition at 100  $\mu\text{M}$  was  $85 \pm 3\%$  ( $n = 10$ ). It was noted however that at 100  $\mu\text{M}$ , there was a large over recovery of current after inhibition ( $201 \pm 28\%$ ,  $n = 7$ ). This suggests that sipatrigine TREK2

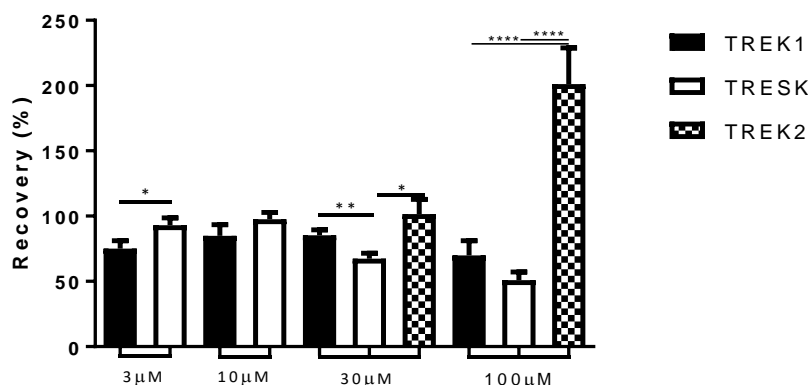


**Figure 5.6:** The recovery of current after sipatrigine inhibition on TREK1, TREK2 and TRESK WT. The recovery of current was measured at a concentration of 3  $\mu\text{M}$  (TREK1  $n = 8$  and TRESK  $n = 11$ ), 10  $\mu\text{M}$  (TREK1  $n = 8$  and TRESK  $n = 10$ ), 30  $\mu\text{M}$  (TREK1  $n = 10$ , TRESK  $n = 16$  and TREK2  $n = 11$ ) and 100  $\mu\text{M}$  (TREK1  $n = 17$ , TRESK  $n = 13$  and TREK2  $n = 7$ ) Unpaired two-tailed Welch's *t*-test was used for 3  $\mu\text{M}$  and 10  $\mu\text{M}$ . One-way ANOVA applying post hoc Tukey was used at 30  $\mu\text{M}$  and 100  $\mu\text{M}$ .

It was therefore hypothesized that this over recovery after sipatrigine inhibition is caused because sipatrigine acts as a fast inhibitor and also a slower activator on TREK2. Therefore, I allowed TREK2 to be exposed to sipatrigine at 100  $\mu\text{M}$  for a longer period of time to see if there is any slow activation.

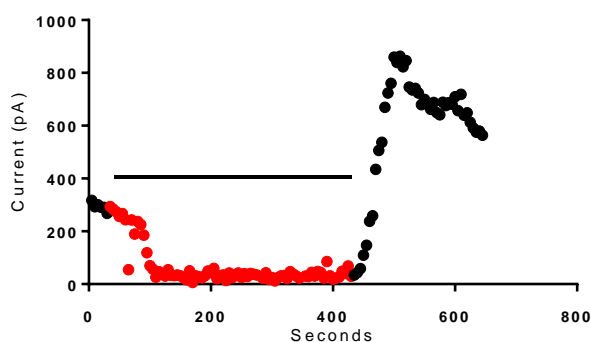


**Figure 5.7:** TREK2 in the presence of sipatrigine (100  $\mu\text{M}$ ) after a longer exposure time.

The results show that the dual action of the drug is there but is only exposed after the drug is washed out.

## 5.8 TREK2 isoforms generated by ATI change sipatrigine effect

The first isoform created was the forced long form of TREK2 which did show over recovery of current. The forced long form TREK2 was inhibited by  $78 \pm 2\%$  ( $n = 11$ ) using  $100 \mu\text{M}$  sipatrigine. There was also over recovery of current after inhibition ( $149 \pm 16\%$ ,  $n = 8$ ) The following shows a representation of general TREK2 isoform currents (see Fig 5.8).

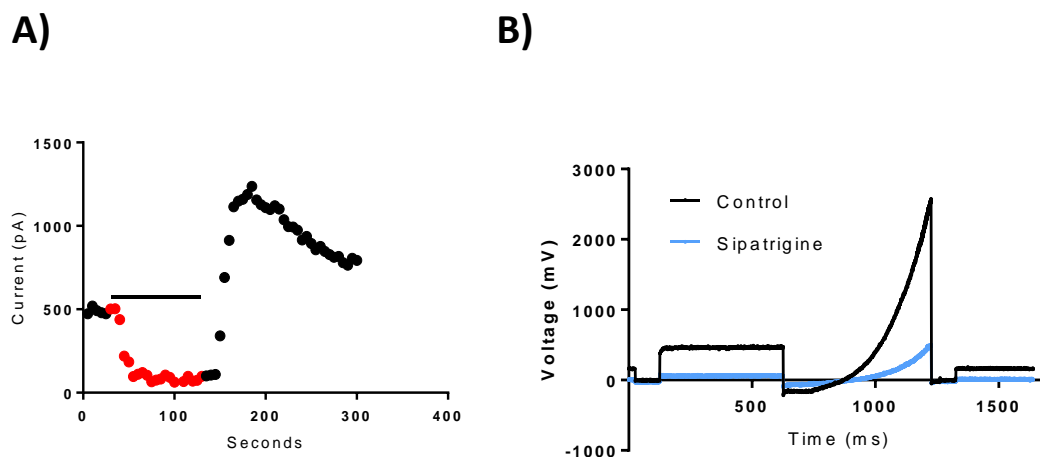


**Figure 5.8:** A) Forced long form TREK2 in the presence of sipatrigine ( $100 \mu\text{M}$ ) and the over recovery in the wash off of sipatrigine. B) Trace of current at different voltages controlled by the protocol. Each trace is an average of five consecutive traces in the presence and absence of sipatrigine.

The intermediate forced form of TREK2 showed inhibition at  $70 \pm 5$  ( $n = 7$ ). The current did show recovery after inhibition however it was not at the same magnitude of the forced long forced. The intermediate forced form showed recovery of current at  $111 \pm 12$  ( $n = 5$ ). The following shows a representation of general TREK2 isoform currents (see Fig 5.9).

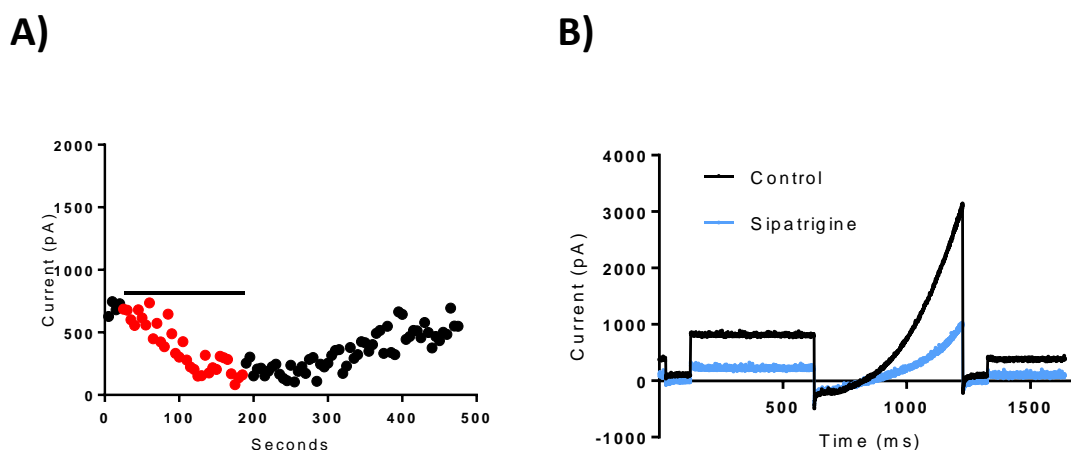


**Figure 5.9:** A) Forced intermediate- form TREK2 in the presence of sipatrigine ( $100 \mu\text{M}$ ) and the recovery of current in the wash-off of sipatrigine. B) Trace of current at different voltages controlled by the protocol. Each trace is an average of five consecutive traces in the presence and absence of sipatrigine.

The forced short form of TREK2 was inhibited by sipatrigine by  $51 \pm 11$  ( $n = 6$ ) and the short form showed recovery of  $115 \pm 18$  ( $n = 5$ ) The following shows a representation of general TREK2 isoform currents (see Fig 5.10).

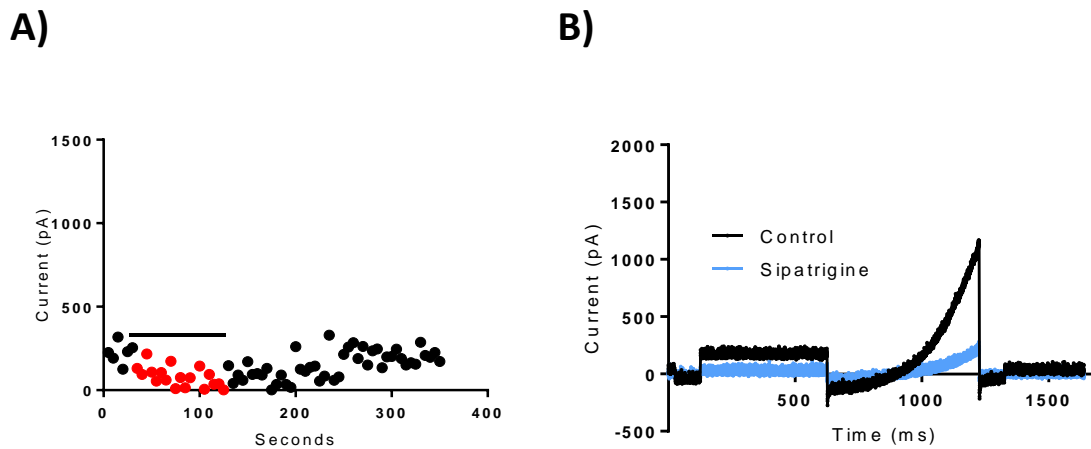


**Figure 5.10:** A) Forced short- form of TREK2 in the presence of sipatrigine ( $100 \mu\text{M}$ ) and the recovery of current in the wash off. B) Trace of current at different voltages controlled by the protocol. Each trace is an average of five consecutive traces in the presence and absence of sipatrigine.

To investigate whether the over recovery of current after sipatrigine inhibition is linked to the N-terminal, the current was measured in the presence of sipatrigine at a concentration of  $100 \mu\text{M}$ . The results showed that at the highest measured concentration, the over recovery was identified when the full-length N terminal is present ( $49 \pm 15\%$ ,  $n = 8$ ). The over recovery of TREK WT was  $101 \pm 28\%$  ( $n = 7$ ) which is considered to not significantly different to the full-length ATI. The results of the intermediate length showed an over recovery of  $11 \pm 13\%$  ( $n = 5$ ) and the short form showed an over recovery of  $15 \pm 18\%$  ( $n = 5$ ). The two smaller isoforms were significantly different to TREK WT over recovery.

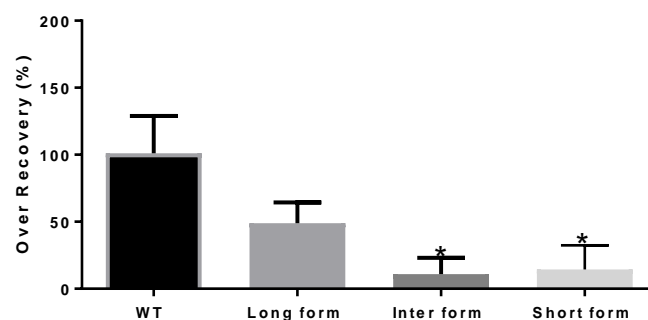


**Figure 5.11:** The measured over recovery of TREK2 WT ( $n = 7$ ) and TREK2 long form ( $n = 8$ ), TREK2 intermediate form ( $n = 5$ ) and TREK2 short form ( $n = 5$ ) after inhibition of sipatrigine ( $100 \mu\text{M}$ ). One-way ANOVA applying post hoc Dunnett's method was used.

When characterising the current of the isoforms of TREK2 it was found that the forced short form expressed a significantly lower current compared to the WT. The current density of WT

was  $68 \pm 9$  pA/pF ( $n = 19$ ), which is significantly greater than the forced short form ( $14 \pm 3$  pA/pF,  $n = 8$ ). The current density of forced long and intermediate isoform was very similar to WT TREK2. The current density of the forced long form is  $64 \pm 13$  pA/pF ( $n = 15$ ) and the intermediate is  $76 \pm 10$  ( $n = 6$ ).

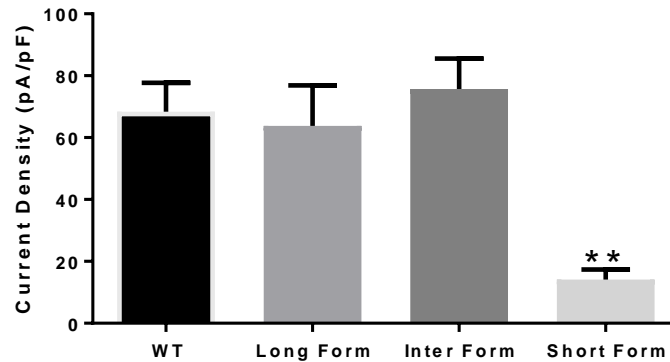


**Figure 5.12:** The current density of TREK2 WT ( $n = 19$ ), TREK2 long form ( $n = 15$ ), TREK2 intermediate form ( $n = 6$ ) and TREK2 short form ( $n = 8$ ). The current density of TREK2 WT versus TREK2 ATI isoforms. One-way ANOVA applying post hoc Dunnett's method was used

The results further show that TREK2 WT inhibition ( $85 \pm 3\%$ ,  $n = 10$ ) was significantly different to the forced short ATI isoform ( $51 \pm 11\%$ ,  $n = 6$ ). The long-forced form showed inhibition of  $78 \pm 2\%$  ( $n = 11$ ) and the intermediate forced form was inhibited by  $70 \pm 5\%$  ( $n = 7$ ). The two longer ATI isoforms showed no significant difference to TREK2 WT.

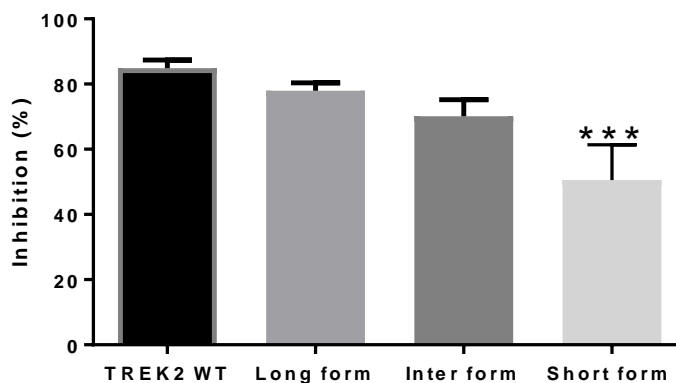


**Figure 5.13:** TREK2 WT ( $n = 10$ ), TREK2 long form ( $n = 11$ ), TREK2 intermediate form ( $n = 7$ ) and TREK2 short form ( $n = 6$ ) inhibition by sipatrigine ( $100 \mu\text{M}$ ). One-way ANOVA applying post hoc Dunnett's method was used.

## 5.9 25 mM K<sup>+</sup> solution effect on TREK2 with sipatrigine

The resting basal current of forced short form TREK2 is significantly lower compared to TREK2 WT and the other two ATI isoforms (see Fig 5.10). The current was therefore measured in 2.5 mM K<sup>+</sup> solution and then perfused 25 mM K<sup>+</sup> solution to increase the current. Sipatrigine (100 μM) was made in 25 mM K<sup>+</sup> solution.

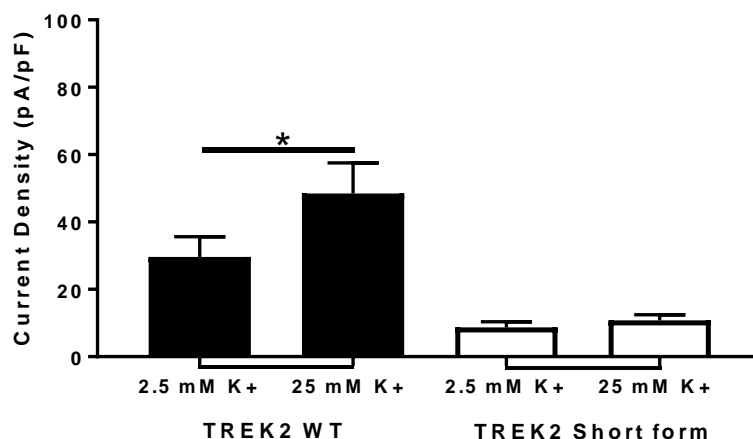


**Figure 5.14:** Current density of TREK2 WT in 2.5mM K<sup>+</sup> solution compared to the same cell in 25mM K<sup>+</sup> solution ( $n = 5$ ). Current density of forced short form TREK2 WT in 2.5mM K<sup>+</sup> solution compared to the same cell in 25mM K<sup>+</sup> solution ( $n = 7$ ). Paired Student *t*-test was used.

TREK2 WT showed that when the channel was exposed to 25 mM K<sup>+</sup> solution, there is a significant increase in current ( $48 \pm 9$  pA/pF,  $n = 5$ ) compared to the channel under 2.5 mM K<sup>+</sup> solution ( $30 \pm 6$  pA/pF,  $n = 5$ ). However, the forced short form TREK2 showed no significant difference in between the channels current 2.5mM K<sup>+</sup> solution ( $9 \pm 2$  pA/pF,  $n = 7$ ) compared to the same cells under 25mM K<sup>+</sup> solution ( $11 \pm 2$  pA/pF,  $n = 7$ ). This shows the importance of the N terminus in channel conductance. The following shows a representation of general TREK2 WT currents (see Fig 5.14).

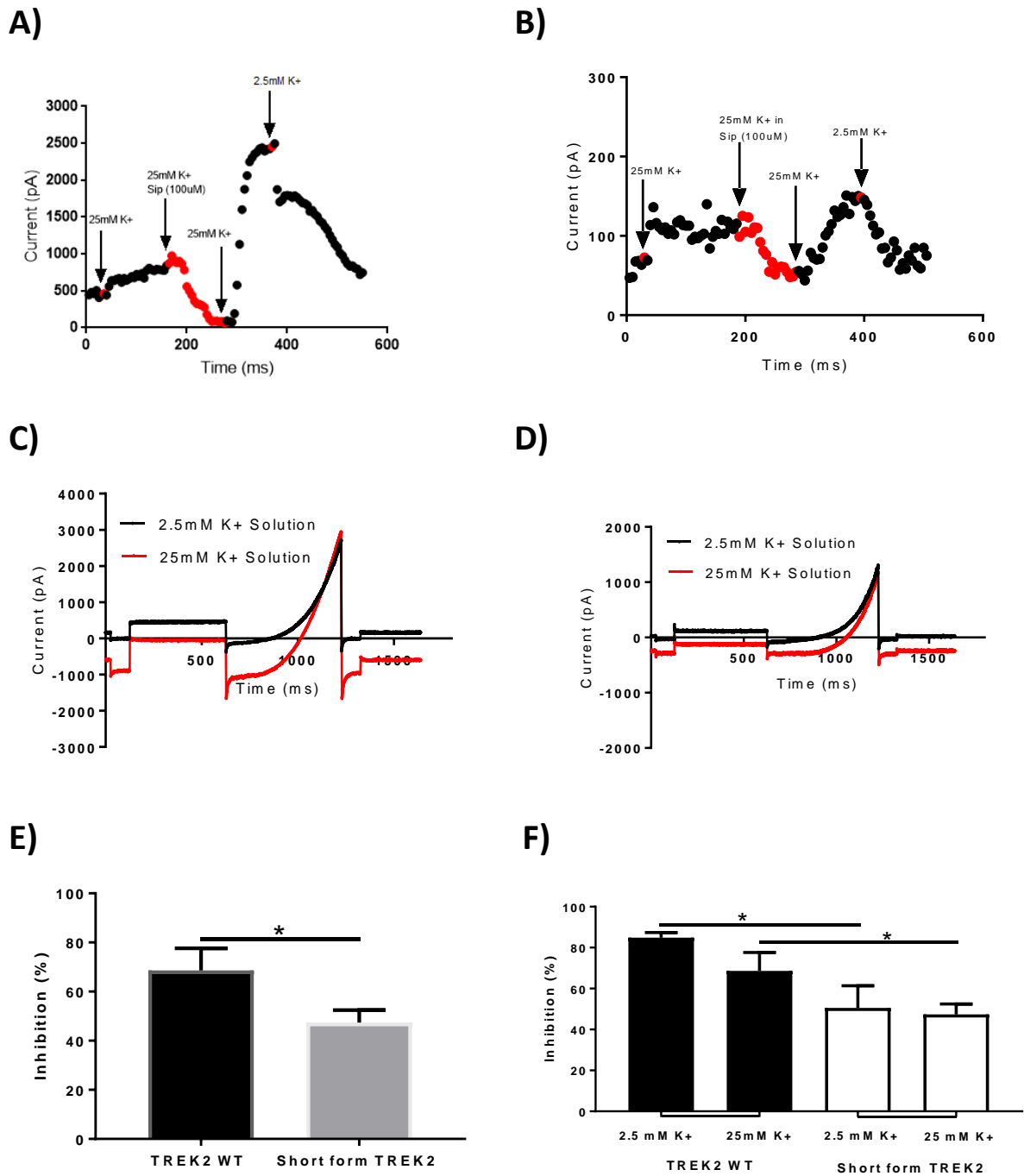


**Figure 5.15:** A) Current change due to external potassium concentration and inhibition caused by sipatrigine (100  $\mu$ M) in TREK2 WT. B) Current change due to external potassium concentration and inhibition caused by sipatrigine (100  $\mu$ M) in TREK2 short form. C) Trace of TREK2 WT current at different voltages controlled by the protocol. Each trace is an average of five consecutive traces. D) TREK2 short form current using the protocol to control the voltage. Each trace is an average of five consecutive traces. E) Sipatrigine inhibition (100  $\mu$ M) in 25 mM K<sup>+</sup> external solution on TREK2 WT (n = 6) and forced short form TREK2 (n = 7). F) There was no significant difference in sipatrigine inhibition (100  $\mu$ M) in 2.5 mM K<sup>+</sup> external solution versus 25mM K<sup>+</sup> solution on the same channel, however there is a significant difference between the degree of sipatrigine inhibition between TREK2 WT and forced short form TREK2. Unpaired two-tailed Welch's t-test was used for 2.5 mM K<sup>+</sup> solution and unpaired one-tailed Welch's t-test was used for 25 mM K<sup>+</sup> solution.

Sipatrigine in 25 mM K<sup>+</sup> external solution produced an inhibition of TREK2 WT ( $69 \pm 9\%$ ,  $n = 6$ ). The forced short form showed a significant change in the degree of inhibition by sipatrigine in 25 mM K<sup>+</sup> solution compared to WT ( $47 \pm 5$ ,  $n = 7$ ) (see Fig 5.14 A-B). The increase in extracellular potassium concentration did not have the desired effect of increasing the current from the forced short form of TREK2, as there was no significant increase in current from the channel (Fig 5.13). However, the results did show no significant difference between sipatrigine inhibition in 2.5mM K<sup>+</sup> solution and 25mM K<sup>+</sup> solution (see Fig 5.14-F).

It was also confirmed that increasing K<sup>+</sup> in the extracellular solution did not change the effect of sipatrigine of the forced short form of TREK2. There was a little to no over recovery of current after sipatrigine inhibition by the forced short form TREK2 ( $18 \pm 8\%$ ,  $n = 5$ ). The over recovery of current after inhibition by TREK2 WT was measured at  $132 \pm 50\%$  ( $n = 5$ ). This shows the importance of the N-terminus in the role of inhibition by sipatrigine and in the over recovery of TREK2 current (see Fig 5.15).

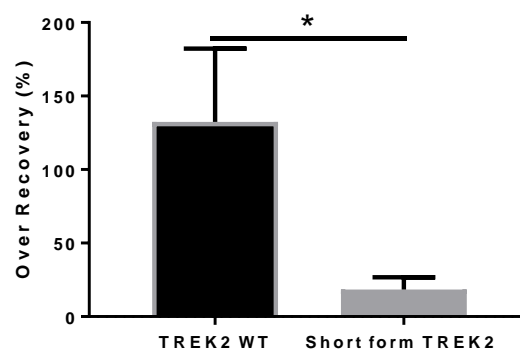


**Figure 5.16:** Over recovery of current seen in TREK2 WT ( $n = 5$ ) and TREK2 short form ( $n = 5$ ) after exposure to sipatrigine ( $100 \mu\text{M}$ ). (One recording was excluded as it showed no recovery). One-tailed Welch's *t*-test was used.

# **CHAPTER SIX**

## **Inhibitor compound Cen-092-C effect on $K_{2P}$ channels**

# Introduction

## 6.1 Cen-092-C

Cen-092-C is a newly developed Na<sup>+</sup> inhibitor which has been investigated in a multiple sclerosis (MS) study in an EAE (experimental autoimmune encephalomyelitis) model. Blocking sodium channels is important in treating MS as sodium accumulation will lead the excitability of neurons. This activity will contribute to axonal injury and will exacerbate the neurological disability (Yang et al 2015). Cen-092-C is derived from lamotrigine and therefore it can only be speculated what effects the compound has on K<sub>2P</sub> channels. The results show that EAE symptoms were significantly decreased in the cumulative disability scores in mice treated with Cen-092-C compared to the untreated rats (unpublished data from Leach).

When investigating neurologic disorders such as MS, the endothelial cells of small brain vessels have become important as the dysfunction of the blood-brain barrier is a common event (Mizee et al 2014). TREK1 is known to play a significant role in regulating inflammatory immune response as the channel regulates immune cell trafficking across the blood-brain barrier like in MS. It was shown that murine lymphocytes migrate with more ease in TREK1<sup>-/-</sup> endothelial cells compared to the wild-type cells (Wang et al 2012). In fact, it was found that in EAE mice model, there was a larger demyelination area and a higher number of infiltrating T cells in the CNS in TREK1<sup>-/-</sup> compared to TREK1 WT. These TREK1<sup>-/-</sup> mice also saw the clinical phenotype worsen in the EAE model (Bittner et al 2013).

TRESK channels have been shown to be expressed in rat thymus and spleen. Both tissues contain T and B - cells which shows that these channels are likely involved in immune response (Han and Kang 2009). It is also seen that TRESK-like K<sup>+</sup> channels are functionally expressed in human leukemic T-cells and Jurkat cells. It was found that in Jurkat cells, TRESK current contributes to the K<sup>+</sup> efflux which will lead to apoptosis (Pottosin et al 2008). Calcineurin is a critical part of pre- T-cell receptor signaling pathway and is also involved in TRESK activation. A high level of calcineurin is detected in leukemic cells and are important regulators of inducible gene expression. When T-cells are activated, binding and dephosphorylation of calcineurin to the docking site on TRESK will lead to an increase in TRESK current. This activation could induce the transcription of new genes as calcineurin-NFAT signaling is critical of mediating cellular activation and the immune response (Bueno et al 2002). Furthermore, TRESK is activated by histamine, a mediator in local immune response. It is known that histamine induces NFAT- mediated transcription through the H1 histamine receptor in human umbilical endothelial cells. The H1 histamine receptor is

involved in decreasing the helper T cell response in the immune system. Therefore, it is likely that TRESK is involved in regulating T-cell function (Han and Kang 2009).

Cen-092-C is derived from lamotrigine and has a similar structure to sipatrigine. As this new compound is closely related to lamotrigine, it would be interesting to find if the same degree of inhibition occurs on each  $K_{2P}$  channel and how this may affect CNS disorders like MS, pain, depression and neuroprotection.

## **6.2 Aim of the chapter**

The effect of Cen-092-C on  $K_{2P}$  channels is unknown. Therefore, I investigated the effect of Cen-092-C on TREK1 and TRESK. This study will aim to see if the compound is an effective antagonist and understand which mechanism the drug takes on to inhibit the channels using electrophysiology recording.

# Results

## 6.3 Cen-092-C inhibition of TRESK current

Cen-092-C at a concentration of 100  $\mu\text{M}$  inhibited TRESK by  $42.7 \pm 5\%$ ,  $n = 9$ . Results carried out at 30  $\mu\text{M}$  showed inhibition at a degree of  $31 \pm 5\%$ ,  $n = 10$ . The following shows a representation of general TRESK WT currents (see Fig 6.1).

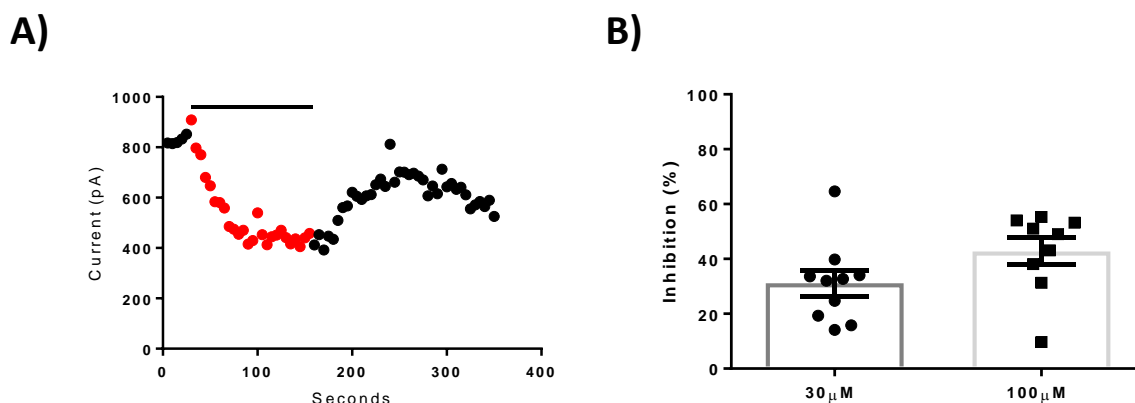


**Figure 6.1:** A) The inhibition of TRESK WT in the presence and absence of 100  $\mu\text{M}$  of Cen-092-C. B) The inhibition of TRESK WT at two different concentrations (30  $\mu\text{M}$ ,  $n = 10$  and 100  $\mu\text{M}$ ,  $n = 9$ ). Paired Student *t*-test was used.

The results show a significantly lower inhibition rate in comparison to sipatrigine (100  $\mu\text{M}$ ), whilst there was no change in the degree of inhibition when compared to lamotrigine (100  $\mu\text{M}$ ). The results also show little to no change in reversal potential. The evidence shows that inhibition is a direct effect of the compound as the double mutated phenylalanine showed a significant decrease in inhibition. This suggests that Cen-092-C may bind to the central cavity of TRESK channels.

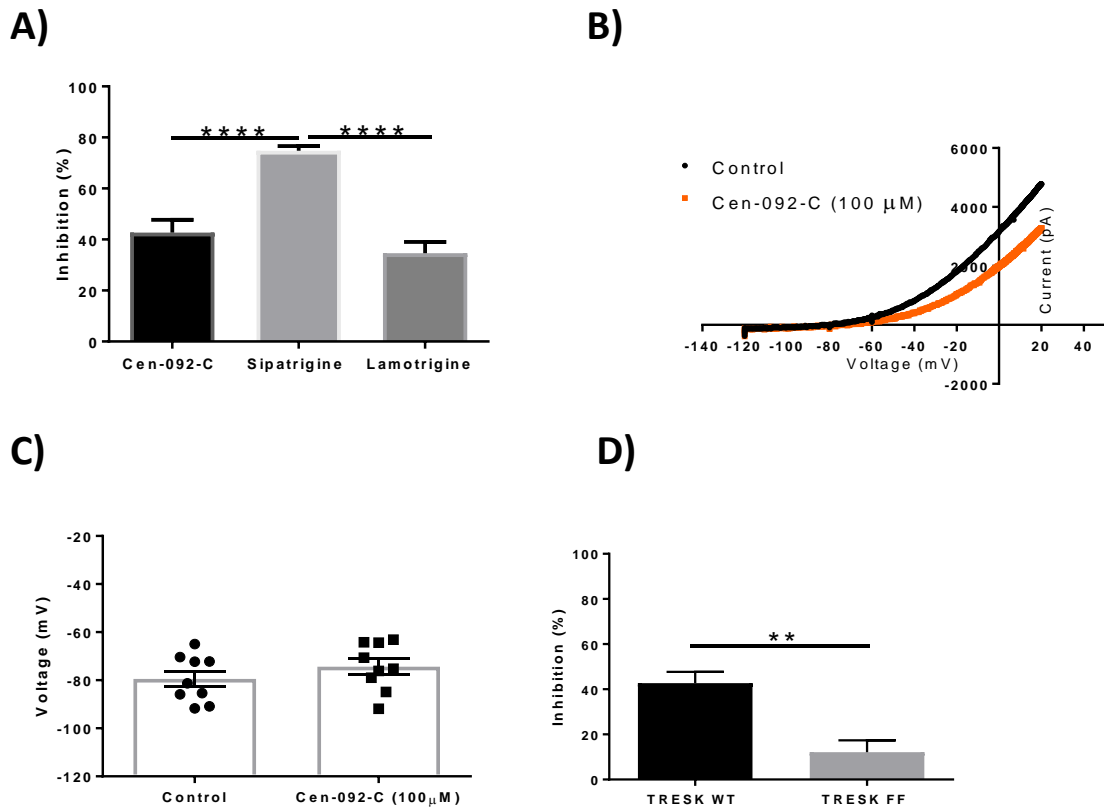


**Figure 6.2:** A) Inhibitory effect of Cen-092-C ( $n = 9$ ), sipatrigine ( $n = 16$ ) and lamotrigine ( $n = 8$ ) (each at a concentration of  $100 \mu\text{M}$ ) on TRESK WT. The inhibitory effect of sipatrigine on TRESK WT versus the inhibitory effect of lamotrigine and Cen-092-C on TRESK. One-way ANOVA applying post hoc Tukey test was used. B) Reversal potential of TRESK WT in the presence of Cen-092-C. C) Average reversal potential of TRESK WT with Cen-092-C ( $100 \mu\text{M}$ ) ( $n = 9$ ). D) The introduction of alanines at residues F145 and F352 ( $n = 6$ ) showed a reduction of Cen-092-C inhibition compared to WT ( $n = 9$ ). The inhibitory effect of Cen-092-C on TRESK WT versus TRESK FF. Paired Student *t*-test was used (C). Unpaired two-tailed Welch's *t*-test was used to analysis mutation inhibition against wild-type (A and D).

## 6.4 Is Cen-092-C inhibition on TRESK state dependent?

It has already been shown that the phosphorylation state of TRESK effects the degree of lamotrigine inhibition. Therefore it would be interesting to see the structurally similar Cen-092-C acts in a similar way (see Fig 4.8). To investigate whether the state of TRESK channel affects the degree of inhibition of Cen-092-C, TRESK was mutated to force a phosphorylation state. The new compound Cen-092-C inhibited TRESK WT at a degree of  $42.8 \pm 5\%$  ( $n = 9$ ). The two states showed no difference of inhibition compared to the WT (TRESK AA inhibition  $49 \pm 7\%$ ,  $n = 6$  and TRESK EE inhibition  $45 \pm 4\%$ ,  $n = 8$ ).

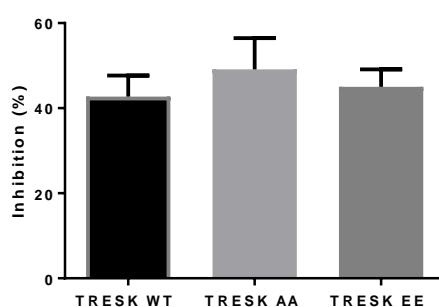


**Figure 6.3:** Cen-092-C (100  $\mu$ M) inhibition of TRESK WT ( $n = 9$ ), TRESK AA ( $n = 6$ ) and TRESK EE ( $n = 8$ ). One-way ANOVA applying post hoc Dunnett's test used.

## 6.5 Cen-092-C inhibition on TREK1

Cen-092-C selectivity was investigated by looking at another  $K_{2P}$  channel. TRESK share about 20% of its sequence with TREK1 (Dobler et al 2007). It was found, however, that inhibition of TREK1 by Cen-092-C (30  $\mu\text{M}$ ) shows little to no inhibition. There were three recordings which showed a high degree of inhibition though these points are believed to be outliers as the majority of recordings showed limited effect on current in the presence of 30  $\mu\text{M}$  Cen-092-C. The inhibition by Cen-092-C at a concentration at 100  $\mu\text{M}$  was  $21.4 \pm 4\%$  ( $n = 9$ ), which was significantly lower than inhibition of TRESK at the same concentration. The inhibitory effect of Cen-092-C on TREK1 was similar to that seen in lamotrigine inhibition at the largest concentration.

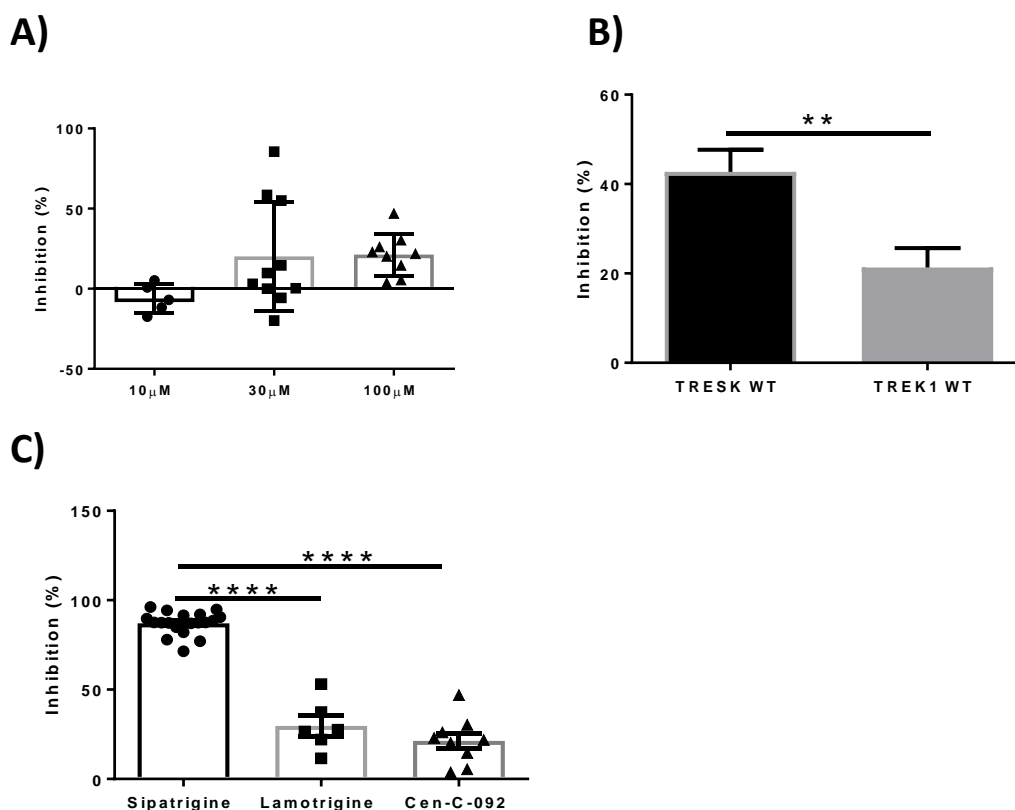


**Figure 6.4:** A) The degree of inhibition of Cen-092-C with a concentration of 10  $\mu\text{M}$  ( $n = 5$ ), 30  $\mu\text{M}$  ( $n = 10$ ) and 100  $\mu\text{M}$  ( $n = 9$ ) on TREK1 current. B) Comparison between TRESK WT ( $n = 9$ ) and TREK1 WT ( $n = 9$ ) inhibition in the presence of Cen-092-C (100  $\mu\text{M}$ ). C) Inhibitory effect of sipatrigine ( $n = 19$ ), lamotrigine ( $n = 6$ ), and Cen-092-C ( $n = 9$ ) (each at a concentration of 100  $\mu\text{M}$ ) on TREK1 WT current. Unpaired two-tailed Welch's *t*-test was used (B). One-way ANOVA applying post hoc Tukey test was used (A and C).

# **CHAPTER SEVEN**

## **GENERAL DISCUSSION**

# General Discussion

## 7.1 Lamotrigine modulates TREK1, TREK2 and TRESK

Lamotrigine has been shown to inhibit TREK1 ( $30 \pm 6\%$ ), TREK2 ( $14 \pm 3\%$ ) and TRESK ( $35 \pm 5\%$ ) at a concentration of  $100 \mu\text{M}$  (see Fig 7.1). This concentration has been shown to have analgesic effects using tail-flick test and is known to induce analgesia in neuropathic pain models (Saber and Chavooshi 2009). Lamotrigine inhibits TREK1 current to a similar degree to TRESK current, while inhibition of TREK2 current by lamotrigine was significantly different to TREK1 and TRESK current inhibition. Lamotrigine has been described to have little or no effect on TREK1 and TREK2 current (Meadows et al 2001; Kang et al 2008). In fact, lamotrigine has been used to identify TRESK channels and distinguish it from other channels (Liu et al 2014; Guo and Cao 2014). The previous study used  $30 \mu\text{M}$  on TREK2 channels and it was then concluded that lamotrigine had no effect on that channel and only TRESK is lamotrigine-sensitive (Kang et al 2008). Lamotrigine ( $10 \mu\text{M}$ ) was found to produce little to no inhibition of TREK1 current expressed in HEK293 cells (Meadows et al 2001). However, my results show that lamotrigine inhibits both TREK1 ( $30 \pm 6\%$ ) and TREK2 ( $14 \pm 3\%$ ), with TREK1 current inhibiting to a similar degree to TRESK ( $35 \pm 5\%$ ) at a concentration of  $100 \mu\text{M}$ . It can therefore be concluded that lamotrigine does inhibit both TREK1 and TREK2 to some degree. Lamotrigine has also been shown to inhibit glutamate-induced TRESK activation. Kang et al 2008 used the inside-out patch configuration to demonstrate that lamotrigine inhibition is a direct action on TRESK. Lamotrigine was originally believed to inhibit only TRESK and so it was claimed to be regulated through a pathway selective for TRESK channels by the blockage of calcium influx (Kang et al 2008). The results here outline that lamotrigine does inhibit TRESK current ( $35 \pm 5\%$ ), however, lamotrigine also inhibits TREK1 ( $30 \pm 6\%$ ) and TREK2 ( $14 \pm 3\%$ ) which shares only 20% of TRESK sequence (Dobler et al 2007) and so, lamotrigine cannot be regarded as a selective inhibitor of TRESK channels.

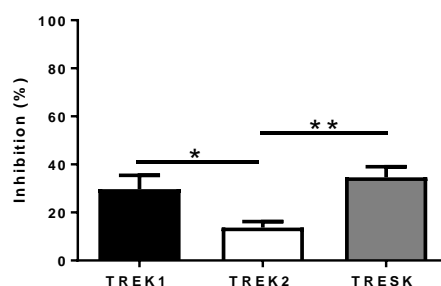


**Figure 7.1:** Lamotrigine ( $100 \mu\text{M}$ ) inhibition of TREK1 WT ( $n=6$ ), TREK2 WT ( $n = 10$ ) and TRESK ( $n=8$ ). One-way ANOVA post hoc Tukey test was used.

## 7.2 Sipatrigine is a potent inhibitor of TREK1, TREK2 and TRESK

The results show that TREK1 and TREK2, and to a lesser extent TRESK current, were effectively inhibited by the neuroprotective agent, sipatrigine. Sipatrigine had not been studied on TRESK previously and has now been shown to be a potent inhibitor. The rapid inhibition and reversible action of sipatrigine could suggest direct action on the channel by binding to TREK1, TREK2 and TRESK. Sipatrigine at a concentration of 3  $\mu\text{M}$  inhibited TREK1 current by  $26.8 \pm 3.8\%$  ( $n = 8$ ) which is significantly different to TRESK current inhibition at the same concentration ( $11 \pm 3\%$ ,  $n = 11$ ). Sipatrigine (10  $\mu\text{M}$ ) inhibition also shows significant difference between TREK1 current ( $40 \pm 5\%$ ,  $n = 10$ ) and TRESK current ( $25 \pm 4\%$ ,  $n = 11$ ). 30  $\mu\text{M}$  of sipatrigine produced TRESK current inhibition ( $46 \pm 3\%$ ,  $n = 19$ ) which was shown to be similar to TREK1 current inhibition of  $56 \pm 5\%$  ( $n = 13$ ). However, TRESK inhibition was significantly different to TREK2 current inhibition ( $66 \pm 5\%$ ,  $n = 11$ ). Sipatrigine (100  $\mu\text{M}$ ) has been seen to inhibit TRESK current by  $73 \pm 3\%$  ( $n = 16$ ) while TRESK current inhibition, was shown to be significantly different to both TREK1 ( $87 \pm 2\%$ ,  $n = 19$ ) and TREK2 ( $85 \pm 3\%$ ,  $n = 10$ ) (see Fig 7.2).

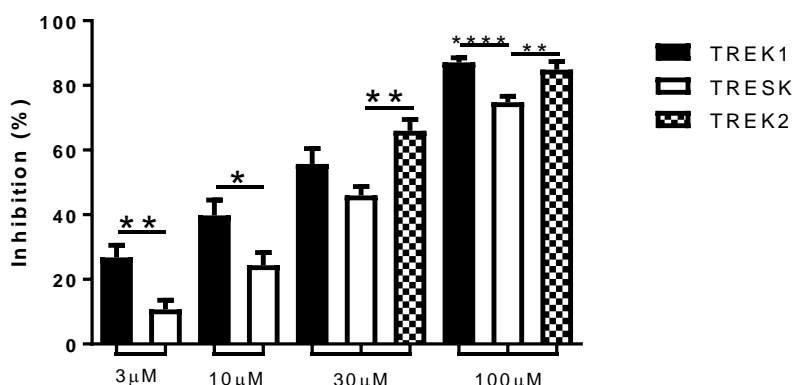


**Figure 7.2:** Sipatrigine inhibition of TREK1, TREK2 and TRESK WT at concentrations of 3  $\mu\text{M}$ , 10  $\mu\text{M}$ , 30  $\mu\text{M}$  and 100  $\mu\text{M}$ . Unpaired two-tailed Welch's *t*-test and one-way ANOVA post hoc Tukey test were used.

Sipatrigine has also been found to inhibit both sodium and calcium channels. The antagonism of both sodium and calcium channels results in attenuation of glutamate release. The inhibitory effect on  $\text{Na}^+$  channel is believed to result in neuroprotection through the down regulation of action potential firing and glutamate release (Hainsworth et al 2000). The inhibition of presynaptic calcium channels by sipatrigine also affects the glutamate release. Therefore, presynaptic calcium channel antagonism is important for neuroprotection (McNaughton et al 1997). Previous *in vitro* studies of CNS white matter ischaemia have

shown that complete protection was seen at a concentration of 100  $\mu\text{M}$  (Garthwaite et al 1999); a concentration which has been demonstrated in this study to show potent inhibition of all three channels. Therefore it must be investigated further what TREK1, TREK2 and TRESK inhibition, at a concentration known to be effective, means for neuroprotection and analgesia.

### 7.3 Central cavity binding sites

Voltage-gated ion channel inhibitors have been shown bind at the central cavity which implies a lack of specificity at this site (Marzian et al 2013). Tetraethylammonium (TEA) is a selective voltage-selective  $\text{K}^+$  channel blocker. TEA has been shown to block potassium channel KcsA current by altering the potassium ion occupancy through binding within the ion conduction pathway in the selectivity filter. TEA is believed to bind to the potassium channel at dehydration transition sites insuring a blockade of potassium ions (Lenaeus et al 2005). Similarly, fatty acids are shown to bind with KcsA on the hydrophobic lining of the central cavity therefore blocking current (Smithers et al 2012). 4-Aminopyridine (4AP) is another “classic” K channel blocker, which is known to interact with the central cavity of KcsA channels. 4AP enters the channel from the cytoplasmic side and will promote a closed conformation (Armstrong and Loboda 2001). The central cavity has also been shown to be imperative in the binding of drugs in  $\text{K}_{2\text{P}}$  channels. The TASK1 blocker A1899 binds on the selectivity filter at residues T93 and T199 on the M2 and the M4 segment of the channel. This region is lined with hydrophobic amino acids which can therefore provide a potential binding surface for small hydrophobic molecules. The hydrophobic lining also allows for rapid movement of  $\text{K}^+$  ions through the cavity. Alanine scanning mutagenesis abolished any inhibition of current which determined the importance of these residues. These threonine residues are conserved in  $\text{K}_{2\text{P}}$  channels and have been indicated in binding studies of various K channels inhibitors (Streit 2011; Piechotta et al. 2011; Schewe et al 2016; Viswanath et al 2016).  $\text{K}_{2\text{P}}$  channel activation also involves the central pore as mutations of threonine close the selectivity filter abolishes activation of TRAAK by AA and  $\text{PIP}_2$  (Schewe et al 2016). Further evidence of the importance of the central pore cavity as a binding site in  $\text{K}_{2\text{P}}$  channels was found through the *in-silico* investigation of TREK1 antagonists. The *in-silico* experiments found that L289 is an important site for binding as it made strong binding interactions with the aliphatic chains of quaternary ammonium blocker compound (QAs) (Viswanath et al 2016). Docking of norfluoxetine to TREK2 again shows strong evidence that binding to the equivalent residue, L320, is important in regulation of the current (Dong et al 2015). Therefore, the docking of the potent antagonist sipatrigine at the central cavity of TREK2 is in line with these studies. The key residue, L289 in TREK1 and L320 in TREK2,

were substituted to an alanine and a significant reduction in sipatrigine inhibition was observed. These results support the proposition that sipatrigine binds to this residue found in TREK1 and TREK2. The same mutated site in TREK1 (L289A) showed no change in the degree of lamotrigine inhibition. It could therefore be proposed that lamotrigine has no interaction with this site. This could be why lamotrigine shows a significantly lower degree of inhibition compared to sipatrigine, even though sipatrigine is derived from lamotrigine. It is therefore proposed that the two compounds act on different sites of the channel.

The *in-silico* study also showed T142 and T251, found close to the selectivity filter, as important sites in channel inhibition (Viswanath et al 2016). However, when these threonine residues were mutated to alanine, there was no significant change in the degree of inhibition of sipatrigine. Therefore, these sites are not involved in TREK1 sipatrigine sensitivity, even though these residues are important for other regulators of TREK channel activity.

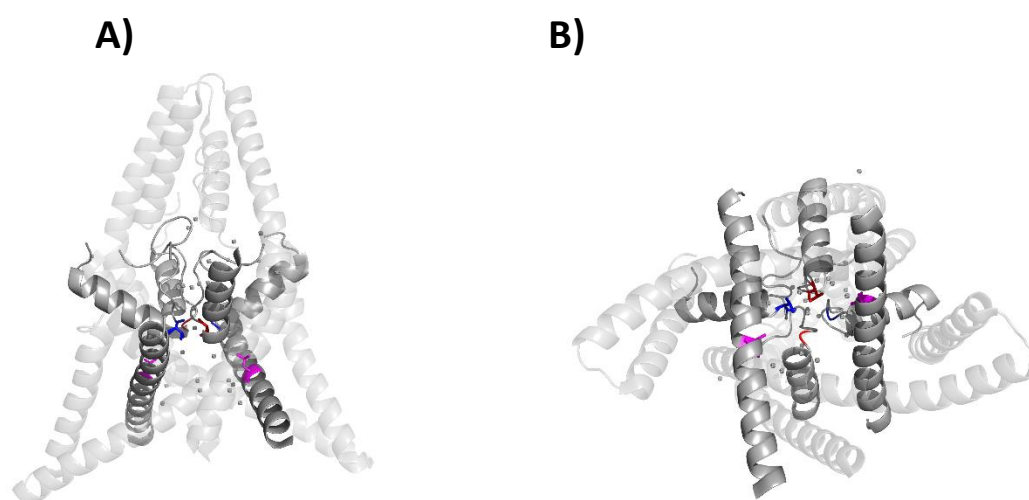


**Figure 7.3:** *TREK1 (4TWK) illustrates sites investigated for sipatrigine and lamotrigine binding. The fenestration site L289 is labelled magenta. The two threonine sites at the pore are also highlighted. T142 is labelled in red and T251 is labelled in blue.*

Furthermore, a very recent study investigating  $K_{2P}$  activation has shown that TREK1 mutation of lysine 271 on the TM4 results in the reversal of ML335 and ML402 activation. The equivalent residue in TRAAK (Q258K) was also found to decrease activation by ML335 and ML402. This mutation also showed to not change the effects of other activators such as arachidonic acid, BL1249 and ML67-33. To further analyse the cation- $\pi$  interaction with ML335 the aliphatic ring was put in place of the original aromatic upper ring called ML335a. It was found that this new compound had no effect on TREK1 which shows that K271 cation- $\pi$  interaction with the C-type gate is important for ML335 and ML402 selectivity and essential for current activation (Lolicato et al 2017). This site could also be of interest in regard to sipatrigine and lamotrigine binding, as K271 is important in influencing the C-type gate.

## 7.4 Dynamic structural changes involving fenestrations in K<sub>2P</sub> channels

The structural gating changes in K<sub>2P</sub> channels have been frequently investigated in recent times, however there have been some conflicting evidence about the conformational changes. A new TRAAK model proposed activation as a tilting with a straight M4 transmembrane helix to reveal the fenestrations. This new conformational change in structure causes the channel to stabilise and lead to channel activation (Lolicato et al 2014). This conflicts with the idea that K<sub>2P</sub> channels activation is caused by a shift from the down to the up state (Brohawn, Campbell and MacKinnon 2014; Dong et al 2015). Consequently, it was questioned if structural activation in K<sub>2P</sub> channels are two-state changes or something more complex. The solution to this problem is the knowledge that activation of the upper selectivity filter gate, can be independent from the conformation of the channel. It was found that when the gain-of-function (GOF) mutations near the selectivity filter (G167I and W306S) were introduced into TREK2 sequence, there were no change in norfluoxetine inhibition. This is interesting as norfluoxetine is a state dependent inhibitor whose binding sites can only be found in the non-conductive down state and the GOF mutation should have abolished this site. This would then indicate that norfluoxetine binding sites still exist and that structural changes did not occur with the GOF. This may explain the new TRAAK model as activation can be independent from conformation change (McClenaghan et al 2016). TREK1 GOF mutations have also shown changes in the inhibitory effect of compounds. TREK1 C terminal GOF mutation showed a reduction in fluoxetine inhibition. This is believed to be due to the E306A mutation causing the channel to couple to the membrane bilayer which is therefore more likely to enter the open-up state resulting in the reduced fluoxetine inhibitory effect (Kennard et al 2005). This is similar to results seen in TREK2 GOF as the mutation in the middle of the TM4 helix (Y315A) shows a dramatic reduction in norfluoxetine inhibition. Hence when the channel enters the open-up state, norfluoxetine exhibits a reduction in sensitivity as a result of the changing state of the fenestration binding sites (McClenaghan et al 2016). The reduced effect of sipatrigine seen in TREK1 E306A could therefore illustrate that the binding of the C terminus to the plasma membrane, does affect the fenestration sites. The other fenestration site (TREK2 F316) may be interesting when investigating further interaction sites. All results then show that structural changes at the TM4 are important for channel gating and current regulation.

## 7.5 Access to TREK through fenestrations

Fenestrations sites are common in K<sup>+</sup> channels and have thought to be used by drugs to access the central cavity of the channel. As aforementioned, fatty acids inhibit KcsA at the central cavity, as the tetrabutylammonium (TBA) ion will displace the blocker and bind itself to the central cavity. To characterise the binding of fatty acid, 11-dansylaminoundecanoic acid (Dauda) was used as a fluorescence probe. The rapid block of Dauda compared to the slower TBA inhibition suggested that TBA needed an open channel to enter the central cavity. Dauda, however, did not require the channel to be open for binding to occur. This implication lead to the idea that fatty acid can bind to the closed KcsA channel via the fenestrations connecting to the lipid bilayer (Smithers et al 2012). This apparent drug access to the central cavity through the fenestrations has also been identified in voltage-gated sodium channels. Small neutral or hydrophobic drugs (for example phenytoin and benzocaine) were found to gain access through the passages when the channel was closed (Payandeh et al 2011). To investigate fenestrations drug access in K<sub>2P</sub>, the “bottleneck radius” of the cavity was measured. In TWIK1, the fenestrations increased its bottleneck radius as lipid membrane molecules entered into the opening. Thus, it is believed that this connection could be used as a drug pathway to the pore.

This is interesting as the TREK2 fenestration sequence, including L320 and L316, is conserved in TWIK1 and therefore it was concluded that K<sub>2P</sub> channels could interact with drugs that access via fenestrations (Jorgensen et al 2016). However, after all this evidence it must still be added that the intracellular gate in K<sub>2P</sub> channels remains permanently open (Piechotta et al 2011). This would mean that drug entrance via the fenestrations is not essential. Moreover, there has been evidence that direct block of the conductive pathway by lipid through the fenestrations does not demonstrate the full mechanism of mechanogating in TREK2 channel. The principal action involving membrane stretch involves ion occupancy in the selective filter (Aryal et al 2017).

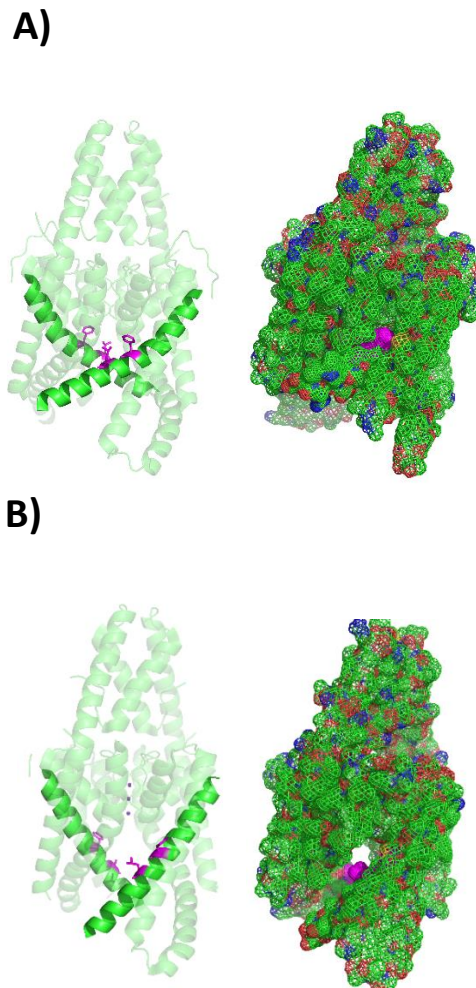


**Figure 7.4:** *TREK2* states which show fenestrations being formed. A) *TREK2* (4BW5) shows the fenestration residues (magenta) in the “upstate”. B) *TREK2* (4XDJ) in the “downstate” state which will lead to fenestration forming as the residues shift.

## 7.6 Sipatrigine has a biphasic effect on TREK2 current

The results showed that sipatrigine potently inhibits TREK2 with the effect also being reversible. The over-recovery of current followed withdrawal of sipatrigine at a concentration of 100  $\mu\text{M}$ . TREK2 current after sipatrigine wash off was significantly higher than the baseline current before the application of the drug. TREK2 current significantly over recovered current by  $101 \pm 28\%$  during washout following application of sipatrigine (100  $\mu\text{M}$ ),

There has been some evidence of dual effects of drugs on ion channels. Riluzole is a known activator of TREK1 and TRAAK and is used as a treatment for amyotrophic lateral sclerosis as it is an anticonvulsant. TRAAK shows a sustained level of activation however TREK2 activation is transient and is followed by inhibition. This inhibition is believed to be caused by riluzole increasing intracellular cAMP concentration. This is followed by a protein kinase A (PKA)-dependent decrease in current as PKA will phosphorylate TREK2 at serine 334 and

352 at C terminus. This biphasic effect is not seen in TRAAK is not regulated by cAMP (Duprat et al 2000). Amitriptyline is a tricyclic antidepressant (TCA) which shows a dual effect on epithelial  $\text{Na}^+$  channel. Amitriptyline is shown to increase current at 0.1 – 50  $\mu\text{M}$  concentrations and inhibits the current at higher concentrations (Pena et al 2002). Most notably however is that sipatrigine (10  $\mu\text{M}$ ) showed a short lived over recovery of TREK1 current after the initial inhibition (Meadows et al 2001). Therefore, it was thought that sipatrigine at high concentrations could have a biphasic effect on TREK2 current. The over recovery of current is rapid and is therefore thought to occur because of a direct action on the channel. This indicates a difference in the time course of the two competing drug effects of TREK2. The inhibition of current counteracts the underlying activation effect of the drug. Fig 5.2-A shows a slight enhancement of current when sipatrigine was initially introduced which may again show the underlying activation. The experiments which used a longer exposure time of sipatrigine (100  $\mu\text{M}$ ) showed long lasting inhibition of TREK2 current which will lead to enhanced over recovery of current which appears after sipatrigine was washed off (see Fig 5.7). It is only through the action of wash-off of sipatrigine at a high concentration (100  $\mu\text{M}$ ) that the over recovery of current is exposed. The observed over recovery of TREK2 current after sipatrigine withdrawal does suggest an activation effect of the drug.

## **7.7 N-terminus is important in over-recovery of TREK2 current following sipatrigine**

It is evident that sipatrigine is a potent inhibitor of TREK2 and exhibits an over-recovery of current after wash-off of compound at a high concentration (100  $\mu\text{M}$ ). Our initial studies established that sipatrigine had a biphasic effect on TREK2 and so the structure of the channel was investigated further.

It has been shown that the N terminus plays a role in the overall sensitivity of the channels to various stimuli. It was demonstrated that the short form TREK1 ( $\Delta\text{N}52$ ) showed less sensitivity to fluoxetine inhibition. This indicates that the N terminus of TREK1 is involved in regulation of the channel (Eckert et al 2011). In addition to blockers of TREK1, the short isoform showed to enhance activity of fenamates all while showing reduced  $\text{K}^+$  selectivity (Veale et al 2014). The truncated form of TREK1 similarly lost its sensitivity to the inhibitor carvedilol. In fact, carvedilol inhibition of full length TREK2 was significantly greater compared to the intermediate and short form TREK2 inhibition (Kisselbach et al 2014). This is similar to the results seen with sipatrigine (100  $\mu\text{M}$ ) and TREK2. The shorter, truncated form showed significantly less sensitivity to sipatrigine compared to TREK2 WT. This illustrates the fact that the distal half of the N terminus is necessary to promote full inhibition

of TREK2 by sipatrigine. The reduced inhibition seen in the short isoform of TREK1 is believed to be connected to the channels newly found Na<sup>+</sup> selectivity of the channel pore. This cannot be said for TREK2 as this channel does not shift the Na<sup>+</sup> conductance (Kisselbach et al 2014). It must be noted however that the truncation may alter the channel gating rather than disrupting the compound binding to the channel.

In addition to the decrease in sipatrigine inhibition, TREK2 ATI isoforms also shows a change in the over-recovery of current. The results demonstrate that there is little to no over-recovery of current in the forced short form and the intermediate form of TREK2. The over-recovery of current seen in the full length TREK2 would suggest that the N-terminal domain is important for the over-recovery of current. A previous study had shown a short lived over-recovery of TREK1 current when sipatrigine was washed off. TREK1 channel used in this experiment had the long form N terminus. This may indicate the importance of the N terminus not only in TREK2 but also TREK1 current over-recovery after wash off (Meadows et al 2001). Furthermore, TREK1 current will also spontaneously increase after several minutes the whole cell configuration i.e. run-up of channel current. To investigate this occurrence, the intercellular proteins which interact with TREK1 were studied. TREK1 is known to interact with the adaptor protein ezrin-radixin-moesin (ERM)-binding phosphoprotein 50 (EBP50) which is known to bind ion channels and stabilise the structure of proteins. EBP50 is colocalised with ezrin, a membrane-organising protein. The interaction of TREK1 with EBP50 is involved in the translocation and formation of actin and ezrin membrane protrusions. TREK1 N terminus has shown to be an important region in the interaction with EBP50. An inhibitor of ezrin decreased the upturn of TREK1 current and the surface expression of TREK1 channel. Therefore, it could be theorised that the N terminus of TREK1 and its interaction with ezrin is important to stabilise the channel to the membrane (Andharia et al 2017). Therefore truncating the N terminus could influence the effects of sipatrigine on TREK2 current. The over-recovery of TREK2 current seen here by sipatrigine (100 µM) could involve the N terminus binding to the plasma membrane. A channel with a truncated N terminus lacks this binding and loses the over-recovery effect.

The initial studies of TREK2 ATI has shown that the N terminal controls the conductance phenotypes. TREK2 isoforms are expressed in a variety of different regions including the brain, heart, pancreas, and kidney (Staudacher et al 2011). It was shown using single channel electrophysiology, that the full length TREK2 produces the small and large conductance, while the intermediate and the short form results in large conductance (Simkin et al 2008). This contrasts with my results where it is the short form TREK2 which produces significantly smaller conductance compared to the intermediate and long form (albeit when measuring the whole cell current through many channels simultaneously). In fact, increasing

the extracellular potassium concentration could not significantly enhance the resting current. This is more in line with TREK1 AT1 isoforms where the short isoforms express smaller currents.

It was discussed that the N terminal could regulate TREK2 at the proximal part near the start of TM1 where there is a predicted short  $\alpha$ -helix. In deletion experiments, if this part is excluded there is a large change in the conductance. It was thought that this region may interact with other, parts of the channel that may affect the function. It could also function in a similar manner to the C terminal by binding to the plasma membrane and influencing the channel conductance (Simkin et al 2008). All of this taken together shows insight into the mechanism of TREK2 and the major influence of the N terminal in current recovery.

## **7.8 Influence of TRESK central cavity**

The identification of the two residues facing the cavity, F145 and F352, has been important in investigating channel regulation. The results here show that the current density of the double mutation TRESK F156A, F364A channel is significantly higher compared to wildtype TRESK current density. A recent study has also found that after injecting TRESK F156A, F364A cRNA into oocytes, the current was five times higher compared to wildtype TRESK. This showed that the double mutation converts the TRESK channel into a more active state (Lengyel et al 2017). Mutating these sites has been shown to reduce the inhibition effect of TRESK blockers quinine, propafenone, lidocaine and loratadine (Kim et al 2013; Bruner et al 2014). Through a structure-activity relationship (SAR) model, these sites are also believed to be involved in the regulation of activators flufenamic acid (FFA) and BL-1249 (Monteillier et al 2016). However, the failure of activators ionomycin and cloxyquin shows that these sites may not be binding sites for compound activators, but rather that the TRESK channel is in a constitutively active state (Lengyel et al 2017). Docking studies showed that F145 and F352 function in a similar way to TREK2 fenestrations. The bulky phenylalanine faces into the pore, which is similar to the fenestration sites in the down state. Further evaluation of channel binding, found that amine linkers of FFA and BL-1249 form hydrogen bonds with backbone oxygen of L321 in the pore loop. Additionally, a hydrogen bond forms between BL-1249 and the side chain of T323. It is therefore thought that activators of TRESK stabilise the open state by pushing the transmembrane domains TM2, TM3 and TM4. The blockers described in this study showed binding to F130, F487 and F490. This binding is a result of  $\pi$ - $\pi$  interactions and causes TM4 and TM2 domains to shift closer together. This shows that these sites are not important in binding activators and that the reduction in activation is a result of the channel being in an activated state (Monteillier et al 2016). Benzocaine, a local anaesthetic, is an inhibitor of TRESK WT, however it has been found to be more potent in

the calcineurin activated TRESK channel. Furthermore, benzocaine efficiently inhibited mouse TRESK F156A, F364A current, which may show that the channel is in the active state (Lengyel et al 2017). It must therefore be investigated whether the double human TRESK F145/F352 alanine mutation simply alters the channel pore and therefore the channel state. The inhibition is abolished in sipatrigine, lamotrigine and Cen-092-C when the double mutation is added to the TRESK channel. This change in degree of inhibition could be due to a direct effect of the binding sites of the compounds or that the change at the pore could alter the channel gating structure. However, it has been shown with benzocaine inhibition of the double mutation showed that the gate was functional. The benzocaine results could show that the TRESK channel is in a more fixed active state which halts the effects of compounds. Further investigation is needed to conclude if the phenylalanine is important in compound binding or if the new active state affects the channel in other ways.

## **7.9 TRESK phosphorylation state influences lamotrigine but not sipatrigine sensitivity**

As previously discussed, TRESK channels have been shown to be directly regulated by intracellular calcium through activation of calmodulin-dependent phosphatase calcineurin (CaN). CaN dephosphorylates the TRESK channel which leads to enhanced current. Under resting conditions, TRESK is phosphorylated. It was investigated whether the inhibition of TRESK channels by sipatrigine, lamotrigine and Cen-092-C are dependent on the phosphorylation state of the channel or whether inhibition is mediated by phosphatase activity. It was found that sipatrigine and the structurally similar Cen-092-C are not reliant on the dephosphorylated pathways, as changes made in TRESK phosphorylation state caused no change in the degree of inhibition. However, it was found that lamotrigine showed a significant increase in inhibition in the permanently “dephosphorylated” form of the channel (S352A/ S264A). A similar result was seen in the inhibition of mouse TRESK current by benzocaine. Benzocaine inhibition is more sensitive when TRESK is constitutively active state. It was discussed here that the compound which acts this way could be used to identify which phosphorylation state the TRESK channel is in (Czirják and Enyedi 2006). This illustrates that lamotrigine distinguishes activated TRESK channel from the resting channel and holds an important role in state-dependent inhibition of TRESK.

## 7.10 Cen-092-C inhibition on TREK and TRESK current

Cen-09-C has been shown to reduce MS symptoms in EAE models (unpublished data from Leach). TREK1 and TRESK channels are thought to serve as a potential target for immune dysfunction. TREK1<sup>-/-</sup> resulted in higher EAE severity score. Spadin, a TREK1 inhibitor, significantly worsened the course of EAE in WT mice, while activation of TREK1 by riluzole showed to attenuate the clinical symptoms. (Bittner et al 2013). TRESK channels are highly expressed in human leukemic T-lymphocytes. TRESK channels have the salient feature of being activated by calcineurin binding at the PQIIS -site. NFAT in T cells will induce calcineurin, which will bind and activate TRESK. NFAT will translocate into the nucleus and will initiate transcription of new genes as well as regulating T-cell immune function. Immunosuppressants such as cyclosporine A and FK506 are known calcineurin inhibitors which will inhibit TRESK current. These immunosuppressants function to suppress activation of NFAT by halting the formation of immunophilin proteins. This suggests that that TRESK could regulate the immune system through its link to T-cells. When the T-cells are activated, TRESK channels will become dephosphorylated by the binding of calcineurin and will regulate transcription and T-cell function (Han and Kang 2009).

Cen-092-C (100  $\mu$ M) inhibition of TRESK was  $43 \pm 5\%$ . Lamotrigine is structurally similar to Cen-09-C and the degree of inhibition is also similar on TRESK at this concentration (Fig 1.15). This inhibition is seen as a direct effect on the channel as the double mutation shows a significant reduction in current inhibition. Cen-092-C did not show state dependent TRESK inhibition, which differs from lamotrigine. Cen-092-C (30  $\mu$ M) was also tested on TRESK which show the degree of inhibition at  $31 \pm 5\%$ . TREK1 effect with Cen-092-C was also tested at a concentration of 30  $\mu$ M and 10  $\mu$ M. However, it was found that these concentrations showed minimal inhibition. TREK1 was shown to have a more steady degree of inhibition at a concentration of 100  $\mu$ M ( $21 \pm 4\%$ ). TREK1 showed comparable inhibition under Cen-092-C and lamotrigine at a concentration of 100  $\mu$ M. These results taken together show that this new compound is more effective on TRESK than on TREK1. This is similar to results seen with lamotrigine. Cen-09-C was developed to target multiple sclerosis and has been shown to be a potent sodium channel blocker. However, the inhibition of TREK1 and TRESK current is not thought to be beneficial in treating multiple sclerosis.

## **7.11 Therapeutic implications of regulating TREK and TRESK channels**

### **7.11.1 TREK and TRESK channels are modulated by antidepressants**

There is significant research which suggests that TREK1 is involved in depression and response to antidepressants. Antidepressants such as serotonin selective reuptake inhibitor (SSRI), work by inhibiting the serotonin transporter (SERT) allowing for an increase of serotonin concentration in the system. It has also been shown that SSRIs block TREK1, leading to downregulation of the presynaptic serotonin 1A (5HT<sub>1A</sub>) receptors. The desensitization of the receptor leads to an increase in postsynaptic serotonin 1A receptors activity through increasing serotonin levels. Furthermore, a development in TREK1 specific antagonist found a new antidepressant named spadin. It was also found that spadin increase the release of serotonin. However, the effect of spadin as an antidepressant was reduced in TREK1<sup>-/-</sup> mice. This shows that the spadin effect and the increase in serotonin release is controlled by the TREK1 current inhibition (Mazella et al 2010). However, the TREK1 knockout also showed a decrease in corticosterone in stress. This effect cannot be linked to an increase in serotonin. This shows that the TREK1<sup>-/-</sup> anti-depressant effect is not solely linked to serotonin. This could lead to a multi drug target treatment for depression using a combination of a TREK1 antagonist with SSRIs (Heurteaux, C., et al 2006). Several antidepressants are known to inhibit TREK and TRESK channels including amitriptyline, citalopram and fluoxetine. This is similar to results seen with lamotrigine and sipatrigine. Lamotrigine is already used in patients with depression linked to bipolar disorder and has reportedly been used in treatment for patients where there is resistance to first line antidepressants. Therefore, the structurally similar sipatrigine could also be a useful for depression treatment as it is a more potent TREK1 and TRESK antagonist. Thus, it could be a more effective agent for depression than lamotrigine (Tsai 2008).

TRESK channels are inhibited by protein kinase A and activated by protein kinase C, however TRESK channels are not regulated by cAMP at all (Czirják et al 2004). TRESK channels are therefore not thought to have any connection to serotonin or depression, however TRESK current is known to be inhibited by antidepressants amitriptyline, bupropion and fluoxetine. Opposing effects can be seen in TRESK and TREK2 as the channels hold different actions when exposed to the antidepressant bupropion. Bupropion inhibits the reuptake of norepinephrine and dopamine and has been found to be useful for neuropathic pain. The compound inhibits TRESK current but has little effect on TREK2. Further studies are needed to account for antidepressants as analgesics and how inhibition of TREK and

TRESK current lead to alleviating pain. This analgesic effect could be connected to activation of inhibitory interneurons resulting in the reduction of pain transmission. However, it must be stated again that there is no known of expression of TREK2 and TRESK in inhibitory interneurons (Park et al 2016). In conclusion, these antidepressants have been shown to have analgesic effects and therefore could be important in pain relief rather than just depression.

### **7.11.2 TREK1 inhibition linked to neuroprotection**

TREK1 is known to be closely related to pathophysiological conditions such as cerebral ischemia and has been shown to be influential in neuroprotection. The mechanism of neuroprotection action is thought to be through activation of  $K_{2P}$  channels which will prevent enhancement of neuronal signalling (Pollema-Mays et al 2013). This is clear when you consider that PUFA will induce neuronal protection linked to TREK1 activation (Heurteaux 2007). TREK1<sup>-/-</sup> are also more sensitive to ischemia and epilepsy (Heurteaux et al 2004). It must also be noted, however, that TREK1 channel expression is upregulation in the DRG of neuropathic pain model. TREK1 was also shown to be higher colocalization with IB4<sup>+</sup> compared to IB4<sup>-</sup> which shows that expression is higher in nociceptive C fibers (Han et al 2016). TREK1 expression has also found to be enhanced after cerebral ischemia. This increase in TREK channels however is thought to protect against glutamate toxicity as glutamate clearance is decreased by TREK1 channel inhibition (Ryoo and Park 2016). It is also noted that excessive potassium efflux, due to cerebral ischemia or hypoxia/anoxia, will also deplete intracellular potassium and will promote apoptosis. Therefore, inhibition of these channels could prevent potassium efflux and against ischemia-induced neuronal apoptosis. It was found that a compound named lig4-4 would selectively inhibit TREK1 current and was shown to reduce the apoptotic-effect. Therefore, in therapeutic practice, it may be necessary to activate TREK1 during the early stage of cerebral ischemia, but then inhibit the channel to prevent neuronal apoptosis (Wang et al 2018).

### **7.11.3 Analgesic effects linked to TREK and TRESK regulation**

TREK1 channels are highly expressed in small and medium DRG sensory neurons and are extensively localised with capsaicin-activated non-selective ion channel named TRPV1. In inflammatory models, mRNA levels of TREK1 in DRG neurons increased 3-fold. TREK1 KO mice however, showed an increase thermal and mechanical hyperalgesia by induced inflammation. This suggests that TREK1 plays a role in the regulation of nociceptor excitation. It may be observed that depolarisation of TRPV1 nociceptors could be controlled

by hyperpolarisation of TREK1 (Alloui et al 2006). TREK2 channels are expressed in small DRG neurons and are selectively expressed in IB4<sup>+</sup> C fibres, which modulate excitability of neurons. TREK2 is important in setting the resting membrane potential as was seen in siRNA knockdown of DRG neuron where TREK2 depolarised the neuron by 10mV. Hyperpolarisation of DRG C-fiber limits the electrical excitability so knockout TREK2 will enhance the excitability and increase the pain (Acosta et al 2014). TRESK channel is expressed in all different sizes of DRG neurons which suggests a role for TRESK in the regulation of the resting membrane potential. TRESK dysfunction has been shown to cause migraine and activation of current was seen to alleviate pain (Lafrenière and Rouleau 2011). Blocking of TRESK channels through pharmacological means causes pain while over-expression of TRESK relieves pain via inhibition of capsaicin mediated substance P release in DRG neurons (Zhou et al 2012).

The evidence shown suggests that upregulation of K<sub>2P</sub> current may be a novel strategy for analgesia. The overall activation of TREK1, TREK2 and TRESK will depress neuronal activity and therefore suppress pain neurotransmission. This effect can be seen in non-steroidal anti-inflammatory drug, Flufenamic Acid (FFA), which activates TREK1, TREK2 and TRESK channels (Takahira et al 2005; Monteillier et al 2016). However, there are known analgesics which inhibit some K<sub>2P</sub> channels. Acetaminophen, ibuprofen and nabumetone will inhibit TRESK current but has no effect on TREK2.

A traditional analgesic aristolochic acid holds opposing result as it blocks TRESK current but enhances TREK2. This difference in activity between TRESK and TREK2 may be due to the differences in how the channels are regulated. TREK2 channels are activated by arachidonic acid and inhibited by PKC activity. While TRESK channels are inhibited by arachidonic acid and activated by PKC (Park et al 2016). TRESK are expressed in DRG neurons are known to be co-expressed with the pain mediator lysophosphatidic acid (LPA). LPA signalling is known to influence neurological disorders such as neuropathic pain and has been shown to activate TRESK, whereas LPA transmission will lead to the inhibition of TREK1 currents. The activation of LPA and TRESK will have limited excitation of TRPV1 channels as TRESK will cause hyperpolarisation. The opposite will occur with the inhibition of TREK1 via LPA leading to TRPV1 excitation. The effect of TRESK and the co-activation by LPA will decrease excitability of DRG neurons. This effect was clearly seen in TRESK<sup>-/-</sup> mice under analgesic compounds which saw an enhancement of hyperpolarisation. This is shown to activate TRESK by the inflammatory mediator LPA will reduce TRPV1 activity and reduce pain (Kollert et al 2015).

Hydroxyl-  $\alpha$ -sanshool, the active ingredient of Szechuan peppers, is another known traditional analgesic and has been seen to block TRESK current. This effect however is

believed to be caused by desensitising the excitatory neurons which leads to a numbing sensation. Therefore, the two natural analgesics are predicted to be similar pathway to produce pain relief (Veale and Mathie 2016). It has been documented that activation of inhibitory interneurons could also have an analgesic effect. So, antagonism here could lead to enhanced activity of inhibitory neurons and lead to neuroprotection. However, there is no known expression of TREK2 and TRESK channels in inhibitory neurons (Park et al 2016). Another hypothesis, relates to the effect that sipatrigine and lamotrigine has on TREK and TRESK current inhibition. The antagonism of these channels leads to depolarisation and thus calcium channel inactivation as the channel becomes inactive at  $-45$  mV. As calcium channels stimulate exocytosis of glutamate, the blockade of TREK and TRESK current and resulting depolarisation will lead to the elimination of glutamate release (Meadows et al 2001). All this taken together shows that further studies into the mechanism of analgesia through TREK and TRESK channels. The expression of these  $K_{2P}$  channels are different among individuals and reactions to analgesics are different as each type of pain condition is unique. This will lead to a novel method of how pain could be alleviated through pharmacological modulation.

All this taken together brings into question the function of TREK and TRESK channels regarding pain. Pain killers and antidepressants with analgesic effects will inhibit TREK2 and TRESK currents however there is evidence will suggest that activation of these currents will lead to the depression of neuronal activity leading to pain relief. More evidence is needed to determine the specific action of  $K_{2P}$  channels which results in analgesia. Investigating the distribution and expression of these channels in inhibitory neurons could be an approach in examining TREK and TRESK physiological role in pain.

## **7.12 Future work**

Previous studies have shown that TREK2 is subject to alternative translation initiation (ATI) which will lead to differing lengths of intracellular N terminal domain and changes in functional properties (Veale et al 2010). The results shown here highlight the importance of the N terminal regarding over recovery of current after sipatrigine wash off. However, it should be determined if all TREK2 structures are trafficked to the plasma membrane. Cellular localization of TREK2 ATI isoforms should be examined under confocal microscope using membrane staining and GFP tagging.

Norfluoxetine binds within intramembrane fenestrations found in the down state of TREK2 (Dong et al 2015). Sipatrigine, but not lamotrigine, has shown a decrease in inhibition when one fenestration site is mutated (L289A). Furthermore, the second fenestration site (L285)

may be of interest in sipatrigine sensitivity. Mutating this site could show further evidence of sipatrigine interaction at the fenestration sites.

A recent paper has also shown that TREK1 K271Q lacks activation by ML335 and ML402, showing that this site is important for stabilising the primary gate at the selective filter (Lolicato M et al 2017). To investigate binding sites further, a mutation of site K271 could be used with sipatrigine, lamotrigine and Cen-092-C to see if there is any change in current inhibition.

## **7.13 Conclusion**

This study suggests that the binding site for sipatrigine is within the intramembrane fenestration site of TREK1 and TREK2. TREK1 was found to exhibit no change in the degree of inhibition with the structurally similar lamotrigine when the fenestration site was mutated. This shows that this site is profoundly important in the inhibition of both TREK1 and TREK2. Furthermore, the binding of the N terminal to the plasma membrane is believed to be important in this over recovery of TREK2 current. This may alter the functional profile of TREK1 and the excitability of cells. Phosphorylation of TRESK channels resulted in a change in lamotrigine sensitivity. This could show that lamotrigine inhibition is state dependent. Cen-092-C has also been identified as a TREK1 and TRESK antagonist with a similar degree of inhibition to lamotrigine. This means that the change in structure had little change in TREK1 and TRESK inhibition, however there was no sensitivity to TRESK dephosphorylation state. These results clearly demonstrate that sipatrigine sensitivity is regulated at the central cavity TREK1 and TREK2. It also could illustrate how state dependent inhibition of TRESK channels by lamotrigine may contribute to a possible off-target effect of the drug.

## REFERENCES

- Acosta, C., et al. (2014). TREK2 expressed selectively in IB4-binding C-fiber nociceptors hyperpolarizes their membrane potentials and limits spontaneous pain. *Journal of Neuroscience*, 34(4), 1494-1509.
- Alexander, S. P., Mathie, A. and Peters, J. A. (2011). Guide to Receptors and Channels (GRAC), 5th edition. *British Journal of Pharmacology*, 164 Suppl 1, S1-324.
- Alloui, A., et al. (2006). TREK-1, a K<sup>+</sup> channel involved in polymodal pain perception. *EMBO Journal*, 25(11), 2368-2376.
- Anderson, P. A. V. and Greenberg, R. M. (2001). Phylogeny of ion channels: clues to structure and function. *Comparative Biochemistry and Physiology*, Part B 128 17-18.
- Andharia, N., et al. (2017). Involvement of intracellular transport in TREK-1c current run-up in 293T cells. *Channels*, 1-12.
- Andres-Enguix, I., et al. (2012). Functional analysis of missense variants in the TRESK (KCNK18) K<sup>+</sup> channel. *Scientific Reports*, 2.
- Armstrong, C. M. and Loboda, A. (2001). A model for 4-aminopyridine action on K channels: Similarities to tetraethylammonium ion action. *Biophysical Journal*, 81(2), 895-904.
- Armstrong, C.M., et al (1973). Destruction of sodium conductance inactivation in squid axons perfused with pronase. *J Gen Physiol*, 62,375–391.
- Aryal, P., et al. (2015). Influence of lipids on the hydrophobic barrier within the pore of the TWIK-1 K2P channel. *Channels*, 9(1), 44-49.
- Aryal, P., Sansom, M. S. P. and Tucker, S. J. (2015). Hydrophobic gating in ion channels. *Journal of Molecular Biology*, 427(1), 121-130.
- Aryal, P., et al. (2014). A hydrophobic barrier deep within the inner pore of the TWIK-1 K2P potassium channel. *Nature Communications*, 5.
- Aryal, P., et al. (2017). Bilayer-Mediated Structural Transitions Control Mechanosensitivity of the TREK-2 K2P Channel. *Structure*.

Ashmole, I., et al. (2009). The response of the tandem pore potassium channel TASK-3 (K2P9.1) to voltage: Gating at the cytoplasmic mouth. *Journal of Physiology*, 587(20), 4769-4783.

Bagal, S. K., et al. (2013). Ion channels as therapeutic targets: A drug discovery perspective. *Journal of Medicinal Chemistry*, 56(3), 593-624.

Bagriantsev, S. N., et al. (2011). Multiple modalities converge on a common gate to control K2P channel function. *EMBO Journal*, 30(17), 3594-3606.

Bagriantsev, S. N., Clark, K. A. and Minor, D. L. (2012). Metabolic and thermal stimuli control K2P 2.1 (TREK-1) through modular sensory and gating domains. *EMBO Journal*, 31(15), 3297-3308.

Bang, H., Kim, Y. and Kim, D. (2000). TREK-2, a new member of the mechanosensitive tandem-pore K<sup>+</sup> channel family. *Journal of Biological Chemistry*, 275(23), 17412-17419.

Bautista, D. M., et al. (2008). Pungent agents from Szechuan peppers excite sensory neurons by inhibiting two-pore potassium channels. *Nature Neuroscience*, 11(7), 772-779.

Barnett, M. W. and Larkman, P. M. (2007). The action potential. *Practical Neurology*, 7(3), 192-197.

Ben-Abu, Y., et al. (2009). Inverse coupling in leak and voltage-activated K<sup>+</sup> channel gates underlies distinct roles in electrical signaling. *Nature Structural and Molecular Biology*, 16(1), 71-79.

Bittner, S., et al. (2013). Endothelial TWIK-related potassium channel-1 (TREK1) regulates immune-cell trafficking into the CNS. *Nature Medicine*, 19(9), 1161-1165.

Booth, I. R., Edwards, M. D, and Miller, S. (2003) Bacterial ion channels. *Biochemistry*. 42:10045–10053.

Braun, G., et al. (2011). TRESK background K<sup>+</sup> channel is inhibited by PAR-1/MARK microtubule affinity-regulating kinases in *Xenopus* oocytes. *Plos One*, 6(12).

- Brohawn, S. G., Del Marmol, J. and MacKinnon, R. (2012). Crystal structure of the human K2P TRAAK, a lipid- and mechano-sensitive K<sup>+</sup> ion channel. *Science*, 335(6067), 436-441.
- Brohawn, S. G., Campbell, E. B. and MacKinnon, R. (2013). Domain-swapped chain connectivity and gated membrane access in a Fab-mediated crystal of the human TRAAK K<sup>+</sup> channel. *Proceedings of the National Academy of Sciences of the United States of America*, 110(6), 2129-2134.
- Brohawn, S. G., Campbell, E. B. and MacKinnon, R. (2014). Physical mechanism for gating and mechanosensitivity of the human TRAAK K<sup>+</sup> channel. *Nature*, 516(729), 126-130.
- Brohawn, S. G. (2015). How ion channels sense mechanical force: Insights from mechanosensitive K2P channels TRAAK, TREK1, and TREK2. *Annals of the New York Academy of Sciences*, 1352(1), 20-32.
- Bruner, J. K., et al. (2014). Identification of novel small molecule modulators of K2P18.1 two-pore potassium channel. *European Journal of Pharmacology*, 740, 603-610.
- Bueno, O. F., et al. (2002). Defective T cell development and function in *calcineurin* A $\beta$ -deficient mice. *Proceedings of the National Academy of Sciences of the United States of America*, 99(14), 9398-9403.
- Cadaveira-Mosquera, A., et al. (2012). Expression of K2P channels in sensory and motor neurons of the autonomic nervous system. *Journal of Molecular Neuroscience*, 48(1), 86-96.
- Campbell, J. N. and Meyer, R. A. (2006). Mechanisms of Neuropathic Pain. *Neuron*, 52(1), 77-92.
- Caterina, M. J., et al. (2000). Impaired nociception and pain sensation in mice lacking the capsaicin receptor. *Science*, 288(5464), 306-13.
- Catterall, W. A. (2000). From ionic currents to molecular mechanism: the structure and function of voltage-gated sodium channels. *Neuron*, 26, 13-25.

- Chae, Y. J., et al. (2010). Discrete change in volatile anesthetic sensitivity in mice with inactivated tandem pore potassium ion channel TRESK. *Anesthesiology*, 113(6), 1326-1337.
- Chatelain, F. C., et al. (2012). TWIK1, a unique background channel with variable ion selectivity. *Proceedings of the National Academy of Sciences of the United States of America*, 109(14), 5499-5504.
- Chemin, J., et al. (2003). Mechanisms underlying excitatory effects of group I metabotropic glutamate receptors via inhibition of 2P domain K<sup>+</sup> channels. *EMBO Journal*, 22(20), 5403-5411.
- Chemin, J., et al. (2005). Lysophosphatidic acid-operated K<sup>+</sup> channels. *Journal of Biological Chemistry*, 280(6), 4415-4421.
- Chemin, J., et al. (2007). *Regulation of the Mechano-Gated K2P Channel TREK-1 by Membrane Phospholipids Current Topics in Membranes*. Vol. 59., pp. 155-170.
- Chu, K. C., et al. (2010). Functional identification of an outwardly rectifying pH- and anesthetic-sensitive leak K<sup>+</sup> conductance in hippocampal astrocytes. *The European Journal of Neuroscience*. 32(5), 725-35.
- Choi, K. L., Aldrich, R. W. and Yellen, G. (1991). Tetraethylammonium blockade distinguishes two inactivation mechanisms in voltage-activated K<sup>+</sup> channels. *Proceedings of the National Academy of Sciences of the United States of America*, 88(12), 5092-5095.
- Cohen, A., Ben-Abu, Y. and Zilberberg, N. (2009). Gating the pore of potassium leak channels. *European Biophysics Journal*, 39(1), 61-73.
- Copper, D. C. (2012). The Neuron. In: Donald C. Copper *Introduction to Neuroscience 1*. University of Colorado: CU Neuroscience Series. p35-71.
- Czirják, G., Tóth, Z. E. and Enyedi, P. (2004). The Two-pore Domain K<sup>+</sup> Channel, TRESK, Is Activated by the Cytoplasmic Calcium Signal through Calcineurin. *Journal of Biological Chemistry*, 279(18), 18550-18558.

Czirjak, G. and Enyedi, P. (2002). Formation of functional heterodimers between the TASK-1 and TASK-3 two-pore domain potassium channel subunits. *Journal of Biological Chemistry*, 277, 5426–5432.

Czirják, G. and Enyedi, P. (2006). Targeting of calcineurin to an NFAT-like docking site is required for the calcium-dependent activation of the background K<sup>+</sup> channel, TRESK. *Journal of Biological Chemistry*, 281(21), 14677-14682.

Czirják, G. and Enyedi, P. (2006). Zinc and mercuric ions distinguish TRESK from the other two-pore-domain K<sup>+</sup> channels. *Molecular Pharmacology*, 69(3), 1024-1032.

Czirják, G. and Enyedi, P. (2010). TRESK background K<sup>+</sup> channel is inhibited by phosphorylation via two distinct pathways. *Journal of Biological Chemistry*, 285(19), 14549-14557.

Czirják, G. and Enyedi, P. (2014). The LQLP calcineurin docking site is a major determinant of the calcium-dependent activation of human TRESK background K<sup>+</sup> channel. *Journal of Biological Chemistry*, 289(43), 29506-29518.

Czirják, G., Vuity, D. and Enyedi, P. (2008). Phosphorylation-dependent binding of 14-3-3 proteins controls TRESK regulation. *Journal of Biological Chemistry*, 283(23), 15672-15680.

Decher, N., et al. (2017). Sodium permeable and "hypersensitive" TREK-1 channels cause ventricular tachycardia. *EMBO Molecular Medicine*.

Derry, S., et al. (2009). Topical capsaicin for chronic neuropathic pain in adults. *The Cochrane Database of Systematic Reviews*. 4 CD 007393.

Devilliers, M., et al. (2013). Activation of TREK-1 by morphine results in analgesia without adverse side effects. *Nature Communications*, 4.

DiFrancesco, D. (1993). Pacemaker mechanisms in cardiac tissue. *Annual Review of Physiology*, 55: 455–472.

Dobler, T., et al. (2007). TRESK two-pore-domain K<sup>+</sup> channels constitute a significant component of background potassium currents in murine dorsal root ganglion neurones. *Journal of Physiology*, 585(3), 867-879.

- Dong, Y.Y., et al. (2015). K2P channel gating mechanisms revealed by structures of TREK-2 and a complex with Prozac. *Science*, 347(6227), pp.1256-1259.
- Doyle, D. A., et al. (1998). The structure of the potassium channel: Molecular basis of K<sup>+</sup> conduction and selectivity. *Science*, 280(5360), 69-77.
- Dudev, T. and Lim, C. (2010). Factors governing the Na<sup>+</sup> vs K<sup>+</sup> selectivity in sodium ion channels. *Journal of the American Chemical Society*, 132(7), 2321-2332.
- Duprat, F., et al. (2000). The Neuroprotective Agent Riluzole Activates the Two P Domain K1 Channels TREK-1 and TRAAK. *Molecular Pharmacology*, 57(5), 906-12.
- Duprat, F., et al. (1997). TASK, a human background K<sup>+</sup> channel to sense external pH variations near physiological pH. *EMBO Journal*, 16(17), 5464-5471.
- Dutzler, R., et al. (2002). X-ray structure of a ClC chloride channel at 3.0 Å reveals the molecular basis of anion selectivity. *Nature*, 415(6869), 287-94.
- Eckert, M., et al. (2011). TREK-1 isoforms generated by alternative translation initiation display different susceptibility to the antidepressant fluoxetine. *Neuropharmacology*, 61(5-6), 918-923.
- Efremov, R. G., et al. (2015). Architecture and conformational switch mechanism of the ryanodine receptor. *Nature*, 517(7532), 39-43.
- Enyedi, P., Braun, G. and Czirják, G. (2012). TRESK: The lone ranger of two-pore domain potassium channels. *Molecular and Cellular Endocrinology*, 353(1-2), 75-81.
- Enyedi, P. and Czirják, G. (2014). Properties, regulation, pharmacology, and functions of the K2P channel, TRESK. *Pflugers Archiv European Journal of Physiology*.
- Eilers, J. P., Plant, T. and Konnerth, A. (1996). Localized calcium signaling and neuronal integration in cerebellar Purkinje neurones. *Cell Calcium*, 20(2), 215-226.
- Feliciangeli, S., et al. (2015). The family of K2P channels: Salient structural and functional properties. *Journal of Physiology*, 593(12), 2587-2603.
- Ferrari, U., et al. (2005). Calcineurin inhibitor-induced headache: Clinical characteristics and possible mechanisms. *Headache*, 45(3), 211-214.

- Fink, M., et al. (1996). Cloning, functional expression and brain localization of a novel unconventional outward rectifier K<sup>+</sup> channel. *EMBO Journal*, 15(24), 6854-6862.
- Flinta, C., et al. (1986). Sequence determinants of N-terminal protein processing. *European Journal of Biochemistry* **154**, 193–196
- Franks, N. P. and Honoré, E. (2004). The TREK K 2P channels and their role in general anaesthesia and neuroprotection. *Trends in Pharmacological Sciences*, 25(11), 601-608.
- Garthwaite, G., et al. (1999). Mechanisms of ischaemic damage to central white matter axons: A quantitative histological analysis using rat optic nerve. *Neuroscience*, 94(4), 1219-1230.
- Girard, C., et al. (2001). Genomic and functional characteristics of novel human pancreatic 2P domain K<sup>+</sup> channels. *Biochemical and Biophysical Research Communications*, 282(1), 249-256.
- Goldin, A. L. (2003). Mechanisms of sodium channel inactivation. *Current opinion in Neurobiology*, 13(3), 284-90
- Goldstein, S. A. N., et al. (1996). ORK1, a potassium-selective leak channel with two pore domains cloned from *Drosophila melanogaster* by expression in *Saccharomyces cerevisiae*. *Proceedings of the National Academy of Sciences of the United States of America*, 93(23), 13256-13261.
- Goldstein, S. A. N., et al. (2005). International union of pharmacology. LV. Nomenclature and molecular relationships of two-P potassium channels. *Pharmacological Reviews*, 57(4), 527-540.
- Golzari, S. E. J., et al (2014). Lidocaine and Pain Management in the Emergency Department: A Review Article. *Anesthesiology and Pain Medicine*. 4(1) e15444.
- Gordon, J. A. and Hen, R. (2006). TREKKing toward new antidepressants. *Nature Neuroscience*, 9(9), 1081-1083.
- Gruss, M., et al (2004). Two-pore-domain K<sup>+</sup> channels are a novel target for the anesthetic gases xenon, nitrous oxide, and cyclopropane. *Molecular Pharmacology*, 65, 443-452.

- Guo, Z. and Cao, Y. -. (2014). Over-expression of TRESK K<sup>+</sup> channels reduces the excitability of trigeminal ganglion nociceptors. *Plos One*, 9(1).
- Hainsworth, A. H., et al. (2000). Sipatrigine (BW 619C89) is a neuroprotective agent and a sodium channel and calcium channel inhibitor. *CNS Drug Reviews*, 6(2), 111-134.
- Halliwel, J.V., Whitaker M., and Ogden, D (1994). Using microelectrodes. In: D.C. Ogden *Microelectrode Techniques. The Plymouth Workshop Handbook*. 2nd ed. Cambridge, UK: The Company of Biologists Ltd. p1-15.
- Halliwel, J.V., et al (1994). Voltage clamp techniques. In: D.C Ogden *Microelectrode Techniques. The Plymouth Workshop Handbook*. 2nd ed. Cambridge, UK: The Company of Biologists Ltd. p17-35.
- Hamill, O. P., et al. (1981). Improved patch-clamp techniques for high-resolution current recording from cells and cell-free membrane patches. *Pflügers Archiv European Journal of Physiology*, 391(2), 85-100.
- Han, J. and Kang, D. (2009). TRESK channel as a potential target to treat T-cell mediated immune dysfunction. *Biochemical and Biophysical Research Communications*, 390(4), 1102-1105.
- Han, H. J., et al. (2016). Enhanced expression of TREK-1 is related with chronic constriction injury of neuropathic pain mouse model in dorsal root ganglion. *Biomolecules and Therapeutics*, 24(3), 252-259.
- Heurteaux, C., et al. (2004). TREK-1, a K<sup>+</sup> channel involved in neuroprotection and general anesthesia. *EMBO Journal*, 23(13), 2684-2695.
- Heurteaux, C., et al. (2006). Deletion of the background potassium channel TREK-1 results in a depression-resistant phenotype. *Nature Neuroscience*, 9(9), 1134-1141
- Heurteaux, C. (2007). PUFA-induced neuroprotection against cerebral or spinal cord ischemia via the TREK-1 channel. *OCL*, 14(3-4), 190-193
- Hille, B. (2001) *Ion Channels of Excitable Membranes*, Sinauer, Sunderland, MA
- Hofmann, F., Lacinová, L and Klugbauer, N. (1999). Voltage-dependent calcium channels: from structure to function. *Rev Physiol Biochem Pharmacol*, 139, 33-87.

Honoré, E., et al. (2002). An intracellular proton sensor commands lipid- and mechano-gating of the K<sup>+</sup> channel TREK-1. *EMBO Journal*, 21(12), 2968-2976.

Honoré, E. (2007). The neuronal background K<sub>2</sub>P channels: Focus on TREK1. *Nature Reviews Neuroscience*, 8(4), 251-261.

Huang, D. -, Yu, B. -. and Fan, Q. -. (2008). Roles of TRESK, a novel two-pore domain K<sup>+</sup> channel, in pain pathway and general anesthesia. *Neuroscience Bulletin*, 24(3), 166-172.

Ji, R. -. and Woolf, C. J. (2001). Neuronal plasticity and signal transduction in nociceptive neurons: Implications for the initiation and maintenance of pathological pain. *Neurobiology of Disease*, 8(1), 1-10.

Jiménez-Pérez, L., et al (2016). Molecular determinants of K<sub>v</sub>1.3 potassium channels-induced proliferation. *Journal of Biological Chemistry*, 291(7), 3569-3580.

Jorgensen, C., et al. (2016). Lateral fenestrations in K<sup>+</sup>-channels explored using molecular dynamics simulations. *Molecular Pharmaceutics*, 13(7), 2263-2273.

Kang, D. and Kim, D. (2006). TREK-2 (K<sub>2</sub>P10.1) and TRESK (K<sub>2</sub>P18.1) are major background K<sup>+</sup> channels in dorsal root ganglion neurons. *American Journal of Physiology - Cell Physiology*, 291(1), C138-C146.

Kang, D, Han, J. and Kim, D. (2006). Mechanism of inhibition of TREK-2 (K<sub>2</sub>P10.1) by the Gq-coupled M<sub>3</sub> muscarinic receptor. *Am J Physiol Cell Physiol* 291, C649-C656

Kang, D, Mariash, E. and Kim, D. (2004). Functional expression of TRESK-2, a new member of the tandem-pore K<sup>+</sup> channel family. *The Journal of Biological Chemistry*, 279(27), 28063-70.

Kang, D., et al. (2008). Lamotrigine inhibits TRESK regulated by G-protein coupled receptor agonists. *Biochemical and Biophysical Research Communications*, 367(3), 609-615.

Katanosaka, K., et al (2008). Contribution of TRPV1 to the bradykinin-evoked nociceptive behavior and excitation of cutaneous sensory neurons. *Neuroscience Research*, 62(3) 168-175.

- Kennard, L. E., et al. (2005). Inhibition of the human two-pore domain potassium channel, TREK-1, by fluoxetine and its metabolite norfluoxetine. *British Journal of Pharmacology*, 144(6), 821-829.
- Keshavaprasad, B., et al. (2005). Species-specific differences in response to anesthetics and other modulators by the K2P channel TRESK. *Anesthesia and Analgesia*, 101(4), 1042-1049.
- Ketchum, K. A., et al. (1995). A new family of outwardly rectifying potassium channel proteins with two pore domains in tandem. *Nature*, 376(6542), 690-695.
- Kim S., et al. (2013). Identification of blocker binding site in mouse TRESK by molecular modeling and mutational studies. *Biochimica et biophysica acta*, 1828:1131-1142.
- Kisselbach, J., et al. (2014). Modulation of K2P2.1 and K2P10.1 K<sup>+</sup> channel sensitivity to carvedilol by alternative mRNA translation initiation. *British Journal of Pharmacology*, 171(23), 5182-5194.
- Knotkova, H., Pappagello, M. and Szallasi, A. (2008). Capsaicin (TRPV1 Agonist) therapy for pain relief: farewell or revival? *The Clinical Journal of Pain*, 24(2), 142-54.
- Kollert, S., et al. (2015). Activation of TRESK channels by the inflammatory mediator lysophosphatidic acid balances nociceptive signalling. *Scientific Reports*, 5.
- Kollewe, A., et al. (2009). A structural model for K2P potassium channels based on 23 pairs of interacting sites and continuum electrostatics. *Journal of General Physiology*, 134(1), 53-68.
- Kosharsky, B et al. (2013). Intravenous infusions in chronic pain management. *Pain Physician*, 16(3), 231-49.
- Kucheryavykh, L. Y., et al (2009). Ischemia Increases TREK-2 Channel Expression in Astrocytes: Relevance to Glutamate Clearance. *The Open Neuroscience Journal*. 1(3), 40-47.
- Lafrenière, R. G., et al. (2010). A dominant-negative mutation in the TRESK potassium channel is linked to familial migraine with aura. *Nature Medicine*, 16(10), 1157-1160.

- Lafrenière, R. G. and Rouleau, G. A. (2011). Migraine: Role of the TRESK two-pore potassium channel. *International Journal of Biochemistry and Cell Biology*, 43(11), 1533-1536.
- Larsson, H. P. and Elinder, F. (2000). A conserved glutamate is important for slow inactivation in K<sup>+</sup> channels. *Neuron*, 27(3), 573-583.
- Lauritzen, I., et al. (2005). Cross-talk between the mechano-gated K2P channel TREK-1 and the actin cytoskeleton. *EMBO Reports*, 6(7), 642-648.
- Leach, M. J., et al. (1993). BW619C89, a glutamate release inhibitor, protects against focal cerebral ischemic damage. *Stroke*, 24(7), 1063-1067.
- Lee, E. S., et al. (2013). Lamotrigine increases intracellular Ca<sup>2+</sup> levels and Ca<sup>2+</sup>/calmodulin-dependent kinase II activation in mouse dorsal root ganglion neurones. *Acta Physiologica*, 207(2), 397-404.
- Lenaeus, M. J., et al. (2005). Structural basis of TEA blockade in a model potassium channel. *Nature Structural and Molecular Biology*, 12(5), 454-459.
- Lengyel, M., et al. (2017). Selective and state-dependent activation of TRESK (K2P18.1) background potassium channel by cloxyquin. *British Journal of Pharmacology*, 174(13), 2102-2113.
- Lesage, F., et al. (1996a). TWIK-1, a ubiquitous human weakly inward rectifying K<sup>+</sup> channel with a novel structure. *EMBO Journal*, 15(5), 1004-1011.
- Lesage, F., et al. (1996b). A pH-sensitive yeast outward rectifier K<sup>+</sup> channel with two pore domains and novel gating properties. *The Journal of Biological Chemistry*, 271, 4183-4187.
- Lesage, F., et al. (2000). Human TREK2, a 2P domain mechano-sensitive K<sup>+</sup> channel with multiple regulations by polyunsaturated fatty acids, lysophospholipids, and Gs, Gi, and Gq protein-coupled receptors. *The Journal of Biological Chemistry*, 275(37), 28298-405.
- Lesage, F. (2003). Pharmacology of neuronal background potassium channels. *Neuropharmacology*, 44(1):1-7

Levitz, J., et al. (2016). Heterodimerization within the TREK channel subfamily produces a diverse family of highly regulated potassium channels. *Proceedings of the National Academy of Sciences of the United States of America*, 113(15), 4194-4199.

Lodish H, et al. *Molecular Cell Biology*. 4th edition. New York: W. H. Freeman; 2000. Section 21.2, The Action Potential and Conduction of Electric Impulses.

Lolicato, M., et al. (2014). Transmembrane helix straightening and buckling underlies activation of mechanosensitive and thermosensitive K2P channels. *Neuron*, 84(6), 1198-1212.

Lolicato, M., et al. (2017). K2P2.1 (TREK-1)-activator complexes reveal a cryptic selectivity filter binding site. *Nature*, 547(7663), 364-368.

Lopes, C. M., et al (2005). PIP2 hydrolysis underlies agonist-induced inhibition and regulates voltage gating of two-pore domain K<sup>+</sup> channels. *The Journal of Physiology*, 564(1), 117-29.

Liu, C., et al. (2004). Potent activation of the human tandem pore domain K channel TRESK with clinical concentrations of volatile anesthetics. *Anesthesia and Analgesia*, 99(6), 1715-1722.

Liu, P., et al. (2013). Functional analysis of a migraine-associated TRESK K<sup>+</sup> channel mutation. *Journal of Neuroscience*, 33(31), 12810-12824.

Li, C. (2008). A reliable whole cell clamp technique. *American Journal of Physiology - Advances in Physiology Education*, 32(3), 209-211.

Li, H., et al. (2007). Structure of Calcineurin in Complex with PVIVIT Peptide: Portrait of a Low-affinity Signalling Interaction. *Journal of Molecular Biology*, 369(5), 1296-1306.

Liang, B., et al. (2014). Genetic variation in the two-pore domain potassium channel, TASK-1, may contribute to an atrial substrate for arrhythmogenesis. *Journal of Molecular and Cellular Cardiology*, 67, 69-76.

López-Barneo, J., et al. (1993). Effects of external cations and mutations in the pore region on C-type inactivation of Shaker potassium channels. *Receptors & Channels*, 1(1), 61-71.

Ma, X-Y., et al. (2011). External Ba<sup>2+</sup> Block of the Two-pore Domain Potassium Channel TREK-1 Defines Conformational Transition in Its Selectivity Filter. *J Biol Chem*, 286(46), 813-822.

MacKenzie, G., Franks, N. P. and Brickley, S. G. (2015). Two-pore domain potassium channels enable action potential generation in the absence of voltage-gated potassium channels. *Pflugers Archiv European Journal of Physiology*, 467(5), 989-999.

MacKinnon, R., 2004. Potassium channels and the atomic basis of selective ion conduction (Nobel Lecture). *Angewandte Chemie International Edition*, 43(33), pp.4265-4277.

Maingret, F., et al. (1999). Mechano- or acid stimulation, two interactive modes of activation of the TREK-1 potassium channel. *Journal of Biological Chemistry*, 274(38), 26691-26696.

Maingret, F., et al. (2000). TREK-1 is a heat-activated background K<sup>+</sup> channel. *EMBO Journal*, 19(11), 2483-2491.

Maingret, F., et al. (2002). Molecular basis of the voltage-dependent gating of TREK-1, a mechano-sensitive K<sup>+</sup> channel. *Biochemical and Biophysical Research Communications*, 292(2), 339-346.

Martinac, B., Adler, J. and Kung, C. (1990). Mechanosensitive ion channels of *E.coli* activated by amphipaths. *Nature*, 348, 261-263.

Mathie, A. (2007). Neuronal two-pore-domain potassium channels and their regulation by G protein-coupled receptors. *Journal of Physiology*, 578(2), 377-385.

Mathie, A., Al-Moubarak, E. and Veale, E. L. (2010). Gating of two pore domain potassium channels. *Journal of Physiology*, 588(17), 3149-3156.

Mathie, A. (2010). Ion channels as novel therapeutic targets in the treatment of pain. *Journal of Pharmacy and Pharmacology*, 62(9), 1089-1095.

Mazella, J., et al. (2010). Spadin, a sortilin-derived peptide, targeting rodent TREK-1 channels: A new concept in the antidepressant drug design. *PLoS Biology*, 8(4).

McClenaghan, C., et al. (2016). Polymodal activation of the TREK-2 K<sub>2</sub>P channel produces structurally distinct open states. *Journal of General Physiology*, 147(6), 497-505.

McNaughton, N. C. L., et al. (1997). Inhibition of human N-type voltage-gated Ca<sup>2+</sup> channels by the neuroprotective agent BW619C89. *Neuropharmacology*, 36(11-12), 1795-1798.

McNaughton, N. C. L., et al. (2000). Inhibition of recombinant low-voltage-activated Ca<sup>2+</sup> channels by the neuroprotective agent BW619C89 (Sipatrigine). *Neuropharmacology*, 39(7), 1247-1253.

Meadows, H. J., et al. (2001). The neuroprotective agent sipatrigine (BW619C89) potently inhibits the human tandem pore-domain K<sup>+</sup> channels TREK-1 and TRAAK. *Brain Research*, 892(1), 94-101.

Medhurst, A. D., et al. (2001). Distribution analysis of human two pore domain potassium channels in tissues of the central nervous system and periphery. *Molecular Brain Research*, 86(1-2), 101-114.

Millán-Guerrero., et al. (2008). Subcutaneous histamine versus topiramate in migraine prophylaxis: a double-blind study. *European Neurology*, 59(5), 237-242

Miller, A. N. and Long, S. B. (2012). Crystal structure of the human two-pore domain potassium channel K<sub>2</sub>P1. *Science*, 335(6067), 432-436.

Mizee, M. R., et al (2014). Astrocyte-derived retinoic acid: a novel regulator of blood-brain barrier function in multiple sclerosis. *Acta Neuropathol* 128(5):691–703.

Moczydlowski, E. and Latorre, R. (1983). Gating kinetics of Ca<sup>2+</sup>-activated K<sup>+</sup> channels from rat muscle incorporated into planar lipid bilayers. Evidence for two voltage-dependent Ca<sup>2+</sup> binding reactions. *J. Gen. Physiol.* 82, 511-542.

Molleman, A. (2003). Patch Clamping An Introductory Guide to Patch Clamp Electrophysiology. West Sussex, UK: John Wiley & Sons, Ltd.

- Monteillier, A., et al. (2016). Investigation of the structure activity relationship of flufenamic acid derivatives at the human TRESK channel K2P18.1. *Bioorganic and Medicinal Chemistry Letters*, 26(20), 4919-4924.
- Murbartián, J., et al. (2005). Sequential phosphorylation mediates receptor- and kinase-induced inhibition of TREK-1 background potassium channels. *Journal of Biological Chemistry*, 280(34), 30175-30184.
- National Research Council (US) Committee on Recognition and Alleviation of Pain in Laboratory Animals. Recognition and Alleviation of Pain in Laboratory Animals. Washington (DC): National Academies Press (US); 2009. 2, *Mechanisms of Pain.*: [http://www.ncbi.nlm.nih.gov/books/NBK32659/.](http://www.ncbi.nlm.nih.gov/books/NBK32659/)
- Naylor, C. E., et al. (2016). Molecular basis of ion permeability in a voltage-gated sodium channel. *EMBO Journal*, 35(8), 820-830.
- Newman-Tancredi, A. (2011) Biased agonism at serotonin 5-HT<sub>1A</sub> receptors: preferential postsynaptic activity for improved therapy of CNS disorders. *Neuropsychiatry*. 1(2):149-164.
- Niemeyer, M. I., et al. (2016). Gating, Regulation, and structure in K2P K<sup>+</sup> Channels: In varietate concordia?. *Molecular Pharmacology*, 90(3), 309-317.
- Nilius, B. and Owsianik, G. (2011). The transient receptor potential family of ion channels. *Genome Biology*. 12(3), 218.
- Noda, M., et al. (1984). Primary structure of electrophorus electricus sodium channel deduced from cDNA sequence. *Nature*, 312 (5990), 121-7.
- Oral, E. T. and Vahip, S. (2004). Bipolar depression: An overview. *Idrugs*, 7(9), 846-850.
- Panyi, G. and Deutsch, C. (2006). Cross talk between activation and slow inactivation gates of Shaker potassium channels. *Journal of General Physiology*, 128(5), 547-559.
- Papazian, D. M., et al. (1987). Cloning of genomic and complementary DNA from Shaker, a putative potassium channel gene from *Drosophila*. *Science*, 237(4816), 749-753.
- Park, H., et al. (2016). Effects of analgesics and antidepressants on TREK-2 and TRESK currents. *Korean Journal of Physiology and Pharmacology*, 20(4), 379-385.

- Patel, A. J., et al. (1998). A mammalian two pore domain mechano-gated S-like K<sup>+</sup> channel. *EMBO Journal*, 17(15), 4283-4290.
- Patel, A. J., et al. (1999). Inhalational anesthetics activate two-pore-domain background K<sup>+</sup> channels. *Nature Neuroscience*, 2(5), 422-426.
- Patel, A. J., Lazdunski, M. and Honoré, E. (2001). Lipid and mechano-gated 2P domain K<sup>+</sup> channels. *Current Opinion in Cell Biology*, 13(4), 422-427.
- Payandeh, J., et al. (2011). The crystal structure of a voltage-gated sodium channel. *Nature*, 475(7356), 353-359.
- Pena, F., et al. (2002). Amitriptyline has a dual effect on the conductive properties of the epithelial Na channel. *Journal of Pharmacy and Pharmacology*, 54(10), 1393-1398.
- Pereira, V., et al. (2014). Role of the TREK2 potassium channel in cold and warm thermosensation and in pain perception. *Pain*, 155(12), 2534-2544.
- Piechotta, P.L. et al. (2011). The pore structure and gating mechanism of K2P channels. *The EMBO journal*, 30(17), pp.3607-3619.
- Plant, L. D. (2012). A role for K2P channels in the operation of somatosensory nociceptors. *Frontiers in Molecular Neuroscience*.
- Pollema-Mays, S. L., et al. (2013). Expression of background potassium channels in rat DRG is cell-specific and down-regulated in a neuropathic pain model. *Molecular and Cellular Neuroscience*, 57, 1-9.
- Pottosin, I. I., et al. (2008). TRESK-like potassium channels in leukemic T cells. *European Journal of Physiology*, 456(6), 1027-48.
- Purves D, Augustine GJ, Fitzpatrick D, et al., editors. Neuroscience. 2nd edition. Sunderland (MA): Sinauer Associates; 2001. The Ionic Basis of the Resting Membrane Potential.
- Rahm, A. -, et al. (2012). PKC-dependent activation of human K<sub>2</sub>P18.1 K<sup>+</sup> channels. *British Journal of Pharmacology*, 166(2), 764-773.

- Rajan, S., et al. (2001). THIK-1 and THIK-2, a Novel Subfamily of Tandem Pore Domain K<sup>+</sup> Channels. *Journal of Biological Chemistry*, 276(10), 7302-7311.
- Rajan, S., et al. (2002). Interaction with 14-3-3 proteins promotes functional expression of the potassium channels TASK-1 and TASK-3. *Journal of Physiology*, 545(1), 13-26.
- Ren, D. (2011). Sodium Leak Channels in Neuronal Excitability and Rhythmic Behaviors. *Neuron*, 72(6), 899-911.
- Renigunta, V., Schlichthörl, G. and Daut, J. (2015). Much more than a leak: Structure and function of K2P-channels. *Pflügers Archiv European Journal of Physiology*, 467(5), 867-894.
- Ressler, K. J. and Nemeroff, C. B. (2000). Role of serotonergic and noradrenergic systems in the pathophysiology of depression and anxiety disorders. *Depression and Anxiety*, 12(SUPPL. 1), 2-19.
- Rowe, P (2016). *Essential statistics for the pharmaceutical sciences*. 2nd ed. West Sussex: Wiley. 50-54.
- Roberds, S. L. and Tamkun, M. M. (1991). Cloning and tissue-specific expression of five voltage-gated potassium channel cDNAs expressed in rat heart, *Proceedings of the National Academy of Sciences*, 88 (5), 1798-1802.
- Ruxton, G. D. (2006). The unequal variance t-test is an underused alternative to Student's t-test and the Mann-Whitney U test. *Behavioral Ecology*, 17(4), 688-690.
- Ryoo, K. and Park, J. -. (2016). Two-pore domain potassium channels in astrocytes. *Experimental Neurobiology*, 25(5), 222-232.
- Saberi, M. & Chavooshi, B. (2009) Suppressive effects of lamotrigine on the development and expression of tolerance to morphine-induced antinociception in the male mouse. *Brain Res* 1291, 32–39.
- Sandoz, G., et al. (2009). Extracellular acidification exerts opposite actions on TREK1 and TREK2 potassium channels via a single conserved histidine residue. *Proceedings of the National Academy of Sciences of the United States of America*, 106(34), 14628-14633.

Sandoz, G., Bell, S. C. and Isacoff, E. Y. (2011). Optical probing of a dynamic membrane interaction that regulates the TREK1 channel. *Proceedings of the National Academy of Sciences of the United States of America*, 108(6), 2605-2610.

Sangameswaran L., et al. (1996) Structure and function of a novel voltage-gated, tetrodotoxin-resistant sodium channel specific to sensory neurons. *Journal of Biology Chemistry* 271:5953–5956.

Sano, Y., et al. (2003). A novel two-pore domain K<sup>+</sup> channel, TRESK, is localized in the spinal cord. *Journal of Biological Chemistry*, 278(30), 27406-27412.

Schewe, M., et al. (2016). A Non-canonical Voltage-Sensing Mechanism Controls Gating in K2P K<sup>+</sup> Channels. *Cell*, 164(5), 937-949.

Shrivastava, I. H., et al. (2002). K<sup>+</sup> versus Na<sup>+</sup> ions in a K channel selectivity filter: A simulation study. *Biophysical Journal*, 83(2), 633-645.

Siegelbaum, S. A., et al (1982). Serotonin and cyclic AMP close single K<sup>+</sup> channels in Aplysia sensory neurones. *Nature*, 299(5882): 413-7.

Simkin, D., Cavanaugh, E. J. and Kim, D. (2008). Control of the single channel conductance of K2P10.1 (TREK-2) by the amino-terminus: Role of alternative translation initiation. *Journal of Physiology*, 586(23), 5651-5663.

Simms, B. A. and Zamponi, G. W. (2014). Neuronal voltage-gated calcium channels: Structures, function, and dysfunction. *Neuron*, 82(1), 24-25.

Smithers, N., et al. (2012). Characterizing the fatty acid binding site in the cavity of potassium channel KcsA. *Biochemistry*, 51(40), 7996-8002.

Snyders. D. J. (1999). Structure and function of cardiac potassium channels. *Cardiovascular Research*. 42(2). 377-90.

Sontheimer, H and Ransom, C.B (2002). Whole-Cell Patch-Clamp Recordings. In: Wolfgang W, Boulton AA and Baker GB Patch-Clamp Analysis Advanced Techniques. New York, USA: Humana Press. p35-65.

- Staudacher, K., et al. (2011). Alternative splicing determines mRNA translation initiation and function of human K<sub>2</sub>P10.1 K<sup>+</sup> channels. *Journal of Physiology*, 589(15), 3709-3720.
- Streit, A. K., et al. (2011). A specific two-pore domain potassium channel blocker defines the structure of the TASK-1 open pore. *Journal of Biological Chemistry*, 286(16), 13977-13984.
- Strong, M., Chandy, K. G., and Gutman, G. A. (1993). Molecular evolution of voltage-sensitive ion channel genes: on the origins of electrical excitability. *Molecular Biology and Evolution*. 10, 221-242.
- Tally, E. M., et al. (2001). Cns distribution of members of the two-pore-domain (KCNK) potassium channel family. *The Journal of Neuroscience*, 21 (19), 7491-505.
- Takahira, M., et al. (2005). Fenamates and diltiazem modulate lipid-sensitive mechano-gated 2P domain K<sup>+</sup> channels. *Pflugers Archiv European Journal of Physiology*, 451(3), 474-478.
- Thomas, D., et al. (2008). Alternative Translation Initiation in Rat Brain Yields K<sub>2</sub>P2.1 Potassium Channels Permeable to Sodium. *Neuron*, 58(6), 859-870.
- Tombola, F., Pathak, M. M. and Isacoff, E. Y. (2006). How does voltage open an ion channel? *Annual Review of Cell and Developmental Biology*. Vol. 22., pp. 23-52.
- Tong, L., et al. (2014). Activation of K<sub>2</sub>P channel-TREK1 mediates the neuroprotection induced by sevoflurane preconditioning. *British Journal of Anaesthesia*, 113(1), 157-167.
- Tsai, S. -. (2008). Sipatrigine could have therapeutic potential for major depression and bipolar depression through antagonism of the two-pore-domain K<sup>+</sup> channel TREK-1. *Medical Hypotheses*, 70(3), 548-550.
- Tulleuda, A., et al. (2011). TRESK channel contribution to nociceptive sensory neurons excitability: Modulation by nerve injury. *Molecular Pain*, 7.
- Veale, E. L. and Mathie, A. (2016). Aristolochic acid, a plant extract used in the treatment of pain and linked to Balkan endemic nephropathy, is a regulator of K<sub>2</sub>P channels. *British Journal of Pharmacology*, 173(10), 1639-1652.

- Veale, E. L., et al. (2014). Influence of the N terminus on the biophysical properties and pharmacology of TREK1 potassium channels. *Molecular Pharmacology*, 85(5), 671-681.
- Viswanath, A. N. I., et al. (2016). Identification of the first in silico-designed TREK1 antagonists that block channel currents dose dependently. *Chemical Biology and Drug Design*.
- Wang, M., et al. (2012). Changes in lipid-sensitive two-pore domain potassium channel TREK-1 expression and its involvement in astrogliosis following cerebral ischemia in rats. *European Journal of Physiology*, 46(2):384–392
- Wang, W., et al (2018). Lig4-4 selectivity inhibits TREK-1 and plays potent neuroprotective roles *in vitro* and in rat MCAO model. *Neuroscience Letters*, 671, 93-98
- Wu, X., et al. (2013). Involvement of TREK-1 Activity in Astrocyte Function and Neuroprotection under Simulated Ischemia Conditions. *Journal of Molecular Neuroscience*, 49(3), 499-506.
- Xie, X. M. and Garthwaite, J. (1996). State-dependent inhibition of Na<sup>+</sup> currents by the neuroprotective agent 619C89 in rat hippocampal neurons and in a mammalian cell line expressing rat brain type IIA Na<sup>+</sup> channels. *Neuroscience*, 73(4), 951-962.
- Yamane, D (2007). *The Axon Guide: A Guide to Electrophysiology & Biophysics Laboratory Techniques*. California, USA: MDS Analytical Technologies. 58-66.
- Yang, C., et al (2015). Sodium channel blockers for neuroprotection in multiple sclerosis. *Cochrane Database of Systematic Reviews*, 10 (CD010422).
- Yellen, G., et al. (1994). An engineered cysteine in the external mouth of a K<sup>+</sup> channel allows inactivation to be modulated by metal binding. *Biophysical Journal*, 66(4), 1068-1075.
- Yoo, S., et al. (2009). Regional expression of the anesthetic-activated potassium channel TRESK in the rat nervous system. *Neuroscience Letters*, 465(1), 79-84.
- Yu, F. H., et al. (2005). Overview of molecular relationships in the voltage-gated ion channel superfamily. *Pharmacological Reviews*, 57(4), 387-395.

- Yu, F. H. and Catterall, W. A. (2003). Overview of the voltage-gated sodium channel family. *Genome Biology*, 4(3).
- Zhou, Y., et al. (2001). Chemistry of ion coordination and hydration revealed by a K<sup>+</sup> channel-Fab complex at 2.0 Å resolution. *Nature*, 414(6859), 43-48.
- Zhuo, R. -, et al. (2016). Allosteric coupling between proximal C-terminus and selectivity filter is facilitated by the movement of transmembrane segment 4 in TREK-2 channel. *Scientific Reports*, 6.
- Zhou, J., et al. (2017). Reversal of TRESK Downregulation Alleviates Neuropathic Pain by Inhibiting Activation of Gliocytes in the Spinal Cord. *Neurochemical Research*, 1-11.
- Zhou, J., et al. (2012). TRESK gene recombinant adenovirus vector inhibits capsaicin-mediated substance P release from cultured rat dorsal root ganglion neurons. *Molecular Medicine Reports*, 5(4), 1049-1052.
- Zhou, Y. and MacKinnon, R. (2003). The occupancy of ions in the K<sup>+</sup> selectivity filter: Charge balance and coupling of ion binding to a protein conformational change underlie high conduction rates. *Journal of Molecular Biology*, 333(5), 965-975.
- Zilberberg, N., Ilan, N. and Goldstein, S. A. N. (2001). KCNKØ: Opening and closing the 2-P-domain potassium leak channel entails "C-type" gating of the outer pore. *Neuron*, 32(4), 635-648.

# 8 Appendix

## Identified regions of TREK and TRESK two pore domain potassium channels critical for inhibition by sipatrigine and lamotrigine

Y Walsh<sup>1</sup>, MJ Leach<sup>2</sup>, EL Veale<sup>1</sup>, A Mathie<sup>1</sup>

Email: yw200@kent.ac.uk

Medway School of Pharmacy, <sup>1</sup>University of Kent and <sup>2</sup>University of Greenwich, Chatham Maritime, Kent, ME4 4TB



### Introduction

Two pore domain potassium (K<sup>2P</sup>) channels are responsible for background currents that regulate membrane potential and neuronal excitability. Compounds which alter the activity of these channels are predicted to have therapeutic potential in treating CNS disorders. The TREK family of K<sup>2P</sup> channels (TREK1, TREK2 and TRAAK) has been shown to play an active role in neuroprotection, schizophrenia, depression and pain, whilst TRESK, with high expression in sensory neurons, has a role in nociception (1). Sipatrigine, a neuroprotective agent and a derivative of the anticonvulsant, lamotrigine, is a known antagonist of TREK channels, whilst lamotrigine is thought to primarily inhibit TRESK channels (2, 3). The aim of this study is to clarify differences in the inhibition of these channels by sipatrigine and lamotrigine and investigate the mechanism of inhibition.

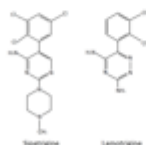


Figure 1: Structure of sipatrigine and lamotrigine

### Method

Modified HEK-293 cells (hA 201) were transiently transfected with wild type (WT) and mutated channels. The whole cell patch clamp electrophysiology technique was used to obtain current recordings in the presence and absence of sipatrigine and lamotrigine (100 μM).

### Results

#### Sipatrigine and lamotrigine inhibit current through TREK 1 and TREK2 channels

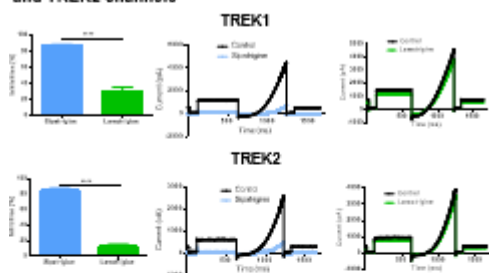


Figure 2: Sipatrigine was a more potent inhibitor of TREK1 channels than lamotrigine. TREK2 channels were similarly inhibited by sipatrigine, whilst lamotrigine had little inhibitory effect.

#### Sipatrigine and lamotrigine are potent inhibitors of TRESK current

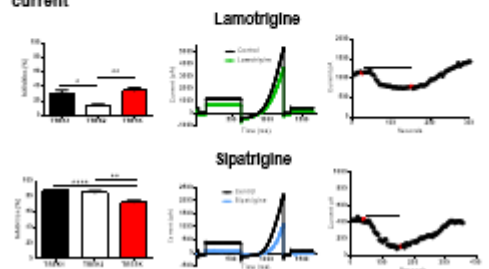


Figure 3: Lamotrigine inhibited TRESK channels to a similar degree as that seen for TREK1 inhibition. More surprisingly however sipatrigine was found to potently inhibit TRESK channels.

#### A leucine residue in M4 is important for sipatrigine inhibition

The recent crystal structure of TREK2 bound to a molecule of the anti-depressant, norfloxacin, has revealed several amino acids important for binding. This included leucine (L) at position 320 (equivalent to 289 for TREK1) which saw a decrease in norfloxacin inhibition when mutated (4).

TREK-2 K P I **V V F W I L V G L A Y F A A V** S M I 320  
 TREK-1 K P V **V V F W I L V G L A Y F A A V** S M I 289

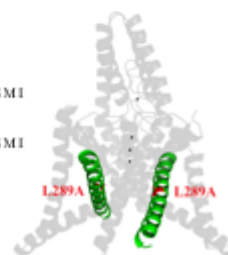


Figure 4: Homology model of TREK1 based on crystal structure 4TWK shows location of L289 mutated to alanine (labelled in red)

#### Mutation L289A reduces inhibition by sipatrigine of TREK1

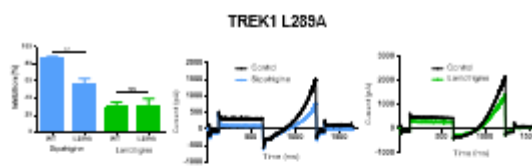


Figure 5: The TREK L289A mutated channel showed a significantly reduced inhibition by sipatrigine compared to WT TREK1, however, inhibition by lamotrigine was unaffected

#### Regulation of TRESK by sipatrigine and lamotrigine is affected by mutations in the pore

Homology models for TRESK channels have identified two key cavity-facing residues, F145 and F362 required for the effectiveness of certain channel blocking compounds (5).

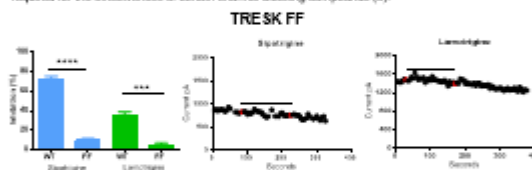


Figure 6: Mutations of bulky phenylalanine residues (F145A and F362A) in the M2 and M4 inner pore regions of the channel, thought to be involved in gating, substantially reduced inhibition by both sipatrigine and lamotrigine compared to WT TRESK.

### Conclusions

Our findings show that lamotrigine does indeed inhibit TRESK channels however the compound also inhibits TREK channels to the same degree. Furthermore, sipatrigine is a potent inhibitor of both TREK and TRESK channels. Mutations of TREK1 and TRESK have demonstrated sites on these channels important for the inhibitory actions of both sipatrigine and lamotrigine. For TREK1 channels, we hypothesize that L289 is important for sipatrigine inhibition but not for lamotrigine binding. For TRESK channels, F156 and F364 are important residues for inhibition by both compounds.

### References

1. Eryed P & Czejka G (2010) *Physiol Rev* 90, 559-625.
2. Moolenaar WJ et al (2001) *Brain Res* 892, 94-101.
3. Liu P et al (2013) *J Neurosci* 33, 12810-12824.
4. Dang YY et al (2015) *Science* 347, 1256-1259.
5. Kim S et al (2013) *Biochim Biophys Acta* 1828, 1131-1142.